Asymptotic Hecke Categories

submitted by
Liam Rogel

Date of the defense: 7th November 2025

1st referee: Prof. Dr. Ulrich Thiel
2nd referee: Prof. Dr. Geordie Williamson

Vom Fachbereich Mathematik der Rheinland-Pfälzischen Technischen Universität Kaiserslautern-Landau zur Verleihung des akademischen Grades Doktor der Naturwissenschaften (Doctor rerum naturalium, Dr. rer. nat.) genehmigte Dissertation

DE-386

Abstract

This thesis explores a conjecture of Lusztig about the correspondence of Fourier matrices combinatorially constructed for non-crystallographic Coxeter groups and S-matrices of the Drinfeld center of the asymptotic Hecke category associated to a two-sided cell $\mathbf{c}$ of a Coxeter group W. We construct these asymptotic Hecke categories using the diagrammatic approach of Elias–Williamson inside the diagrammatic Hecke category of Soergel bimodules. Through explicit calculations in dihedral groups, and some cells in type H_3, H_4, and certain infinite Coxeter groups with finite cells, we verify Lusztig's conjecture by showing that the asymptotic Hecke categories are known in the literature as fusion categories with type A_k fusion rules. For smaller cells these are either Fibonacci categories or $\mathbb{Z}/2\mathbb{Z}$-graded vector spaces. Our calculations establish an algorithmic framework that, in the future, could be extended to compute the asymptotic Hecke category of the 'so-called' middle cell in type H_4.

Zusammenfassung

Diese Dissertation untersucht eine Vermutung von Lusztig über die Korrespondenz zwischen kombinatorisch konstruierten Fourier-Matrizen für nicht-kristallographische Coxeter-Gruppen und S-Matrizen des Drinfeld-Zentrums der asymptotischen Hecke-Kategorie, die einer zweiseitigen Zelle $\mathbf{c}$ einer Coxeter-Gruppe W zugeordnet ist. Wir konstruieren diese asymptotischen Hecke-Kategorien mit dem diagrammatischen Ansatz von Elias–Williamson innerhalb der diagrammatischen Hecke-Kategorie der Soergel-Bimoduln. Durch explizite Berechnungen in Diedergruppen, sowie in einigen Zellen von Typ H_3, H_4 und bestimmten unendlichen Coxeter-Gruppen mit endlichen Zellen verifizieren wir Lusztigs Vermutung, indem wir zeigen, dass die asymptotischen Hecke-Kategorien in der Literatur als Fusionskategorien mit Fusionsregeln vom Typ A_k bekannt sind. Für kleinere Zellen handelt es sich entweder um Fibonacci-Kategorien oder $\mathbb{Z}/2\mathbb{Z}$-graduierte Vektorräume. Unsere Berechnungen motivieren einen algorithmischen Rahmen, der in der Zukunft benutzt werden könnte, um die asymptotische Hecke Kategorie der mittlere Zelle im Typ H_4 zu beschreiben.

Contents

Introduction

Historical background

The Kazhdan–Lusztig Framework. The theory of Soergel bimodules and the diagrammatic Hecke category has been one recent major development in representation theory, providing a new categorification of old structures in representation theory.

The roots trace back to [40] when Kazhdan and Lusztig introduced a new basis for Hecke algebras. The base change entries are now known as Kazhdan–Lusztig polynomials and it was conjectured that they are always positive. This positivity conjecture was proven through geometric methods relating to intersection cohomology of Schubert varieties [3].

In recent times, there has been a second proof. Soergel established in [60, 62] the category of Soergel bimodules $\mathbb{S}\mathrm{Bim}$ that can be constructed for any Coxeter group, not just Weyl groups coming from geometry. In a series of papers, Elias and Williamson [17, 23] then gave a diagrammatic description of this category, proving the positivity conjecture for any Coxeter group.

Lusztig's Conjecture for Non-crystallographic Coxeter Groups. These new discoveries then gave a motivation for a conjecture by Lusztig that tries to explain combinatorial values that have been studied in the last century.

In the study of reductive groups, Lusztig found in [46] that certain so-called unipotent characters can be parametrized by a finite set $U(W)$ only depending on the underlying Weyl group W, not on the order of the finite field. To these families, certain structure constants, called the Fourier matrix, have been observed to fulfill certain symmetries. This lead to attempts to describe these kind of matrices for non-crystallographic Coxeter groups. For the finite examples of the dihedral groups $I_2(n)$, and H_3, H_4, Lusztig [49], Malle [52], and Broué–Malle [8] constructed such Fourier matrices $F_W^{\mathbf{c}}$ for certain two-sided cells $\mathbf{c}$ of W.

These Coxeter groups have no geometry behind them, so Broué, Malle, and Michel coined the term 'spetses' in [7] for possible categorical objects behind these numbers.

Conjecture (Lusztig [50, Section 10]). *Let W be a non-crystallographic finite Coxeter group and let $\mathbf{c}$ be a two-sided cell in W. The S-matrix of the Drinfeld center of $C_{\mathbf{c}}$, $\mathcal{Z}^{\mathbf{c}}$ is equal to the Fourier matrix $F_W^{\mathbf{c}}$ from [49, 52]. In particular, the number of simple objects of $\mathcal{Z}^{\mathbf{c}}$ is equal to the number of unipotent characters supported in $\mathbf{c}$.*

Here $C_{\mathbf{c}}$ is a new category described by Lusztig. It is constructed out of the category of Soergel bimodules by imitating the same process that turns the Hecke algebra into the asymptotic Hecke algebra. One forms certain quotients and disregards summands of smaller cells. However, because of degree reasons in Soergel bimodules, the naive generalization does not work. Only following the new results on the hard Lefschetz theorem in [18] did a possible construction emerged. Result on the bijection where also observed in [56, Section 5.4].

We aim in this thesis to construct and define all structures needed to describe the asymptotic Hecke category associated to a two-sided cell **c**. We will calculate it explicitly in all cases in H_3, some in H_4, all dihedral groups, and even some infinite Coxeter groups. We will also compute the S-matrix of their centers to verify Lusztig's conjecture.

Overview of this thesis

Cell Theory and the Asymptotic Hecke Algebra. In chapter 1 we lay the algebraic groundwork for this thesis. All structures we look at are constructed using Coxeter groups. We denote a Coxeter system by (W, S), where W is the group and S is the set of simple reflections. We consider the Iwahori–Hecke algebra $\mathbf{H}(W)$, a deformation of the group ring $\mathbb{Z}[W]$. In our notation, the standard basis elements are denoted $\{\delta_x\}_{x\in W}$, while the Kazhdan–Lusztig basis elements are $\{b_w\}_{w\in W}$.

We introduce the general notions of cells following Green's theory, see [33]. Originally defined for monoids, cells structure the multiplication in algebraic systems. Certain equivalence classes formed by left and right multiplication are called L-cells and R-cells, respectively. The intersection of these relations gives rise to H-cells, while the smallest equivalence relation containing both is the J-relation. In general, the representation theory of monoids depends only on the representations of certain subgroups associated with the H-cells. The technique of reducing general problems to these is called H-reduction.

This framework can be extended to the Hecke algebra, though the cell structure depends critically on the choice of basis. For the standard basis $\{\delta_x\}$, the cell structure is trivial, while for the Kazhdan–Lusztig basis $\{b_w\}$, we obtain the Kazhdan–Lusztig cells. Here, H-reduction is also applicable. For every cell **c** one can use the multiplication of the Kazhdan–Lusztig basis to define a new structure, the asymptotic Hecke algebra $J_{\mathbf{c}}$. It has generators only coming from elements of the cells, where in the product one quotients out elements of higher cells and certain summands with high gradings.

For finite Weyl groups, the asymptotic algebras $J_{\mathbf{c}}$ are fusion rings of the form $\mathbf{Conv}_G(X \times X)$, i.e., G-graded coherent sheaves on a finite set. For $X = \{*\}$ or $X = G$ with the group action, this gives, for example, group-theoretical fusion rings, i.e., Grothendieck rings of categories of the form $\mathrm{Rep}(G)$ or $\mathbf{Vec}_G$. The only possibilities that occur for G are S_3, S_4, S_5 and some elementary abelian 2-groups.

In dihedral groups, H_3, and H_4, however, we find interesting new examples. A common occurrence is the Fibonacci ring, a commutative ring with two generators 1 and x satisfying $x^2 = 1 + x$. In dihedral groups, we observe a generalization with more terms following a Clebsch–Gordan-like rule of multiplication.

Furthermore, we describe finite cells in infinite Coxeter groups of small **a**-value (particularly $\mathbf{a} = 1$ and $\mathbf{a} = 2$), identifying specific representatives that will be essential for our later constructions. For example, in $\mathbf{a}(1)$-finite groups, the cell structure can be characterized by elements having unique reduced expressions, while the classification of $\mathbf{a}(2)$-finite groups includes types A_n, B_n, $\tilde{C}_n$, $E_{q,r}$, F_n, H_n, and I_n.

Categorical Structures and Monoidal Categories. In chapter 2 we then introduce the categorical structures needed for our framework. We build upon monoidal categories, which generalize the familiar tensor product from algebra. However, from a categorical viewpoint, we must carefully track associators $\alpha_{X,Y,Z} : (X \otimes Y) \otimes Z \xrightarrow{\sim} X \otimes (Y \otimes Z)$. These isomorphisms between different bracketings of a triple tensor product must satisfy the pentagon axiom to ensure coherence. The main reference for monoidal categories will be [24].

As base examples, we present two different categorical versions of the rings introduced in the first chapter. For the relation $x^2 = 1$, the category $\mathbf{Vec}_{\mathbb{Z}/2\mathbb{Z}}$ admits both a strict version

where all associators are identity maps, and a non-strict version where $\alpha_{1,1,1} = -\mathrm{id}$. For the Fibonacci relation $x^2 = 1 + x$, we also have two non-equivalent categorifications given by different associators corresponding to the two solutions of the polynomial $x^2 - x - 1 = 0$.

The Drinfeld center and H-reduction. We further introduce the Drinfeld center $\mathcal{Z}(C)$ of a monoidal category C. Objects in the center are pairs (X, γ), where $X \in C$ and γ is a family of natural isomorphisms $\gamma_Y : X \otimes Y \xrightarrow{\sim} Y \otimes X$ satisfying a hexagon axiom, see [24, Section 2.4], related to associativity and braiding.

Here we also state H-reduction for the center. The center of a multifusion category is equivalent to the center of the fusion subcategories $C_{i,i}$. One can therefore reformulate Lusztig's Conjecture using an H-cell **h** instead of a J-cell. With the knowledge from chapter 1, we now understand that the corresponding asymptotic Hecke algebras $J_{\mathbf{h}}$ are all group theoretical. The center of group theoretical fusion categories, such as $\mathbf{Vec}_G$ or $\mathrm{Rep}(G)$, has the exact same combinatorial description as the sets $U(W)$ Lusztig constructed for reductive groups. They are pairs consisting of a conjugacy class of G and a simple representation of its centralizer. Furthermore, the S-matrix of this center category also has the same entries as the corresponding Fourier matrices.

Finishing the groundwork, we introduce Soergel bimodules, following the approaches of Soergel, Elias and Williamson. We present both the algebraic formulation as well as the diagrammatic version. For dihedral groups, we give an explicit connection between Soergel bimodules and a two-colored version of the Temperley–Lieb category. This will be used when doing concrete calculations in the asymptotic category.

Constructing Idempotents and Computational Challenges. We know that for most H-cells in type H_3, H_4 there are only two possible categorifications, differing only by a few entries in the associators. To distinguish them we will therefore later need to explicitly calculate certain fusion structures, such as the associators or dimensions of objects. Hence we need a skeletal version of the asymptotic categories. For these to be constructed, we need to be able to construct idempotents in the diagrammatic category corresponding to the elements in the H-cells we introduced.

A general construction of idempotents in this category has not been described before. The author was made aware of notes from Ben Elias and Dani Tubbenhauer calculating some idempotents during a research stay at the University of Oregon with Ben Elias in 2022. A detailed description of the construction of idempotents is given in [21], with a companion paper [22] featuring a computer construction inside the localized category.

In Chapter 3 we give a short introduction to the construction. In the same way as the construction for the Kazhdan–Lusztig polynomials, one can build the idempotents inductively. For $B_w B_s \simeq \bigoplus B_z$ one needs to describe pairwise orthogonal projection and inclusion maps to the summands. Here we keep to specific calculations for the H-cells, while in the coming paper more general notions will be introduced. Surprisingly, idempotents for an object are not unique; for us it is however enough to find one working representative. Calculations can get out of hand if many smaller summands occur; the second longest cell in H_3 is computable, while currently there is no hope for the middle and higher cells in H_4.

We compute all idempotents for the H-cells introduced in Chapter 1.4, from the relatively simple cases in $\mathbf{a}(2)$-finite groups to the more complex idempotents in type H_3 with **a**-value 6.

The Asymptotic Hecke Category Construction. In chapter 4, we then give the detailed construction of the asymptotic Hecke category $\mathcal{J}_{\mathbf{c}}$ associated to a two-sided Kazhdan–Lusztig cell **c** in a Coxeter group, following the work of Lusztig, Elias, and Williamson.

We begin by explaining in section 4.1 why the algebraic construction of the asymptotic algebra cannot be directly categorified: projecting tensor products $B_x \otimes B_y$ to their lowest degree summands fails because the necessary projection and inclusion morphisms lack canonicity.

The resolution to this difficulty comes from Elias and Williamson's hard Lefschetz theorem for Soergel bimodules, presented in section 4.2. For a dominant regular weight $\rho \in \mathfrak{h}^*$ and elements $x, y \in W$, multiplication by ρ induces isomorphisms $\eta^i : H^{-i}(B_x \otimes_R B_y) \xrightarrow{\sim} H^i(B_x \otimes_R B_y)$ between perverse cohomology. This provides the canonical isomorphisms needed to define projection and inclusion maps in our construction.

We apply this algorithm systematically to all H-cells listed before. In small examples where $\mathcal{J}_{\mathbf{c}}$ categorifies the Fibonacci category or $\mathbb{Z}/2\mathbb{Z}$ ring, we demonstrate how the exact associator is determined by the dimensions of the objects.

Verification of Lusztig's Conjecture and Future Directions. Our work then culminates in the last chapter. We identify the asymptotic Hecke categories as adjoint parts of type A_k fusion categories, whose centers and S-matrices are known in the literature. The main classification results are:

Theorem (Theorem 5.25, Corollary 5.27). *The* H*-cell subcategory $\mathcal{J}_{\mathbf{h}_s}$ in the subregular cell of type $I_2(k)$ is equivalent to* $\mathrm{Ad}(C_{k-1})$*, the adjoint part of the type A_{k-1} fusion category. For* $\mathbf{a}(1)$*-finite Coxeter groups the same holds with $k = m_{s,t}$.*

For infinite Coxeter groups with finite cells of $\mathbf{a}$-value ≤ 2, the H-cell asymptotic categories are $\mathbf{Vec}_{(\mathbb{Z}/2\mathbb{Z})^2}$ (type $\tilde{C}_n$, Theorem 5.34), $\mathbf{Vec}_{\mathbb{Z}/2\mathbb{Z}}$ (types B_n and F_n, Theorem 5.37), and the Fibonacci category (type H_n). For types H_3 and H_4 the H-cells yield either the Fibonacci category or $\mathbf{Vec}_{\mathbb{Z}/2\mathbb{Z}}$; see Theorems 5.33, 5.40, 5.38, and 5.39.

Together these identifications yield the main result:

Theorem (Theorem 5.45). *The S-matrix of $\mathcal{Z}(\mathcal{J}_{\mathbf{c}})$ equals the Fourier matrix $F_W^{\mathbf{c}}$ of [49, 52] for all two-sided cells* $\mathbf{c}$ *in dihedral groups, in type H_3, and in the smaller cells of type H_4.*

One final observation worth noting is that different conventions for S-matrices exist in the literature. The treatments in [24] and [49] differ by certain normalizations and orderings of rows and columns. After appropriate reordering and rescaling, our results perfectly match Lusztig's original claim.

While our approach has enabled us to handle all cases of two-sided cells except the middle and higher cells in H_4, where the calculations become prohibitively complex for paper-based methods, we have established an algorithmic framework that could be implemented computationally. We hope that further developments in computer algebra systems will allow these remaining cases to be tackled using the methods described in this work.

Acknowledgements

First I want to thank my supervisor Ulrich Thiel for introducing me to the wonderful world of diagrammatic categories and the in-person and online discussions, especially during the first Corona Lockdown. I am grateful to the 'Jürgen Group' of my earliest PhD office mates: Johannes Schmidt, Dario Mathiä and Maria Walch. The livelihood in office 48-420 was a wonderful restart after Corona. My thanks goes to the SFB-TRR 195 for many important conference opportunities and meetings, as well as the chance to visit faraway places. I would like to thank Ben Elias for hosting me for nine weeks in 2022 at his university in Eugene, Oregon on a research stay and for the progress I made there in

understanding the diagrammatic calculations. Thanks also to other mathematicians whose conversations have helped me, including Victor Ostrik on associators, Dani Tubbenhauer on cell structures, and Abel Lacabanne on centers. Furthermore, I appreciate Fabian and Erec for our exchanges, computer assistance, and joint seminar organization. For their proofreading, I thank Maria Walch and Michael Will. Finally, my gratitude goes to my family and friends for their support throughout this journey. This work is a contribution to the SFB-TRR 195 ‘Symbolic Tools in Mathematics and their Application’ of the German Research Foundation (DFG).

CHAPTER 1

The asymptotic Algebra

To define the asymptotic Hecke algebra, we first introduce Coxeter groups and their Hecke algebras with their standard and Kazhdan–Lusztig bases. The Kazhdan–Lusztig basis leads naturally to the theory of cells in the Hecke algebra, generalizing Green's theory for monoids. Using the structure constants of multiplication in this basis, we then construct the asymptotic algebra. The computer implementations for these calculations are detailed in [22]. We focus particularly on the cases where the cells are finite, including finite Coxeter groups and certain cells of small **a**-value in infinite Coxeter groups, as these will be relevant for our later categorification results.

1.1. The Hecke algebra and the Kazhdan–Lusztig basis

In this section, we introduce Coxeter groups, define the Hecke algebra, and describe the Kazhdan–Lusztig basis. The conventions chosen here will be used throughout this thesis.

1.1.1. Coxeter groups. Coxeter groups, introduced and studied in [11] are groups that are only generated by involutions, i.e. elements of order 2. They include a variety of often studied groups, such as Weyl groups of semisimple Lie algebras.

Definition 1.1 (Coxeter System). A Coxeter group is a group with a presentation of the form $W = \langle s_i \mid (s_i s_j)^{m_{ij}} = 1,\ i, j \in I\rangle$ with index set I, where $m_{ii} = 1$ and $m_{ij} = m_{ji} \geq 2$ for $i \neq j$. The pair (W, S) with $S = \{s_i \mid i \in I\}$ is called a Coxeter system.

The Dynkin diagram serves as a visual representation of the relations of the generators.

Definition 1.2 (Dynkin Diagram). The Dynkin diagram of a Coxeter system (W, S) is an undirected graph where:

- Vertices are generators $s_i \in S$.
- An edge connects s_i and s_j if $m_{ij} \geq 3$.
- Edges are labeled with m_{ij} when $m_{ij} \geq 4$.

A Coxeter system is *irreducible* if its Dynkin diagram is connected.

The classification of finite Coxeter systems was completed by [11]. Since the Dynkin diagram of $(W \times W', S \times S')$ is the disjoint union of the individual diagrams, it suffices to classify irreducible systems. The following example lists all finite irreducible Coxeter groups as well as other infinite Coxeter groups that we will investigate.

Example 1.3. All finite irreducible Coxeter groups can be found in the following list. Here n is a positive natural number. It is common to not use $B_2, D_2, D_3, I_2(2)$ for disambiguity. Some sources also prefer to use H_2 instead of $I_2(5)$. Since we will focus more on dihedral groups we also use $I_2(6)$ instead of G_2.

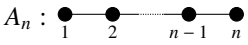

(1.1)

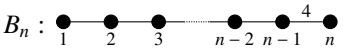

(1.2)

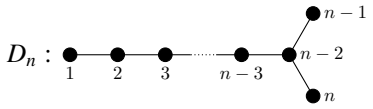

(1.3)

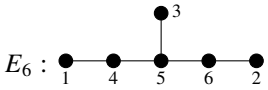

(1.4)

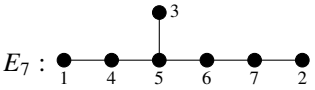

(1.5)

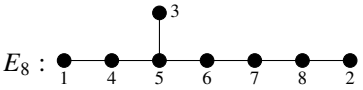

(1.6)

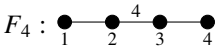

(1.7)

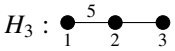

(1.8)

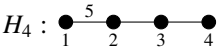

(1.9)

(1.10)

While finite Coxeter groups have well-established notation, the notation for infinite Coxeter groups varies considerably in the literature. For our work with infinite groups, we establish the following conventions:

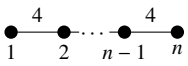

(1.11)

for $n \geq 3$,

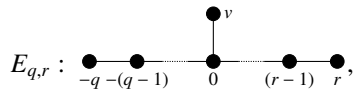

, (1.12)

for $r \geq q \geq 1$,

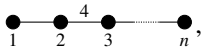

, (1.13)

for $n \geq 4$,

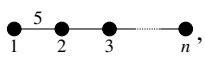

, (1.14)

for $n \geq 3$.

Notation 1.4. In a Coxeter group (W, S), every element $w \in W$ can be written as a product of generators $s_i \in S$. Such an expression $w = s_{i_1} s_{i_2} \dots s_{i_k}$ is called a *word* representing w. For elements of a Coxeter system (W, S), we use unadorned letters (e.g., w) to denote the element itself, and underlined letters (e.g., $\underline{w} = (s_1, \dots, s_n)$) to denote a specific expression.

Example 1.5. The *length* of w, denoted $\ell(w)$, is the minimum number of generators needed in any expression $(s_1, \dots, s_n)$ expressing w.

A word of minimal length representing w is called a *reduced expression* for w. Furthermore we define the *Bruhat order* as the relation $x < y$ defined by: $\ell(x) < \ell(y)$ and there is a $t \in W$ with $xt = y$.

In a finite group there is an unique longest word denoted w_0. In type A_2 we have for example $w_0 = sts$.

Remark 1.6. While elements of W may have multiple reduced expressions, any two such expressions are related by *braid relations* of the form $\underbrace{st\dots}_{m_{s,t}} = \underbrace{ts\dots}_{m_{s,t}}$. For instance, in type A_3 with simple reflections r, s, t satisfying $m_{rs} = 3 = m_{st}$ and $m_{rt} = 2$ (i.e., r and t commute):

$$rstr = rsrt = srst. \tag{1.15}$$

Definition 1.7 (Coxeter Complex). Let (W, S) be a Coxeter system of rank n, i.e. $|S| = n$. The *Coxeter complex* $\Sigma(W, S)$ is a simplicial complex defined as follows:

- For each element $w \in W$ we take one $n-1$-dimensional simplex Δ_w.
- We label its faces by the reflections $s \in S$.
- We glue any Δ_w and Δ_v along the edge labeled s if and only if $ws = v$.

The Coxeter complex of a dihedral group can be viewed as a $2n$-gon in the plane. More generally, the Coxeter complex of a finite rank 3 Coxeter system is a triangulation of the 2-sphere. In the next example, we use the same color coding as for Hecke algebras and Soergel bimodules introduced in subsection 2.4.2.

Example 1.8. For type $I_2(3) = A_2$ the Coxeter complex is:

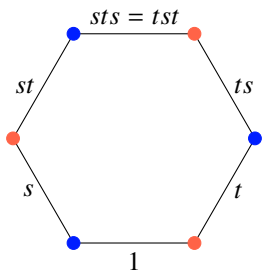

(1.16)

1.1.2. Realizations of Coxeter Groups. The concept of a realization of a Coxeter group is due to Soergel [62]. He used this to algebraically define Soergel bimodules. We follow the notation of Elias and Williamson [17, Section 3] and [20, Section 5.7]. These realizations will be needed again in section 2.4.

Definition 1.9 ([20], Definition 5.37). Let (W, S) be a Coxeter system and $\Bbbk$ a commutative integral domain. A *realization* of (W, S) over $\Bbbk$ consists of a triple $(\mathfrak{h}, \{\alpha_s\}_{s\in S}, \{\alpha_s^\vee\}_{s\in S})$ where:

- $\mathfrak{h}$ is a free $\Bbbk$-module of finite rank.

- $\alpha_s^\vee \in \mathfrak{h}$ and $\alpha_s \in \mathfrak{h}^* = \mathrm{Hom}_{\mathbb{k}}(\mathfrak{h}, \mathbb{k})$ for all $s \in S$.

satisfying:

- We have $\alpha_s(\alpha_s^\vee) = 2$ for all $s \in S$.
- The map $(s, v) \mapsto v - \alpha_s(v)\alpha_s^\vee$ extends to a W-action on $\mathfrak{h}$.
- A technical condition holds (see [20, Section 5.7]).

The *Cartan matrix* of the realization is defined as:

$$(\alpha_t(\alpha_s^\vee))_{s,t\in S}. \tag{1.17}$$

We will only consider realizations satisfying:

- *Demazure surjectivity:* For all $s \in S$, the maps $\alpha_s : \mathfrak{h} \to \mathbb{k}$ and $\alpha_s^\vee : \mathfrak{h}^* \to \mathbb{k}$ are surjective.
- *Balancedness:* The balancedness condition is as defined in [20, Assumption 5.57].

We set $R \coloneqq \mathrm{Sym}(\mathfrak{h}^*)$ and consider it as the polynomial ring $\mathbb{k}[\alpha_s \mid s \in S]$ where α_s has degree 2. We will primarily work over the real or complex numbers. For most Coxeter groups, the following realization satisfies the required criteria.

Definition 1.10 (Geometric Representation). The geometric representation $V \coloneqq V_{geom}$ of (W, S) is a real vector space spanned by $\{\alpha_s\}_{s\in S}$, equipped with a symmetric bilinear form $(-,-)$ such that:

$$(\alpha_s, \alpha_t) \coloneqq -\cos\left(\frac{\pi}{m_{s,t}}\right). \tag{1.18}$$

We set $\frac{\pi}{m_{s,t}} \coloneqq 0$ if $m_{s,t} = \infty$. Setting $\alpha_s^\vee \coloneqq 2(\alpha_s, -)$, we obtain the data of a realization. The action of W on V is then given on the generators by:

$$s.\lambda \coloneqq \lambda - 2(\lambda, \alpha_s)\alpha_s. \tag{1.19}$$

1.1.3. Demazure Operators and Positive Roots. To finish the overview on all Coxeter groups that we are interested in we will also fix dominant regular elements for all types. These will play a role in the hard Lefschetz theorem of section 4.2.

Definition 1.11. For $I \subseteq S$, let $W_I \coloneqq \langle I \rangle \subseteq W$ be the standard parabolic subgroup generated by I. Define $R^I \coloneqq \{f \in R \mid w.f = f \text{ for all } w \in W_I\}$. For singleton sets $I = \{s\}$, we write R^s instead of $R^{\{s\}}$.

Definition 1.12 (Demazure Operator). For each simple reflection $s \in S$, the Demazure operator $\partial_s : R \to R^s(-2)$ is defined as:

$$\partial_s(f) \coloneqq \frac{f - s.f}{\alpha_s}. \tag{1.20}$$

For any $w \in W$ with reduced expression $\underline{w} = (s_1, s_2, \ldots, s_n)$, we define:

$$\partial_w \coloneqq \partial_{\underline{w}} \coloneqq \partial_{s_1}\partial_{s_2}\cdots\partial_{s_n}. \tag{1.21}$$

The well-definedness of ∂_w follows from the fact that the Demazure operators satisfy the braid relations, [20, Equation 4.25].

For later purposes, we need an element $\rho \in R$ such that $\partial_s(\rho) > 0$ for all $s \in S$. We call such an element *dominant regular*. For finite Coxeter systems the Cartan matrix is invertible, and we can compute a dominant regular element ρ satisfying $\partial_s(\rho) = 1$ for all $s \in S$.

For type $I_2(n)$, we verify that $\partial_s(\alpha_s + \alpha_t) = \frac{(\alpha_s+\alpha_t)-(-\alpha_s+\alpha_t+2\cos(\frac{\pi}{n})\alpha_s)}{\alpha_s} = 2 - 2\cos\left(\frac{\pi}{n}\right)$ is positive.

[1]Here ϕ denotes the golden ratio $\frac{1+\sqrt{5}}{2}$.

Type	Coxeter matrix	Cartan matrix	dominant regular element
$I_2(n)$	$\begin{pmatrix} 1 & n \\ n & 1 \end{pmatrix}$	$\begin{pmatrix} 2 & -2\cos(\pi/n) \\ -2\cos(\pi/n) & 2 \end{pmatrix}$	$\alpha_s + \alpha_t$
A_3	$\begin{pmatrix} 1 & 3 & 2 \\ 3 & 1 & 3 \\ 2 & 3 & 1 \end{pmatrix}$	$\begin{pmatrix} 2 & -1 & 0 \\ -1 & 2 & -1 \\ 0 & -1 & 2 \end{pmatrix}$	$\frac{3}{2}\alpha_1 + 2\alpha_2 + \frac{3}{2}\alpha_3$
B_3	$\begin{pmatrix} 1 & 3 & 2 \\ 3 & 1 & 4 \\ 2 & 4 & 1 \end{pmatrix}$	$\begin{pmatrix} 2 & -1 & 0 \\ -1 & 2 & -\sqrt{2} \\ 0 & -\sqrt{2} & 2 \end{pmatrix}$	$\frac{4+\sqrt{2}}{2}\alpha_1 + (3+\sqrt{2})\alpha_2 + \frac{3+3\sqrt{2}}{2}\alpha_3$
B_4	$\begin{pmatrix} 1 & 3 & 2 & 2 \\ 3 & 1 & 3 & 2 \\ 2 & 3 & 1 & 4 \\ 2 & 2 & 4 & 1 \end{pmatrix}$	$\begin{pmatrix} 2 & -1 & 0 & 0 \\ -1 & 2 & -1 & 0 \\ 0 & -1 & 2 & -\sqrt{2} \\ 0 & 0 & -\sqrt{2} & 2 \end{pmatrix}$	$\frac{6+\sqrt{2}}{2}\alpha_1 + (5+\sqrt{2})\alpha_2 + \frac{12+3\sqrt{2}}{2}\alpha_3 + (2+3\sqrt{2})\alpha_4$
F_4	$\begin{pmatrix} 1 & 3 & 2 & 2 \\ 3 & 1 & 4 & 2 \\ 2 & 4 & 1 & 3 \\ 2 & 2 & 3 & 1 \end{pmatrix}$	$\begin{pmatrix} 2 & -1 & 0 & 0 \\ -1 & 2 & -\sqrt{2} & 0 \\ 0 & -\sqrt{2} & 2 & -1 \\ 0 & 0 & -1 & 2 \end{pmatrix}$	$(5+3\sqrt{2})\alpha_1 + (9+6\sqrt{2})\alpha_2 + (9+6\sqrt{2})\alpha_3 + (5+3\sqrt{2})\alpha_4$
H_3	$\begin{pmatrix} 1 & 5 & 2 \\ 5 & 1 & 3 \\ 2 & 3 & 1 \end{pmatrix}$	$\begin{pmatrix} 2 & -\phi & 0 \\ -\phi & 2 & -1 \\ 0 & -1 & 2 \end{pmatrix}$	$\frac{9\phi+6}{2}\alpha_1 + (5\phi+4)\alpha_2 + \frac{5\phi+5}{2}\alpha_3$
H_4	$\begin{pmatrix} 1 & 5 & 2 & 2 \\ 5 & 1 & 3 & 2 \\ 2 & 3 & 1 & 3 \\ 2 & 2 & 3 & 1 \end{pmatrix}$	$\begin{pmatrix} 2 & -\phi & 0 & 0 \\ -\phi & 2 & -1 & 0 \\ 0 & -1 & 2 & -1 \\ 0 & 0 & -1 & 2 \end{pmatrix}$	$(42\phi+26)\alpha_1 + (51\phi+33)\alpha_2 + (34\phi+23)\alpha_3 + (17\phi+12)\alpha_4$[1]

TABLE 1.1. Overview on dominant regular elements in finite Coxeter groups.

REMARK 1.13. For affine Coxeter groups, the geometric realization fails to satisfy Demazure surjectivity, as the Cartan matrix is not invertible. For types F_5 and $\tilde{C}_n$, which we will consider later, there exists an alternative realization called the *Kac–Moody realization* (see [20, Section 5.6], following Soergel's construction in [62]).

For example, in F_5, where $\alpha_1, \ldots, \alpha_5$ are linearly dependent, one works over an extension $\mathfrak{h}' = \mathfrak{h} \oplus \mathbb{k} \cdot e$ with e fixed under the W-action. This yields a larger polynomial ring R, where one can find a dominant regular element ρ as before.

In this Kac–Moody realization, one can still normalize the roots. Thus, we will assume throughout that we have a dominant regular element ρ satisfying:

$$\partial_s(\rho) = 1 \quad \text{for all } s \in S. \tag{1.22}$$

REMARK 1.14. For a dominant regular element ρ, we have $\partial_w(\rho^{\ell(w)}) > 0$ for all $w \in W$. This follows from the *twisted Leibniz rule* (see [20, Equation 4.22]):

$$\partial_s(fg) = \partial_s(f)g + s.f\partial_s(g). \tag{1.23}$$

For example, taking $f = g = \rho$, we get

$$\partial_s(\rho^2) = \partial_s(\rho)\rho + s.\rho\partial_s(\rho) = \rho + s.\rho. \tag{1.24}$$

Then for any $t \neq s$, we have $\partial_t(\rho + s(\rho)) = 1 + \partial_t(s.\rho) > 0$, since $s.\rho$ remains dominant with respect to t.

For a given Coxeter system (W, S), we denote by ρ_W its dominant regular element, writing simply ρ when the context is clear.

1.1.4. Iwahori–Hecke algebra. Hecke algebras are deformations of the group algebras of Coxeter groups. They were originally introduced by Iwahori and Matsumoto in the context of p-adic groups [38]. We again follow the notation of [20].

DEFINITION 1.15 (Hecke Algebra). Let (W, S) be a Coxeter system and $\mathbb{Z}[v^{\pm 1}]$ the ring of Laurent polynomials over $\mathbb{Z}$. The Iwahori–Hecke algebra $\boldsymbol{H} := \boldsymbol{H}(W)$ is the unital associative algebra over $\mathbb{Z}[v^{\pm 1}]$ generated by the elements $\{\delta_s \mid s \in S\}$, subject to the following relations:

- (Quadratic relation) $\delta_s^2 = (v^{-1} - v)\delta_s + 1$ for all $s \in S$.
- (Braid relation) $\underbrace{\delta_s\delta_t\dots}_{m_{s,t}} = \underbrace{\delta_t\delta_s\dots}_{m_{s,t}}$ for all $s, t \in S$.

For a word $\underline{x} = (s_1, \dots, s_n)$, we define $\delta_x \coloneqq \delta_{s_1} \dots \delta_{s_n}$. The elements $\{\delta_x \mid x \in W\}$ form the *standard basis* of $\boldsymbol{H}$.

Remark 1.16. The statement that $\{\delta_x\}$ forms a basis is non-trivial, see [20, Theorem 3.5]. Note that δ_x is independent of the chosen word due to the braid relation and Remark 1.6. Furthermore, one has the following multiplication rules:

- $\delta_w\delta_s = \delta_{ws}$ if $ws > w$;
- $\delta_w\delta_s = (v^{-1} - v)\delta_w + \delta_{ws}$ if $ws < w$.

Any δ_s (and hence any δ_x) is invertible with $\delta_s^{-1} = \delta_s + (v - v^{-1})$. This follows from the quadratic relation Definition 1.15:

$$\delta_s\delta_s^{-1} = \delta_s^2 + (v - v^{-1})\delta_s = 1 \tag{1.25}$$

We denote by $\bar{\cdot} : \boldsymbol{H} \to \boldsymbol{H}$ the *involution* on $\boldsymbol{H}$ which sends the generators δ_s to δ_s^{-1} and v to v^{-1}.

Remark 1.17. Some further remarks on the Hecke algebra. It is a deformation of the ordinary group ring $\mathbb{Z}[v^{\pm 1}][W]$, which we can recover by setting $v \coloneqq 1$.

In the literature, there are different conventions for the variable used. For example, in [40] they use an isomorphic representation with variable $q^{1/2}$.

Also note that our Hecke algebra is also called the equal parameter or one-parameter Hecke algebra. One can also define a variant using variables q_s for every conjugacy class of reflection, as in [45].

1.1.5. Kazhdan–Lusztig polynomials. The *Kazhdan–Lusztig basis* is a second basis of $\boldsymbol{H}(W)$ introduced in [40]. We will focus on the purely algebraic definition and not refer to the geometric background of their construction. Again, our notation coincides with [20, Chapter 3]. In this subsection, W is always a Coxeter group with generating reflections S. If we focus on a specific group, we will mention it.

Definition 1.18. The *Kazhdan–Lusztig basis* $\{b_w \mid w \in W\}$ is the uniquely defined basis of $\boldsymbol{H}(W)$ with

- (self duality) $\overline{b_w} = b_w$,
- (degree bound) $b_w = \delta_w + \sum_{x<w} h_{x,w}\delta_x$, for $h_{x,w} \in v\,\mathbb{Z}[v]$.

The polynomials $h_{x,w}$, i.e. the base change coefficients to the standard basis are called *Kazhdan–Lusztig polynomials*.

Example 1.19. For any reflection s, we have $b_s = \delta_s + v\delta_1$. Indeed, $\overline{b_s} = \overline{\delta_s} + v^{-1}\delta_1 = (\delta_s + (v - v^{-1})\delta_1) + v^{-1}\delta_1 = b_s$, and all coefficients are of positive degree excluding the leading term.

Remark 1.20. The existence and uniqueness of Definition 1.18 can be found in [20, Section 3.2]. For motivational purposes, we will give the inductive construction. Later in chapter 3, we will also build idempotents inductively in a similar fashion.

By Example 1.19, we have the Kazhdan–Lusztig basis for the simple reflections. Also note that trivially one has $b_1 = \delta_1$.

Now we would like to construct b_{ws} from b_w if s is a reflection such that $ws > w$. Consider the product $b_w b_s$. It has a summand of the form $\delta_w\delta_s = \delta_{ws}$ and all other summands correspond to δ_v for $v < ws$. By the degree bound condition, we must find b_{ws} as

a summand inside $b_w b_s$. By subtracting minimal multiples $\mu_s(v,w)b_v$ for $v < ws$ starting with v of biggest possible length until the term $b_w b_s - \sum_v \mu_s(v,w)b_v$ satisfies the degree bound, we will have found the Kazhdan–Lusztig basis element b_{ws}.

We show this graphically in type A_2:

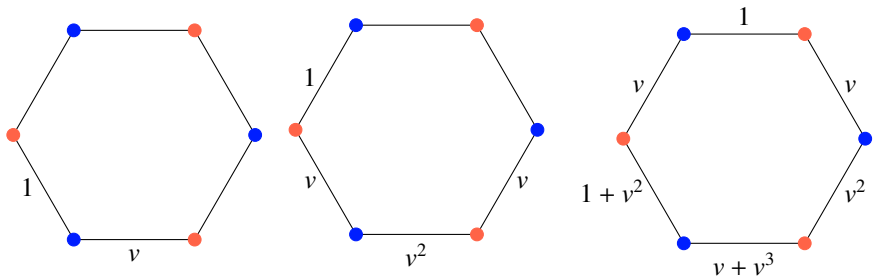

Basis element b_s. Product $b_s b_t = b_{st}$. Product $b_{st} b_t = b_{sts} + b_s$. (1.26)

In dihedral groups, this calculation can be easily extended to show that the Kazhdan–Lusztig polynomials are always monomials. We have:

$$b_x = \sum_{y \le x} v^{\ell(x)-\ell(y)} \delta_y. \tag{1.27}$$

We will introduce some more notation for further use.

Definition 1.21. Since $\{b_x\}$ forms a basis of the Hecke algebra $\boldsymbol{H}(W)$, we can express any product of two basis elements in the basis. We write

$$b_x b_y = \sum_{z \in W} h_{x,y,z} b_z.$$

and call $h_{x,y,z} \in \mathbb{Z}[v^{\pm 1}]$ the *structure constants*. We then have $\mu_s(v,w) = h_{w,s,v}$. One also defines the *μ-coefficient* $\mu(v,w)$ as the coefficient of v^1 in $h_{v,w}$. For $vs < v$, we have $\mu(v,w) = \mu_s(v,w)$.

1.2. Cell theory

The construction of the asymptotic algebra requires knowledge on the Kazhdan–Lusztig cells of a Coxeter system. Cell theory originated in the study of monoids, we introduce the general notation following Green's original work.

1.2.1. Green's relations. The notion of cells was introduced by Green [33] in the context of semigroups – sets equipped with an associative binary operation. For our purposes, we will primarily work with monoids (semigroups with identity), as this simplifies many definitions. These concepts will later be extended to algebras.

For the theory of H-reduction, we rely on the fundamental results of Clifford–Munn–Ponizovskiĭ [10, 55]. A modern treatment of monoid representation theory can be found in [63].

Definition 1.22 (Green's Relations [33]). Let M be a monoid. For $a, b \in M$, define:

- $a \le_{\mathrm{L}} b$ if there exists $c \in M$ such that $ca = b$.
- $a \le_{\mathrm{R}} b$ if there exists $c \in M$ such that $ac = b$.
- $a \le_{\mathrm{J}} b$ if there exist $c, c' \in M$ such that $cac' = b$.

We extend this to a relation and add two more. For $a, b \in M$ and $x \in \{\mathrm{L}, \mathrm{R}, \mathrm{J}\}$ we define:

- $a \sim_x b$ if $a \leq_x b$ and $b \leq_x a$.
- $a \sim_{\mathrm{H}} b$ if $a \sim_{\mathrm{L}} b$ and $a \sim_{\mathrm{R}} b$.
- $a \sim_{\mathrm{D}} b$ if there exists $c \in M$ such that $a \sim_{\mathrm{L}} c$ and $c \sim_{\mathrm{R}} b$.

We call the equivalence classes with respect to $\{\mathrm{L}, \mathrm{R}, \mathrm{J}\}$ the left-, right-, or two-sided cells.

Green showed that for finite monoids the D- and J-relations are equivalent. We will therefore only work with the latter. We will also use notation such as $x <_{\mathrm{L}} y$ to mean $x \leq_{\mathrm{L}} y$ but $x \not\sim_{\mathrm{L}} y$.

Example 1.23. Let M be a group. Then for any $a, b \in M$ we have $a \sim_x b$ for any Green relation. This follows from the existence of inverses, as we have, for example, $(ba^{-1})a = b$ demonstrating the left relation.

Extending the previous example, it is clear that the invertible elements $G \subset M$ inside a monoid form their own x-cell, for $x \in \{\mathrm{L}, \mathrm{R}, \mathrm{J}, \mathrm{H}\}$. Furthermore, since $a = a \cdot 1 = 1 \cdot a = 1 \cdot a \cdot 1$, we have $1 \leq_x a$ for all $a \in M$ and $x \in \{\mathrm{L}, \mathrm{R}, \mathrm{J}\}$, and therefore G can be regarded as the lowest cell.

1.2.2. Eggbox-diagram. Before we introduce more notation on the cells, we will first present a representation of the cells of a monoid called the eggbox-diagram. These diagrams will often be used in this thesis to give an overview of Kazhdan–Lusztig cells. The name is self-explanatory.

Definition 1.24. An eggbox diagram is a visual representation of a monoid M with respect to Green's relations:

- Every vertex represents a J-cell.
- We connect two J-cells j_1, j_2 by an edge $j_1 \to j_2$ if $j_1 \leq_{\mathrm{J}} j_2$. Usually, we read eggbox diagrams from bottom to top and therefore omit the arrowheads.
- The vertices themselves are $m \times n$-box diagrams.
- Each box represents an H-class (where $\mathrm{H} = \mathrm{L} \cap \mathrm{R}$).
- Rows form L-classes, columns form R-classes.
- We mark H-cells containing an idempotent.

Example 1.25. The transformation monoid T_X is the set of all functions from a finite set X to itself, equipped with function composition as the binary operation. For $n \in \mathbb{N}$, we write T_n for T_X where X is any set of n elements. A function can be written in shorthand notation as $(i_1 i_2 \dots i_n)$, which sends j to i_j. We depict these maps by diagrams, where composition is performed by vertical stacking and connecting arches:

$$\mathrm{id}_n \leftrightarrow \begin{array}{c} 1\ 2\ 3 \\ \big|\ \big|\ \big| \\ 1\ 2\ 3 \end{array}, \quad (121) \leftrightarrow \begin{array}{c} 1\ 2\ 3 \\ \big\backslash\!\big|\ \bullet \\ 1\ 2\ 3 \end{array}. \tag{1.28}$$

Often we will omit the labelings at the top and bottom. A calculation shows that the eggbox diagram is as given in Figure 1.1.

The motivation why we color cells containing idempotents is the next definition. Note, that each idempotent e gives rise to a submonoid eMe of M. Although it has a different neutral element.

The subgroup of invertible elements can be found at the bottom. The next layer contains all maps having only two elements in their image. We can see from the diagram that the position of the endpoints at the top is the defining characteristic for R-cells, as multiplication from the right corresponds to stacking a diagram below.

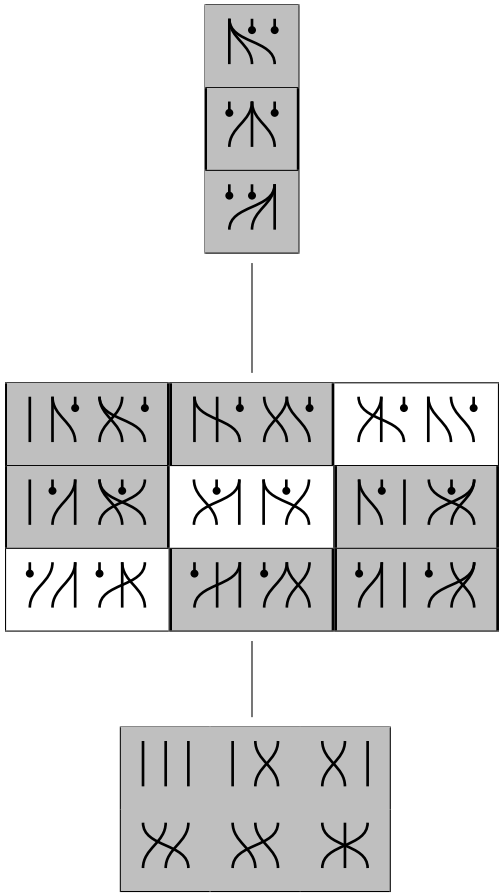

FIGURE 1.1. Eggbox diagram of T_3.

Conversely, the L-cells are characterized by their preimages. If i, j point to the same k at the top, they will continue to do so after stacking another diagram on top.

The H-cells are characterized by permutations in their image.

The motivation for coloring cells containing idempotents comes from the next definition. Note that each idempotent e gives rise to a submonoid eMe of M, albeit with a different neutral element.

DEFINITION 1.26. For a monoid M, denote by G_1, as in Example 1.23, the subgroup of invertible elements of M. For an idempotent $e \in M$, we set G_e to be the group of invertible elements of the monoid eMe. We call the G_e's the maximal subgroups of M.

REMARK 1.27. One can show that the relations $\{\mathrm{L}, \mathrm{R}, \mathrm{J}, \mathrm{H}\}$ hold in M if and only if they hold in eMe for any idempotent e. Hence, by the observations of Example 1.23, the set G_e forms one H-cell inside M and contains exactly one idempotent.

One can further show that all groups G_e within one J-cell are isomorphic. Representations of the monoid M can be restricted to each maximal subgroup; conversely, there is a construction to induce any representation of G_e to one of M. Note that all cells not higher

than the cell containing e will be represented by zero. We will not describe the construction completely, but only state the main theorem of Clifford–Munn–Ponizovskiĭ theory. This motivates why we will later focus only on H-cells.

Theorem 1.28 (Clifford–Munn–Ponizovskiĭ Theory). *Let M be a finite monoid and $\Bbbk$ a field. There is a one-to-one correspondence between isomorphism classes of simple $\Bbbk M$-modules and isomorphism classes of simple $\Bbbk G_e$-modules, where e ranges over representatives of* J*-equivalence classes of idempotents in M.*

This shows that the representation theoretic study of simple monoids reduces to the study of the groups G_e. As these are all H-cells inside the monoid we call this process H-*reduction*. We will see similar results for the center of the asymptotic category.

1.3. Kazhdan–Lusztig cells

We have now defined Green cells for monoids. We use this definition to extend the concept of cells to algebras. In the context of the Hecke algebra with the Kazhdan–Lusztig basis, these are called *Kazhdan–Lusztig* cells and were introduced in [40]. As with monoids, these cells are used to find representations of the Hecke algebra.

We use the general notation from Green and more specific notation introduced by Lusztig for these special cells. The main references are a series of papers on the cells of affine Weyl groups, beginning with [47, 48], and for an overview, see [45]. We first extend Green cells to algebras, then provide a small example in the dihedral case, and then present the main notation introduced by Lusztig. Finally, we show how H-reduction can also work for the Hecke algebra; we will call the resulting algebras the *asymptotic (Hecke) algebra*.

Throughout (W, S) always denotes an arbitrary Coxeter system and $\boldsymbol{H}$ the corresponding Hecke algebra.

1.3.1. Green relations on algebras.

Definition 1.29. Let A be an R-algebra with basis $B = \{b_i \mid i \in I\}$. Any product $b_i b_j = \sum_k \alpha_{i,j}^k b_k$ for $b_i, b_j \in B$ decomposes as a sum, where $\alpha_{i,j}^k \in R$. We say $b_k \prec b_i b_j$ if $\alpha_{i,j}^k \neq 0$. We can then define Green's relations on (A, B):

- $b_i \leq_{\mathrm{L}} b_j$ if there exists a $b_k \in B$ such that $b_j \prec b_k b_i$.
- $b_i \leq_{\mathrm{R}} b_j$ if there exists a $b_k \in B$ such that $b_j \prec b_i b_k$.
- $b_i \leq_{\mathrm{J}} b_j$ if there exist $b_k, b_l \in B$ such that $b_j \prec b_k b_i b_l$.

Similar to the monoid case, we also define the H-relation as $b_i \sim_{\mathrm{H}} b_j$ if $b_i \sim_{\mathrm{L}} b_j$ and $b_i \sim_{\mathrm{R}} b_j$.

Remark 1.30. The relations and the cells strongly depend on the chosen basis. Take for example a Hecke algebra $\boldsymbol{H}(W)$. If we choose the standard basis $B = \{\delta_w \mid w \in W\}$, then we get only one cell, as the based algebra is a deformation of the group ring and therefore $\delta_1 \prec \delta_x \delta_{x^{-1}}$ and hence all basis elements lie in the same H-cell, comparable to a group being a single H-cell.

If we choose the Kazhdan–Lusztig basis, however, we get different cells. These we call *Kazhdan–Lusztig cells*, and from now on we will always assume that we are working with these. Note that the coefficients $\alpha_{i,j}^k$ have been called $h_{x,y,z}$, see Definition 1.21.

Remark 1.31. To visualize these cells, we will also use eggbox diagrams. Similar to the monoid case, an idempotent $e \in A$ gives rise to a sub R-algebra eAe. However, since we do not assume A to be unital, nor the unit to be one of the basis elements, there is no a priori connection to the cell structure (as e may not be part of the basis).

The concept of H-reduction requires additional assumptions. For any J- or H-cell, we denote by A_{J} and A_{H} respectively the corresponding restrictions. As it turns out in Kazhdan–Lusztig cells we will always have pseudo idempotents in exactly one H-cell per L- or R-cell. We will always give the eggbox diagram such that these H-cells lie on the diagonal and therefore do not color the diagrams anymore.

1.3.2. Small example in type A_2. Before we introduce more Kazhdan–Lusztig cell notation, we look at the symmetric group on 3 letters, i.e. we consider W of type A_2. As it is a dihedral group, we have seen a description of all Kazhdan–Lusztig polynomials in (1.27) and can compute:

$$b_s b_t = b_{st},\ b_s b_s = [v]b_s,\ b_{st}b_s = b_{sts} + b_s \quad \text{and} \quad b_{sts}b_s = [v]b_{sts}, \tag{1.29}$$

for $[v] \coloneqq [v]_2 \coloneqq v + v^{-1}$. Multiplication with $b_1 = \delta_1$ on the other hand is always trivial. Using symmetry and applying these repeatedly, we get the multiplication in Table 1.2. Here, we also set $[v]_3 \coloneqq [v]_2[v]_2 - 1 = v^2 + 1 + v^{-2}$.

$\cdot$	b_1	b_s	b_t	b_{st}	b_{ts}	b_{sts}
b_1	b_1	b_s	b_t	b_{st}	b_{ts}	b_{sts}
b_s	b_s	$[v]b_s$	b_{st}	$[v]b_{st}$	$b_{sts} + b_s$	$[v]b_{sts}$
b_t	b_t	b_{ts}	$[v]b_t$	$b_{sts} + b_t$	$[v]b_{ts}$	$[v]b_{sts}$
b_{st}	b_{st}	$b_{sts} + b_s$	$[v]b_{st}$	$[v]b_{sts} + b_{st}$	$[v](b_{sts} + b_s)$	$[v]^2 b_{sts}$
b_{ts}	b_{ts}	$[v]b_{ts}$	$b_{sts} + b_t$	$[v](b_{sts} + b_t)$	$[v]b_{sts} + b_{ts}$	$[v]^2 b_{sts}$
b_{sts}	b_{sts}	$[v]b_{sts}$	$[v]b_{sts}$	$[v]^2 b_{sts}$	$[v]^2 b_{sts}$	$[v]_3[v]b_{sts}$

TABLE 1.2. Multiplication of Kazhdan–Lusztig basis in type $I_2(3)$.

This gives for example

$$h_{s,ts,sts} = 1,\ h_{s,s,s} = (v + v^{-1}),\ h_{st,ts,s} = (v + v^{-1}). \tag{1.30}$$

We can read of the cell structure:

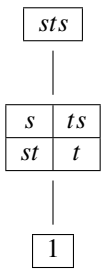

FIGURE 1.2. Eggbox diagram of A_2.

We have three J-cells. The top $\mathbf{c}_3 \coloneqq \{sts\}$ and bottom $\mathbf{c}_0 \coloneqq \{1\}$ contain only one L-, R- and H-cell, while the middle one $\mathbf{c}_1 \coloneqq \{s, t, st, ts\}$ contains 2, 2, and 4 cells respectively:

$$\mathbf{c}_s^L \coloneqq \{s, ts\},\ \mathbf{c}_t^L \coloneqq \{t, st\},\ \mathbf{c}_s^R \coloneqq \{s, st\},\ \mathbf{c}_t^R \coloneqq \{t, ts\}. \tag{1.31}$$

We will see the general setting for the dihedral group in the overview, see subsection 1.4.1.

1.3.3. Lusztig's conjectures for cells. We introduce more notation to state 15 conjectures on the cell structure in the Hecke algebra, see [45, Conjecture 14.2].

Remark 1.32. In [45], one defines the relations $z \leftarrow_{\mathrm{L}} y$ if and only if there exists an $s \in S$ with $h_{s,y,z} \neq 0$. This is then extended to the relation $\leq_{\mathrm{L}}$. Different results, e.g. [29, Section 1.6], show that both notions yield the same cell structure. As the 15 conjectures use this different notation, we will also mention it here.

Lemma 1.33. *Let c^L be a left cell of W. Then*

$$c^R := \{w^{-1} \mid w \in c^L\} \tag{1.32}$$

is a right cell of W.

Proof. This follows from [45, 13.1(e)]:

$$h_{x,y,z} = h_{x^{-1},y^{-1},z^{-1}}. \tag{1.33}$$

The main idea is to use the anti-automorphism $\boldsymbol{H} \to \boldsymbol{H}, b_w \mapsto b_{w^{-1}}$. Then $z \leftarrow_{\mathrm{L}} y$ is equivalent to $z^{-1} \leftarrow_{\mathrm{R}} y^{-1}$, which proves our claim. □

For $w \in W$ we define the *left descent set* and *right descent set* to be

$$L(w) := \{s \in S \mid \ell(sw) < \ell(w)\} \quad \text{and} \quad R(w) := \{s \in S \mid \ell(ws) < \ell(w)\}. \tag{1.34}$$

Lemma 1.34. *For any elements y, z in a Coxeter group W we have*

$$z \leq_{\mathrm{L}} y \Rightarrow R(z) \supseteq R(y) \tag{1.35}$$

and

$$z \leq_{\mathrm{R}} y \Rightarrow L(z) \supseteq L(y). \tag{1.36}$$

Proof. This is [45, Lemma 8.6]. □

Remark 1.35. Lemma 1.34 implies that for $z \sim_{\mathrm{L}} y$ we have $R(y) = R(z)$. Hence the number of left cells is at least the number of unique sets $R(w)$ for $w \in W$. In an irreducible Coxeter group there is always one cell containing all elements having a unique reduced expression, the *subregular cell*, see [44, Theorem 3.8]. Together with Lemma 1.34 we can say that the L-cells inside the subregular cell are classified by the last reflection, the R-cells by the first and the H-cells by both. If the group is not irreducible the cells splits into multiple ones. For example in $I_2(2)$ the cells $\{s\}$ and $\{t\}$ are not related.

Corollary 1.36. *For any element $x \neq 1$ of a Coxeter group W, we have*

$$1 \leq x, \quad x \not\leq 1 \tag{1.37}$$

for any of the relations $\leq \in \{\leq_{\mathrm{L}}, \leq_{\mathrm{R}}, \leq_{\mathrm{J}}\}$. In particular, the set $\{1\}$ is always the lowest left, right, and two-sided cell of W.

Proof. The Kazhdan–Lusztig polynomial of the identity basis element has the form $b_1 = \delta_1$. This gives $b_1 b_x = b_x = b_x b_1$, so $1 \leq x$. However, we have $L(1) = \emptyset = R(1)$ while the descending sets for x are non-empty. By Lemma 1.34, this implies that $x \not\leq 1$. □

Corollary 1.37. *Let (W, S) be a finite Coxeter group and denote by w_0 the longest element. Then for any $x \in W \setminus \{w_0\}$, we have*

$$x \leq w_0, \quad w_0 \not\leq x \tag{1.38}$$

for any of the relations $\leq \in \{\leq_{\mathrm{L}}, \leq_{\mathrm{R}}, \leq_{\mathrm{J}}\}$. In particular, the set $\{w_0\}$ is always the highest left, right, and two-sided cell of W.

Proof. We argue similarly to Corollary 1.36. Since $L(w_0) = S = R(w_0)$, we have $w_0 \not\leq x$ for any $x \in W \setminus \{w_0\}$. For any such x, we can find an element $x' \in W$ with $x'x = w_0$ and $\ell(x') + \ell(x) = \ell(w_0)$. Then by an inductive argument from [20, Theorem 3.27], we see that $b_{x'}b_x$ equals a sum of $b_{x'x} = b_{w_0}$ and some other A-multiples of terms $b_{w'}$ where $\ell(w') < \ell(w_0)$. This shows that $x \leq_{\mathrm{L}} w_0$, and similarly we obtain $x \leq_{\mathrm{R}} w_0$. □

Definition 1.38. On W we define the **a**-*function*

$$\mathbf{a} : W \to \mathbb{N} \cup \{\infty\} \tag{1.39}$$

to be the map sending z to the smallest positive integer $\mathbf{a}(z) \in \mathbb{N}$ such that

$$v^{\mathbf{a}(z)} h_{x,y,z} \in \mathbb{Z}[v] \text{ for all } x, y \in W, \tag{1.40}$$

or to ∞ if no such integer exists. If $\mathbf{a}(z) \in \mathbb{N}$ for all $z \in W$, we call W *bounded*.

Proposition 1.39. *Let W be a finite Coxeter group and $w_0 \in W$ the longest element. Then*

$$\mathbf{a}(w_0) = \ell(w_0). \tag{1.41}$$

Proof. By [20, Theorem 3.27], we have for any $s \in S$ that

$$b_s b_{w_0} = [v] b_{w_0},$$

where $[v] \coloneqq v + v^{-1}$, since $L(w_0) = S$. By induction, this shows that

$$b_{w_0} b_{w_0} = (v^{-\ell(w_0)} + \text{ terms of higher degree}) b_{w_0},$$

hence $\mathbf{a}(w_0) \geq \ell(w_0)$. Since the length of the longest element is an upper bound for the **a**-function, we conclude that $\mathbf{a}(w_0) = \ell(w_0)$. □

Remark 1.40. It is clear that any finite Coxeter group is bounded, with the maximal **a**-value given by the length of the longest element w_0 (see Proposition 1.39). Recent work shows that the **a**-function is also bounded in general, see [9]. Therefore it can be assumed that all W we work with are bounded.

For any $x, y, z \in W$, let

$$\gamma_{x,y,z^{-1}} \coloneqq h_{x,y,z} v^{\mathbf{a}(z)}(0) \in \mathbb{Z} \tag{1.42}$$

be the coefficient of the $v^{-\mathbf{a}(z)}$-term in $h_{x,y,z}$. Note that we use z^{-1} in the definition of γ.

Remark 1.41. For finite W we always have $\gamma_{x,y,z} \geq 0$. If W is crystallographic this was shown in [47, Lemma 5.2(d)] and [48, 1.1(e)]. For the non-crystallographic types H_3, H_4 and $I_2(m)$ there have been explicit calculations, see [12]. We will see the dihedral case explicitly in subsection 1.3.2.

Definition 1.42 ([45, Section 14.1]). Let $d(z)$ be the degree of the smallest term in the Kazhdan–Lusztig polynomial $h_{1,z}$. We define the set of *Duflo involutions* by

$$D \coloneqq \{z \in W \mid \mathbf{a}(z) = d(z)\}. \tag{1.43}$$

Let n_z denote the coefficient of the $v^{d(z)}$-term in $h_{1,z}$.

Note that in Lusztig's paper, the polynomials $h_{x,y,z}$ lie in $\mathbb{Z}[v^{-1}]$, hence he instead uses the highest exponent.

Example 1.43. For the dihedral group, we know that $h_{1,z} = v^{\ell(z)}$, hence by Example 1.45 we have $D = \{1, s, t, w_0\}$.

We can now describe the conjectures of [45, Conjecture 14.2].

Proposition 1.44. *For a bounded Coxeter group (W, S), we have:*

- *(P1) For any $z \in W$:* $\mathbf{a}(z) \leq d(z)$.
- *(P2) If $d \in D$ and $x, y \in W$ satisfy $\gamma_{x,y,d} \neq 0$, then $x = y^{-1}$.*
- *(P3) For $y \in W$, there exists a unique $d \in D$ with $\gamma_{y^{-1},y,d} \neq 0$.*
- *(P4) If $z \leq_{\mathrm{J}} y$, then $\mathbf{a}(z) \geq \mathbf{a}(y)$. Hence $z \sim_{\mathrm{J}} y$ implies $\mathbf{a}(z) = \mathbf{a}(y)$.*
- *(P5) In the case of (P3), this value is $n_d = \pm 1$.*
- *(P6) For $d \in D$, we have $d^2 = 1$.*
- *(P7) For any $x, y, z \in W$, we have $\gamma_{x,y,z} = \gamma_{y,z,x}$.*
- *(P8) If for $x, y, z \in W$ we have $\gamma_{x,y,z} \neq 0$, then $x \sim_{\mathrm{L}} y^{-1}$.*
- *(P9) If $z \leq_{\mathrm{L}} y$ and $\mathbf{a}(y) = \mathbf{a}(z)$, then $z \sim_{\mathrm{L}} y$.*
- *(P10) If $z \leq_{\mathrm{R}} y$ and $\mathbf{a}(y) = \mathbf{a}(z)$, then $z \sim_{\mathrm{R}} y$.*
- *(P11) If $z \leq_{\mathrm{J}} y$ and $\mathbf{a}(y) = \mathbf{a}(z)$, then $z \sim_{\mathrm{J}} y$.*
- *(P12) Let $I \subseteq S$. If w lies in the subgroup W_I generated by I, then $\mathbf{a}(w)$ computed in W_I equals $\mathbf{a}(w)$ computed in W.*
- *(P13) Any left cell contains a unique element $d \in D$.*
- *(P14) For any $z \in W$, we have $z \sim_{\mathrm{J}} z^{-1}$.*
- *(P15) If $h'_{x,y,z}$ denotes the image of $h_{x,y,z}$ under the map $\mathbb{Z}[v, v^{-1}] \to \mathbb{Z}[v', v'^{-1}]$, $v \mapsto v'$, and $\mathbf{a}(w) = \mathbf{a}(y)$ for some $w, y \in W$, then*

$$\sum_{y' \in W} h'_{w,x',y'} h_{x,y',y} = \sum_{y' \in W} h_{x,w,y'} h'_{y',x',y}.$$

- *($\tilde{P}$) If for $x, y, z, z' \in W$ we have $\gamma_{x,y,z^{-1}} \neq 0$ and $z' \leftarrow_{\mathrm{L}} z$, then there exists $x' \in W$ such that $v^{\mathbf{a}(z)} h_{x',y,z'}(0) \neq 0$. In particular, $\mathbf{a}(z') \geq \mathbf{a}(z)$.*

Proof. In [45, Section 15], Lusztig shows that (P1)–(P3) and $\tilde{P}$ imply (P4)–(P15). Furthermore, in Section 15 he proves that for bounded W, one has (P1)–(P3) and $\tilde{P}$. □

Example 1.45. Reading off from Figure 1.2, we see that $\mathbf{c}_0$ and $\mathbf{c}_1$ have $\mathbf{a}$-value 1, while $\mathbf{c}_3$ has value 3. This explains our choice of indices. By Proposition 1.39 and Conjecture (P4) see Proposition 1.44, in the dihedral group $I_2(n)$ we always have the $\mathbf{a}$-values 0, 1, and n.

Remark 1.46. Using the term 'involution' in the name of *Duflo involution* is justified by property (P6).

Proposition 1.47. *For a bounded Coxeter group W, we have:*

(A) $\mathbf{a}(w) = \mathbf{a}(w^{-1})$.
(B) $\mathbf{a}(w) = 0$ *if and only if* $w = 1$.
(C) $\mathbf{a}(w) \leq \ell(w)$ *for any* $w \in W$.

Proof. (A) This follows from (P14) and (P4).
(B) We have $b_1 = \delta_1$, hence by (P1), $0 \leq \mathbf{a}(1) \leq d(1) = 0$. If $w \in W$ is non-trivial and $s \in L(w)$, then $b_s b_w = [v] b_w$, so $1 \leq \mathbf{a}(w)$.
(C) The highest exponent in the Kazhdan–Lusztig polynomial $h_{1,z}$ is bounded by $\ell(z)$, hence by (P1) the claim follows.

□

1.3.4. The J-ring. We again assume that (W, S) is a bounded Coxeter system. Lusztig used the coefficients $\gamma_{x,y,z}$ to define a new ring structure on the $\mathbb{Z}$-module $\langle j_w \mid w \in W \rangle_{\mathbb{Z}}$. Using this structure, he proved the following theorem for crystallographic Coxeter groups in [48, Theorem 2.2]. This theorem was then generalized to a more general notion, which we present there.

On a vector space generated by e_s for $s \in S$ we define a symmetric bilinear form $(e_s, e_t) \coloneqq -\cos\left(\frac{\pi}{m_{s,t}}\right)$. We say the Coxeter system is *tame* if this form is positive semi-definite, see [45, Section 1.11]. Tame groups are all bounded, see [47, Section 7.2].

Theorem 1.48. *Let W be a bounded and tame Coxeter group satisfying properties (P1) to (P15). Then:*

(A) *W has finitely many left cells.*
(B) *W has finitely many right cells.*
(C) *W has finitely many two-sided cells.*
(D) *The set D is finite.*

Proof. This is [45, Theorem 18.2]. □

Remark 1.49. In general one can construct Coxeter groups with infinitely many left cells, see for example [4, Theorem 5.3].
Recently boundness was proven for all Coxeter groups of finite rank, see [9].

We will now describe the ring he used and will list some properties for it. Most calculations follow directly from Proposition Proposition 1.44.

Definition 1.50. For a bounded Coxeter group W, we define $J \coloneqq J_W$ to be the free abelian group generated by $\{j_x \mid x \in W\}$ with multiplication given by

$$j_x j_y = \sum_{z \in W} \gamma_{x,y,z^{-1}} j_z, \tag{1.44}$$

and call it the *J-ring associated to W*. For a commutative ring A, we call $A \otimes_{\mathbb{Z}} J$ the *asymptotic Hecke algebra* of W over A.

We will use the terms J-ring and asymptotic Hecke algebra interchangeably.

Lemma 1.51. *If W is a bounded Coxeter group, then J is a ring with unit. The unit element is given by*

$$1_J = \sum_{d \in D} n_d j_d. \tag{1.45}$$

Proof. This follows from Proposition Proposition 1.44; see [48, Chapter 2] or [45, Section 18.3]. We outline the main steps:

- The multiplication is well-defined since there are only finitely many $z \in W$ with $h_{x,y,z} \neq 0$.
- The product is associative by (P15).
- The element 1_J is well-defined by Theorem 1.48 (D).
- For the unit property, we show $j_w 1_J = j_w = 1_J j_w$ for every $w \in W$. Let $d \in D$. By (P7), we have $\gamma_{w,d,x} = \gamma_{x,w,d}$ for any $x \in W$. By (P2), (P3), and (P8), this is non-zero if and only if $x = w^{-1}$ and $x \sim_{\mathrm{L}} d$. In this case,

  $$j_w j_d = \gamma_{w^{-1},w,d} j_w = n_d j_w$$

  by (P3). Hence,

  $$j_w 1_J = j_w \sum_{d \in D} n_d j_d = \sum_{d \in D} n_d^2 j_w \overset{(P5)}{=} j_w.$$

  Similarly, we show $1_J j_w = j_w$.

□

While Lusztig showed these properties hold in general, for the cases we are interested in the ring J has additional structure. To make this precise, we introduce the following definition.

Definition 1.52 ([24, Section 3.1]). Let R be a unital ring which is free as a $\mathbb{Z}$-module. We call R a *based ring* if, for a fixed basis $B = \{b_i\}_{i\in I}$ of R, we have:

(A) $b_i b_j = \sum_{k\in I} c_{i,j}^k b_k$, where $c_{i,j}^k \in \mathbb{Z}_{\geq 0}$.
(B) The unit $1 \in R$ is a non-negative linear combination of basis elements. We denote by I_0 the set of indices i for which b_i occurs in the decomposition of 1. Let $\tau : R \to \mathbb{Z}$ be the group homomorphism sending b_i to 1 if $i \in I_0$ and to 0 otherwise.
(C) There exists an involution $i \mapsto i^*$ on I such that the induced map $R \to R$, $kb_i \mapsto kb_{i^*}$ is an anti-involution on R and $\tau(b_i b_j)$ equals 1 if $j = i^*$ and 0 otherwise. This means that in $b_i b_{i^*}$ exactly one basis element from the decomposition of the unit occurs exactly once.

If the basis is finite, i.e., R is of finite rank, we call it a *multifusion ring*. If furthermore $1 \in B$, we call it a *fusion ring*.

Remark 1.53. For finite W, we always have $\gamma_{x,y,z} \geq 0$. For crystallographic W, this was shown in [47, Lemma 5.2(d)] and [48, 1.1(e)]. For the non-crystallographic types H_3, H_4, and $I_2(m)$, this follows from explicit calculations (see [12]).

The result was generalized to all Coxeter groups by Elias and Williamson in [23, Corollary 1.2] and extended to show unimodularity in [18, Corollary 1.5]. The constructions in these two papers form the main basis for chapter 4.

The J-ring of a finite Coxeter group is a multifusion ring. To see this, note that it is a based ring with basis $\{j_w \mid w \in W\}$ satisfying: (1) the structure constants $\gamma_{x,y,z} \geq 0$ (shown above), (2) the unit element $\sum_{t\in D} j_t$ where D is the set of *Duflo involutions* in W is a non-negative linear combination of basis elements, and (3) the anti-involution $w \mapsto w^{-1}$ on the basis (which maps L-cells to R-cells by Lemma 1.33) satisfies the required properties. Since the basis is finite for finite Coxeter groups, the J-ring is multifusion. It is conjectured that the J-ring remains locally unital in general bounded Coxeter groups, meaning that the formal sum $\sum_{t\in D} j_t$ acts as an identity would. For details, see [45, Section 13.4, Conjecture 14.2 and Section 18.3].

For any subset $V \subseteq W$, we define

$$J_V \coloneqq \langle j_w \mid w \in V\rangle_{\mathbb{Z}} \tag{1.46}$$

to be the $\mathbb{Z}$-submodule of J generated by the elements of V.

Proposition 1.54. *Let $\{\mathbf{c}_i \mid 1 \leq i \leq n\}$ denote the two-sided cells of W. Then we have a decomposition*

$$J = \bigoplus_{i=1}^{n} J_{\mathbf{c}_i} \tag{1.47}$$

into two-sided ideals. Every $J_{\mathbf{c}_i}$ itself is an algebra with unit given by

$$1_i \coloneqq \sum_{d\in D\cap \mathbf{c}_i} j_d. \tag{1.48}$$

Proof. We follow [48, p. 3.1]. The idea is as follows: Let x be in some two-sided cell $\mathbf{c}$ and $y \in W$ arbitrary. Then by properties (P8), (P14), and (P7), for any $z \in W$ the coefficient $\gamma_{x,y,z}$ is non-zero if and only if $x \sim_{\mathrm{J}} y \sim_{\mathrm{J}} z$. Hence, j_z occurs as a summand of $j_x j_y$ only if

they all lie in the same cell $\mathbf{c}$. This shows that $J_{\mathbf{c}}$ is a right ideal of J. The arguments for the left ideal property and the unit element are analogous. □

Remark 1.55. In the language of Green, Proposition 1.54 implies that we find smaller algebras $J_{\mathbf{c}}$ associated to J-cells inside the Coxeter group. The elements j_d for $d \in D$ act similarly to idempotents in the monoid case. Note that for an H-cell $\mathbf{h} \subset \mathbf{c}$, we can also restrict to $J_{\mathbf{h}}$. This is our candidate for H-reduction. Even when the full asymptotic algebra J is not globally defined, one can still define the algebra $J_{\mathbf{c}}$ for individual cells $\mathbf{c}$ using the same construction.

1.4. Overview of Cells and Asymptotic Hecke Algebras

For finite Coxeter groups, most of the cell structure and also the structure of the asymptotic algebra is known. For non-crystallographic groups and exceptional types, explicit calculations have been performed by Ducloux [12] and Geck [28]. For dihedral groups, this is a straightforward calculation which we will show here. For the infinite groups like A_n, there are general results.

Remark 1.56. The author used a variety of computer algebra programs to perform computations in the Hecke algebra and asymptotic Hecke algebra. The computational methods and implementations used here are based on the work in [28, 12], with additional code available in [32]. We fix H-cells here for further use.

Example 1.57. To give an overview of the different Coxeter groups and their properties, we present the following data:

Group	Order	Length of longest element	Number of KL cells
A_n	$(n+1)!$	$\frac{n(n+1)}{2}$	†
B_n	$2^n n!$	n^2	†
D_n	$2^{n-1} n!$	$n(n-1)$	†
E_6	511,840	36	17
E_7	2,903,040	63	35
E_8	696,729,600	120	45
F_4	1,152	24	11
G_2	12	6	3
H_3	120	15	7
H_4	14,400	60	13
$I_2(n)$	$2n$	n	3

Table 1.3. Properties of Coxeter Groups.

† : Note that for the infinite series A_n, B_n, and D_n, the number of Kazhdan–Lusztig cells depends on n and follows a more complex pattern.

1.4.1. Example: Dihedral Groups. In this subsection we will consider $W := I_2(m)$ for $m \in \mathbb{N} \cup \{\infty\}$, generated by $S = \{s, t\}$. The case $m = 3$ was analyzed in subsection 1.3.2. Using concise notation, we can show that the cell structure is similar for all cases.

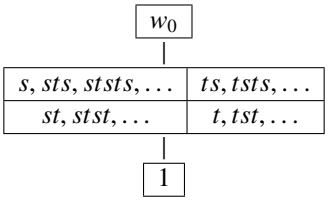

TABLE 1.4. Cells in dihedral groups.

To work more efficiently with the group W, we use the following notation (see [45, Corollary 1.4]). For any natural number k we set

$$1_k := \underbrace{st\ldots}_{k \text{ factors}}, \quad 2_k := \underbrace{ts\ldots}_{k \text{ factors}} \in W. \tag{1.49}$$

Note that $1_0 = 1_W = 2_0$ and $1_m = w_0 = 2_m$, where w_0 is the longest word in W for $m < \infty$. Further, we have $1_{m+n} = 2_{m-n}$ for $0 \leq n \leq m$. This leads to the following rules:

$$s1_k = 2_{k-1}, \quad t1_k = 2_{k+1}, \quad 1_{2k}s = 1_{2k+1}, \quad 1_{2k+1}s = 1_{2k}. \tag{1.50}$$

By (1.29) we obtain:

$$b_t b_{1_k} = b_{2_{k+1}} + b_{2_{k-1}}, \quad b_s b_{2_k} = b_{1_{k+1}} + b_{1_{k-1}}, \tag{1.51}$$

for $2 \leq k \leq m-1$, hence we have:

$$2_{k-1} \leftarrow 1_k \rightarrow 2_{k+1}, \quad 1_{k-1} \leftarrow 2_k \rightarrow 1_{k+1} \tag{1.52}$$

for the relation $\leftarrow_L$. Further, we compute:

$$b_{1_1} b_{2_1} = b_{1_2}, \quad b_{2_1} b_{1_1} = b_{2_2} \text{ and } b_{1_0} b_{1_m} = [v] b_{1_m} = b_{1_m} b_{1_0}. \tag{1.53}$$

This yields for the relation $\leftarrow_L$:

$$1_0 \rightarrow 2_1 \rightleftarrows 1_2 \rightleftarrows 2_3 \rightleftarrows \ldots, \tag{1.54}$$

and

$$1_0 = 2_0 \rightarrow 1_1 \rightleftarrows 2_2 \rightleftarrows 1_3 \rightleftarrows \ldots. \tag{1.55}$$

For $m < \infty$, we also have:

$$\ldots \rightleftarrows 1_{m-3} \rightleftarrows 2_{m-2} \rightleftarrows 1_{m-1} \rightarrow 2_m = 1_m \tag{1.56}$$

and

$$\ldots \rightleftarrows 2_{m-3} \rightleftarrows 1_{m-2} \rightleftarrows 2_{m-1} \rightarrow 1_m = 2_m. \tag{1.57}$$

For $m \geq 3$, this again gives three J-cells: the top and bottom cells have one element each, while the middle cell splits into two left and right cells. The eggbox diagram is:

The multiplication table of the J-ring can be found in [12, Section 4]. The coefficients $\gamma_{x,y,z}$ are either 0 or 1. The multiplication in the J-ring is given by:

$$j_{1_k} j_{i_l} = \begin{cases} 0 & \text{if } i \text{ even and } i = 1 \text{ or } k \text{ odd and } i = 2, \\ \sum_{u=\max\{0,k+l-m\}}^{\min\{k,l\}-1} j_{1_{k+l-1-2u}} & \text{otherwise.} \end{cases} \tag{1.58}$$

We can read off directly that the neutral element is $j_s + j_t$. For type $I_2(5)$, this gives:

$\cdot$	j_s	j_{st}	j_{sts}	j_{ststs}
j_s	j_s	j_{st}	j_{sts}	j_{ststs}
j_{ts}	j_{ts}	$j_t + j_{tst}$	$j_{ts} + j_{tsts}$	j_{tst}
j_{sts}	j_{sts}	$j_{st} + j_{ststs}$	$j_s + j_{sts}$	j_{st}
j_{tsts}	j_{tsts}	j_{tst}	j_{ts}	j_t

(1.59)

Remark 1.58 (Verlinde Fusion Rings). The structure of the multiplication is similar to the Clebsch–Gordan rule for the monoidal products of $U(\mathfrak{sl}_2)$ representations. We see this explicitly for an H-cell.

For the diagonal H-cells $\mathbf{h}_s := c_s^L \cap c_s^R = \{s, sts, ststs, \ldots\}$, we get for odd $1 \leq i, j \leq n$ and $i + j \leq m - 1$:

$$j_{s_i} j_{s_j} = j_{s_{|i-j|+1}} + j_{s_{|i-j|+3}} + \ldots + j_{s_{i+j-1}}, \tag{1.60}$$

where terms are truncated whenever $i + j \geq n$. We will explore categorifications of such rings later in subsection 5.1.1.

1.4.2. Type A. In type A_n, the Kazhdan–Lusztig cells have a natural correspondence to partitions via the Robinson–Schensted correspondence. The partial order on two-sided cells matches the dominance order on partitions. For type A_3, we get:

Label of J-cell **c**	$\lvert\mathbf{c}\rvert$	**a**-value	$\lvert h\rvert$ for diagonal H-cell	Representative of H-cell
0	1	0	1	$\{1\}$
1	9	1	1	$\{r\}$
2	4	2	1	$\{rt\}$
3	9	3	1	$\{rsrts\}$
4	1	6	1	$\{rsrtsr\}$

(1.61)

The relationship between the partition ordering and the cell structure is illustrated in Figure 1.3b.

1.4.3. Type H_3. We have the following data for the Kazhdan–Lusztig cells.

label	$\lvert c\rvert$	**a**-value	$\lvert h\rvert$	representative
0	1	0	1	
1	18	1	2	$\{a, aba\}$
2	25	2	1	
3	32	3	2	$\{bcb, bcbabc\}$
4	25	5	1	
5	18	6	2	$\{ababacbaba, ababacbabacbab\}$
6	1	15	1	

(1.62)

The H-cells $\mathbf{h}_1, \mathbf{h}_5$ follow the same multiplication rules as in type $I_2(5)$. I.e., we have $j_{aba}^2 = j_a + j_{aba}$. We call those *Fibonacci cells*. In $\mathbf{h}_3$ the J-ring multiplication is $j_{bcbabc}^2 = j_{bcb}$, we call this the $(\mathbb{Z}/2\mathbb{Z})$-ring. For **a**-value 6 the Duflo involution is the element of length 14. All 7 cells can be found in Figure 1.4.

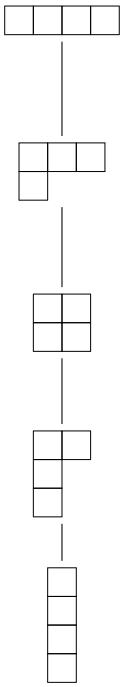

(A) Dominance order on partitions of 4.

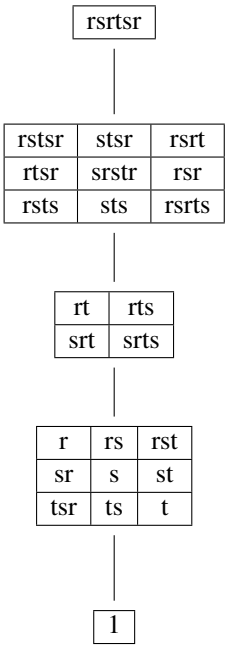

(B) Eggbox diagram for Kazhdan–Lusztig cells.

FIGURE 1.3. Comparison of partition order and Kazhdan–Lusztig cell structure in type A_3.

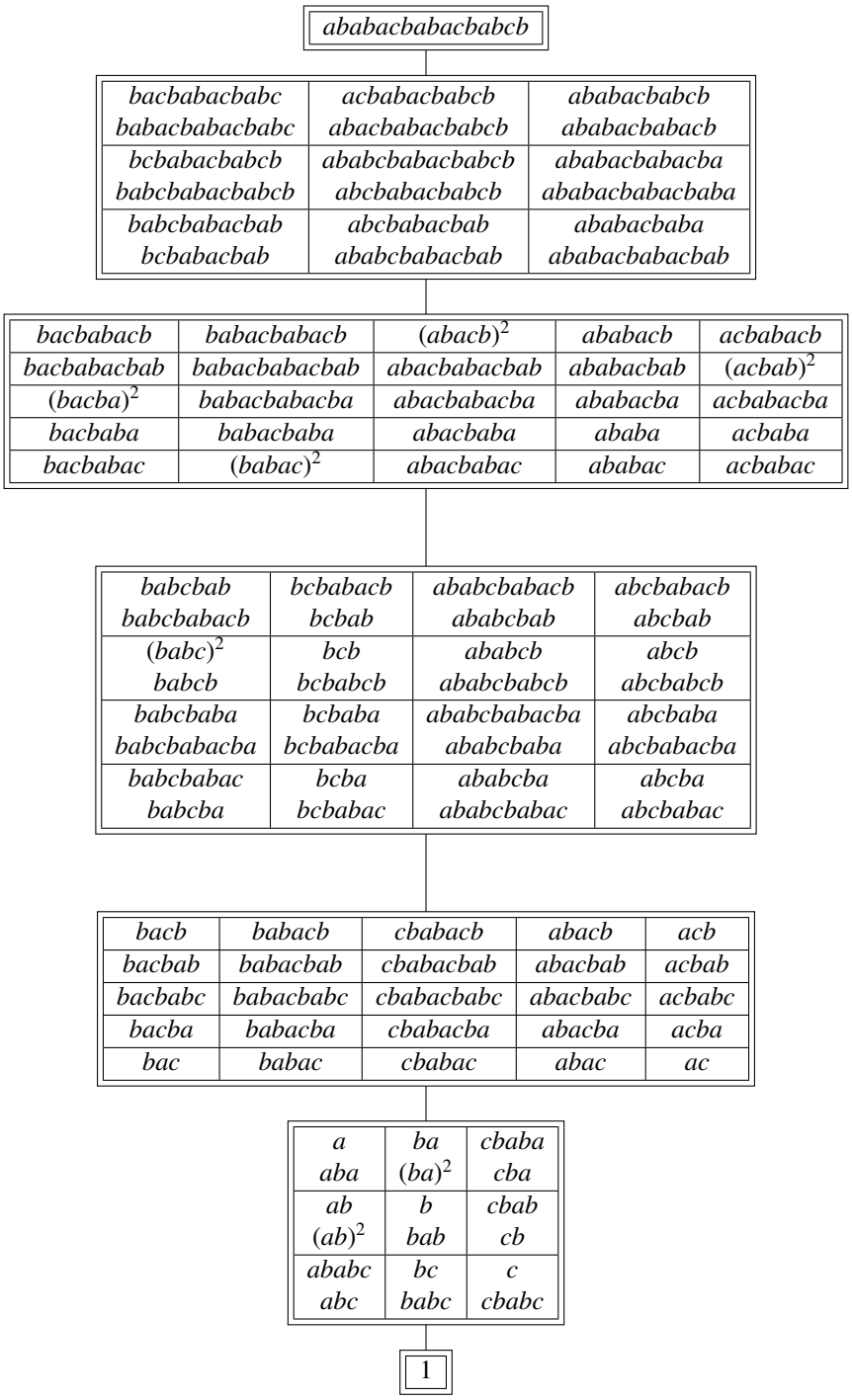

FIGURE 1.4. Eggbox diagram for Kazhdan–Lusztig cells in type H_3.

1.4.4. Type H_4. The cell structure has many similarities to H_3. In many small cases one can choose the same representative. However there is a significant difference: the middle cell is much larger and gives rise to new fusion rings.

label	$\lvert c\rvert$	**a**-value	$\lvert h\rvert$	representative
0	1	0	1	
1	32	1	2	(a)
2	162	2	2	{ca,cabadc}
3	512	3	2	(a)
4	625	4	1	
5	1296	5	1	
6	9144	6	14,18,24	(c)
7	1296	15	1	
8	625	16	1	
9	512	18	2	(b)
10	162	22	2	(b)
11	32	31	2	(b)
12	1	60	1	

(1.63)

In the cases (a) we can choose the same representative as in type H_3, for (b) we multiply both elements by w_0 and for (c) it is way more complicated. The asymptotic Hecke algebra has been described by Alvis in [1] based on calculations by [12]. In this thesis, we will analyze the lower cells in H_4 and use the notation from [21]. In $\mathbf{h}_2$, i.e., the representative of **a**-value 2, we also have Fibonacci rules.

1.4.5. Finite Cells of Small a-value in Infinite Coxeter Groups. So far we have only considered finite Coxeter groups, where all two-sided cells are necessarily finite. The situation becomes more interesting when investigating finite two-sided cells within infinite Coxeter groups.

While there are conjectured results on the structure of cells in infinite Coxeter groups (see [5, 6]), to the author's knowledge there are no classification results for finite two-sided or H-cells.

In this subsection, we focus on finite cells with **a**-value less than or equal to 2, as these are completely understood. The simplest case is the cell of **a**-value 0, which is always finite as it contains only the unit element. For this case, the asymptotic Hecke algebra is the trivial algebra.

1.4.5.1. *The Case of* **a**(1)*-Finite Coxeter Groups.* Let W denote a Coxeter group with generating set S. For any integer i, we write $W_i := \{x \in W \mid \mathbf{a}(x) = i\}$ for the subset of elements with **a**-value i. We say that W is $\mathbf{a}(i)$*-finite* if W_i is finite. A characterization of **a**(1)-finite Coxeter groups was given by Hart in [37]. The set W_1 has been described in Remark 1.35. It contains the elements having a unique reduced expression.

Lemma 1.59 ([37, Theorem 2.1]). *Let W be an irreducible Coxeter group with generating set S. The set W_1 of elements of* **a***-value* 1 *is finite if and only if all of the following conditions hold:*

(A) *The set S is finite.*
(B) *The Dynkin diagram of W is a tree.*
(C) *There is no relation $m_{s,t} = \infty$ and at most one relation $m_{s,t} > 3$ for $s, t \in S$.*

Proof. The idea of the proof is the following: In a reduced expression $(s_1, s_2, \ldots, s_n) \in W$, there cannot be an i such that s_i and s_{i+1} commute; hence we must have $m_{s_i,s_{i+1}} > 2$ for all i. This implies that any word of a reduced expression corresponds to a path in the Dynkin diagram of W. The question is therefore to determine when a path represents a reduced expression and when there are only finitely many such expressions.

A path represents a reduced expression if and only if there is no subsequence $(s, t, \ldots)$ of length $m_{s,t}$. Hence, if S is infinite, we can construct infinitely many reduced expressions. Similarly, this occurs if there is a cycle in the Dynkin diagram or if we have $m_{s,t} = \infty$ for some s, t.

Now assume that there are two pairs (s, t) and (u, v) with $m_{s,t}, m_{u,v} > 3$, and let p be a path connecting both pairs. Without loss of generality, we have $p = (t = r_0, r_1, \ldots, r_n = u)$. Let p^{-1} denote the reverse path. Then the composition (p, v, p^{-1}, s) represents a reduced expression, and any power of it does too; hence W_1 is infinite.

If all our assumptions are satisfied, we show that there is a finite number of paths giving a reduced expression. Let $m_{s,t}$ be the largest relation occurring. Any reduced expression of a path starting at some $r \in S$ of length more than $|S|$ includes one element $u \in S$ at least twice. As the Dynkin diagram contains no cycles, we therefore can find a subsequence of the form $(\ldots, u, v, u, \ldots)$. This implies that (u, v) is the edge (s, t) with $m_{s,t} > 3$. Any path corresponding to a reduced expression can now repeat u, v at most $m_{s,t} - 1$ times. Once the path leaves this edge, it cannot return; hence the length of a reduced expression is bounded, and therefore the size of W_1 is bounded as well. □

We can extend the classification of $\mathbf{a}(1)$-finite Coxeter groups to non-irreducible cases as well.

Lemma 1.60. *Let W be a Coxeter group with generating set M and let $K, L \subset M$ be subsets of M such that $m_{k,l} = 2$ for all $k \in K, l \in L$. Let U and V denote the Coxeter groups generated by K and L respectively. Then $U \times V \subset W$ is a subgroup of W. For two-sided cells $\mathbf{c}_1 \subset U$ and $\mathbf{c}_2 \subset V$ of $\mathbf{a}$-value i and j respectively, the Cartesian product $\mathbf{c} \coloneqq \mathbf{c}_1 \times \mathbf{c}_2 \subset W$ is a two-sided cell of $\mathbf{a}$-value $i + j$ in W. Moreover, the asymptotic Hecke algebra $J_{\mathbf{c}}$ is isomorphic to the tensor product $J_{\mathbf{c}_1} \otimes J_{\mathbf{c}_2}$.*

Proof. This follows from the observation that for $x \in \mathbf{c}_1$ and $y \in \mathbf{c}_2$, the Kazhdan–Lusztig basis elements commute, i.e., we have $b_x b_y = b_y b_x$ and therefore $b_{(x,y)} = b_x b_y$. The cell and $\mathbf{a}$-value computations then work independently in both factors. □

Corollary 1.61. *The conclusion of Lemma 1.59 still holds when W is not assumed to be irreducible. The conditions (2) and (3) then need to hold for each connected component of the Dynkin diagram.*

Proof. By Lemma 1.60, the $\mathbf{a}$-value of a cell $\mathbf{c} \times \mathbf{d}$, where $\mathbf{c}$ and $\mathbf{d}$ lie in different Coxeter groups, is the sum of their $\mathbf{a}$-values. Let $S = \coprod S_i$ be a disjoint union where each S_i represents a connected component of the Dynkin diagram. Then any cell $\mathbf{c} \subset W(S)$ of $\mathbf{a}$-value 1 has the form $\{1\} \times \{1\} \times \ldots \times \mathbf{c}_i \times \ldots \times \{1\}$, where $\mathbf{c}_i$ is a cell of $\mathbf{a}$-value 1 lying in $W(S_i)$. The result follows by applying Lemma 1.59. □

Corollary 1.62. *Let W be an $\mathbf{a}(1)$-finite irreducible Coxeter group and let $\mathbf{c} \subset W$ be a two-sided cell. Let m be the largest relation occurring in the Dynkin diagram. For any pair of reflections (r, s) in W, there exists a unique* H*-cell $h_{r,s}$ containing all elements whose reduced expressions start with r and end with s. The cardinality of $h_{r,s}$ is $\lfloor \frac{m}{2} \rfloor$ if the shortest path connecting r and s contains the edge labeled by m, and $\lfloor \frac{m-1}{2} \rfloor$ otherwise.*

Proof. This follows from the proof of Lemma 1.59 by counting the number of paths corresponding to reduced expressions. We use the characterization of left and right cells inside W_1 by initial and terminal letters as shown in Remark 1.35. An explicit enumeration of W_1 can also be found in [37, Theorem 2.5]. □

Example 1.63. We can now extend the dihedral example of Figure 1.2 to any finite cell of **a**-value 1 in an irreducible Coxeter group.

Consider a Dynkin diagram satisfying the conditions of Lemma 1.59:

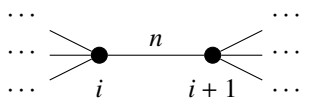

(1.64)

Assume there are i edges to the left and j edges to the right. The eggbox diagram of the cell of **a**-value 1 is then

$\lfloor \frac{n+1}{2} \rfloor_{i,i}$	$\lfloor \frac{n-1}{2} \rfloor_{i,j}$
$\lfloor \frac{n-1}{2} \rfloor_{j,i}$	$\lfloor \frac{n+1}{2} \rfloor_{j,j}$

(1.65)

Here, the index (i, i) indicates that we have i rows and i columns with the corresponding labeling. The elements in each H-cell are characterized by their initial and terminal elements.

One such Coxeter group appears in [6, Figure 1]. The Coxeter group is a hyperbolic triangle group,of type W_{237} with generators $\langle r, s, t \mid r^2 = s^2 = t^2 = (rs)^3 = (st)^7 = (rt)^2 = 1\rangle$. Following Corollary 1.62, we can enumerate all elements of **a**-value 1 by finding paths corresponding to reduced expressions. We organize these elements by their initial and terminal letters, partitioning them into left and right cells:

$\{r, rstsr, rststsr\}$	$\{sr, stsr, ststsr\}$	$\{tsr, tstsr, tststsr\}$
$\{rs, rsts, rstsrs\}$	$\{s, sts, stsrs\}$	$\{ts, tsts, tstsrs\}$
$\{rst, rstst, rststst\}$	$\{st, stst, ststst\}$	$\{t, tst, tstst\}$

On the diagonal H-cells coming from the dihedral subgroup of type $I_2(7)$, the multiplication in the asymptotic Hecke algebra can be read off directly. For example, we have $j_{sts}^2 = j_s + j_{sts} + j_{stsrs}$. Similarly, one can work out the complete multifusion ring structure and obtain, for instance, $j_{sr} j_{rststsr} = j_{ststsr}$.

1.4.5.2. *The case of* **a**(2)*-finite Coxeter groups.* Recent results by Green and Xu have classified all irreducible Coxeter groups which are **a**(2)-finite. Coxeter groups whose Dynkin diagram contains a cycle have either none or infinitely many elements of **a**-value 2. For all other cases, they have further described one H-cell lying in W_2. We refer to the Dynkin diagrams of (1.11) through (1.14).

Proposition 1.64 ([35, Theorem 3.31 and Proposition 4.15] and [34, Proposition 4.1]). *An irreducible Coxeter group W with elements of* **a***-value* 2 *is* **a**(2)*-finite if and only if it is of one of the following types:*

$$A_n,\ B_n,\ \tilde{C}_n,\ E_{q,r},\ F_n,\ H_n,\ I_n. \tag{1.66}$$

In the case $E_{q,r}$ where $r = q = 1$ (i.e., D_4), the set W_2 consists of three two-sided cells; if $r > q = 1$ (i.e., type D_{r+3}), we have two cells in $E_{q,r}$. In all other cases, W_2 itself is a two-sided cell.

One representative of an H*-cell is given by the following:*

- *Type* A_n*:* $\mathbf{h} = \{13\}$.
- *Type* B_3*:* $\mathbf{h} = \{13\}$.
- *Type* B_n *(*$n > 3$*):* $\mathbf{h} = \{24, 2124\}$.
- *Type* $\tilde{C}_{n-1}$ *(*$n \geq 5$*):* $\mathbf{h} = \{24, 2124, 2z, 212z\}$*, where* $z = 45\ldots(n-1)n(n-1)\ldots54$.
- *Type* $E_{q,r}$ *(*$r \geq q \geq 2$*):* $\mathbf{h} = \{1v\}$.
- *Type* F_4*:* $\mathbf{h} = \{24\}$.
- *Type* F_n *(*$n > 4$*):* $\mathbf{h} = \{24, 243524\}$.
- *Type* H_3*:* $\mathbf{h} = \{13\}$.
- *Type* H_n *(*$n > 3$*):* $\mathbf{h} = \{24, 2124\}$.

If we have 2 entries we are in the Fibonacci case for H_n and in the $\mathbb{Z}/2\mathbb{Z}$ case for F_n and B_n. Note, that in $\tilde{C}_{n-1}$ the cell can be written as a product of two $\mathbf{a} = 1$-cells in smaller type: $\{2, 212\}$ and $\{4, z\}$, since there are no relations between the respective generators. Both of these H-cells are also $\mathbb{Z}/2\mathbb{Z}$-cases, hence in total the asymptotic algebra is isomorphic to the group ring of $(\mathbb{Z}/2\mathbb{Z})^2$.

In the next chapter we introduce all categorical concepts. This will also allow us to construct idempotents to all these chosen H-cells in chapter 3.

CHAPTER 2

Categorical Structures and Soergel Diagrammatics

In this chapter, we develop the categorical framework necessary for our subsequent study of idempotents in the diagrammatic Hecke category and the construction of the asymptotic Hecke category.

We begin with fundamental categorical structures in section 2.1, establishing the language of abelian and monoidal categories that forms the foundation for later work. In section 2.2 we then introduce fusion categories, which arise naturally in representation theory and provide the setting for many of our key examples. Finally, section 2.3 presents the Temperley–Lieb category, which will serve as a crucial bridge to understanding Soergel bimodules for dihedral groups in section 2.4.

2.1. Category Theory Basics and Monoidal Structures

We introduce the basic categorical notions of monoidal categories and the center. Here we mostly keep to the notation of [24].

We denote categories by calligraphical letters such as $\mathcal{C}$. We write $X \in \mathcal{C}$ instead of $X \in \mathrm{Obj}(\mathcal{C})$ for objects. Our focus will be on *essentially small* categories, i.e., categories where for any objects $X, Y \in \mathcal{C}$, the class $\mathrm{Hom}_{\mathcal{C}}(X, Y)$ is a set (called a Hom-set), and where the isomorphism classes of objects form a set.

2.1.1. Abelian Categories. We begin by introducing two fundamental categorical structures:

Definition 2.1. An *additive category* is a category $\mathcal{C}$ satisfying:

- (A1) Each Hom-set carries the structure of an abelian group with bilinear composition.
- (A2) There exists a *zero object* $0 \in \mathcal{C}$ with unique morphisms to and from every object.
- (A3) Binary direct sums exist: for any objects $X_1, X_2 \in \mathcal{C}$, there exists an object $X_1 \oplus X_2$ with morphisms $i_k : X_k \to X_1 \oplus X_2$ and $p_k : X_1 \oplus X_2 \to X_k$ satisfying $p_k \circ i_{k'} = \delta_{k,k'} id_{X_k}$, and $i_1 \circ p_1 + i_2 \circ p_2 = \mathrm{id}_{X_1 \oplus X_2}$.

The direct sum property is illustrated by the following diagram:

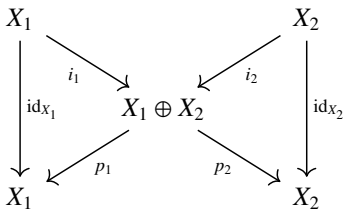

(2.1)

In most applications, the Hom-spaces carry the structure of a $\Bbbk$-vector space, in which case we call the category $\Bbbk$-linear. For a morphism $f : X \to Y$, a *kernel* is a pair (K, k) with

$k : K \to X$ such that $f \circ k = 0$ and which is universal with this property. Dually, a *cokernel* is a pair (C, c) with $c : Y \to C$ such that $c \circ f = 0$ and which is universal with this property.

Definition 2.2. An *abelian category* is an additive category where every morphism $\phi : X \to Y$ fits into an exact sequence

$$K \xrightarrow{k} X \xrightarrow{i} I \xrightarrow{j} Y \xrightarrow{c} C \tag{2.2}$$

where $(K, k) = \mathrm{Ker}(\phi)$, $(C, c) = \mathrm{Coker}(\phi)$, $(I, i) = \mathrm{Coker}(k)$, $(I, j) = \mathrm{Ker}(c)$, and $ji = \phi$. Here, $I = \mathrm{Im}(\phi)$ is called the image.

A $\Bbbk$-linear abelian category is called *finite semisimple* if it has finitely many isomorphism classes of simple objects and every object is isomorphic to a finite direct sum of simple objects. In this work, we primarily consider such categories. For any field $\Bbbk$, the category of finite-dimensional vector spaces $\mathbf{Vec} \coloneqq \mathbf{Vec}_{\Bbbk}$ provides a fundamental example of such a category.

2.1.2. Monoidal Categories. We now focus on monoidal categories. This is a structure that formalized the notion of 'tensor products'.

Definition 2.3. A *monoidal category* is a quintuple $(C, \otimes, \alpha, 1, \iota)$ where:

- C is a category,
- $\otimes : C \times C \to C$ is a bifunctor,
- α is a natural isomorphism $(- \otimes -) \otimes - \xrightarrow{\sim} - \otimes (- \otimes -)$ with components $\alpha_{X,Y,Z} : (X \otimes Y) \otimes Z \xrightarrow{\sim} X \otimes (Y \otimes Z)$ for objects $X, Y, Z \in C$, called the *associativity constraints*,
- $1 \in C$ is a *unit object* with natural isomorphisms $\lambda_X : 1 \otimes X \xrightarrow{\sim} X$ and $\rho_X : X \otimes 1 \xrightarrow{\sim} X$,

subject to the following axioms:

(A) *(Pentagon axiom)* The diagram

$$\begin{array}{ccc}
 & ((W \otimes X) \otimes Y) \otimes Z & \\
{\scriptstyle \alpha_{W,X,Y} \otimes \mathrm{id}_Z} \swarrow & & \searrow {\scriptstyle \alpha_{W \otimes X,Y,Z}} \\
(W \otimes (X \otimes Y)) \otimes Z & & (W \otimes X) \otimes (Y \otimes Z) \\
{\scriptstyle \alpha_{W,X \otimes Y,Z}} \downarrow & & \downarrow {\scriptstyle \alpha_{W,X,Y \otimes Z}} \\
W \otimes ((X \otimes Y) \otimes Z) & \xrightarrow{\mathrm{id}_W \otimes \alpha_{X,Y,Z}} & W \otimes (X \otimes (Y \otimes Z))
\end{array} \tag{2.3}$$

commutes for all objects $W, X, Y, Z \in C$.

(B) *(Triangle axiom)* For all objects $X, Y \in C$, the diagram

$$\begin{array}{ccc}
(X \otimes 1) \otimes Y & \xrightarrow{\alpha_{X,1,Y}} & X \otimes (1 \otimes Y) \\
 & {\scriptstyle \rho_X \otimes \mathrm{id}_Y} \searrow \quad \swarrow {\scriptstyle \mathrm{id}_X \otimes \lambda_Y} & \\
 & X \otimes Y &
\end{array} \tag{2.4}$$

commutes.

For the remainder of this work, we will frequently encounter two fundamental examples of monoidal categories: the graded vector spaces $\mathbf{Vec}_{\mathbb{Z}/2\mathbb{Z}}$ (with both trivial and non-trivial associators) and the Fibonacci category $\mathcal{F}$. These examples will serve as running examples throughout our discussion. Their Grothendieck rings we call the Fibonacci ring and the $(\mathbb{Z}/2\mathbb{Z})$-graded ring.

Example 2.4. Let G be a group. With $\mathbf{Vec}_G$ we denote the category of finite dimensional G-graded vector spaces, see [24, Example 2.3.6].

An object $V \in \mathbf{Vec}_G$ is a collection of vector spaces $V = (V_g)_{g\in G}$ indexed by elements of G, where V_g is the component 'lying above' g. The simple objects are denoted δ_g for $g \in G$, where δ_g is the one-dimensional vector space concentrated at g (i.e., $(\delta_g)_h = \Bbbk$ if $\mathbf{h} = g$ and 0 otherwise).

The tensor product is defined component-wise by

$$(V \otimes W)_g \coloneqq \bigoplus_{hk=g} V_h \otimes W_k \tag{2.5}$$

for objects $V, W \in \mathbf{Vec}_G$. On simple objects, this gives $\delta_g \otimes \delta_h = \delta_{gh}$. For any normalized 3-cocycle $\omega \in Z^3(G, \Bbbk^*)$, we can define a monoidal structure on $\mathbf{Vec}_G$, denoted $\mathbf{Vec}_G^\omega$, where the associator on simple objects is given by

$$\alpha_{g,h,k} : (\delta_g \otimes \delta_h) \otimes \delta_k \xrightarrow{\omega(g,h,k)} \delta_g \otimes (\delta_h \otimes \delta_k). \tag{2.6}$$

On $G = \mathbb{Z}/2\mathbb{Z}$ this gives two non-equivalent monoidal structures:

(A) The *non-twisted* version $\mathbf{Vec}_G$: Here we use the trivial 3-cocycle $\omega(g, h, k) = 1$ for all $g, h, k \in G$. The simple objects are δ_0 and δ_1, with tensor product $\delta_i \otimes \delta_j = \delta_{i+j}$ (addition modulo 2) and trivial associator $\alpha_{g,h,k} = \mathrm{id}$ for all $g, h, k \in G$.

(B) The *twisted* version $\mathbf{Vec}_G^\upsilon$: Here we use the non-trivial 3-cocycle υ defined by

$$\upsilon(g, h, k) = \begin{cases} -1 & \text{if } g = h = k = 1, \\ 1 & \text{otherwise.} \end{cases}$$

This gives an associator

$$\alpha_{g,h,k} = \begin{cases} -\mathrm{id} & \text{if } g = h = k = 1, \\ \mathrm{id} & \text{otherwise.} \end{cases}$$

These two categories, $\mathbf{Vec}_G$ and $\mathbf{Vec}_G^\upsilon$, are not monoidally equivalent. The twisted version represents the non-trivial element in the cohomology group $H^3(\mathbb{Z}/2\mathbb{Z}, \Bbbk^*) \cong \mathbb{Z}/2\mathbb{Z}$.

Example 2.5. The Fibonacci category $\mathcal{F}$ is a fusion category with two simple objects: $\mathbf{1}$ (the unit object) and $\mathbf{X}$. The tensor product rules are given by:

$$\mathbf{1} \otimes \mathbf{1} = \mathbf{1},\ \mathbf{1} \otimes \mathbf{X} = \mathbf{X} \otimes \mathbf{1} = \mathbf{X},\ \mathbf{X} \otimes \mathbf{X} = \mathbf{1} \oplus \mathbf{X} \tag{2.7}$$

Only for $X = Y = Z = \mathbf{X}$ is the associator $\alpha_{X,Y,Z} : (X \otimes Y) \otimes Z \to X \otimes (Y \otimes Z)$ non-trivial. In this case, we have:

$$\alpha_{\mathbf{X},\mathbf{X},\mathbf{X}} : (\mathbf{X} \otimes \mathbf{X}) \otimes \mathbf{X} \to \mathbf{X} \otimes (\mathbf{X} \otimes \mathbf{X}). \tag{2.8}$$

Both sides of this isomorphism decompose as:

$$(\mathbf{X} \otimes \mathbf{X}) \otimes \mathbf{X} = (\mathbf{1} \oplus \mathbf{X}) \otimes \mathbf{X} = \mathbf{X} \oplus (\mathbf{X} \otimes \mathbf{X}) = \mathbf{X} \oplus (\mathbf{1} \oplus \mathbf{X}) = \mathbf{1} \oplus \mathbf{X} \oplus \mathbf{X}. \tag{2.9}$$

With respect to this decomposition, the associator $\alpha_{\mathbf{X},\mathbf{X},\mathbf{X}}$ is represented by block matrices:

$$\alpha_{\mathbf{X},\mathbf{X},\mathbf{X}} = \begin{pmatrix}1\end{pmatrix} \oplus \begin{pmatrix}\phi^{-1} & -\phi^2 \\ 1 & -\phi^{-1}\end{pmatrix}. \tag{2.10}$$

where ϕ is satisfying $\phi^2 = \phi + 1$. Both possibilities on ϕ create non-equivalent monoidal categories. For $\phi = \frac{1+\sqrt{5}}{2}$ the golden ratio we write $\mathcal{F}$, the other case is denoted by $\mathcal{F}'$.

Remark 2.6. By Ostrik's classification of fusion categories of rank 2 [57], the Fibonacci categories $\mathcal{F}$ and $\mathcal{F}'$ together with the category of graded vector spaces $\mathbf{Vec}_{\mathbb{Z}/2\mathbb{Z}}$ (from Example 2.4) constitute the complete list of non-trivial fusion categories with exactly two isomorphism classes of simple objects.

Both $\mathbf{Vec}_{\mathbb{Z}/2\mathbb{Z}}$ and $\mathcal{F}$ are a special case of so-called type A_k fusion categories. We will explore them further in subsection 5.1.1, where we will see that they provide the categorification we seek for all cells in H_3 and the lower cells in H_4.

2.1.3. Center. The construction of the categorical center is due to Drinfeld. Let C denote a monoidal category. The center captures those objects in C, that commute via the monoidal action.

Definition 2.7. A *braiding* γ on an object Z in the category C is a family of natural isomorphisms

$$\{\gamma_X \in \mathrm{Hom}_C(X \otimes Z, Z \otimes X) \mid X \in C\}, \tag{2.11}$$

such that we have the following properties:

- (Braid relation) For any objects $X, Y \in C$ the diagram

$$\begin{array}{ccccc} & & X\otimes(Z\otimes Y) & \xrightarrow{\alpha^{-1}_{X,Z,Y}} & (X\otimes Z)\otimes Y & & \\ & \nearrow^{\mathrm{id}_X\otimes\gamma_Y} & & & & \searrow^{\gamma_X\otimes\mathrm{id}_Y} & \\ X\otimes(Y\otimes Z) & & & & & & (Z\otimes X)\otimes Y \\ & \searrow_{\alpha^{-1}_{X,Y,Z}} & & & & \nearrow_{\alpha^{-1}_{Z,X,Y}} & \\ & & (X\otimes Y)\otimes Z & \xrightarrow{\gamma_{X\otimes Y}} & Z\otimes(X\otimes Y) & & \end{array} \tag{2.12}$$

  commutes.
- (Unit property)

$$\gamma_1 = r_Z^{-1} \circ l_Z. \tag{2.13}$$

We then define the *center* $\mathcal{Z}(C)$ *of the category* C to be the category with objects (Z, γ) for $Z \in C$ and γ a braiding on Z. A morphism from (Z, γ) to (Z', δ) is a morphism $f \in \mathrm{Hom}_C(Z, Z')$ satisfying

$$(f \otimes \mathrm{id}_X) \circ \gamma_X = \delta_X \circ (\mathrm{id}_X \otimes f) \tag{2.14}$$

for all objects $X \in C$ which can equivalently be expressed by the following commutative diagram:

$$\begin{array}{ccc} X \otimes Z & \xrightarrow{\mathrm{id}_X \otimes f} & X \otimes Z' \\ {\scriptstyle \gamma_X}\downarrow & & \downarrow{\scriptstyle \delta_X} \\ Z \otimes X & \xrightarrow{f \otimes \mathrm{id}_X} & Z' \otimes X \end{array} . \tag{2.15}$$

The category $\mathcal{Z}(C)$ inherits a lot of structure from C. By [25, Theorem 2.15], the center of a fusion category is fusion. This term will be introduced in section 2.2.

Example 2.8. For the category of G-graded vector spaces $\mathbf{Vec}_G$ one can describe the objects in $\mathcal{Z}(\mathbf{Vec}_G)$ as tuples (C, V), where C is a conjugacy class of G and V is a simple representation of an elements of the conjugacy class, see [24, Example 8.5.4].

2.1.4. String Diagrams. String diagrams provide a graphical approach to calculations in monoidal categories. Following [59], we can interpret a monoidal category C as a 2-category with one object, where 1-morphisms correspond to objects of C (composed via tensor product), and 2-morphisms correspond to the original morphisms of C.

In this notation, diagrams are read from bottom to top, and the basic elements are:

- A morphism $f : X \to Y$ is represented as a box with input and output strings:

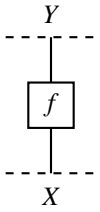

- Composition $(g \circ f) : X \to Z$ for $f : X \to Y$ and $g : Y \to Z$ is done with vertical stacking:

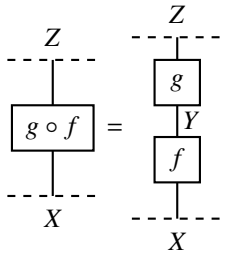

- Tensor product $(f \otimes g) : X_1 \otimes X_2 \to Y_1 \otimes Y_2$ works by horizontal composition:

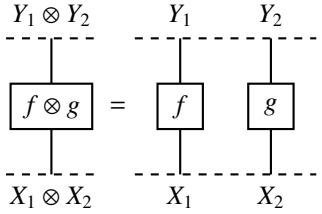

- The identity morphism $\mathrm{id}_X : X \to X$ is represented by a vertical string:

A key feature of string diagrams is their invariance under planar isotopy: two diagrams represent the same morphism if one can be continuously deformed into the other without breaking or crossing strings, see [59, Theorem 3.1]. For example, the relative height of boxes in a tensor product is irrelevant, as illustrated by the equality:

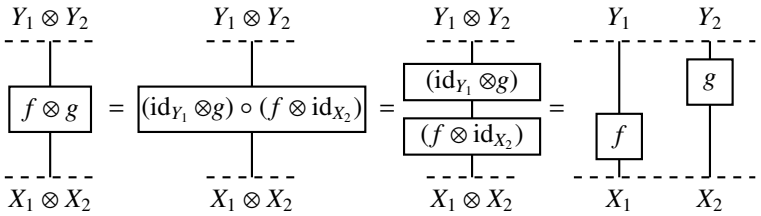

(2.16)

It is important to note that these diagrams are most naturally suited to strict monoidal categories. For non-strict categories, the associator and unitor isomorphisms are implicit in the diagrams, which requires care when performing calculations. In section 4.4, we will examine how this diagrammatic calculus extends to Soergel bimodules.

Following [54] and [36] we represent a braiding $c_{X,Y} : X \otimes Y \xrightarrow{\sim} Y \otimes X$ as an overlap of lines:

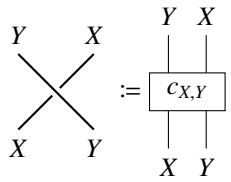

(2.17)

The axioms on the braidings guarantee that we can use diagrammatic notation. For example, the braid relation is

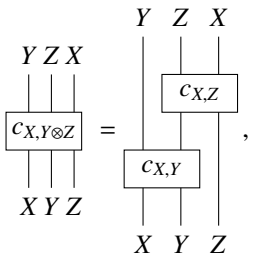

(2.18)

and naturality is shown in

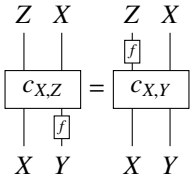

(2.19)

for a morphism $f : Y \to Z$.

2.2. Fusion and Multifusion Categories

The examples we have introduced so far, $\mathbf{Vec}_G$ and the Fibonacci category, carry more structure than just a monoidal category. They are examples of fusion categories. We introduce these and describe the desired properties.

2.2.1. Rigidity. The notion of rigidity generalizes the concept of duality from linear algebra to monoidal categories. Just as finite-dimensional vector spaces have dual spaces with canonical evaluation and coevaluation maps, objects in monoidal categories can possess dual objects with analogous structural morphisms.

Definition 2.9 ([24, Section 2.10]). Let X be an object of a monoidal category C. A *left dual* of X is an object X^* together with morphisms $\mathrm{ev}_X : X^* \otimes X \to 1$ (evaluation) and $\mathrm{coev}_X : 1 \to X \otimes X^*$ (coevaluation) such that the compositions

$$X \xrightarrow{\mathrm{coev}_X \otimes \mathrm{id}_X} (X \otimes X^*) \otimes X \xrightarrow{\alpha_{X,X^*,X}} X \otimes (X^* \otimes X) \xrightarrow{\mathrm{id}_X \otimes \mathrm{ev}_X} X \tag{2.20}$$

and

$$X^* \xrightarrow{\mathrm{id}_{X^*} \otimes \mathrm{coev}_X} X^* \otimes (X \otimes X^*) \xrightarrow{\alpha^{-1}_{X^*,X,X^*}} (X^* \otimes X) \otimes X^* \xrightarrow{\mathrm{ev}_X \otimes \mathrm{id}_{X^*}} X^* \tag{2.21}$$

are the identity morphisms on X and X^*, respectively. Similarly, we call an object ${}^*X$ a *right dual* of X in C if there are morphisms $\mathrm{ev}'_X : X \otimes {}^*X \to 1$ and $\mathrm{coev}'_X : 1 \to {}^*X \otimes X$ such that

$$X \xrightarrow{\mathrm{id}_X \otimes \mathrm{coev}'_X} X \otimes ({}^*X \otimes X) \xrightarrow{\alpha^{-1}_{X,{}^*X,X}} (X \otimes {}^*X) \otimes X \xrightarrow{\mathrm{ev}'_X \otimes \mathrm{id}_X} X \tag{2.22}$$

and

$${}^*X \xrightarrow{\mathrm{coev}'_X \otimes \mathrm{id}_{{}^*X}} ({}^*X \otimes X) \otimes {}^*X \xrightarrow{\alpha^{*}_{X,X,{}^*X}} {}^*X \otimes (X \otimes {}^*X) \xrightarrow{\mathrm{id}_{{}^*X} \otimes \mathrm{ev}'_X} {}^*X \tag{2.23}$$

are the identity morphisms on X and ${}^*X$, respectively. We call the object X *rigid* in C if there is a left dual X^* and a right dual ${}^*X$ of X; if all objects of the category C are rigid we call C *rigid*. If left and right duals agree in a category we will use X^*.

Example 2.10. The category **Vec** of finite-dimensional vector spaces over $\Bbbk$ is rigid. For any object $V \in \mathbf{Vec}$, the left dual is the dual vector space $V^* = \mathrm{Hom}_{\Bbbk}(V, \Bbbk)$. Given a basis $\{e_i\}_{i=1}^n$ of V, the dual basis $\{e_i^*\}_{i=1}^n$ is defined by $e_i^*(e_j) = \delta_{ij}$ (the Kronecker delta). The evaluation map is $\mathrm{ev}_V : V^* \otimes V \to \Bbbk$, $\mathrm{ev}_V(f \otimes v) = f(v)$, and the coevaluation map is $\mathrm{coev}_V : \Bbbk \to V \otimes V^*$, $\mathrm{coev}_V(1) = \sum_{i=1}^n e_i \otimes e_i^*$.

Example 2.11. For the category of G-graded vector spaces $\mathbf{Vec}_G^\omega$ from Example 2.4, one can check that $\delta_g^* = \delta_{g^{-1}} = {}^*\delta_g$, i.e., left and right duals correspond to assigning to each constituent its inverse. The evaluation and coevaluation maps are inherited from the standard duality in **Vec**.

In the Fibonacci category from Example 2.5, all objects possess duals; specifically, each object is self-dual. If we take elements from the one-dimensional Hom-space $f_{\mathbf{X}} \in \mathrm{Hom}_{\mathcal{F}}(\mathbf{X} \otimes \mathbf{X}, \mathbf{1})$ and $g_{\mathbf{X}} \in \mathrm{Hom}_{\mathcal{F}}(\mathbf{1}, \mathbf{X} \otimes \mathbf{X})$ such that $f_{\mathbf{X}} \circ g_{\mathbf{X}} = \mathrm{id}_{\mathbf{1}}$, then the associator from Definition 2.9 implies that any pair $(\mathrm{ev}_{\mathbf{X}}, \mathrm{coev}_{\mathbf{X}})$ must be a scalar multiple of $(f_{\mathbf{X}}, g_{\mathbf{X}})$ with the product of scalars equal to ϕ.

Remark 2.12. We draw the evaluation and coevaluation in string diagrams by using cups and caps:

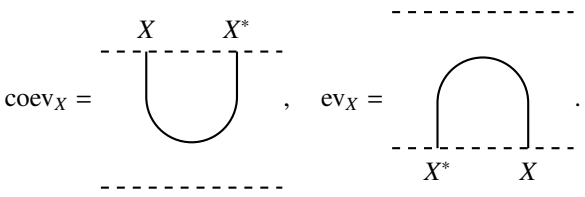

(2.24)

Then rigidity, Equation 2.20 and Equation 2.21, are represented via:

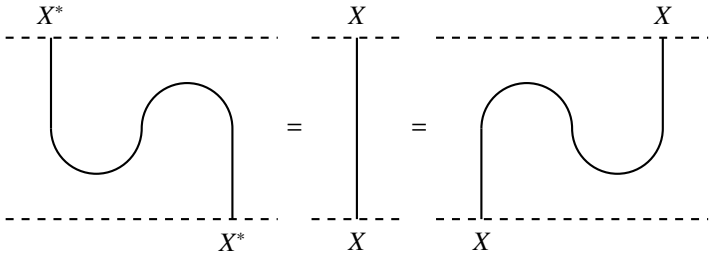

(2.25)

Here the associator morphism, while not visible in the diagrammatic notation, is crucial for the mathematical consistency. The string diagram notation allows us to omit drawing vertical lines, as any planar isotopy preserves the morphism. In categories where left and right duals do not coincide one often uses arrows to distinguish the orientation. For us we will always have ${}^*X \simeq X^*$.

Remark 2.13. Dual objects possess several important properties that we list here for later use:

- The unit object $1 \in C$ of any monoidal category C is always rigid. Its dual is $1^* = 1 = {}^*1$, with evaluation $\mathrm{ev}_1 = \iota$ and coevaluation $\mathrm{coev}_1 = \iota^{-1}$, using the triangle axiom (2.4) and properties of l_1.
- Left and right duals, when they exist, are unique up to unique isomorphism (see [24, Proposition 2.10.5]).
- The *tensor-hom adjunction*: the tensor-hom adjunction provides several natural isomorphisms (see [24, Proposition 2.10.8] for all variations). One such isomorphism for an object V with left dual V^* is:

$$\mathrm{Hom}_C(U \otimes V, W) \xrightarrow{\sim} \mathrm{Hom}_C(U, W \otimes V^*),\ f \mapsto (f \otimes \mathrm{id}_{V^*}) \circ (\mathrm{id}_U \otimes \mathrm{coev}_V) \tag{2.26}$$

Diagrammatically we can construct this by:

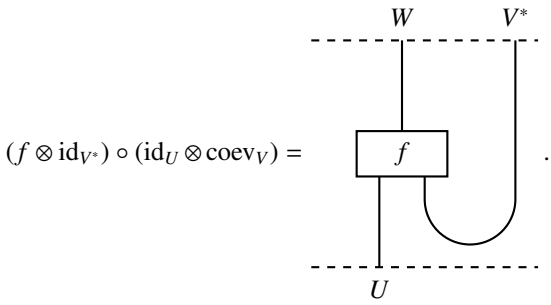

(2.27)

- For an object X with left dual X^*, the evaluation and coevaluation maps $\mathrm{ev}_X : X^* \otimes X \to 1$ and $\mathrm{coev}_X : 1 \to X \otimes X^*$ induce a right dual structure on X^* by setting $\mathrm{ev}'_{X^*} := \mathrm{ev}_X$ and $\mathrm{coev}'_{X^*} := \mathrm{coev}_X$. This yields canonical isomorphisms ${}^*(X^*) \simeq X$ and $({}^*X)^* \simeq X$.

2.2.2. Fusion and Multifusion Categories. We now introduce the main categories of interest in our study. Here $\Bbbk$ is assumed to be algebraically closed. While Soergel bimodules of section 2.4 are mostly defined over $\mathbb{R}$ we will see there is no harm in assuming $\mathbb{C}$. Being algebraically closed will also be needed for the results on the center.

We assume that all categories are $\Bbbk$-linear abelian and *locally-finite*, i.e. for any objects the Hom-space is a finite dimensional $\Bbbk$-vector space, and each object has finite length.

Definition 2.14 ([24, Definition 4.1.1]). Let C be a locally-finite, finite semisimple, $\Bbbk$-linear abelian rigid monoidal category. We call C a *multifusion category* over $\Bbbk$ if the bifunctor $\otimes : C \times C \to C$ is $\Bbbk$-bilinear on morphisms. If additionally $\mathrm{End}_C(1) \simeq \Bbbk$, we call C a *fusion category*.

One can also define a *monoidal functor* between two monoidal categories as a functor that preserves the monoidal structure (see [24, Definition 2.4.1]). A monoidal equivalence is then an equivalence of categories that is also a monoidal functor.

The condition $\mathrm{End}_C(1) \simeq \Bbbk$ is equivalent to the unit object being simple. When C is multifusion but not fusion, the unit object decomposes as a direct sum of simple objects $1 = \bigoplus_{1 \le i \le m} S_i$. This decomposition induces a natural splitting of C as an abelian category:

$$C = \bigoplus_{1 \le i,j \le m} C_{i,j}. \tag{2.28}$$

where each *component subcategory* $C_{i,j} := S_i \otimes C \otimes S_j$ is the full subcategory of C consisting of objects of the form $S_i \otimes C \otimes S_j$ for $C \in C$.

The monoidal structure interacts with this decomposition in a natural way: for objects $X \in C_{i,j}$ and $Y \in C_{k,l}$, their tensor product $X \otimes Y$ lies in $C_{i,l}$ if $j = k$, and is zero otherwise. Moreover, the duality structure is compatible with this decomposition: the left or right dual of an object in $C_{i,j}$ must lie in $C_{j,i}$. Consequently, each diagonal component $C_{i,i}$ forms a fusion subcategory of C. This structure explains the terminology 'multifusion' – it describes a category containing multiple fusion categories interacting with each other.

There is also the slightly weaker notion of a *multitensor category*, which is defined as a locally-finite, $\Bbbk$-linear abelian rigid monoidal category C. Thus, multifusion categories form a special class of multitensor categories, with the additional property of being finite semisimple. Despite not requiring finite semisimplicity, multitensor categories still exhibit a key structural property: as shown in [24, Corollary 4.3.2], their unit object always decomposes as a direct sum of pairwise non-isomorphic indecomposable objects. A multitensor category C is called a *tensor category* if it cannot be written as a direct sum of multitensor categories and satisfies $\mathrm{End}_C(1) \simeq \Bbbk$.

For a finite group G and 3-cocycle ω on G, the category $\mathbf{Vec}_G^\omega$ from Example 2.4 provides a fundamental example of a fusion category. Its fusion structure arises naturally: it is locally-finite and $\Bbbk$-linear by construction, abelian from the underlying vector space structure, finite semisimple with simple objects $\{\delta_g\}_{g \in G}$, and rigid monoidal as seen earlier. Moreover, since δ_1 is simple, we have $\mathrm{End}_{\mathbf{Vec}_G^\omega}(\delta_1) \simeq \Bbbk$, making it a fusion category. In the same way the Fibonacci category is fusion.

2.2.3. The H-reduction of the center. Recall from above that a multifusion category C decomposes as a direct sum of component subcategories $C = \bigoplus_{i,j} C_{i,j}$, with the diagonal

components $C_{i,i}$ being fusion subcategories. This structure resembles the eggbox diagram picture from section 1.2, where H-cells form a similar block diagonal structure. Building on this analogy, one can introduce the concepts of cells on tensor categories, using the decomposition of the monoidal product. Since we only need one key result of this theory we do not introduce all notation in full generality; we only remark that the terminology 'H-reduction' comes from this connection to the monoid-theoretic H-reduction discussed in section 1.2.

The main objective of this subsection is to establish that for an indecomposable multifusion category, the center is equivalent to the center of its fusion subcategories. Precisely: if a multifusion category is not itself a direct sum of smaller tensor categories, then the center $\mathcal{Z}(C)$ is equivalent to $\mathcal{Z}(C_{ii})$ for any diagonal fusion component. We call this phenomenon the H-*reduction* for monoidal categories. Later we will use this to reduce the computation of the center of categories associated to J-cells to that of categories associated to H-cells.

We again denote by $C_{i,j}$ the component subcategories of a given multifusion category. We assume this to be indecomposable, i.e. we cannot write $C \simeq C_1 \oplus C_2$ as a direct sum of monoidal categories, or in other words all components $C_{i,j}$ are non-empty.

Proposition 2.15 ([41]). *For a multifusion category C with component fusion subcategories C_{ii} for $1 \leq i \leq n$ we have*

$$\mathcal{Z}(C) \simeq \mathcal{Z}(C_{ii}). \tag{2.29}$$

Therefore, the center of an indecomposable multifusion category is fusion.

Idea of proof. This is Theorem 2.5.1 in [41]. One can define the notion of a module category $\mathcal{M}$ over a multifusion category. On the Grothendieck level this categorifies the notion of a module over a ring. Since inside C the component subcategory C_{ij} maps C_{jk} into C_{ik}, one can regard C_{ij} as a (C_{ii}, C_{jj})-bimodule category. Then the action of the component subcategories on each other extends to the following equation (here $\boxtimes$ denotes the Deligne tensor product of bimodule categories, the categorical analogue of tensor product of modules over a ring; see [24, Section 1.11]):

$$C_{ij} \boxtimes_{C_{jj}} C_{jl} \simeq C_{il} \tag{2.30}$$

as (C_{ii}, C_{ll})-bimodules. Now define the (C_{ii}, C)-bimodule and (C, C_{ii})-bimodule categories $\mathcal{M}_i \coloneqq \bigoplus_j C_{ij}$ and $\mathcal{N}_i \coloneqq \bigoplus_j C_{ji}$. They are what is called *invertible* in [41], i.e.

$$\mathcal{M}_i \boxtimes_C \mathcal{N}_i \simeq C_{ii} \tag{2.31}$$

and

$$\mathcal{N}_i \boxtimes_{C_{ii}} \mathcal{M}_i \simeq C. \tag{2.32}$$

Now following [41, Proposition 2.4.4] these equations show

$$\mathcal{Z}(C_{ii}) \simeq \mathcal{Z}(C). \tag{2.33}$$

□

We apply this result in the next section to the asymptotic Hecke category.

2.2.4. Traces and Dimensions. Let C be a rigid monoidal category. For an object $V \in C$ and a morphism $a \in \mathrm{Hom}_C(V, V^{**})$, we define the *left categorical trace*, see [24, Definition 4.7.1], as

$$\mathrm{tr}^L(a) : 1 \xrightarrow{\mathrm{coev}_V} V \otimes V^* \xrightarrow{a \otimes \mathrm{id}_{V^*}} V^{**} \otimes V^* \xrightarrow{\mathrm{ev}_{V^*}} 1. \tag{2.34}$$

For a $\Bbbk$-linear tensor categories, this trace can be interpreted as the element of the ground field determined by the following string diagram:

$\mathrm{tr}^L(a)\,\mathrm{id}_1 =$ 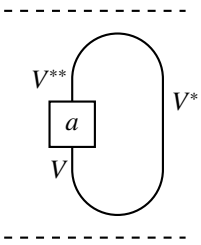

. (2.35)

Similarly, we define the *right categorical trace* (see [24, Definition 4.7.1]) as

$$\mathrm{tr}^R(a) : 1 \xrightarrow{\mathrm{coev}_{{}^*V}} {}^*V \otimes V \xrightarrow{\mathrm{id}_{{}^*V} \otimes a} {}^*V \otimes {}^{**}V \xrightarrow{\mathrm{ev}_{{}^{**}V}} 1, \tag{2.36}$$

which for tensor categories corresponds to the field element:

$\mathrm{tr}^R(a)\,\mathrm{id}_1 =$ 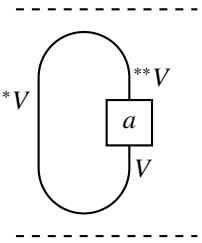

(2.37)

Definition 2.16 ([24, Definition 4.7.7, 4.7.11 and 4.7.14, Section 7.21]). A *pivotal* structure
on a rigid monoidal category C is a collection of natural isomorphisms $a_X : X \to X^{**}$ satisfying $a_{X\otimes Y} = a_X \otimes a_Y$ for all $X, Y \in C$. For a tensor category C, we define the *(left) dimension* of an object X as

$$\dim_a(X) \coloneqq \mathrm{tr}^L(a_X) \in \mathrm{End}_C(1). \tag{2.38}$$

A pivotal structure is called *spherical* if $\dim_a(V) = \dim_a(V^*)$ for all objects V.

For a multifusion category C, we can consider the *categorical dimension* of simple objects in the component subcategories $C_{i,j} = S_i \otimes C \otimes S_j$ as a value in $\mathrm{End}_C(S_i) \otimes_{\Bbbk} \mathrm{End}_C(S_j) \simeq \Bbbk$.

Example 2.17. Continuing with Example 2.11, we can choose the identity morphisms for the isomorphisms to the double duals in both categories. In $\mathbf{Vec}_G$, the dimension agrees with the dimension of the underlying vector space. In the Fibonacci category $\mathcal{F}$, we obtain $\dim(\mathbf{X}) = \phi$.

This illustrates how fusion categories naturally generalize vector spaces, with categorical dimensions that can take values beyond the natural numbers.

Remark 2.18. While general categories may exhibit differences between left and right duals and their corresponding dimensions, these distinctions often vanish in categories of our interest. By [24, Proposition 4.8.1], we have ${}^*V \simeq V^*$ in semisimple multitensor

categories over an algebraically closed field. When working with pivotal categories, we conventionally use the left trace for dimension calculations.

2.2.5. Skeletal Fusion Categories. In studying fusion categories, it is often convenient to work with a simpler representation where we eliminate redundant isomorphic objects. This leads to the notion of skeletal categories and their associated numerical data, particularly the 6j-symbols, which play a crucial role in explicit computations. For the notation in this subsection we refer to [2].

Definition 2.19. A category is called *skeletal* if it has exactly one object in each isomorphism class.

For a skeletal fusion category C, we can encode its structure through the following data. First, we have a finite set of simple objects $\{X_1, \dots, X_s\}$, where X_1 is the monoidal unit. Every object in the category can be expressed as a direct sum of these simples. When we tensor two simple objects, we obtain a direct sum of simples: $X_i \otimes X_j = \bigoplus_k X_k^{\oplus N_{i,j}^k}$, where the exponents $N_{i,j}^k \in \mathbb{N}$ are called the *fusion coefficients*. These coefficients completely determine the multiplicative structure of the Grothendieck ring.

To fully specify the monoidal structure, we must also encode the morphisms and associativity constraints. For each triple (i, j, k) of simple objects, we fix vector spaces $\mathrm{Hom}_C(X_i \otimes X_j, X_k)$ of dimension $N_{i,j}^k$. The monoidal structure is then determined by associator isomorphisms that relate different bracketings of tensor products. Specifically, the associator provides an isomorphism

$$\bigoplus_m \mathrm{Hom}_C(X_i \otimes X_j, X_m) \otimes \mathrm{Hom}_C(X_m \otimes X_k, X_l) \simeq \bigoplus_n \mathrm{Hom}_C(X_i \otimes X_n, X_l) \otimes \mathrm{Hom}_C(X_j \otimes X_k, X_n) \tag{2.39}$$

which encodes how morphisms on the left side (grouping as $(X_i \otimes X_j) \otimes X_k$) relate to those on the right side (grouping as $X_i \otimes (X_j \otimes X_k)$).

To make this structure explicit, we fix bases $B_{i,j}^k = \{(\alpha_{i,j}^k)_t \mid 1 \le t \le N_{i,j}^k\}$ of $\mathrm{Hom}_C(X_i \otimes X_j, X_k)$. The associator isomorphism between morphisms in $(X_i \otimes X_j) \otimes X_k \to X_l$ and $X_i \otimes (X_j \otimes X_k) \to X_l$ then becomes a linear map. Since we have simple objects on both sides and $\mathrm{Hom}_C(X_i, X_j) = \Bbbk$ if $i = j$ and 0 otherwise, this linear map can be represented by a matrix once we have fixed our bases. The entries of these matrices are the *6j-symbols*, since they encode six indices: the initial objects i, j, k, the final object l, the intermediate object m in the left grouping, and the intermediate object n in the right grouping.

In string diagram notation, basis elements are represented as:

$(\alpha_{i,j}^k)_t \leftrightarrow$ 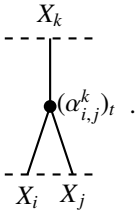 . (2.40)

For a triple tensor product we can write the composition of basis elements on the left side as a linear combination of basis elements on the right side:

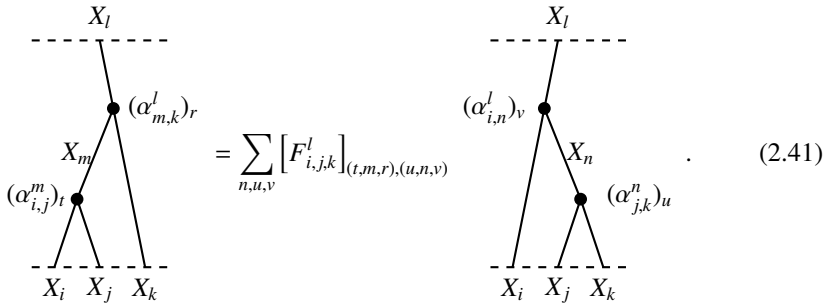

(2.41)

The matrix of coefficients is called *F-matrix*, the entries are the 6*j-symbols*.

We also choose dual bases $\overline{B^k_{i,j}} = \{\overline{(\alpha^k_{i,j})_t} \mid 1 \le t \le N^k_{i,j}\}$ of $\mathrm{Hom}_C(X_k, X_i \otimes X_j)$ satisfying the duality relation:

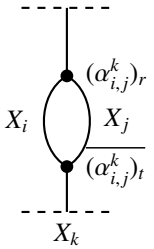

$= \delta_{tr} \, \mathrm{id}_{X_k}$. (2.42)

This duality relation provides a method for computing the F-matrices once bases are fixed, through the relation:

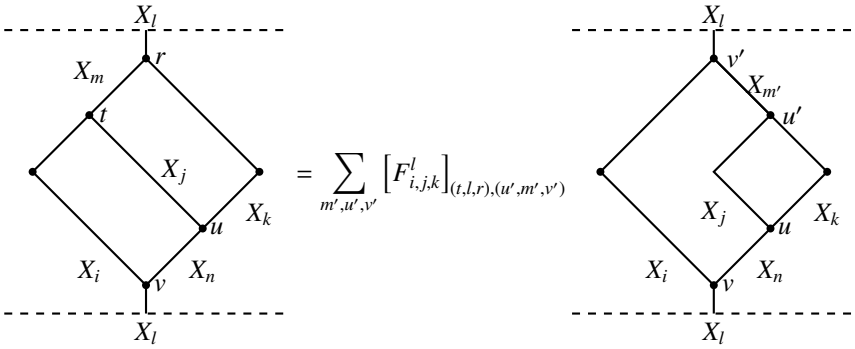

(2.43)

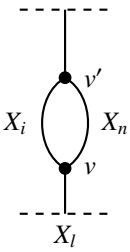

(2.44)

Remark 2.20. The choice of bases for the morphism spaces $\mathrm{Hom}_C(X_i \otimes X_j, X_k)$ introduces a gauge freedom in the F-symbols. Specifically, if we change bases via invertible

matrices $u^k_{i,j} \in \mathrm{GL}_{N^k_{i,j}}(\Bbbk)$, where $N^k_{i,j} = \dim \mathrm{Hom}_C(X_i \otimes X_j, X_k)$

$$(\alpha^k_{i,j})_t \mapsto \sum_{t'} (u^k_{i,j})_{t,t'} (\alpha^k_{i,j})_{t'}, \tag{2.45}$$

then the F-symbols transform, see [2, Equation 5a]. We will see such a gauge transformation in subsubsection 5.2.2.1.

2.2.6. Modular data. For spherical braided categories we introduce the S-matrix.

Definition 2.21. Let C be a ribbon fusion category, i.e. a fusion category equipped with a spherical structure φ and a braiding c. We denote the set of simple objects by $\{X_1, \dots, X_s\}$. The S-matrix is then defined to be the matrix of entries:

$$S(C) \coloneqq (s_{(X),(Y)})_{X,Y \in \{X_1,\dots,X_s\}}, \quad \text{where } s_{(X),(Y)} = \mathrm{tr}(c_{Y,X} c_{X,Y}). \tag{2.46}$$

Diagrammatically this looks like:

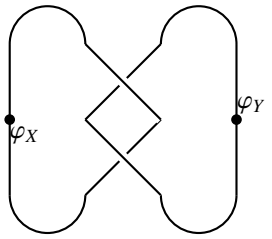

(2.47)

Here we have a composition of coevaluations, braidings, associators and the spherical structure.

2.3. Temperley–Lieb category

We study the Temperley–Lieb category here for two reasons: it demonstrates key concepts of diagrammatic categories, and its structure closely parallels that of Soergel bimodules for dihedral groups.

To handle multiple dihedral types simultaneously, we use quantum numbers, which allow for uniform calculations that can later be specialized to specific cases. We begin with these quantum numbers, then define the Temperley–Lieb category, and finally study its Karoubian envelope through Jones–Wenzl projectors.

2.3.1. Quantum numbers. Let us introduce quantum numbers, which play a fundamental role in representation theory, particularly in the study of $\mathfrak{sl}_2$ and its categorification. Following [20, Example 5.51] and [17, Section 3.1], we define:

Definition 2.22. Let $\mathbb{Z}[q^{\pm 1}]$ be the ring of Laurent polynomials. For any integer n, the *quantum number* $[n] \in \mathbb{Z}[q^{\pm 1}]$ is defined as

$$[n] \coloneqq \frac{q^n - q^{-n}}{q - q^{-1}} = q^{n-1} + q^{n-3} + \cdots + q^{1-n}. \tag{2.48}$$

Remark 2.23. For natural numbers b, c, we can specialize q to $e^{\frac{c\pi i}{b}}$, a $2b$-th root of unity; the resulting quantum number $[n]^c_b \in \mathbb{C}$ is a complex algebraic number. When $c = 1$, we omit the superscript. If b is clear from context, we omit both indices. For $b = \infty$, we set $[n] = n$.

A key example arises in dihedral groups, where $[2]^1_{m_{s,t}} = e^{\frac{\pi i}{m_{s,t}}} + e^{-\frac{\pi i}{m_{s,t}}} = 2\cos(\frac{\pi}{m_{s,t}}) = -a_{s,t}$ for $a_{s,t}$ the entry of the Cartan matrix. These numbers allow unified calculations across different dihedral types through specialization of the parameter q.

The quantum numbers satisfy the following fundamental relations:

$$[0] = 0, \quad [1] = 1, \quad [-n] = -[n], \tag{2.49}$$

and for any $n > 1$:

$$[2][n] = [n+1] + [n-1]. \tag{2.50}$$

More generally, for any positive integers m, n:

$$[m][n] = [n+m-1] + [n+m-3] + \cdots + [|n-m|+1], \tag{2.51}$$

see [20, Section 5.7].

We define the *quantum factorial* $[n]! \in \mathbb{Z}[q^{\pm 1}]$ for $n \in \mathbb{N}$ as:

$$[n]! := \prod_{i=1}^{n} [i], \tag{2.52}$$

Lemma 2.24. *For $m, n, p \in \mathbb{N}$, we have:*

$$[m+p][n+p] - [m][n] = [m+n+p][p]. \tag{2.53}$$

Proof. Using the expansion of quantum numbers and collecting terms, we observe that $[m+p][n+p]$ yields the sum of alternating terms from $q^{m+n+2p-1}$ to $q^{|m-n|+1}$. The product $[m][n]$ contributes terms from q^{m+n-1} to $q^{|n-m|+1}$. The difference yields precisely the terms corresponding to $[m+n+p][p]$. □

Example 2.25. For small values of b, we list frequently used quantum numbers:

b	$[2]$	$[3]$	$[4]$	$[5]$	$[6]$
2	0	-1	0	1	0
3	1	0	-1	-1	0
4	$\sqrt{2}$	1	0	-1	$-\sqrt{2}$
5	ϕ	ϕ	1	0	-1
6	$\sqrt{3}$	2	$\sqrt{3}$	1	0
∞	2	3	4	5	6

Table 2.1. Quantum numbers for small values.

Here $\phi := \frac{1+\sqrt{5}}{2}$ denotes the golden ratio. Note that $[b]_b = 0$ for any positive integer b.

2.3.2. The Temperley–Lieb Category. The Temperley–Lieb algebra was first introduced by Temperley and Lieb in 1971 in statistical mechanics. We present here a categorification, which emerged through the study of quantum groups and knot theory in the 1980s. For a comprehensive treatment, we refer to [39].

Definition 2.26. For a field $\Bbbk$, let q be the indeterminate of the Laurent polynomials $\Bbbk[q, q^{-1}]$. We set $[2] = q + q^{-1}$ and fix a bubble evaluation $\delta = -[2]$. The *Temperley–Lieb category* $\mathcal{TL}(q)$ is a strict monoidal $\Bbbk(q)$-linear category defined as follows:

(A) **Objects:** The category is generated by a single object $\overline{1}$, represented diagrammatically as a point on a horizontal line:

(2.54)

(B) **Monoidal Product:** On objects the monoidal product is defined by concatenation $\overline{n} \otimes \overline{m} := \overline{n+m}$. For instance, $\overline{3}$ is represented as:

(C) **Morphisms:** All morphisms are $\Bbbk[q^{\pm 1}]$-linearly generated by three elementary diagrams:

(a) The *cap morphism* $\cap\colon \overline{2} \to \overline{0}$:

(2.55)

(b) The *cup morphism* $\cup\colon \overline{0} \to \overline{2}$:

(2.56)

(c) The *identity morphism* $\mathrm{id}_{\overline{1}}\colon \overline{1} \to \overline{1}$:

(2.57)

(D) **Relations:** The morphisms satisfy two fundamental relations:

(a) The *bubble relation*: A closed loop evaluates to $-[2]$ times the identity:

$$= -(q+q^{-1}) \cdot \mathrm{id}_{\overline{0}}\,. \tag{2.58}$$

(b) The *rigidity relations*: Compositions yielding planar isotopic diagrams are equal:

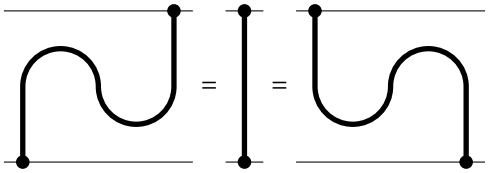

(2.59)

Proposition 2.27. *The object $\overline{1}$ in $\mathcal{TL}(q)$ is self-dual. Specifically, the cap and cup morphisms provide the evaluation and coevaluation maps exhibiting $\overline{1}$ as both left and right dual to itself.*

Proof. This follows from the rigidity relations in (2.59), which are precisely the triangle identities for duality in a monoidal category. □

2.3.3. Karoubian envelope and Jones–Wenzl projectors. The Temperley–Lieb category $\mathcal{TL}(q)$ is not abelian – it lacks kernels and cokernels because even idempotents do not split. To remedy this, we introduce the Karoubian envelope construction, which formally adjoins the images of all idempotents. In the special case of $\mathcal{TL}(q)$, this construction yields an abelian category, and the Jones–Wenzl projectors provide a way to construct a complete set of simple objects in this envelope.

In what follows, we work in $\mathcal{TL}(q)$ where a bubble evaluates to $\delta = -[2]$. Following [20, Section 9.3], we first introduce the Jones–Wenzl projectors – certain idempotent morphisms with remarkable properties – and then study how they behave in the Karoubian envelope.

Remark 2.28. To see why $\mathcal{TL}(q)$ is not abelian, note that even idempotents do not split. Consider the Hom space $\mathrm{Hom}_{\mathcal{TL}(q)}(\overline{2},\overline{2})$, spanned by the identity morphism $\mathrm{id}_{\overline{2}}$ and a non-trivial composite. Define

$$e := \frac{1}{\delta}$$

(2.60)

where $\delta = [2]$. Then e is an idempotent ($e^2 = e$), as is $1 - e$. For an abelian category, the idempotent $1 - e$ would split: we would need a section $r : \mathrm{Im}(1 - e) \to \overline{2}$ such that $(1-e)\circ r = \mathrm{id}_{\mathrm{Im}(1-e)}$. However, such a section cannot exist in $\mathcal{TL}(q)$ because any morphism from a lower-rank object to $\overline{2}$ must contain cup morphisms to increase the number of strands, and composing any cup-containing morphism with $1 - e$ yields zero. Thus the category is not abelian.

Note that each $\mathrm{Hom}_{\mathcal{TL}(q)}(\overline{n},\overline{n})$ is a finite-dimensional $\Bbbk[q^{\pm 1}]$-module spanned by non-crossing diagrams, and always contains the identity morphism $\mathrm{id}_{\overline{n}}$ with coefficient 1 in any endomorphism.

Theorem 2.29. *For each $n \in \mathbb{N}$, there exists a unique idempotent endomorphism $JW_n \in \mathrm{End}_{\mathcal{TL}(q)}(\overline{n})$, called the* Jones–Wenzl projector*, satisfying:*

- $JW_n \circ f = 0$ *for any morphism f containing a cup.*
- $f \circ JW_n = 0$ *for any morphism f containing a cap.*
- *The coefficient of the identity morphism* $\mathrm{id}_{\overline{n}}$ *in JW_n is* 1.

Proof. The Jones–Wenzl projectors can be defined recursively by either of the following equivalent formulas:

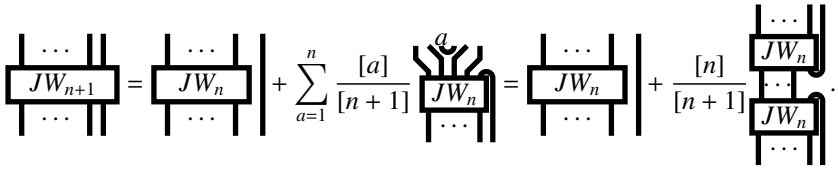

(2.61)

The proof proceeds by induction. For JW_1, the claim is immediate as it equals the identity morphism. For $n > 1$:

(A) The inductive hypothesis ensures any cup or cap composed with JW_n in the first term yields zero.
(B) The second term guarantees the killing of cups and caps on the $(n + 1)$-st strand via Lemma 2.31.
(C) The identity morphism appears only in the first term with coefficient 1.
(D) Idempotency follows from the cup and cap killing properties.

□

Example 2.30. The Jones–Wenzl projectors for $n \in \{2, 3\}$ are:

$$JW_2 =$$ 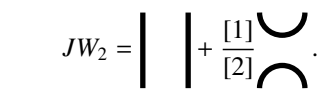

(2.62)

$$JW_3 =$$ 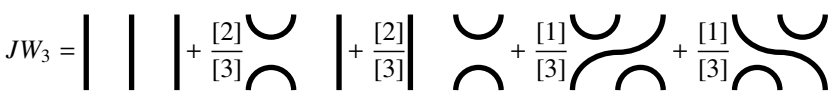

(2.63)

They always include all possible morphisms of $\mathrm{End}_{\mathcal{TL}(q)}(\overline{n})$.

Lemma 2.31. *For the Jones–Wenzl projectors, we have:*

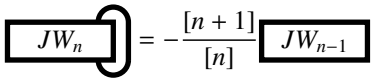

(2.64)

Proof. The proof proceeds by induction. The case $n = 1$ is immediate. For $n > 1$, we use the second recursion from Theorem 2.29 and the identity:

$$-[2] + \frac{[n-1]}{[n]} = -\frac{[2][n] - [n-1]}{[n]} = -\frac{[n-1] + [n+1] - [n-1]}{[n]} = -\frac{[n+1]}{[n]}.$$

□

Recall that, as shown in item 2.55 and item 2.56, the cap and cup morphisms serve as the evaluation and coevaluation maps for the self-dual object $\overline{1}$. This construction extends naturally to $\overline{n}$: one can compose n nested cups on top of any morphism, followed by n nested caps on the bottom, forming a closed diagram that evaluates to a scalar. This scalar is called the *trace* of the morphism.

Proposition 2.32 ([20, Exercise 9.28]). *The trace of JW_n equals $(-1)^n[n+1]$.*

Proof. This follows by induction using Lemma 2.31. □

To better understand the structure of the Temperley–Lieb category, we introduce the Karoubian envelope, see [20, Section 11.2.3].

Definition 2.33. For a category C, the *Karoubian envelope* is the category $\mathrm{Kar}(C)$ with:

- Objects are pairs (X, p) where $X \in C$ and $p \in \mathrm{End}_C(X)$ is idempotent.
- Morphisms in $\mathrm{Hom}_{\mathrm{Kar}(C)}((X, p), (Y, q))$ are morphisms $f \in \mathrm{Hom}_C(X, Y)$ satisfying $fp = f = qf$.

The complete proof of the following proposition is very lengthy; we refer to [64, Section 3.2] for the full argument. Instead, we illustrate the key idea with a concrete example below.

Proposition 2.34. *The Karoubian envelope $\mathrm{Kar}(\mathcal{TL}(q))$ is semisimple, and all simple objects are of the form $(\overline{n}, JW_n)$.*

The decomposition $(\overline{n}, JW_n) \otimes (\overline{1}, JW_1) \simeq (\overline{n-1}, JW_{n-1}) \oplus (\overline{n+1}, JW_{n+1})$ can, for example, be derived from (2.61).

Example 2.35. The simplicity of objects $(\overline{n}, JW_n)$ is evident: while $\mathrm{End}_{\mathcal{TL}}(\overline{3})$ has 5 generators (see (2.63)), all morphisms except the identity vanish when composed with JW_3, yielding $\mathrm{End}_{\mathrm{Kar}(\mathcal{TL})}(\overline{n}, JW_n) \simeq \Bbbk$. Morphisms in $\mathrm{Kar}(\mathcal{TL}(q))$ are diagrammatically represented by pre- and postcomposing with the respective idempotents. For example $\mathrm{Hom}_{\mathrm{Kar}(\mathcal{TL})}((\overline{2}, JW_2) \otimes (\overline{2}, JW_2), (\overline{2}, JW_2))$ is only one dimensional as all other morphisms vanish because of the cap and cup vanishing.

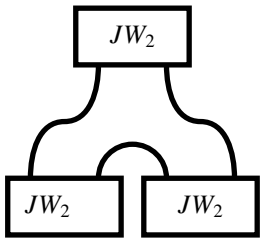

.

(2.65)

Remark 2.36. The trace computed in Proposition 2.32 coincides with the categorical dimension of $(\overline{n}, JW_n)$ in $\mathrm{Kar}(\mathcal{TL}(q))$. Note that one Jones–Wenzl projector in the composition of evaluation and coevaluation vanishes due to the cup/cap killing property:

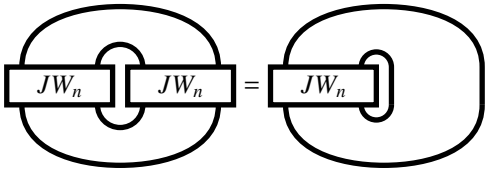

. (2.66)

These computations parallel those we will encounter in the study of Soergel bimodules for dihedral groups.

2.4. Soergel bimodules

Soergel bimodules, introduced in a series of fundamental papers [60, 61, 62], provide a categorification of Hecke algebras. In this section, we develop their theory in three stages:

First, we present the original algebraic construction of Soergel bimodules as polynomial bimodules. Then we introduce their diagrammatic presentation, developed by Elias–Williamson [17], which proved instrumental in resolving Soergel's conjecture. Finally, we explore their connection to the Temperley–Lieb category in the case of dihedral groups, yielding computational tools that will be essential for our later study of the asymptotic category.

2.4.1. Algebraic Definition. Let (W, S) be a Coxeter system with realization V over a field $\Bbbk$ of characteristic 0. As in subsection 1.1.2, let $R = \mathrm{Sym}(V^*)$ be the symmetric algebra on the dual space, with V having grading 2.

We work in the category R-gbim of graded (R, R)-bimodules that are finitely generated as left and as right R-modules. For N an (R, R)-bimodule we denote the shift to one degree higher by $N(1)$. The morphisms are homogeneous graded bimodule maps of degree 0. We set:

$$\mathrm{Hom}^\bullet(M, N) := \bigoplus_{i\in\mathbb{Z}} \mathrm{Hom}(M, N(i)). \tag{2.67}$$

By $\mathrm{rk}_{\mathbb{Z}[v^{\pm 1}]}\,\mathrm{Hom}^\bullet(B, B')$, we denote the graded rank of the morphism space, this is the Laurent polynomial $\sum_{i\in\mathbb{Z}} \mathrm{rk}(\mathrm{Hom}(B, B(i)))v^i$. Then R-gbim is a monoidal category with tensor product by R. We will often omit $\otimes_R$ if it is clear from context, i.e. we write MN instead of $M \otimes_R N$.

In this category we will work with a certain subset of Bott–Samelson bimodules. They will form the basis of Soergel bimodules, our objects of desire.

Definition 2.37 (Bott–Samelson Bimodules). For $s \in S$, define the elementary Bott–Samelson bimodule by

$$B_s := R \otimes_{R^s} R(1), \tag{2.68}$$

with R^s the s-invariant elements, see Definition 1.11. For an expression $\underline{w} = (s_1, \ldots, s_n)$ in S, we define:

$$\mathrm{BS}(\underline{w}) := B_{s_1} \otimes_R B_{s_2} \otimes_R \cdots \otimes_R B_{s_n} \cong R \otimes_{R^{s_1}} R \otimes_{R^{s_2}} \cdots \otimes_{R^{s_n}} R(\ell(\underline{w})). \tag{2.69}$$

Definition 2.38 (Soergel Bimodules). The category of Soergel bimodules $\mathbb{S}\mathrm{Bim}(W)$ is the full subcategory of graded (R, R)-bimodules whose objects are direct summands of finite direct sums of shifts of Bott–Samelson bimodules.

Remark 2.39. There is a notion of a standard bimodule R_w, for any $w \in W$ which is defined as R with the left action twisted by w:

$$f \cdot r \cdot g = fw(r)g,$$

for $f, g, r \in R$, see [20, Section 5]. Using these standard bimodules one can define a unique so called Δ- or ∇-filtration on any Soergel bimodule B. The subquotients of those are then isomorphic to a certain number of copies of R_x, denoted by $\mathbf{h}_x(B)$. For example B_s has quotients $R(1)$ and $R_s(-1)$. From this data we can then define the character of a Soergel bimodule as:

$$\mathrm{ch}_\Delta(B) \coloneqq \sum_{x \in W} v^{l(x)} h_x(B) \delta_x \in H(W). \tag{2.70}$$

This character map provides the bridge between Soergel bimodules and the Hecke algebra. We write $[\mathbb{S}\mathrm{Bim}(W)]_\oplus$ for the *split Grothendieck group* of the Soergel bimodules, see [20, Section 4.8]. This is an abelian group generated by equivalence classes of objects with the relation $[B]+[B'] \coloneqq [B \oplus B']$. Using the monoidal structure and grading it becomes a $\mathbb{Z}[v^{\pm 1}]$-algebra via $[B] \cdot [B'] \coloneqq [B \otimes_R B']$ and $v.[B] \coloneqq [B(1)]$.

The following theorem can be seen in [20, Theorem 5.24].

Theorem 2.40 (Soergel's Categorification Theorem). *There exists an isomorphism of $\mathbb{Z}[v^{\pm 1}]$-algebras:*

$$H(W) \xrightarrow{\sim} [\mathbb{S}\mathrm{Bim}(W)]_\oplus, \tag{2.71}$$

sending b_s to $[B_s]$ for each $s \in S$. The inverse is ch*. Moreover:*

(A) *For each $w \in W$, there exists an indecomposable Soergel bimodule B_w whose class $[B_w]$ corresponds to b_w.*
(B) *For any reduced expression $\underline{w}$ of w, the Soergel bimodule B_w appears as a direct summand of* $\mathrm{BS}(\underline{w})$ *with multiplicity one.*
(C) *If B_w appears as a summand of* $\mathrm{BS}(\underline{x})$*, then $x \geq w$ in the Bruhat order.*

A key computational tool is the following formula for morphism spaces, see [20, Theorem 5.27].

Theorem 2.41 (Soergel Hom Formula). *For Soergel bimodules B, B':*

$$\mathrm{rk}_{\mathbb{Z}[v^{\pm 1}]} \mathrm{Hom}^\bullet(B, B') = (\mathrm{ch}(B), \mathrm{ch}(B')), \tag{2.72}$$

where ch *is the character map to the Hecke algebra and $(-,-)$ is the standard pairing: $(a, b) \coloneqq \epsilon(\omega(a)b)$, where $\epsilon(\cdot)$ gives the coefficient of δ_1 and $\omega(\cdot)$ is the* Kazhdan–Lusztig anti-involution*, defined as $\omega(\delta_x) = \delta_x^{-1}$.*

Corollary 2.42. *For $x, y \in W$ and $i \in \mathbb{N}$ we have:*

$$\mathrm{rk}_{\mathbb{Z}[v^{\pm 1}]} \mathrm{Hom}^\bullet(B_x, B_y) = \begin{cases} 1 + v r_{x,y} & \text{if } x = y, \\ v r_{x,y} & \text{otherwise,} \end{cases} \tag{2.73}$$

for some Laurent polynomial $r_{x,y}$.

Proof. This follows from Theorem 2.41 using knowledge on orthogonality of Kazhdan–Lusztig basis, see[20, Theorem 3.21]. □

In particular this means that the zero degree Hom space is empty is $x \neq y$.

The explicit construction of the indecomposable bimodules B_w is highly non-trivial. This motivates the diagrammatic approach we will develop in the next section, which provides a more combinatorial way to understand these objects.

2.4.2. Diagrammatic Soergel Bimodules. We now introduce the diagrammatic category $\mathcal{H}_{BS}$ of Bott–Samelson bimodules. Following [17], we define this category by generators and relations, and simultaneously give a functor $\mathcal{F}$ to $\mathbb{S}$Bim. By [20, Chapters 10-11], this functor induces an equivalence between the Karoubian envelope of the additive and shift closure of $\mathcal{H}_{BS}$, which we denote by $\mathcal{H}$, and the category of Soergel bimodules $\mathbb{S}$Bim defined in the previous section. We discuss idempotents and the Karoubian envelope in more detail in chapter 3. When taking the additive and shift closure of a category, we denote this by subscripting with $\oplus$ (additive closure via finite direct sums) and $\cong$ (equivalence under isomorphism).

We fix a Coxeter system (W, S) with $S = \{s_1, \dots, s_n\}$ and choose a color scheme for the reflections. In Example 1.8, we already used different colors to distinguish between reflections. For improved readability, we also assign different styles to the various markings. In all examples we consider 5 reflections are enough.

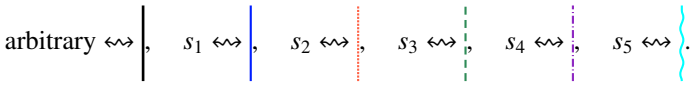

(2.74)

Definition 2.43 ([20, Chapters 8-9]). The diagrammatic Hecke category $\mathcal{H}_{BS}$ of Bott–Samelson bimodules and the functor $\mathcal{F} : \mathcal{H}_{BS} \to \mathbb{S}$Bim are defined by generators and relations as follows:

(A) **Objects:** Sequences of colors $(s_1, \dots, s_n)$ with $s_i \in S$ drawn as a horizontal line with n points colored by the s_i. The functor $\mathcal{F}$ sends a sequence $(s_1, \dots, s_n)$ to the tensor product $B_{s_1} \otimes_R \dots \otimes_R B_{s_n}$:

$$\mapsto B_{s_1} \otimes_R B_{s_2} \otimes_R B_{s_3} \simeq \mathrm{BS}(s_1, s_2, s_3). \tag{2.75}$$

(B) **One-color generators:** For each $s \in S$:

- Box (degree f):

$$\mapsto R \to R(\deg(f)),\ 1 \mapsto f. \tag{2.76}$$

- Start dot (degree 1):

$$\mapsto B_s \to R(1),\ f \otimes g \mapsto fg. \tag{2.77}$$

- End dot (degree 1):

$$\mapsto R \to B_s(1),\ 1 \mapsto \frac{1 \otimes \alpha_s + \alpha_s \otimes 1}{2}. \tag{2.78}$$

- Merge (degree -1):

$$\mapsto B_s \otimes_R B_s \to B_s(-1),\ 1 \otimes g \otimes 1 \mapsto \partial_s(g) \otimes 1. \tag{2.79}$$

- Split (degree -1):

$$\mapsto B_s \to B_s \otimes_R B_s(-1),\ f \otimes g \mapsto f \otimes 1 \otimes g. \tag{2.80}$$

(C) **One-color relations**:

- Unit relations:

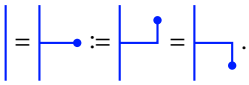

(2.81)

We also use cap and cup for the composition of enddot with split and merge with start dot:

(2.82)

- Associativity:

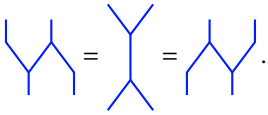

(2.83)

- Barbell:

(2.84)

- Needle:

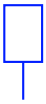

(2.85)

- Polynomial forcing:

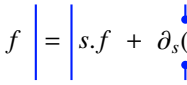

(2.86)

(D) **Two-color generators:** For adjacent $s, t \in S$ with $m_{st} < \infty$:

- The m_{st}-valent vertex (degree 0) (Here shown for $m_{s,t} = 5$):

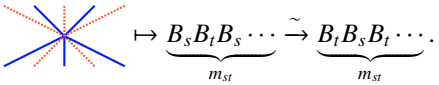

(2.87)

(E) **Two-color relation:**

- For any $m_{s,t} < \infty$ two-color associativities. We show it again for $m_{s,t} = 5$

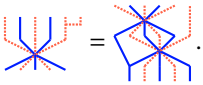

(2.88)

- Two-color dot contraction:

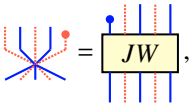

(2.89)

where JW is a Jones–Wenzl projector similar to the Jones–Wenzl from Temperley–Lieb categories. We see an exact definition in subsection 2.4.4.

(F) **Three color relations:** Further for any longest word in a finite Coxeter group on 3 generators there are is a cycle in the graph of reduced expressions of w_0 where the edges are the possible rex moves. We need relations on the two ways in this graph. These are called *Zamolodchikov equations*, see [17].

THEOREM 2.44 ([20, Theorem 4.2, Chapters 10-11]). *The functor $\mathcal{F} : \mathcal{H}_{BS} \to \mathbb{S}\mathrm{Bim}$ induces an equivalence of categories between the Karoubian envelope of the additive and shift closure of $\mathcal{H}_{BS}$, denoted by $\mathcal{H}$, and the category of Soergel bimodules $\mathbb{S}\mathrm{Bim}(W)$.*

Example 2.45. We demonstrate how Theorem 2.40 works by computing some idempotent decompositions.

First, consider the equality $b_s b_s = (v + v^{-1})b_s$ in the Hecke algebra. This suggests we should find $B_s \otimes_R B_s \simeq B_s(1) \oplus B_s(-1)$ in $\mathcal{H}$. Indeed, we can decompose the identity morphism as:

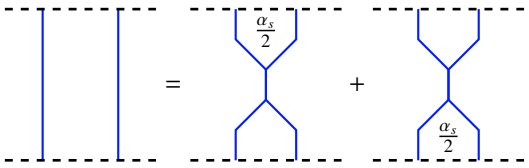

(2.90)

Both summands are idempotent since $\partial_s(\alpha_s) = 2$ and using the needle relation. Further they are orthogonal as $\partial_s(1) = \partial_s(\alpha_s^2) = 0$:

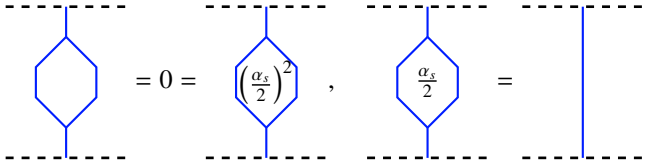

(2.91)

For a more complex example, consider $b_s b_t b_s = b_{sts} + b_s$ in type A_2. The corresponding idempotent in $\mathcal{H}$ is:

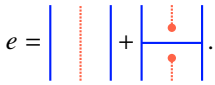

(2.92)

To verify this is idempotent, we use that $\partial_s(\alpha_t) = -1$ in type A_2:

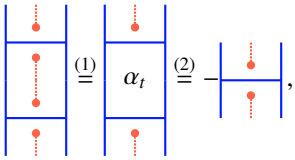

(2.93)

where (1) uses polynomial forcing and (2) uses the needle relation.

While we could write these decompositions explicitly in $\mathbb{S}$Bim using the functor $\mathcal{F}$, the diagrammatic calculations are far more manageable. This illustrates the power of the diagrammatic approach.

2.4.3. Light Leaves. The light leaves construction, introduced by Libedinsky [43] and further developed by Elias and Williamson [23], provides a systematic way to construct bases for morphism spaces between Bott–Samelson bimodules.

Definition 2.46. For an expression $\underline{w} = (s_1, \dots, s_n)$ in S, a *subexpression* is a sequence $\underline{e} = (e_1, \dots, e_n)$ where each $e_i \in \{0, 1\}$. This defines a sequence of elements in W by:

$$w_k := \begin{cases} w_{k-1} s_k, & \text{if } e_k = 1, \\ w_{k-1}, & \text{if } e_k = 0. \end{cases} \tag{2.94}$$

We write $\underline{w}^{\underline{e}}$ for the final element w_n.

To each index k in a subexpression, we assign one of four decorations based on two criteria:

- Direction: U (up) if $\ell(w_{k-1}s_k) > \ell(w_{k-1})$, otherwise D (down).
- Value: the value of e_k (0 or 1).

The light leaf $LL_{\underline{w},\underline{e}} \in \mathrm{Hom}(\mathrm{BS}(\underline{w}), \mathrm{BS}(\underline{w}^{\underline{e}}))$ is constructed recursively by applying one of four operations at each step, determined by these decorations:

Map		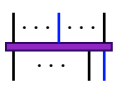		
Decoration	$U0$	$U1$	$D0$	$D1$
Degree	1	0	-1	0

Table 2.2. Light leaf operations.

To ensure the construction is well-defined, we fix:

- A reduced expression $\underline{x}$ for each $x \in W$.
- For each $x \in W$ and $s \in R(x)$, a reduced expression $\underline{x}_s$ ending in s.
- For any two reduced expressions of the same element, a sequence of braid moves connecting them.

By $\overline{LL}_{\underline{w},\underline{e}} \in \mathrm{Hom}(\mathrm{BS}(\underline{w}^{\underline{e}}), \mathrm{BS}(\underline{w}))$ we denote the vertical flip of $LL_{\underline{w},\underline{e}}$. The light leaves provide bases for morphism spaces:

Theorem 2.47 ([20, Theorem 10.32]). *For expressions $\underline{x}, \underline{y}$ in S, the double leaves*

$$\mathbb{LL}^{z}_{\underline{f},\underline{e}} := \overline{LL}_{\underline{y},\underline{f}} \circ LL_{\underline{x},\underline{e}}, \tag{2.95}$$

where $\underline{e}, \underline{f}$ range over subexpressions with $\underline{x}^{\underline{e}} = z = \underline{y}^{\underline{f}}$, form a basis of $\mathrm{Hom}_{\mathcal{H}_{BS}}(\mathrm{BS}(\underline{x}), \mathrm{BS}(\underline{y}))$.

For indecomposable Soergel bimodules B_x and B_y, represented by idempotents ψ_x and ψ_y, the morphism space is obtained by composition:

$$\mathrm{Hom}_{\mathcal{H}}(B_x, B_y) = \psi_y \circ \mathrm{Hom}_{\mathcal{H}_{BS}}(\mathrm{BS}(\underline{x}), \mathrm{BS}(\underline{y})) \circ \psi_x. \tag{2.96}$$

The dimension of these morphism spaces is given by Soergel's Hom formula in terms of Kazhdan–Lusztig polynomials. We will see explicit examples of light leaf calculations in the dihedral case in the next section, as here $\mathcal{H}$ is closely related to the Temperley–Lieb category.

Example 2.48. Consider the expression $\underline{w} = sts$ in type A_2. Each subexpression $\underline{e}$ produces a light leaf morphism $LL_{\underline{w},\underline{e}}$ as shown below:

$\underline{e}$	$(1,1,1)$	$(1,1,0)$	$(1,0,1)$	$(1,0,0)$
$LL_{\underline{w},\underline{e}}$				
Element	sts	st	1	s
Degree	0	1	1	0

The double leaves $\mathbb{LL}^{z}_{\underline{f},\underline{e}} = \overline{LL}_{\underline{w},\underline{f}} \circ LL_{\underline{w},\underline{e}}$ between $\mathrm{BS}(sts)$ and itself give a basis for $\mathrm{Hom}(\mathrm{BS}(sts), \mathrm{BS}(sts))$. By Soergel's Hom formula, this space has graded dimension $1 +$

$\underline{e}$	$(0,1,1)$	$(0,1,0)$	$(0,0,1)$	$(0,0,0)$
$LL_{\underline{w},\underline{e}}$				
Element	ts	t	s	1
Degree	1	2	2	3

TABLE 2.3. Light leaves for sts in type A_2.

$2v^2 + 2v^4 + v^6$. Only combinations of expressions $(1,1,1)$, $(1,1,0)$, $(0,1,1)$, $(0,1,0)$, and $(0,0,0)$ contribute non-zero maps to this basis.

2.4.4. Two-colored Temperley–Lieb Category. Building on the ordinary Temperley–Lieb category introduced in subsection 2.3.2, we now develop a colored variant that will connect directly to Soergel bimodules for dihedral groups, following [20, Definition 9.11 and 9.12]. Originally this is due to Elias in [15, Section 4.3].

DEFINITION 2.49. Let $\Bbbk$ be a field and consider the Laurent polynomials $\Bbbk[q^{\pm 1}]$. We set $\delta := q + q^{-1}$. The *two-colored Temperley–Lieb category* $\mathcal{TL}_2(\delta)$ is a $\Bbbk$-linear 2-category defined as follows:

- **Objects:** Objects are finite sequences of colors from $\{r, b\}$ representing boundary points colored red or blue.
- **1-Morphisms:** For $n \in \mathbb{N}$ and $c \in \{r, b\}$, the notation $\overline{n}_c$ represents the object consisting of n boundary points, where the first point has color c, and colors alternate between red and blue. For example, $\overline{1}_r$ represents a single red point transitioning to blue, and $\overline{3}_r$ represents red-blue-red-blue alternation. The 1-morphisms are generated by the following basic generators.

$$\overline{1}_r \quad \longleftrightarrow \quad \text{  }, \qquad \overline{1}_b \quad \longleftrightarrow \quad \text{  }. \tag{2.97}$$

General 1-morphisms are composed horizontally. For example:

$$\overline{3}_r \quad \longleftrightarrow \quad \text{  }. \tag{2.98}$$

- **2-Morphisms:** The 2-morphisms are $\Bbbk[v^{\pm 1}]$-linear combinations of diagrams (where morphisms are graded by degree). These are generated by the following basic generators.
  - Lines (identity morphisms):

$$\overline{1_r} \to \overline{1_r}: \quad \text{ 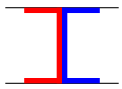 }, \tag{2.99}$$

$$\overline{1_b} \to \overline{1_b}: \quad \text{ 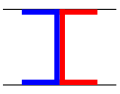 }. \tag{2.100}$$

  - Caps (evaluations):

$$\overline{2}_r \to \overline{0}_r: \quad \text{  }, \tag{2.101}$$

$$\overline{2}_b \to \overline{0}_b: \quad \text{  }. \tag{2.102}$$

– Cups (coevaluations):

$\overline{0}_r \to \overline{2}_r$:  , (2.103)

$\overline{0}_b \to \overline{2}_b$:  . (2.104)

- **Relations:** The 2-morphisms satisfy the following relations:
  (A) Bubble relations: Closed loops of a single color evaluate to δ times the corresponding identity:

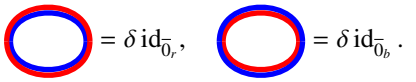 (2.105)

  (B) Isotopy relations: Each color acts independently with the standard Temperley–Lieb relations. For red (or blue) strands, the standard Reidemeister moves and isotopy relations from the ordinary Temperley–Lieb category apply, while strands of different colors do not interact.

Remark 2.50. The two-colored Temperley–Lieb category exhibits a key structural property: there are no 2-morphisms that connect objects starting with different colors (e.g., no morphisms from $\overline{1}_r$ to $\overline{1}_b$ or vice versa). This independence reflects that red and blue strands operate in separate monoidal subcategories. The idempotent structure parallels that of subsection 2.3.2, yielding colored variants of the Jones–Wenzl projectors.

The connection to Soergel bimodules for dihedral groups is established via the following functor, see [20, Definition 9.12].

Definition 2.51. Given a dihedral Coxeter system (W, S) with $S = \{s, t\}$, we have $a_{st} = \partial_s(\alpha_t) = -2\cos(\pi/m_{st}) = a_{ts}$ as in subsection 2.4.2. There is a functor $\Sigma : \mathcal{TL}_2(a_{st}) \to \mathbb{S}\mathrm{Bim}$ defined as follows:

- **On objects:** Red regions map to B_s and blue regions to B_t.
- **On 1-Morphisms:** A sequence of transitions maps to the corresponding tensor product in $\mathbb{S}\mathrm{Bim}$. For example:

 (2.106)

- **On 2-Morphisms:** Apply a deformation retract to obtain morphisms in $\mathbb{S}\mathrm{Bim}$. For instance:

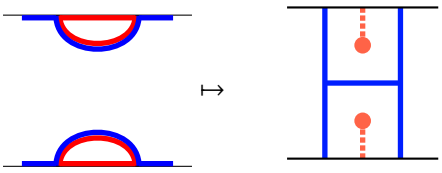 (2.107)

Remark 2.52. The functor Σ exhibits two important properties:

(A) It is not a monoidal functor (or 2-functor). This is because $\mathbb{S}\mathrm{Bim}$ distinguishes between objects like B_sB_s that are not distinguished in $\mathcal{TL}_2(a_{st})$. For example, while $\mathrm{id}_{\overline{0}_r}$ maps to id_{B_s}, the tensor product $\mathrm{id}_{\overline{0}_r} \otimes \mathrm{id}_{\overline{0}_r}$ maps to id_{B_s} rather than $\mathrm{id}_{B_sB_s}$. See [20, Section 24.2.3] for a detailed treatment of this subtlety.

(B) When $\mathcal{TL}_2(\delta)$ is defined over the same field $\Bbbk$ of characteristic 0 as the Soergel bimodules, the functor induces an isomorphism between morphism spaces:

$$\mathrm{Hom}_{\mathcal{TL}_2(a_{st})}(\overline{n}_c, \overline{m}_{c'}) \cong \mathrm{Hom}^0_{\mathbb{S}\mathrm{Bim}}(\mathrm{BS}(\underline{w}), \mathrm{BS}(\underline{w'})), \tag{2.108}$$

where $\underline{w}, \underline{w'}$ are the sequences corresponding to $\overline{n}_c, \overline{m}_{c'}$ respectively, and Hom^0 denotes degree zero morphisms, see [19, Theorem 2.15]. This isomorphism will be essential for our computations in the asymptotic category.

Further, the Jones–Wenzl projectors of the Temperley–Lieb category describe the idempotents in $\mathcal{H}$ for words of the form $sts\ldots$, see [20, Theorem 9.22]. Hence we already have a description of these idempotents that we also denote by JW and have used in (2.89).

CHAPTER 3

Idempotents for Soergel bimodules

The diagrammatic Hecke category was defined to be a Karoubian envelope. Its objects are characterized by idempotent morphisms. Every Soergel bimodule B_w can be found inside $\mathrm{BS}(\underline{w})$ for some reduced expression of w. Therefore, to understand the objects in the diagrammatic Hecke category, we need to compute idempotents. Specifically, to compute the categorical data of the asymptotic Hecke category associated to an H-cell, we need to compute all idempotents of elements thereof. In this chapter, we develop systematic techniques for the computation of idempotents and then use them on all chosen H-cells from the previous chapter.

The computational approach to idempotents presented here has not previously been made explicit in this form. The author is grateful to Ben Elias for sharing computational techniques during a research stay in 2022.

While a detailed treatment appears in the paper [21] with Ben Elias and Dani Tubbenhauer, we focus here on explicit calculations to get all idempotents of our chosen H-cells. We introduce notations that will also be part of [21, Section 3 and 4] particularly those essential to our setting.

In this chapter, (W, S) always denotes a Coxeter system and $\mathcal{H}$ the corresponding diagrammatic Hecke category. We write $i \in S$ instead of $s_i \in S$ and use the color code from (2.74).

3.1. Top idempotents and clasp idempotents

In the Temperley–Lieb category we have seen a complete description of all idempotents, see subsection 2.3.2. When an object X decomposes as a direct sum $X \simeq \bigoplus_j Y_j$, we require inclusion morphisms $i_j : Y_j \to X$ and projection morphisms $p_j : X \to Y_j$ satisfying the relations $p_k \circ i_l = \delta_{k,l} \mathrm{id}_{Y_k}$ and $\sum_j (i_j \circ p_j) = \mathrm{id}_X$. This is exactly the general definition of a direct sum in a category, see Definition 2.1.

We wish to do the same for Soergel bimodules. We remember, that for every $w \in W$, we have an indecomposable Soergel bimodule B_w. Our goal is to construct an idempotent inside $\mathrm{End}_{\mathcal{H}}(\mathrm{BS}(w))$ corresponding to B_w.

Definition 3.1. Let X be an object of $\mathcal{H}$. We say that B_w is a *top summand* of X if we have chosen a decomposition of X into indecomposable direct summands, such that (a summand isomorphic to) B_w appears once, and all other summands are (isomorphic to) shifts of B_y for $y < w$. That is,

$$X \simeq B_w \oplus \bigoplus_{y<w} B_y^{\oplus n_y}, \tag{3.1}$$

for some graded multiplicities $n_y \in \mathbb{N}[v, v^{-1}]$, possibly zero.

When B_w is a top summand of X, we call X a *w-object*, and implicit in this notation is the choice of an explicit decomposition. In this case, the primitive idempotent $e \in \mathrm{End}_{\mathcal{H}}(X)$

whose image is isomorphic to B_w will be called a *top idempotent* (associated to this decomposition of X). Note that different decompositions of the same object X might produce different top idempotents.

In our diagrammatic notation, we represent top idempotents by rectangles: 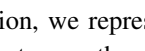

. Unlike in the Temperley–Lieb category, these top idempotents are not unique. There exist situations where an infinite family of distinct idempotents can describe the same B_w. We illustrate this phenomenon with the following example.

Example 3.2. Consider type $W = A_3$ with simple reflections $\{1, 2, 3\}$. Let $\underline{w} = (3, 1, 2, 1, 3)$, a reduced expression for $w = 31213$, and $y = 31$. Note that $B_y \cong B_1 B_3$. A straightforward computation in the Hecke algebra shows that $b_w = b_3 b_{121} b_3$, and consequently we can describe B_w inside $X = B_w$ as the image of the following top idempotent e:

(3.2)

This construction takes the (top) idempotent inside $B_{(1,2,1)}$ from the dihedral case, projects it to B_{121}, and tensors on the left and right with the identity maps of B_3.

The Bott–Samelson bimodule decomposes as $\mathrm{BS}(w) \simeq B_w \oplus B_y(+1) \oplus B_y(-1)$. By the Soergel Hom formula, we compute $\mathrm{rk}_{\mathbb{Z}[v^{\pm 1}]}(\mathrm{Hom}^\bullet(B_w, B_y)) = v + 3v^3 + 3v^5 + v^7$. This implies that $\dim \mathrm{Hom}(\mathrm{BS}(w), \mathrm{BS}(w)) = 2$ in degree 0, where the space is spanned by the identity on B_w and a composition of maps $\mathrm{BS}(w) \to B_w \to B_y(+1)$ and $B_y(-1) \to \mathrm{BS}(w)$. Define the following morphisms:

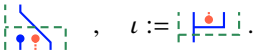

(3.3)

Note that $e \circ \iota = 0$ by the pitchfork rule of the dihedral idempotent. This is expected, as the map has degree -1 but lies in $\mathrm{Hom}(B_y, B_w)$ whose minimal degree is $+1$.

These maps combine to give a family of idempotents for B_w. For any scalar λ, consider:

$e + \lambda(\iota \circ g \circ e) =$ 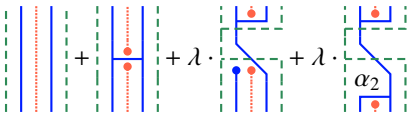

(3.4)

The fact that this is an idempotent for any λ follows from the computation:

$$(e + \lambda(\iota \circ g \circ e))^2 = e + \lambda(\iota \circ g \circ e) \circ e + \lambda e \circ (\iota \circ g \circ e) + \lambda^2 (\iota \circ g \circ e) \circ (\iota \circ g \circ e) = e + \lambda(\iota \circ g \circ e),$$

where we use that $e \circ \iota = 0$.

This issue arises because $\mathrm{BS}((3, 1, 2, 1)) = B_{3121} \oplus B_{31}$, and the final tensor product with B_3 introduces the grading shift. If we had constructed the idempotent from B_{3121}, we would obtain uniqueness. This motivates our preferred approach: constructing idempotents inductively, step by step. While it is possible to construct elements w with grading shifts inside $\mathrm{BS}(w)$ that still yield unique top idempotents, it is most natural to restrict our attention to degree zero objects.

Definition 3.3. A w-object X is called *perverse* if

$$X \cong B_w \oplus \bigoplus_{y<w} B_y^{\oplus n_y}, \tag{3.5}$$

where $n_y \in \mathbb{N}$ (i.e., the summands appear without grading shifts).

Remark 3.4. The terminology "perverse" for such objects follows the convention in [18, Section 2], where this concept is introduced as part of the theory of perverse cohomology on Soergel bimodules. We will return to this more general perspective in chapter 4.

As we will demonstrate, perverse objects always yield unique idempotents.

Example 3.5. Let $x \in W$ and $i \in S$ such that $w = xi > x$. Then $B_x B_i$ is a perverse w-object, which follows from Remark 1.16. This explains the observation following Example 3.2: $B_{3121} \otimes B_3 \cong B_{31213}$, where $B_{3121} \otimes B_3$ is a $w = 31213$-object.

Let X be a w-object and $\underline{y}$ an expression of length lower than $\ell(x)$. We denote maps between X and $B_{\underline{y}}$ by trapezoids:

$$g : X \to B_{\underline{y}} \leftrightarrow \boxed{g}, \quad h : B_{\underline{y}} \to X \leftrightarrow \boxed{h} \tag{3.6}$$

By a corollary of the Soergel Hom formula, Corollary 2.42, any element of $\mathrm{End}(X)$ can be written as a linear combination of the identity id_X or morphisms of the form:

$$\begin{array}{|c|}\hline g \\ \hline h \\ \hline \end{array} \tag{3.7}$$

In other word, the collection of id_X and such trapezoid compositions form a basis of $\mathrm{End}(X)$ as a (left) R-module. For $f \in \mathrm{End}(X)$ we write $\kappa(f)$ for the *identity coefficient* of f, that is, the coefficient of id_X in the expansion of f as an R-linear combination of basis elements. We also write $\mathrm{Hom}^0_{<w}(X, X)$ for the degree zero morphisms of $\mathrm{End}(X)$ factoring over a lower word, i.e. the compositions of trapezoids of degree zero.

Lemma 3.6. *Let X be a w-object and $e \in \mathrm{End}(X)$ a top idempotent. Then for any $\mathbf{h} \in \mathrm{End}^0(X)$ we have*

$$\begin{array}{|c|}\hline e \\ \hline h \\ \hline e \\ \hline \end{array} = \kappa(h) \cdot \boxed{e}. \tag{3.8}$$

Proof. It is enough to show this statement for all basis elements of $\mathrm{End}(X)$, as this diagrammatic morphism is defined to be a linear combination of either id_X or compositions of trapezoids. For the identity the statement is trivial, as e is assumed to be an idempotent.

Let now $g : X \to B_{\underline{y}}$, $f : B_{\underline{y}} \to X$ be trapezoid morphisms. Since $\kappa(f \circ g) = 0$, we wish to show the composition with the idempotent is also zero. If either g or f has non positive degree one part of the composition is already zero by Corollary 2.42. If, for example $\deg(g) \leq 0$, then already

$$\begin{array}{|c|}\hline g \\ \hline e \\ \hline \end{array} = 0, \tag{3.9}$$

since there is no negative degree morphism $B_w \to B_{\underline{y}}$. By assumption $\deg(h) = 0$, hence we always have this case. □

Corollary 3.7. *A direct application of Lemma 3.6 is, that $\kappa(e) = 1$ for any top idempotent e.*

In the diagrammatic Hecke category the composition with positive degree morphisms does not always work in the same way. Idempotents which have these properties work similar to Jones–Wenzl projectors and give us a very nice computable way to construct them. Such idempotents we give a special name.

Definition 3.8. Let $w \in W$ and X be a w-object. An element $e \in \mathrm{End}^0(X)$ is called a *clasp idempotent* if it satisfies the following two properties:

(A) The identity coefficient of e is 1, that is,

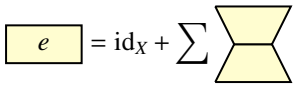

(3.10)

(B) Precomposition and postcomposition with e annihilates all degree 0 morphisms factoring through $v < w$, that is,

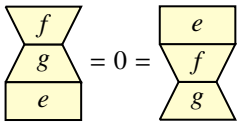

(3.11)

whenever $\deg(f) + \deg(g) = 0$.

Example 3.9. These clasp idempotents do not always exist, we have seen a counterexample already in Example 3.2. There we saw, that there is an infinite family of top idempotents for w, namely $\{e + \lambda(\iota \circ g \circ e)\}$. Hence, $\iota \circ g \circ \neq 0$, contrary to the condition (3.11).

Theorem 3.10. *Let $w \in W$ and X be a w-object. If a clasp idempotent $e \in \mathrm{End}^0(X)$ exists, then it is unique and is an idempotent in the usual sense:*

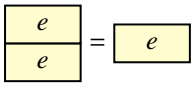

(3.12)

Moreover, e is preserved under vertical reflection:

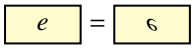

(3.13)

Proof. The idempotent property follows from (3.11):

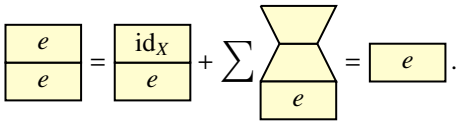

(3.14)

For uniqueness, let $\tilde{e}$ be a second clasp idempotent. By (3.10), we have that $e - \tilde{e}$ is a linear combination of morphisms factoring through smaller elements. Using the defining properties, we calculate:

$$e - e\tilde{e} = e(e - \tilde{e}) = 0 = (e - \tilde{e})\tilde{e} = \tilde{e} - e\tilde{e}, \tag{3.15}$$

which proves uniqueness for a fixed reduced expression. □

Theorem 3.11. *Let $w \in W$ and X be a w-object. The following are equivalent:*

(A) *The clasp idempotent exists.*
(B) *The top idempotent is unique.*

Proof. $\Rightarrow$: Suppose a clasp idempotent e exists. We show that any top idempotent equals e. Let e' be any top idempotent. We extend e' to a complete idempotent decomposition of the identity:

$$\mathrm{id}_X = e' + \sum_j q_j, \tag{3.16}$$

where the q_j are mutually orthogonal idempotents. Their images are therefore isomorphic to $v^k B_y$ for various $y < w$ and $k \in \mathbb{Z}$.

Since $q_j \in \mathrm{Hom}^0_{<w}(X, X)$ and e is a clasp idempotent, we have by (3.11) that $e \circ q_j = 0$ for all j. Therefore:

$$e = e \circ \mathrm{id}_X = e \circ e' + \sum_j e \circ q_j = e \circ e'. \tag{3.17}$$

By the same argument, precomposing with id_X gives:

$$e = \mathrm{id}_X \circ e = e' \circ e + \sum_j q_j \circ e = e' \circ e. \tag{3.18}$$

Combining these equations we get:

$$e = e \circ e' = e' \circ e = e' \circ e \circ e'. \tag{3.19}$$

Now, we can identify $e'\,\mathrm{End}(X)e'$ with $\mathrm{End}(B_w)$ in the usual way (the image of e' is isomorphic to B_w). By the Soergel Hom formula (see Corollary 2.42), we know that $\mathrm{End}^0(B_w)$ is one-dimensional, spanned only by the identity map. Therefore, the only nonzero idempotent in $\mathrm{End}(B_w)$ is the identity itself, which corresponds to the idempotent $e' \in \mathrm{End}^0(X)$ under this identification. Hence $e' \circ e \circ e' = e'$, so $e = e'$ since $e' \circ e \circ e' = e'$. This proves that the top idempotent is unique.

$\Leftarrow$: Suppose the top idempotent e is unique. We will show that e is also a clasp idempotent. By definition, e is an idempotent with identity coefficient $\kappa(e) = 1$, so condition (1) of Definition 3.8 is satisfied. It remains to verify condition (2), namely that e annihilates $\mathrm{Hom}^0_{<w}(X, X)$.

Suppose for contradiction that there exists $g \in \mathrm{Hom}^0_{<w}(X, X)$ with $g \circ e \neq 0$. We will now construct more idempotents, showing that this case can never occur. This works in the same way as Example 3.2. We can write g as a linear combination:

$$g = \sum_i \lambda_i f_i \circ h_i, \tag{3.20}$$

where $f_i : B_{y_i} \to X$ and $\mathbf{h}_i : X \to B_{y_i}$ with $y_i < w$ and $\deg(f_i) + \deg(h_i) = 0$ and $\lambda_i \in \mathbb{R}$.

Since $g \circ e \neq 0$, at least one composition $\mathbf{h}_i \circ e \neq 0$. Let $p : X \to B_w$ denote the projection morphism corresponding to the top idempotent e (so that $e = \iota \circ p$ where $\iota : B_w \to X$ is the inclusion). Then $\mathbf{h}_i \circ e = (h_i \circ \iota) \circ p$ gives a nonzero element in $\mathrm{Hom}(B_w, B_{y_i})$. By the Soergel Hom formula, $\mathrm{Hom}^{\leq 0}(B_w, B_{y_i}) = 0$ for $y_i < w$. Since $\deg(h_i \circ e) = \deg(h_i)$ and $\mathbf{h}_i \circ e \neq 0$, we must have $\deg(h_i) > 0$. Consequently, $\deg(f_i) < 0$. Since $\deg(f_i) < 0$, we have $e \circ f_i = 0$ by Corollary 2.42, as there are no negative degree morphisms from B_{y_i} to B_w.

Let $f := f_i \circ h_i \circ e \in \mathrm{Hom}^0_{<w}(X, X)$. Then:

- $f \circ e = f_i \circ h_i \circ e \circ e = f_i \circ h_i \circ e = f$ (since e is idempotent),
- $e \circ f = e \circ f_i \circ h_i \circ e = 0$ (since $e \circ f_i = 0$),
- $f^2 = f \circ e \circ f = f \circ 0 = 0$.

For any scalar $\lambda \in \mathbb{R}$, consider $e' := e + \lambda f$. We compute:

$$\begin{aligned}
(e')^2 &= (e + \lambda f)^2 && (3.21)\\
&= e^2 + \lambda ef + \lambda fe + \lambda^2 f^2 && (3.22)\\
&= e + \lambda \cdot 0 + \lambda f + \lambda^2 \cdot 0 && (3.23)\\
&= e + \lambda f = e'. && (3.24)
\end{aligned}$$

Thus e' is an idempotent for any choice of λ. Moreover, since $f \in \mathrm{Hom}^0_{<w}(X, X)$, we have $\kappa(e') = \kappa(e + \lambda f) = \kappa(e) = 1$. To verify that e and e' have isomorphic images, we check:

$$e \circ e' \circ e = e \circ (e + \lambda f) \circ e = e^2 + \lambda efe = e + \lambda \cdot 0 = e, \tag{3.25}$$

$$e' \circ e \circ e' = (e + \lambda f) \circ e \circ (e + \lambda f) = e + \lambda fe = e + \lambda f = e'. \tag{3.26}$$

Therefore, e' is another top idempotent for any $\lambda \neq 0$, contradicting uniqueness. This contradiction shows that $g \circ e = 0$ for all $g \in \mathrm{Hom}^0_{<w}(X, X)$. By a symmetric argument (or by applying vertical reflection, which preserves all relevant properties by Lemma 3.6), we also have $e \circ g = 0$ for all $g \in \mathrm{Hom}^0_{<w}(X, X)$.

Therefore, e satisfies both conditions of Definition 3.8 and is a clasp idempotent. □

Our goal is to work with arbitrary reduced expressions for any word. By the theory of Coxeter groups, all reduced expressions are related by rex moves, which correspond to degree 0 maps in the diagrammatic Hecke category. We denote these rex moves by purple strips in our diagrams. For a w-object X and two reduced expressions $\underline{w}, \underline{w}'$, we have B_w as a summand of both. The rex moves provide an isomorphism, and by (3.11) we have:

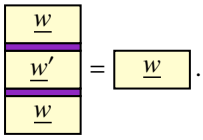

(3.27)

For a detailed treatment of rex moves, we refer to [21]. In what follows, we will make all calculations explicit. The next section focuses on the algorithmic construction of idempotents.

3.2. Inductive computation of idempotents

The key insight driving our approach is that idempotents can be computed inductively, building them step by step. For any element $w \in W$ with reduced expression $\underline{w}$, we construct clasp idempotent e_w by using idempotents of smaller length. This process requires careful tracking of summands that appear at each step of the form $B_v \otimes B_i$. To organize this information efficiently, we introduce the branching graph structure.

Definition 3.12. For a given Coxeter system (W, S), the *branching graph* $\Gamma(W, S)$ is an oriented graph where:

- The vertices are in bijection with elements of W.
- For every summand B_y appearing in the decomposition of $B_x B_i$, we add an i-colored edge from x to y.

Thus, the branching graph encodes all the decompositions $B_x \otimes B_i \simeq \bigoplus B_w^{m_w}$ for $x \in W, s \in S$.

Definition 3.13. Let $\underline{w} = (i_1, \ldots, i_n)$ be a reduced expression for $w \in W$. We write w_m for the element $s_{i_1} \ldots s_{i_m}$ and $N(w_m)$ for the set of all elements x such that B_x appears as a summand of $B_{w_m} \otimes B_{i_{m+1}}$. The *branching graph* $\Gamma(\underline{w})$ is the subgraph of $\Gamma(W, S)$ constructed as follows:

- We include all vertices w_m and $N(w_m)$.
- We include all edges corresponding to the products $w_m \to x$ for $x \in N(w_m)$.

We say that $\Gamma(\underline{w})$ is *linear* if $N(w_m)$ lies in $\{w_{m-1}, w_{m+1}\}$ for all m. Moreover:

- If $N(w_m)$ contains only w_{m+1}, we say w_m is of *type 1* otherwise we say it is of *type 2*.

Note that by construction, $\Gamma(\underline{w}_m)$ is a subgraph of $\Gamma(\underline{w})$.

Example 3.14. Let (W, S) be of type $I_2(n)$. The branching graph of the longest word $\Gamma(w_0) = \Gamma(12\ldots)$ is linear, and its branching graph is:

$$\Gamma(w_0) = \quad \emptyset \rightleftarrows 1 \rightleftarrows 12 \rightleftarrows 121 \rightleftarrows 1212 \rightleftarrows \ldots \longrightarrow w_0 \ . \tag{3.28}$$

Here, the vertex labeled 1 is of type 1, while all vertices corresponding to longer words are of type 2.

If one chooses the other reduced expression $(2, 1, 2, \ldots)$ of w_0 the branching graph looks the same by interchanging the colors. We see that $\Gamma(\underline{w})$ depends on the chosen expression, however if we describe a word by its reflection directly we might drop the underline and write $\Gamma(w)$.

Algorithm 3.15. Let $\underline{w} = (i_1, \ldots, i_n)$ be a fixed reduced expression for an element $w \in (W, S)$, where $n = \ell(w)$ is the length of w. We compute $e = e_{\underline{w}}$ inductively over the length m, for $0 \leq m \leq n$. For each such m, we write $e_m := e_{\underline{w}_m}$, where $\underline{w}_m = (i_1, \ldots, i_m)$.

Initialization: If $n = 0$ we set $e_\emptyset = \mathrm{id}_{B_\emptyset}$, the empty diagram.

Inductive Step: Assume e_m has been constructed. We describe how we construct e_{m+1}.

(A) Compute $\Gamma(w_m)$ by adding all new vertices $N(w_m)$ to $\Gamma(w_{m-1})$. This corresponds to the decomposition

$$B_{w_m} \otimes B_{i_{m+1}} \simeq \bigoplus_{x \in N(w_m)} B_x^{n_x},$$

where $n_x \in \mathbb{N}$. We initially assume that we are multiplicity free, i.e. $n_x = 1$ (see Remark 3.18 for the general case).

(B) For each $x \in N(w_m)$, use the inductively constructed e_x to compute the unique (up to scalar) morphisms:

$p^x_{w_m, i_{m+1}} =$ 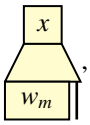

, $i^x_{w_m, i_{m+1}} =$ 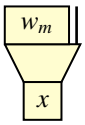

, (3.29)

where $p^x_{w_m, i_{m+1}} \in \mathrm{Hom}^0(B_{w_m} B_{i_{m+1}}, B_x)$ and $i^x_{w_m, i_{m+1}} \in \mathrm{Hom}^0(B_x, B_{w_m} B_{i_{m+1}})$. For $x = w_{m+1}$, we use the trivial middle trapezoid.

(C) Compute the scalar $\kappa_{x, w_{m+1}} \in \mathbb{R}$ satisfying:

$p^x_{w_m, i_{m+1}} \circ i^x_{w_m, i_{m+1}} =$ 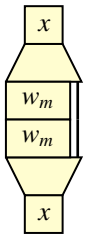

$= \kappa_{x, w_{m+1}} \cdot$ 

(3.30)

for all $x \in N(w_m)$. This is $\kappa_{x, w_{m+1}} = \kappa(p^x_{w_m, i_{m+1}} \circ i^x_{w_m, i_{m+1}})$. Note that $\kappa_{w_{m+1}, w_{m+1}} = 1$.

(D) Define e_{m+1} recursively as follows:

$$\boxed{e_{m+1}} := e_m \otimes \mathrm{id}_{i_{m+1}} - \sum_{x \in N(w_m)\setminus\{w_{m+1}\}} \kappa^{-1}_{x,w_{m+1}} \cdot i^x_{w_m,i_{m+1}} \circ p^x_{w_m,i_{m+1}}, \tag{3.31}$$

which can be expressed diagrammatically as:

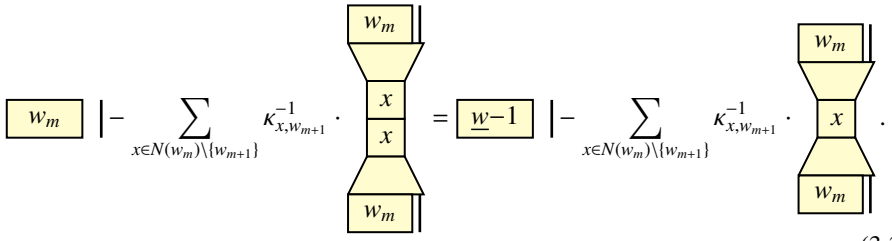

(3.32)

Remark 3.16. The scalar κ from (3.30) can be interpreted as the value of a local intersection form.

See for example [31, Section 3.4] for the computation of so called p-canonical basis, or [20, Section 11.5].

Proposition 3.17. *For any reduced expression $\underline{w} = (i_1, \ldots, i_n)$, Algorithm 3.15 produces a clasp idempotent $e_n \in \mathrm{End}^0(B_{w_{n-1}} \otimes B_{i_n})$.*

Proof. The statement follows from the properties established earlier in this chapter.

The decomposition (3.32) provides an orthogonal decomposition into $\bigoplus_{x \in N(\underline{w}_m)} B_x$ of $B_{w_m} \otimes B_{i_{m+1}}$. The orthogonality follows from the vanishing of homomorphisms $\mathrm{Hom}^0(B_x, B_{\tilde{x}}) = 0$ for distinct $x, \tilde{x} \in N(\underline{w}_m)$. Consequently:

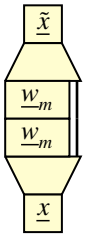

$= 0\,.$ (3.33)

Furthermore, by definition of $\kappa_{x,w_{m+1}}$, the composition $i \circ p$ is idempotent, since:

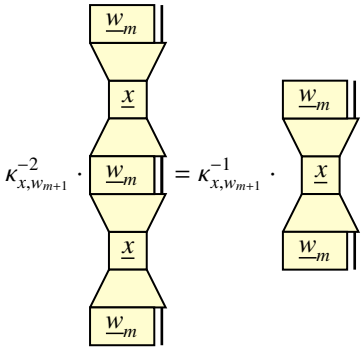

(3.34)

□

In particular, by Theorem 3.11 we obtain a top idempotent for every $w \in W$. The main challenges are now finding the unique projection and inclusion maps and computing the coefficients κ.

Remark 3.18. If we are not in the multiplicity-free case, i.e. in step (A) there was an $x \in N(w_m)$ such that $n_x > 1$, we proceed as in [20, Proposition 11.69]. Specifically, for $w := w_m$, $i := i_{m+1}$ and x where B_x occurs with multiplicity $n_x > 1$, the space $\mathrm{Hom}^0(B_w B_i, B_x)$ is n_x-dimensional. In this case, we select a collection of projection and inclusion maps and apply the algorithm presented there.

All examples considered here are multiplicity-free. Moreover, the scalars κ correspond to values of intersection forms as detailed in [20, Chapter 11].

Lemma 3.19. *Let $\underline{w} = (i_1, \ldots, i_{n+1})$ have a linear branching graph. If it is of type 2, the trapezoid map contains exactly one dot and one merge:*

$$p^{w_{n-1}}_{w_n, i_{n+1}} = \quad , \tag{3.35}$$

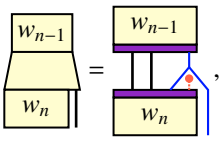

for appropriate rex moves. We use two different colors to emphasize that in a reduced expression, no reflection can appear consecutively (i.e., we never have $i_k = i_{k+1}$).

Proof. This follows from properties of the light leaves basis. We prove that the trapezoid must correspond to a light leaf having the U1 decoration $n-2$ times and exactly one U0 and one D0, with D0 occurring at the end. The total graded homomorphism space $\mathrm{Hom}(B_{w_n} B_{i_{n+1}}, B_{w_{n-1}})$ is constructed using terms of the form $LL(\underline{w}, \underline{e})$.

For degree reasons, we need at least $n-1$ U1's. Since we require a degree zero map, the remaining decoration must be either U0 and D1, or U1 and D1. However, a D1 decoration is only possible if the expression is not reduced or if we had a U0 decoration previously. Thus, we are in the first case. By the same reasoning, we deduce that D0 must occur after U0.

Since we precompose with e_{m-1}, the D1 decoration cannot appear in the first $n-1$ terms, as such a light leaf would vanish by the clasp properties. □

Note that the U0 decoration can appear at any position. In practice, when computing idempotents, one often finds that no $\underline{x}$ appears in the middle of (3.32). This frequently occurs when a trivalent vertex slides around the idempotents. In [21], this property is shown to hold in more general cases. We introduce it as a formal property and verify it in our constructions.

Definition 3.20. Let $\underline{w} = (i_1, \ldots, i_n)$ be a reduced expression for w and $j \in R(w)$, where $R(w)$ denotes the right descending set. We say that (e_w, j) satisfies *trivalent sliding* if:

$$\quad = \quad . \tag{3.36}$$

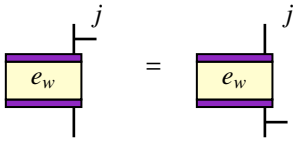

3.3. Examples of Idempotents

Having established the general theory, we now examine explicit computations of idempotents in several important cases. We focus particularly on cases arising from the cells classified in section 1.4.

3.3.1. Dihedral Groups. The dihedral groups $I_2(n)$ provide the simplest non-trivial examples where our construction yields interesting idempotents. As mentioned in subsection 2.4.4, these idempotents can be understood through their connection to the two-color Temperley–Lieb category. The branching graph structure, previously displayed in (3.28), guides our explicit calculations.

LEMMA 3.21. *In type $I_2(n)$ the idempotents e_w for w of length $m+1$ ending in* 21 *have the form:*

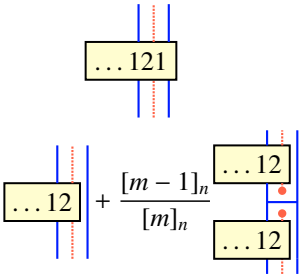

(3.37)

(3.38)

Further we have:

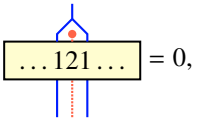

(3.39)

(3.40)

and

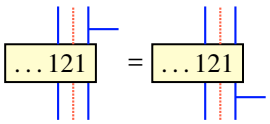

(3.41)

PROOF. This is the recursion formula (2.61) using the functor from Definition 2.51. □

We will also do this computation using Algorithm 3.15:

PROPOSITION 3.22. *Let (W,S) be of type $I_2(n)$. Consider elements w with length $l(w) = m+1 \geq 3$ ending in* 121. *Then the idempotent e_w can be computed explicitly using Algorithm 3.15 and has the form:*

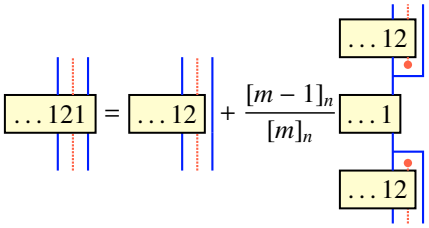

(3.42)

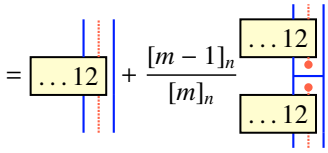

(3.43)

Moreover, these idempotents satisfy the trivalent sliding property (3.36).

Proof. We follow Algorithm 3.15 step by step:
1. Base Cases: We begin with the trivial idempotents:

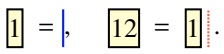

(3.44)

2. Light Leaves Structure: For any expression $\underline{w} = (\ldots, 1, 2)$, the projection $p^{w2}_{w,1}$ is given by the light leaves sequence $(1, \ldots, 1, 0, 0)$, placing U0 and D0 at the end:

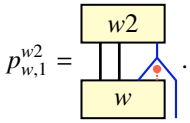

(3.45)

Note that $w2 < w$ is shorter than w.
3. Coefficient Computation: We compute $\kappa_{1,121}$ directly:

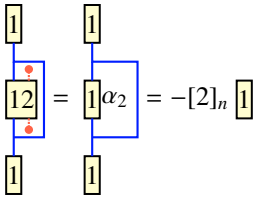

(3.46)

4. General Case: For longer elements, we compute:

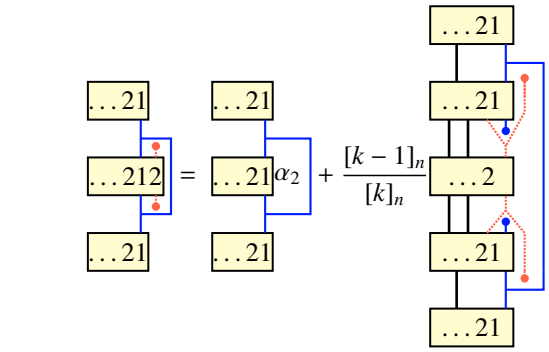

(3.47)

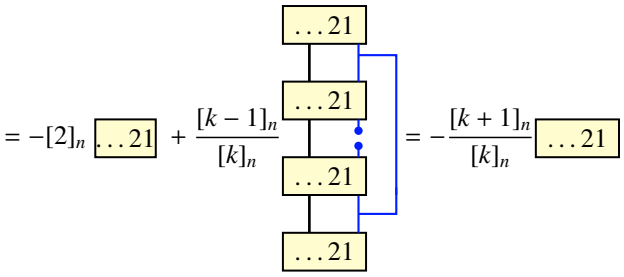

(3.48)

The final step uses trivalent sliding and then the quantum integer identity:

$$-[2]_n + \frac{[k-1]_n}{[k]_n} = \frac{-[2]_n[k]_n + [k-1]_n}{[k]_n} = \frac{-[k+1]_n}{[k]_n}.$$

The trivalent sliding property follows by induction on the length of w, as each step of the construction preserves this property. □

3.3.2. Type H_3. Having established the dihedral case, we now examine idempotents in type H_3. From the cell classification in subsection 1.4.3, we sort idempotents by their **a**-values.

3.3.2.1. *Elements of* **a***-value 1.* The J-cell of **a**-value 1 consists of $W_1 = \{1, 121, 2, 212, 3, 32123\}$. All idempotents except 32123 follow from the dihedral case. For 32123, we compute:

Proposition 3.23. *The branching graph for* 32123 *is linear:*

(3.49)

and the idempotents of W_1 have the form:

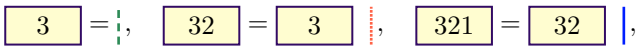

(3.50)

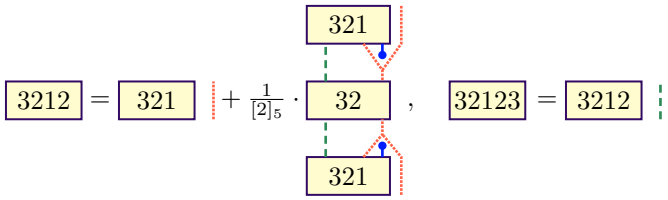

. (3.51)

Proof. Following Algorithm 3.15, we have one coefficient to compute. It works the same as in the dihedral case, but we do it once more as it involves a third color:

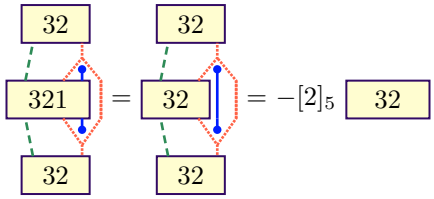

(3.52)

□

3.3.2.2. *Elements of* **a***-value 3.* For **a**-value 3, we focus on the H-cell $\mathbf{h}_3 = \{232, 232123\}$ identified in (1.62).

Proposition 3.24. *Let (W, S) be of type H_3 and $\underline{d} = 232$. The branching graph for $\underline{x} := \underline{d}123$ is linear:*

$$\Gamma(\underline{d}123) = \quad \emptyset \longrightarrow 2 \rightleftarrows 23 \longrightarrow \underline{d} \rightleftarrows \underline{d}1 \rightleftarrows \underline{d}12 \longrightarrow \underline{d}123 \tag{3.53}$$

The idempotents are:

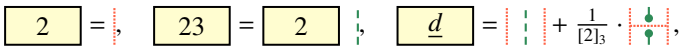

(3.54)

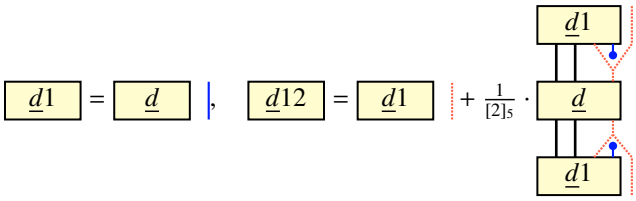

(3.55)

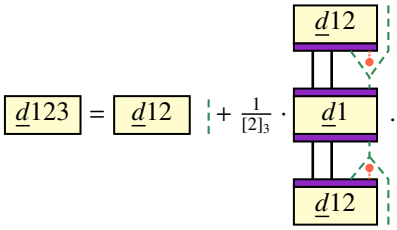

(3.56)

For the final step note that 232123 = 323123 = 321323.

Proof. Following Algorithm 3.15, we compute the critical coefficients. For $\kappa_{d,d12}$, this follows similar to from the calculation in (3.52).

For $\kappa_{d1,d123}$, we compute:

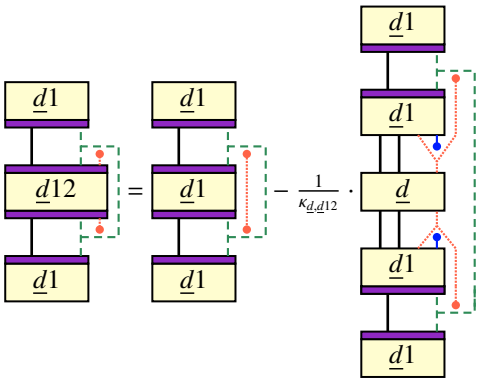

(3.57)

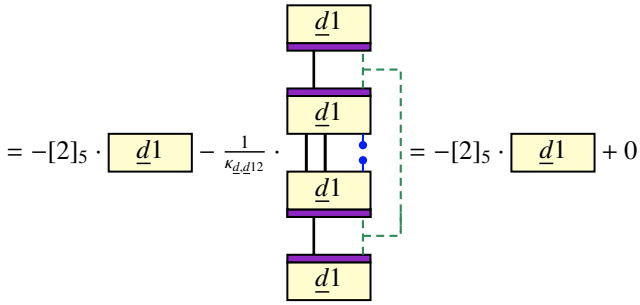

(3.58)

The final summand vanishes due to trivalent sliding and the needle relation:

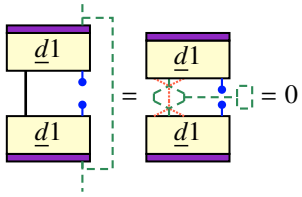

(3.59)

□

3.3.2.3. *Elements of* **a***-value* 6. For **a**-value 6, we encounter more complex computations due to the length of the expressions. The chosen H-cell is $\mathbf{h}_6 = \{1212132121, 12121321213212\}$.

Proposition 3.25. *Let* (W, S) *be of type* H_3. *For* $w := 12121321213212$, *the branching graph is:*

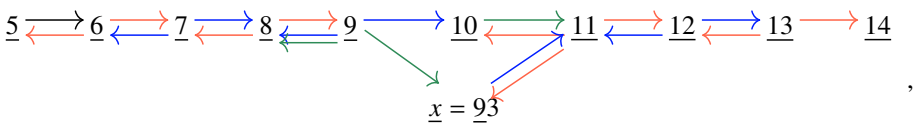

(3.60)

here $\underline{n}$ *is short for* $\underline{w}_n$. *We excluded the dihedral branching graph in the beginning. The idempotents have the form:*

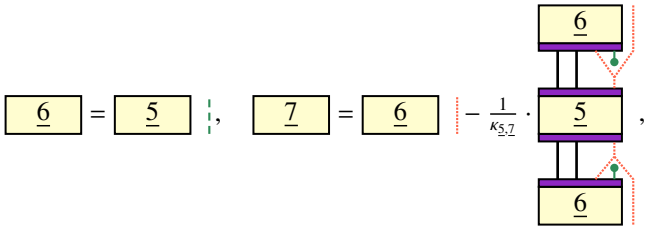

(3.61)

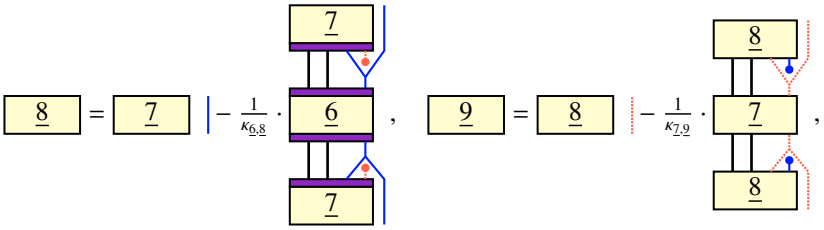

(3.62)

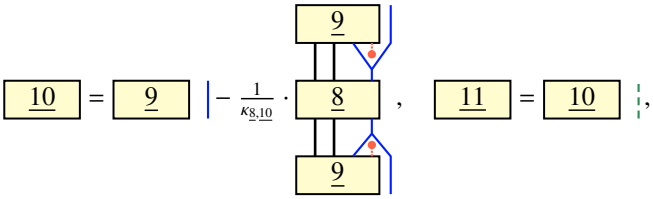

(3.63)

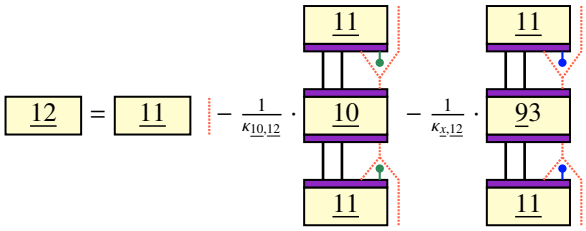

(3.64)

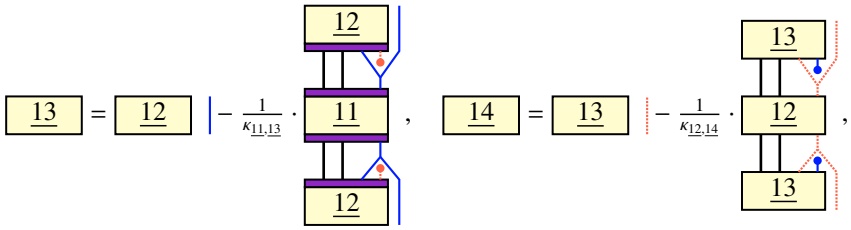

(3.65)

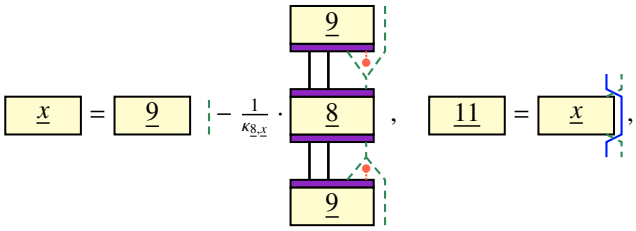

(3.66)

where the coefficients are

$$\kappa_{5,7} = \partial_2(\alpha_3) = [2]_3 = -1, \tag{3.67}$$

$$\kappa_{6,8} = \partial_1(\alpha_2) = [2]_5 = -\varphi, \tag{3.68}$$

$$\kappa_{7,9} = -\varphi + \tfrac{1}{\varphi} = \tfrac{-\varphi^2+1}{\varphi} = -1, \tag{3.69}$$

$$\kappa_{8,10} = \partial_2(\alpha_1) - \tfrac{1}{\kappa_{7,9}} = -\varphi + 1 = \tfrac{-\varphi^2+\varphi}{\varphi} = \tfrac{-1}{\varphi}, \tag{3.70}$$

$$\kappa_{8,x} = \partial_3(\alpha_2) = -1, \quad \kappa_{10,12} = \partial_2(\alpha_3) = -1, \tag{3.71}$$

$$\kappa_{x,12} = \tfrac{1}{\varphi}, \quad \kappa_{11,13} = 1, \quad \kappa_{12,14} = \varphi. \tag{3.72}$$

Here $\varphi = \frac{1+\sqrt{5}}{2}$ *is the golden ratio.*

The computation of these coefficients will be done in tandem with showing trivalent sliding for a couple of cases:

Lemma 3.26. *We have trivalent sliding for the following cases:*

(A) $(\underline{6}, \text{l})$, *(B)* $(\underline{7}, \text{i})$, *(C)* $(\underline{7}, \text{i})$.
(D) $(\underline{8}, \text{l})$, *(E)* $(\underline{8}, \text{i})$, *(F)* $(\underline{11}, \text{l})$.
(G) $(\underline{10}, \text{i})$, *(H)* $(\underline{x}, \text{i})$, *(I)* $(\underline{12}, \text{i})$.

These computations are detailed in [22], with code available in [16]. We need two additional diagrammatic relations which will be applied throughout the calculations.

Lemma 3.27. *The following relations hold in the diagrammatic Hecke category:*

(3.73)

(3.74)

Proof. Direct application of the defining relations. □

We now compute the idempotents step by step following Algorithm 3.15, verifying trivalent sliding at each stage.

Proof of Lemma 3.26, Case (A). We use induction on the computation of $\underline{6}$ to obtain:

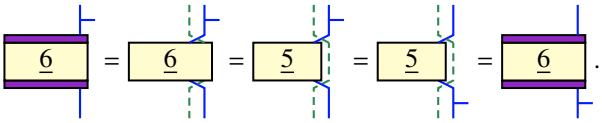

(3.75)

This result follows from the fact that Lemma 3.26 holds for $(\underline{5}, \mathrm{I})$. □

Computation of $\kappa_{\underline{5},\underline{7}}$. The rex move is a 5-valent vertex, therefore we compute:.

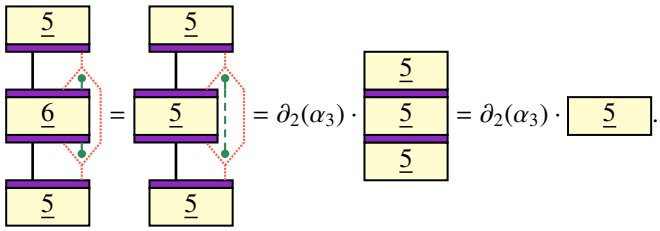

(3.76)

Since $\partial_2(\alpha_3) = [2]_3 = -1$, we conclude that $\kappa_{\underline{5},\underline{7}} = -1$. □

Computation of $\kappa_{\underline{6},\underline{8}}$. We employ a recursion seen in Proposition 3.24, and apply Lemma 3.26 for $\underline{6}$ and the blue strand.

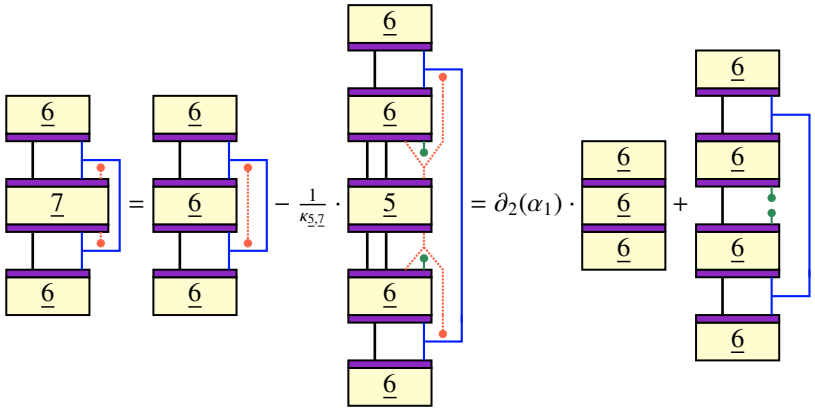

(3.77)

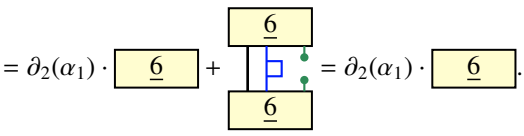

(3.78)

The rex moves around $\underline{6}$ consist solely of a 2-valent vertex from $(\ldots, 1, 3)$ to $(\ldots, 3, 1)$; therefore, by the needle relation, the last term vanishes. Given that $\partial_2(\alpha_1) = [2]_5 = -\phi$ we conclude $\kappa_{\underline{6},\underline{8}} = \frac{1}{\phi}$. □

Proof of Lemma 3.26, Case (B). This result follows from the recursion formula for $\underline{7}$, as Lemma 3.26 holds for $(\underline{5}, \mathrm{I})$. □

Computation of $\kappa_{\underline{7},\underline{9}}$. Recursion on

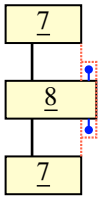

(3.79)

gives again two terms. The first results in

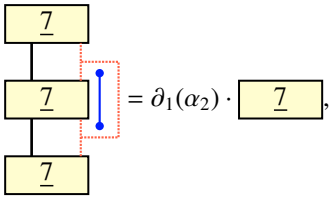

(3.80)

while the second term computes to

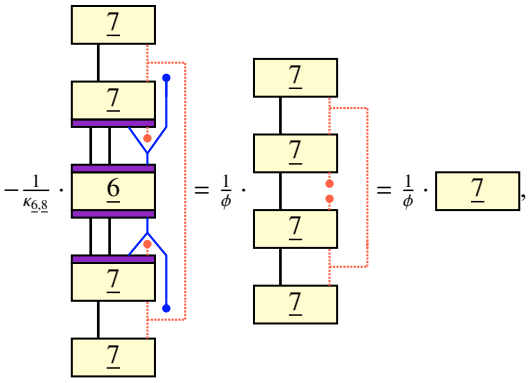

(3.81)

using Lemma 3.26, Case (B). In total we obtain $-\phi + \frac{1}{\phi} = \frac{-\phi^2+1}{\phi} = -1$ for $\kappa_{\underline{7},\underline{9}}$. □

Proof Lemma 3.26, Case (D). Use apply the recursion of $\underline{8}$ and Case (A). □

Computation of $\kappa_{\underline{8},\underline{10}}$. The computation follows a similar pattern to that of $\kappa_{\underline{7},\underline{9}}$. In this case we have no rex moves, and we must apply Lemma 3.26, Case (D), to obtain $\partial_2(\alpha_1) - \frac{1}{\kappa_{\underline{7},\underline{9}}} = -\phi + 1 = \frac{-\phi^2+\phi}{\phi} = \frac{-1}{\phi}$. □

Proof of Lemma 3.26, Case (C). We apply the recursion to $\underline{7}$ and then compose with the rex moves. This, combined with the recursion on $\underline{6}$ and the relation (3.73), yields the

following result.

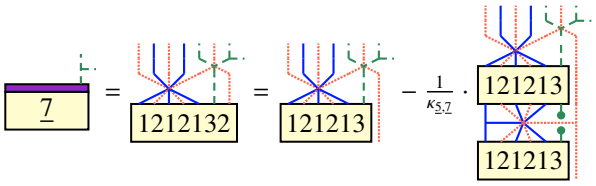

(3.82)

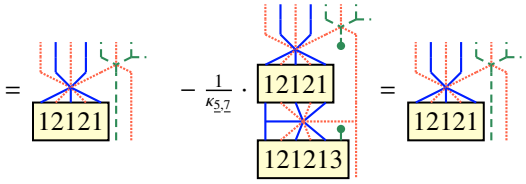

(3.83)

Adding the same rex moves as the bottom and using two-color associativity we get our statement:

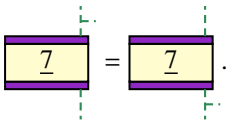

(3.84)

The proof is complete. □

Proof of Lemma 3.26, Case (E). We calculate:

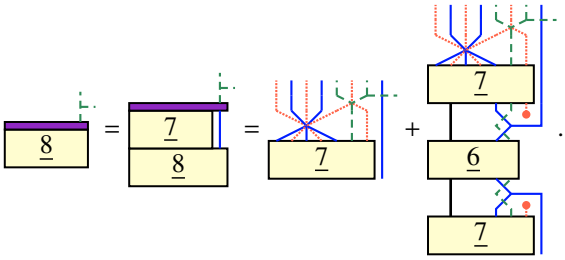

(3.85)

For the first term, we can apply induction, specifically Case (C). In the second term, we also employ induction, incorporation additional rex moves.

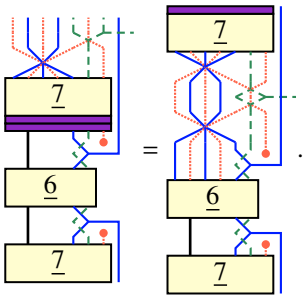

(3.86)

We simplify using the two-color dot contraction:

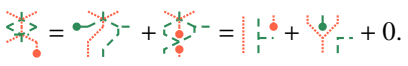

(3.87)

The zero term arises by a needle relation. If we now plug this into (3.86) one term is eliminated due to the pitchfork relation. The remaining term yields:

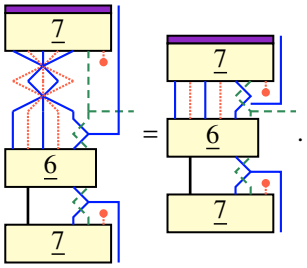

(3.88)

Now, we can use induction to push green around $\underline{6}$. This demonstrates that the diagram is symmetric, i.e., we obtain the same result when starting with a trivalent vertex at the bottom:

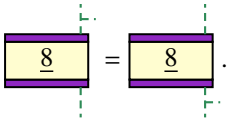

(3.89)

This case is therefore done. □

Computation of $\kappa_{\underline{8},x}$. This works similarly to the calculation of $\kappa_{\underline{7},\underline{9}}$. We obtain one diagram from the tower of idempotents of $\underline{8}$, which gives a term $\partial_3(\alpha_2) = -1$. The second term is derived by induction:

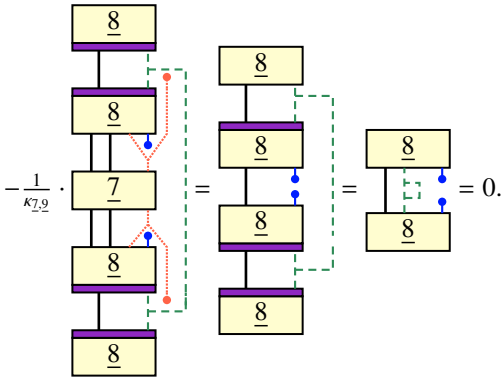

(3.90)

Here we used Lemma 3.26, Case (E). This gives $\kappa_{\underline{8},x} = -1$. □

Computation of $\kappa_{\underline{10},\underline{12}}$. From this point forward, we are no longer linear. Consequently, we must be more careful with the rex moves. In this case, note that the rex moves needed do not involve the last reflection. We use the following rex moves: $121213212132 = 121231212132 = 121232121232$ Hence, by induction, we quickly obtain:

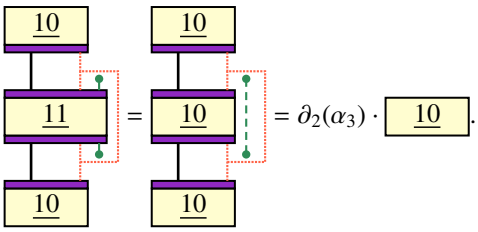

(3.91)

Therefore, we conclude that $\kappa_{\underline{10},\underline{12}} = -1$. □

Computation of $\kappa_{\underline{x},\underline{12}}$. This computation is more complex, as it involves significantly more rex moves. First, we use recursion for the idempotent $\underline{12}$:

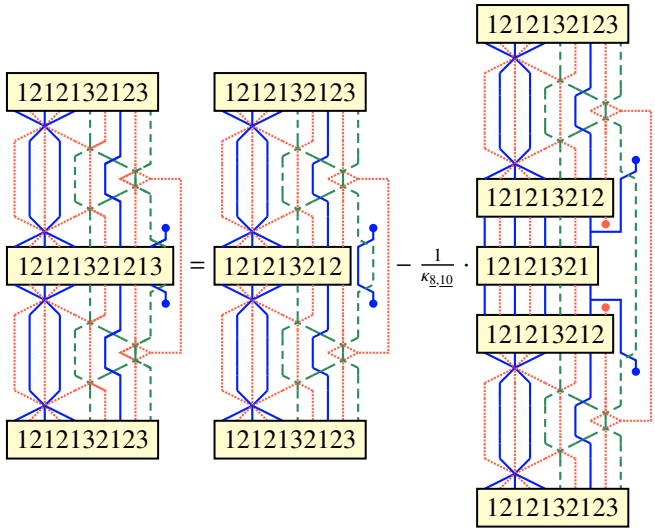

(3.92)

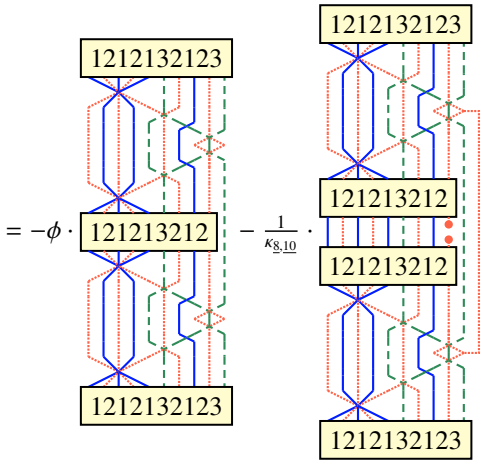

(3.93)

For term (A), we first simplify the rex moves in the second component using two-color associativity.

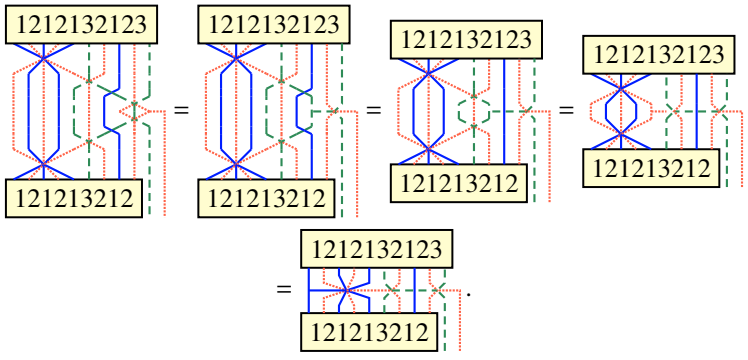

(3.94)

Applying the recursion formula to $\underline{9}$ yields:

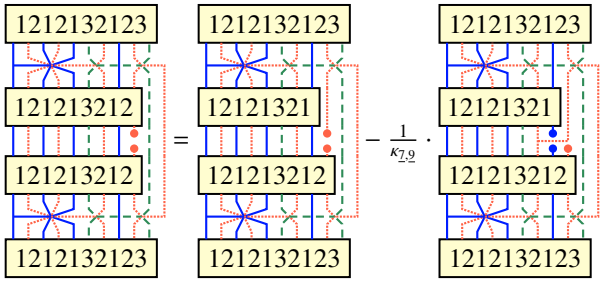

(3.95)

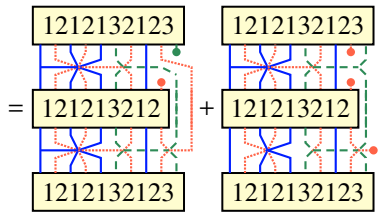

(3.96)

The middle term contains a pitchfork in the top right corner and, therefore, is zero. Specifically, after applying rex moves, we obtain a subterm of the form:

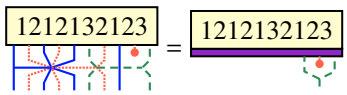

(3.97)

For the first term, we apply the recursion formula of $\underline{9}$ to obtain:

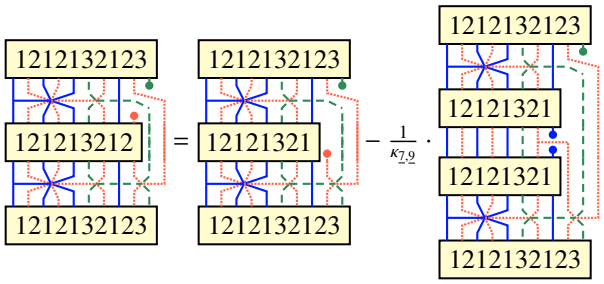

(3.98)

The first term resulting from this operation will equal zero after the two-color dot contraction, due to either a needle or pitchfork relation. We can apply Lemma 3.26, Case (E), in this context.

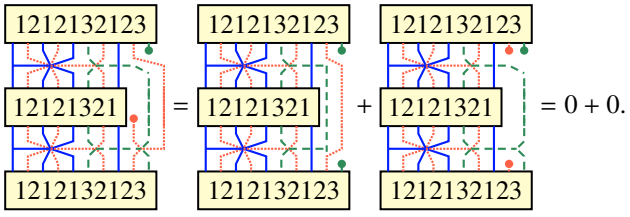

(3.99)

Applying Lemma 3.26, Case (E) to the second term similarly yields a pitchfork on the bottom. Returning to term (B) of (3.95), we apply recursion to $\underline{8}$ and use Lemma 3.26,

Case (B), which gives:

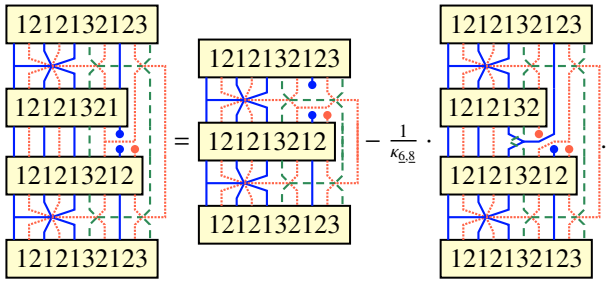

(3.100)

For the first term, we apply the recursion formula of $\underline{9}$ to obtain:

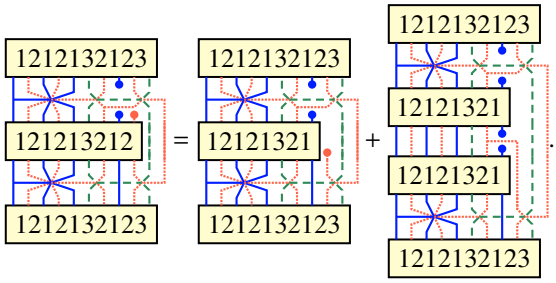

(3.101)

The first term resulting from this operation will equal zero, following the same reasoning as in equation (3.99). The two-color dot contraction produces two terms: one where Lemma 3.26 yields a needle relation, and another that includes a pitchfork. For the second term, we apply the recursion formula to the $\underline{8}$ term at the top to obtain:

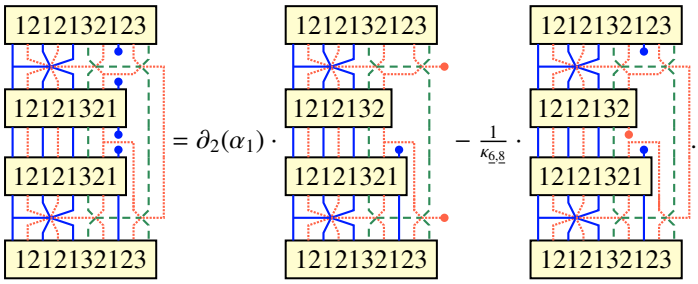

(3.102)

The first summand will equal zero, following the same arguments as in (3.99), using the needle and pitchfork relations. For the second summand, we move red around $\underline{7}$, retract the idempotent, and consequently obtain a pitchfork. This leaves us with the second summand of (3.100). In this case, we apply Lemma 3.26 to ($\underline{7}$,), which yields the following picture for the top part:

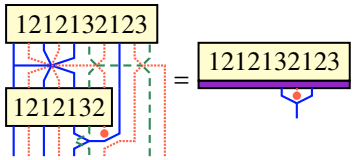

(3.103)

Consequently, all terms originating from (3.3.2.3) evaluate to zero, leading to the result $\frac{1}{\kappa_{\underline{x},12}} = \frac{1}{\phi}$. □

Proof of Lemma 3.26, Case (F). This result can be derived directly from Case (D) using the recursion formula for $\underline{11}$, given that the green and blue colors commute in the diagram.

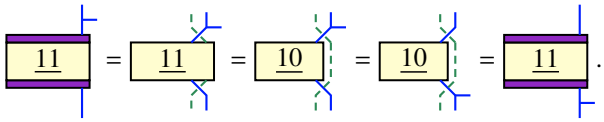

(3.104)

Thus, this case is done. □

Computation of $\kappa_{\underline{11},\underline{13}}$. Only one rex move is required in this case: $121213212\underline{132} = 121213212312$. Based on this, we proceed with the following computation:

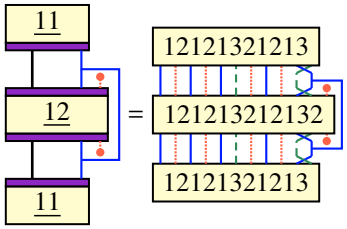

$$= \partial_1(\alpha_2) \cdot \boxed{\underline{11}} + (A) + (B), \tag{3.105}$$

where we have:

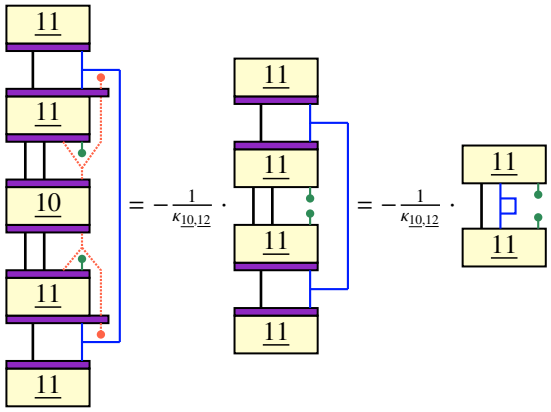

(3.106)

On the other hand, we have:

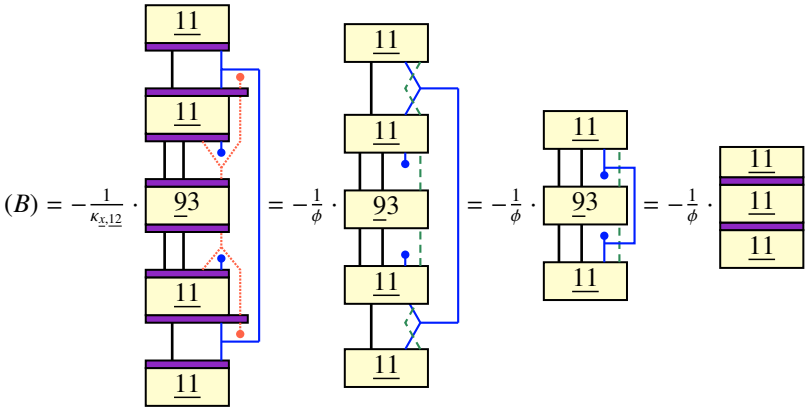

(3.107)

$$= -\frac{1}{\phi} \cdot \boxed{\underline{11}}, \tag{3.108}$$

which therefore gives $\frac{-1}{-\phi+\frac{1}{\phi}} = \frac{-1}{\left(\frac{-\phi^2+1}{\phi}\right)} = 1$ for $\kappa_{\underline{11},\underline{13}}$. □

Proof of Lemma 3.26, Case (G). We will build up to our statement step by step using induction. First we show:

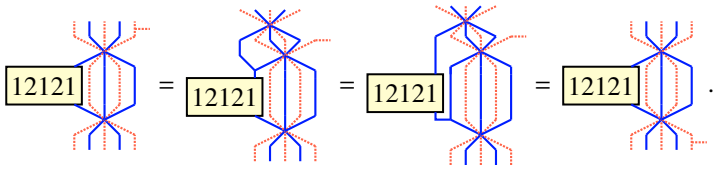

(3.109)

In the same way we get:

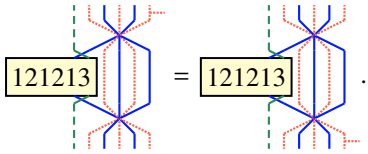

(3.110)

Now we consider a similar statement for $\underline{7}$. We use recursion to get:

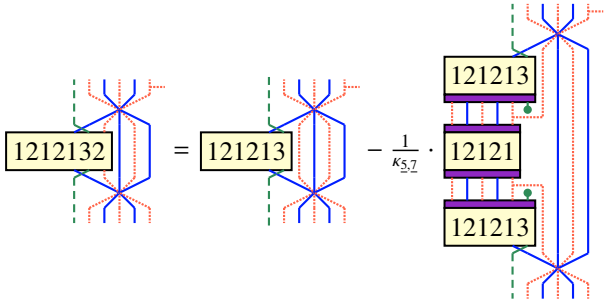

(3.111)

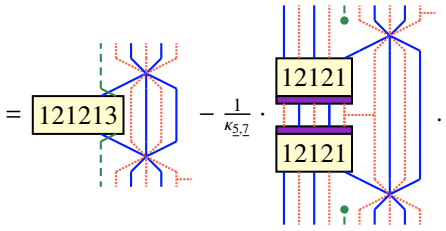

(3.112)

For the first term, we apply induction. For the second term, we employ an argument similar to that in (3.109), utilizing additional two-color associativity to establish the same symmetry. Analogous calculations can be performed for $\underline{8}$:

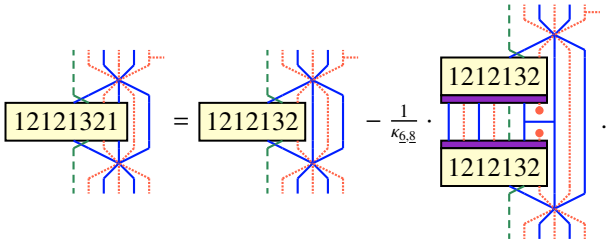

(3.113)

On the first term we use induction, expanding the second term gives some pitchforks, the only nonzero diagram is:

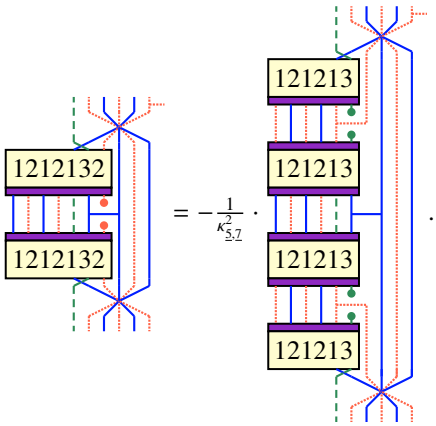

(3.114)

In the middle we get a α_3 term by the barbell relation. Breaking it through any red line nearby also yields a pitchfork and therefore also zero. By a similar induction, although with a few more terms we can show

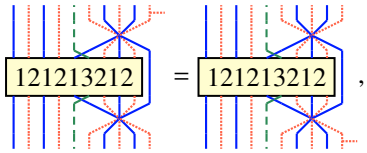

(3.115)

and also

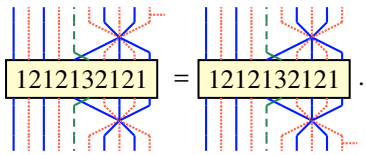

(3.116)

□

Proof of Lemma 3.26, Case (H). Similar to the proof of Case (G), we can compute the following statements step by step using the recursion formulas. Manual calculations produce an even greater number of terms than in previous cases.

(i)

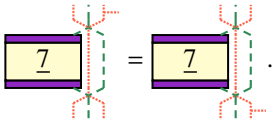

(3.117)

(ii)

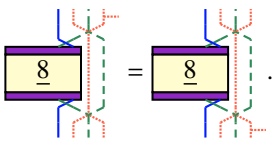

(3.118)

(iii)

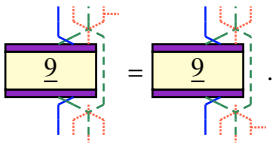

(3.119)

(iv)

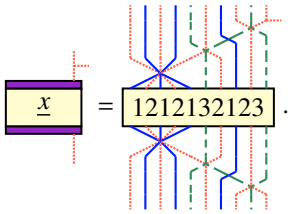

(3.120)

This case is therefore also complete. □

Proof of Lemma 3.26, Case (I). By the recursion of $\underline{12}$ this reduces to cases (G) and (H). □

Computation of $\kappa_{\underline{12},\underline{14}}$. Finally, we compute

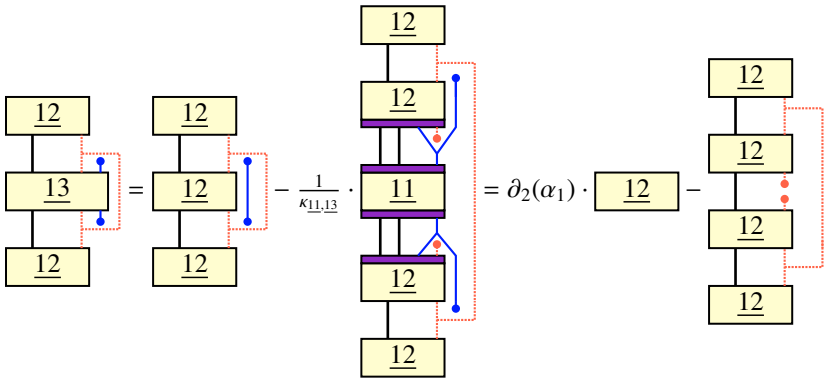

(3.121)

$$= \partial_2(\alpha_1) \cdot \boxed{\underline{12}} - \boxed{\underline{12}}. \tag{3.122}$$

Here the last equality is due to Lemma 3.26, Case (I). In total we get $\frac{-1}{-\phi+1} = \phi$ for $\kappa_{\underline{12},\underline{14}}$. □

3.3.3. Type H_4. Many cells in type H_4 allow us to reuse the idempotent constructions from type H_3. Specifically, for elements of **a**-value 1 and 3, we can choose the same representatives as in type H_3 and apply our previous computations.

The new case appears in the cell $\mathcal{H}_2 = \{\underline{d} = 31, \underline{d}2143\}$ identified in subsection 1.4.4. Here, we choose $\underline{d} = 31$ to minimize the number of rex moves needed in our computation.

Proposition 3.28. *The branching graph for $\underline{d}2143$ exhibits a linear structure:*

$$\Gamma(\underline{d}2143) = \quad \emptyset \dashrightarrow 3 \longrightarrow 31 = \underline{d} \rightleftarrows \underline{d}2 \longrightarrow \underline{d}21 \dashrightarrow \underline{d}214 \dashrightarrow \underline{d}2143 \ . \tag{3.123}$$

The idempotents are:

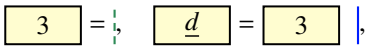

(3.124)

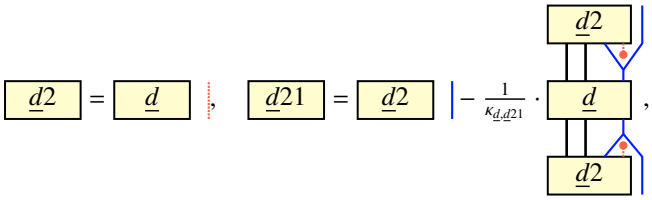

(3.125)

(3.126)

Proof. Here $\kappa_{\underline{d},\underline{d}21} = \partial_1(\alpha_2) = -[2]_5$, since:

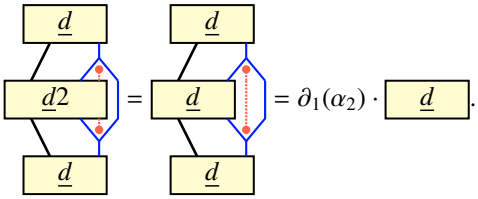

(3.127)

□

3.3.4. Idempotents in the subregular cell. For elements of **a**-value 1 (the subregular cell), the classification in subsubsection 1.4.5.1 shows these are precisely elements with unique reduced expressions. By the observations of Lemma 3.19, this means our idempotent construction requires no rex moves, at least when ignoring potential summands from higher cells (see Remark 3.30).

Lemma 3.29. *Let (W,S) be a Coxeter system and $w := (i_1,\dots,i_{n-2},i_{n-1},i_n)$ a reduced expression. The branching graph $\Gamma(\underline{w})$ contains an edge $\underline{w}_{n-1} \to \underline{w}_{n-2}$ if and only if $i_{n-2} = i_n$. We may have edges to elements having higher* **a***-value.*

Proof. The structure follows from analysing possible light leaves maps. If $B_{\underline{w}_{n-2}}$ is a summand of $B_{\underline{w}_{n-1}} \otimes B_{i_n}$ we can find a light leave, i.e. a degree zero projection map in between. Since $\underline{w}_n$ admits a single reduced expression this contains no rex moves. Following the argumentation of Lemma 3.19 we need $i_{n-2} = i_n$. □

One should keep in mind that an element of **a**-value 1 is characterized by the subexpression being a path inside the Dynkin diagram. Only at such a zigzag move we get smaller summands also lying in the subregular cell. It should be noted that we find cases with summands in bigger cells quite easily:

Remark 3.30. The appearance of summands from higher J-cells is intrinsic to the structure and cannot be avoided in general. Consider the triangle group $W := \Delta(3,3,4)$, defined by the presentation:

$$\langle s_1, s_2, s_3 \mid s_1^2 = s_2^2 = s_3^2 = (s_1s_2)^4 = (s_1s_3)^3 = (s_2s_3)^3 = 1\rangle. \tag{3.128}$$

In the Hecke algebra $\boldsymbol{H}(W)$, we have the decomposition:

$$b_{12312}b_1 = b_{123121} + b_{1231} + b_{1212}, \tag{3.129}$$

where b_{1212} has **a**-value 4, higher than all other terms. The corresponding idempotent takes the form:

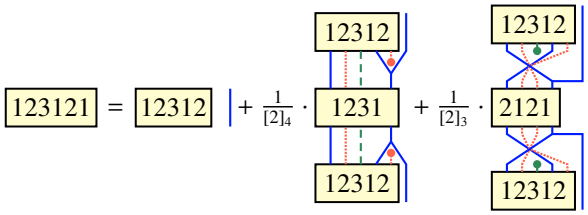

(3.130)

This example demonstrates that even in relatively simple cases, idempotents may require terms from higher cells.

Other than that we can describe the idempotents using the knowledge from the dihedral case, at least if we ignore summands in higher cells.

LEMMA 3.31. *Let* $\underline{w} := (i_1, \dots, i_n)$ *be a reduced expression of a subregular element such that* $i_{n-2} = i_n$. *Let* $l = m_{i_{n-1}, i_{n-2}}$ *and* k *be unique natural number such that the last* $k+1$ *terms of* $\underline{w}$ *are alternating between* i_n *and* i_{n-1}. *Then we have:*

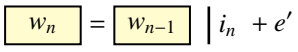

(3.131)

for e' *a possible idempotent corresponding to objects in higher cells. If* $i_{n-2} = i_n$ *we have:*

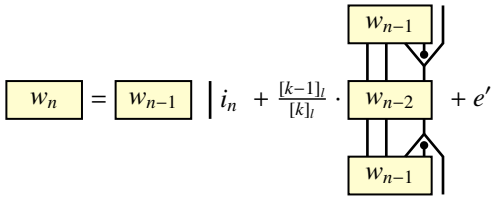

(3.132)

where e' *again is a possible idempotent corresponding to objects in higher cells. Further* k *is defined such that the last* $k+1$ *terms of* $\underline{w}$ *alternate between* i_{n-1} *and* i_n *and we have* $m_{i_{n-1}, i_n} = l$.

PROOF. This is the same computation as in the dihedral case of Proposition 3.22. Note, that if for a smaller $n' < n$ an idempotent of a bigger cell occurs, all other summands with this idempotent lie also in a bigger cell. Hence it is enough to consider subregular elements in $N(w)$. □

3.3.4.1. *Subregular cell in* H_4. The cell of **a**-value 1 contains 32 elements. One can check that here no exception of Lemma 3.31 holds. Hence as an application of Lemma 3.31 we have a description of all idempotents in W_1. As one example consider the element $\underline{w} = (4, 3, 2, 1, 2, 3, 4)$:

(3.133)

and the idempotents are:

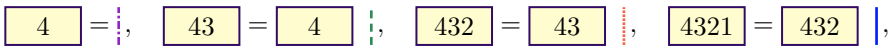

(3.134)

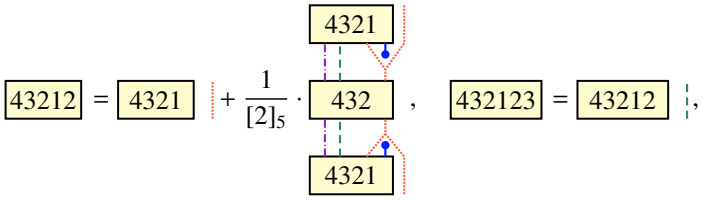

(3.135)

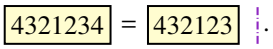

(3.136)

3.3.5. Idempotents in a(2)-finite Coxeter Groups. We give descriptions of idempotents for all H-cells with cardinality greater than 1 as seen in Proposition 1.64 using previous results.

3.3.5.1. *Type $\tilde{C}_n$, B_n and H_n.* In type $\tilde{C}_n$, we focus on the H-cell $\mathbf{h} = \{24, 2124, 2z, 212z\}$ where $z = 45\ldots(n-1)n(n-1)\ldots4$ as classified in Proposition 1.64. A key observation simplifies our computation:

Remark 3.32. Since no reflection of number 3 appears in these expressions, computing idempotents in $\mathcal{H}$ reduces to computing idempotents for two **a**-value 1 cells:

(A) The dihedral cell $\{2, 212\}$.
(B) The zigzag cell $\{4, z\}$.

Both cases are covered by Lemma 3.31. The full idempotents are then tensor products of these simpler cases:

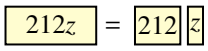

(3.137)

In the same way one can describe the idempotents in type B_n and H_n.

3.3.5.2. *Type F_n.* Finally, we examine the H-cell $\mathbf{h} = \{24, 243524\}$. The branching graph is:

(3.138)

Proposition 3.33. *The corresponding idempotents are computed using the techniques developed in section 3.2:*

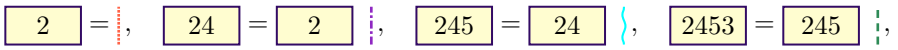

(3.139)

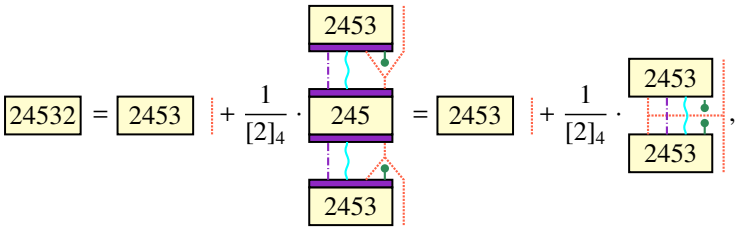

(3.140)

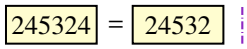

(3.141)

We have now constructed all idempotents corresponding to the H-cells of section 1.4. In the next chapter we give the construction of the asymptotic Hecke category.

CHAPTER 4

The asymptotic Hecke category

After the introductory chapters, we now have all the tools to define the asymptotic Hecke category associated to a two-sided Kazhdan–Lusztig cell in a Coxeter group. This was first motivated in [50, Section 10.1].

We will first see that replicating the construction of the asymptotic algebra poses challenges. While in the J-ring we could simply take the lowest graded summand, in the categorical setting we need inclusion and projection morphisms which are not unique. The solution to this problem comes from ideas of Elias–Williamson [18]. Hard Lefschetz for Soergel bimodules provides an isomorphism between the highest and lowest perverse cohomology of a tensor product. When working in a slight modification of the category of Soergel bimodules, this produces the categorification we seek.

4.1. Motivational problems

Example 4.1 ([18, Example 2.1]). For any Coxeter system (W, S) the reflections lie in the cell of **a**-value 1 (see Remark 1.35). For any $s \in S$ we have $b_s b_s = (v + v^{-1})b_s$ which gives $j_s j_s = j_s$ in the J-ring (see Definition 1.21). In the categorical setting of Soergel bimodules, we would like a similar construction that projects and includes to the degree -1 part.

The decomposition $B_s \otimes B_s \simeq B_s(-1) \oplus B_s(+1)$ is not canonical. We saw one possibility in Example 2.45:

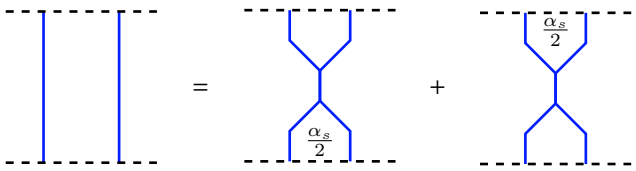

(4.1)

Naming the projections and inclusions i_{+1}, i_{-1} and p_{+1}, p_{-1} we can define alternatives. For any $\lambda \in \mathbb{R}$, we can modify these maps:

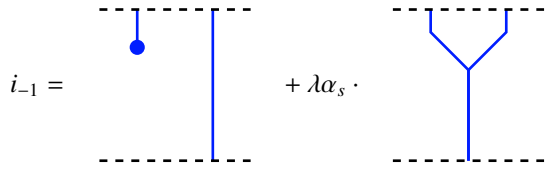

(4.2)

$p_{+1} =$ 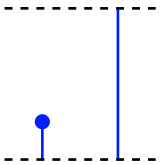 $+ (1-\lambda)\alpha_s \cdot$ 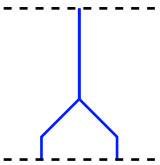 (4.3)

For $\lambda = \frac{-1}{2}$ we recover the original decomposition. The extra term vanishes when composing i_{-1} with p_{+1} (and vice versa) due to the needle relation. This shows that $B_s(-1)$ does not have a canonical inclusion into $B_s \otimes B_s$.

This example demonstrates why we cannot naively replicate the construction of the J-ring by using projection and inclusion onto and into the lowest graded summand. Instead, we will use the Lefschetz and Hodge results of Elias–Williamson to resolve this non-uniqueness.

4.2. Hard Lefschetz for Soergel bimodules

The challenge we encountered earlier arises from the non-canonicity of the decomposition of tensor products in the category of Soergel bimodules. Following Theorem 2.41 and the observations from Remark 1.16 any Bott–Samelson bimodule $\mathrm{BS}(\underline{w})$ exhibits a symmetry: every summand appearing with a positive grading must also appear with a negative grading. This suggests a deeper relationship between highest and lowest degree parts.

The general theory, developed by Elias and Williamson in [23, 18], uses the concept of hard Lefschetz for Soergel bimodules to exploit this symmetry. Their work not only provided a powerful tool for relating highest and lowest degree parts but also led to a proof of the unimodality of Kazhdan–Lusztig polynomials. In this section, we explain their results and show how this machinery enables us to define the asymptotic Hecke category.

4.2.1. Hard Lefschetz. Hard Lefschetz is a concept from geometry with applications in representation theory. In our context, it provides the key tool for relating the highest and lowest degree parts of Soergel bimodules, resolving the non-canonicity issues described earlier. Let us fix our notation following [20, Chapter 17.2].

In the general setting, we have a fixed finite-dimensional $\mathbb{Z}$-graded $\mathbb{R}$-vector space $H = \bigoplus_{i\in\mathbb{Z}} H^i$ together with a symmetric nondegenerate graded bilinear form $\langle -,-\rangle : H\otimes H \to \mathbb{R}$. Here, nondegeneracy means that the map $h \mapsto \langle -, h\rangle$ induces an isomorphism. The form being graded bilinear means $\langle H^i, H^j\rangle = 0$ if $i \neq j$, hence we always have an isomorphism $H^{-i} \simeq (H^i)^*$.

Definition 4.2. An operator $L \in \mathrm{End}_{\mathbb{R}}(H)$ of degree 2 is called a *Lefschetz operator* if $\langle La, b\rangle = \langle a, Lb\rangle$ for all $a, b \in H$. If furthermore $L^i : H^{-i} \to H^i$ is an isomorphism for all i, the operator is said to satisfy *hard Lefschetz*.

Definition 4.3. For a Lefschetz operator L, we define the *Lefschetz form* on H^{-i} via

$$(a,b)_L^{-i} := \langle a, L^i b\rangle \tag{4.4}$$

for all $a, b \in H^{-i}$.

An operator satisfying hard Lefschetz is equivalent to saying that the morphism

$$H^{-i} \xrightarrow{L^i} H^i \xrightarrow{x\mapsto\langle -,x\rangle} (H^{-i})^* \tag{4.5}$$

is an isomorphism $H^{-i} \simeq (H^{-i})^*$.

The Lefschetz operator chosen in the following sections requires additional structure – namely, certain positive or negative definite properties. This requirement arises from *Hodge theory* and is crucial for the results of [23]. Without these positivity conditions, the construction of [18] would not be possible.

Definition 4.4. For L a Lefschetz operator on H satisfying hard Lefschetz, we define the *primitive subspaces*

$$P_L^{-i} \coloneqq \ker(L^{i+1}) \cap H^{-i}. \tag{4.6}$$

The space H then admits a decomposition

$$H = \bigoplus_{i\geq 0} \bigoplus_{i\geq j\geq 0} L^j(P_L^{-i}) \tag{4.7}$$

and each component decomposes as

$$H^{-i} = P_L^{-i} \oplus L\left(P_L^{-i-2}\right) \oplus L^2\left(P_L^{-i-4}\right) \oplus \cdots. \tag{4.8}$$

For an H that is concentrated in odd or even degree, we say that $(H, \langle -, - \rangle, L)$ satisfies the *Hodge-Riemann bilinear relations* if the restriction of the Lefschetz form $(-,-)_L^{m+2i}\big|_{P_L^{m+2i}}$ is $(-1)^i$-definite, where m denotes the minimal degree of H.

One can then show that the Lefschetz form is either positive (or $(+1)$-definite) or negative ((-1)-definite), namely on $L^k(P_L^{-i-2k})$ it is $(-1)^{j+k}$-definite. This additional structure is crucial in Elias and Williamson's proof. They establish hard Lefschetz and Hodge–Riemann for all Soergel bimodules through induction over the length of the element.

This theory will be crucial for our construction of the asymptotic Hecke category. The Hard Lefschetz theorem for Soergel bimodules will provide canonical isomorphisms between highest and lowest degree parts, allowing us to define well-behaved projection and inclusion maps. The Hodge-Riemann relations ensure these maps have the desired positivity properties needed for categorification.

4.2.2. Intersection forms on Soergel bimodules. Finding the right description of Lefschetz operators for Soergel bimodules is not straightforward. The main problem was seen in subsection 2.1.4, where we do not have a canonical decomposition into direct summands. The workaround that Elias and Williamson found was to introduce perverse cohomology on Soergel bimodules, which allows us to talk about perverse filtrations and then use the cohomology spaces.

While Soergel bimodules are graded by definition, considering a Soergel bimodule B as an $\mathbb{R}$-vector space (rather than an R-module) yields an infinite-dimensional vector space. To handle this, we construct a bilinear form by considering only the highest degree part of fixed basis of B as an R-module. Consider a fixed expression $\underline{w} = (s_1, \ldots, s_m)$. For each subexpression $e = (e_1, \ldots, e_m) \in \{0,1\}^m$, we define

$$c_e \coloneqq c_{s_1}^{e_1} \otimes \cdots \otimes c_{s_m}^{e_m},$$

where $c_s^0 = 1 \otimes 1$ and $c_s^1 = \frac{\alpha_s}{2} \otimes 1 + 1 \otimes \frac{\alpha_s}{2}$ in $B_s = R \otimes_R R(1)$ (see [20, Section 12.1]). The set $\{c_e \mid e \subset w\}$ forms a right (and left) R-module basis for $\mathrm{BS}(\underline{w})$, called the 01-*basis*.

Definition 4.5. For a Bott–Samelson bimodule $\mathrm{BS}(\underline{w})$ we define the *trace* as

$$\mathrm{BS}(\underline{w}) \to R,\ b \mapsto \mathrm{tr}(b), \tag{4.9}$$

where $\mathrm{tr}(b)$ is the coefficient of $c_{\underline{w}}$ (the top element where all $e_i = 1$) when b is expanded in the 01-basis. For elements $a, b \in \mathrm{BS}(\underline{w})$ we can then define the intersection form

$$\langle a, b \rangle_{\underline{w}} \coloneqq \mathrm{tr}(ab). \tag{4.10}$$

Example 4.6. On BS(s) the pairing has the following Gram matrix in the 01-basis:

	c_0	c_1
c_0	0	1
c_1	1	α_s

Table 4.1. Intersection form on BS(s).

Remark 4.7. A fundamental result of [23] shows that every Soergel bimodule admits a unique (up to positive scalar) non-degenerate invariant form. The proof proceeds as follows:

First, one shows that every Bott–Samelson bimodule admits a non-degenerate invariant form using the trace. For any $x \in W$, one can then restrict this form to the summand B_x and prove it remains non-degenerate.

The proof of non-degeneracy is a major achievement of [23] and relies crucially on positivity properties. The key insight is that for any polarized Soergel bimodule B (one equipped with a non-degenerate intersection form), the intersection form behaves well under induction, and the induced form on BB_s inherits important positivity properties.

Example 4.8. For a polarized Soergel bimodule $(B, \langle -, - \rangle_B)$, we have a canonical isomorphism with its dual $\mathbb{D}B := \mathrm{Hom}^\bullet_{-,R}(B, R)$ given by

$$B \cong \mathbb{D}B : b \mapsto \langle -, b \rangle. \tag{4.11}$$

In particular, we always have $\mathbb{D}B_x \cong B_x$. For B_s, this can be verified directly from the Gram matrix in Example 4.6.

Example 4.9. Let us extend Example 4.6 to BS((s, s)). Computing in the 01-basis gives:

	c_{00}	c_{01}	c_{10}	c_{11}
c_{00}	0	0	0	1
c_{01}	0	0	1	α_s
c_{10}	0	1	1	α_s
c_{11}	1	α_s	α_s	α_s^2

Table 4.2. Intersection form on BS((s, s))

This example illustrates the inductive structure mentioned in Remark 4.7. After an appropriate basis change, the matrix takes the form

$$\begin{pmatrix} \partial_s(G_s) & G_s \\ G_s & \alpha_s G_s \end{pmatrix}, \tag{4.12}$$

where G_s is the Gram matrix of the intersection form on B_s. When restricting to the summands $B_s(-1)$ and $B_s(+1)$ as in Equation 4.1, we obtain a non-generated form.

4.2.3. Perverse cohomology of Soergel bimodules. Having established the intersection form on Soergel bimodules, we can now introduce the perverse filtration and cohomology as in [18, Section 2]. These concepts, inspired by perverse sheaves, provide the key tools for relating the highest and lowest degree parts of Soergel bimodules. Soergel bimodules will mostly be denoted by $B_x(m) \in \mathbb{S}\mathrm{Bim}$.

In Definition 3.3 we defined a perverse w-object. More generally we can say:

Definition 4.10. We call a Soergel bimodule B *perverse* if its character $\mathrm{ch}(B)$ can be written as a sum $\sum a_x b_x$ for $a_x \in \mathbb{Z}$ without grading shifts (see [18, Section 2]).

For any $i \in \mathbb{Z}$, we define full additive subcategories of $\mathbb{S}\mathrm{Bim}$ that capture different grading ranges:

$$\begin{aligned} \mathbb{S}\mathrm{Bim}^{\leq i} &:= \langle B_x(m) \mid x \in W, m \geq -i \rangle_{\oplus,\cong}, \\ \mathbb{S}\mathrm{Bim}^{>i} &:= \langle B_x(m) \mid x \in W, m < -i \rangle_{\oplus,\cong}. \end{aligned} \tag{4.13}$$

Here we use the notation from subsection 2.4.2 for the additive and shift closure.

Similarly, we define $\mathbb{S}\mathrm{Bim}^{<i}$ and $\mathbb{S}\mathrm{Bim}^{\geq i}$. The category of *perverse Soergel bimodules*, denoted ${}^{p}\mathbb{S}\mathrm{Bim} := \mathbb{S}\mathrm{Bim}^{\geq 0} \cap \mathbb{S}\mathrm{Bim}^{\leq 0}$, consists precisely of the perverse objects from Definition Definition 4.10.

Any Soergel bimodule $B \in \mathbb{S}\mathrm{Bim}$ decomposes as $B \cong \bigoplus_{i \in \mathbb{Z}, x \in W} B_x^{\oplus m_{x,i}}(i)$ for non-negative integers $m_{x,i}$. This decomposition allows us to define:

$$\tau_{\leq i}(B) := \bigoplus_{j \geq -i, x \in W} B_x^{\oplus m_{x,j}}(j) \in \mathbb{S}\mathrm{Bim}^{\leq i} \tag{4.14}$$

This gives rise to the *perverse filtration* on B:

$$\ldots \subset \tau_{\leq i} B \subset \tau_{\leq i+1} B \subset \ldots \tag{4.15}$$

Dually, we define $\tau_{\geq i} B := B / \tau_{\leq i-1} B \in \mathbb{S}\mathrm{Bim}^{\geq i}$ which yields the *perverse cofiltration*:

$$\ldots \twoheadrightarrow \tau_{\geq i} B \twoheadrightarrow \tau_{\geq i+1} B \twoheadrightarrow \ldots \tag{4.16}$$

The *perverse cohomology* of a Soergel bimodule B is then defined as:

$$H^i(B) := (\tau_{\leq i} B / \tau_{\leq i-1} B)(i) \tag{4.17}$$

Example 4.11. Let us examine the Bott–Samelson bimodule $B := \mathrm{BS}((s,s)) \cong B_s(+1) \oplus B_s(-1)$ for $s \in S$. Using the perverse filtration, we obtain:

i	≥ 1	0	-1	≤ -2
$\tau_{\leq i} B$	B	$B_s(+1)$	$B_s(+1)$	$\{0\}$
$\tau_{\geq i} B$	$\{0\}$	$B_s(-1)$	$B_s(-1)$	B

Table 4.3. Perverse filtration of $\mathrm{BS}(s,s)$.

This yields the following perverse cohomology:

i	≥ 2	1	0	-1	≤ -2
$H^i(B)$	0	B_s	0	B_s	0

Table 4.4. Perverse cohomology groups of $\mathrm{BS}((s,s))$.

Perverse cohomology provides a natural setting for hard Lefschetz operators, as demonstrated in the following theorem:

Theorem 4.12 (Relative Hard Lefschetz for Soergel bimodules, [18, Theorem 1.2]). *Let $x, y \in W$ be arbitrary and let $\rho \in \mathfrak{h}^*$ be the dominant regular element fixed in subsection 1.1.3. The multiplication map*

$$\eta : B_x \otimes_R B_y \to B_x \otimes_R B_y(2),\ b \otimes b' \mapsto b \otimes \rho b' = b\rho \otimes b' \tag{4.18}$$

induces isomorphisms (for all $i \geq 0$)

$$\eta^i : H^{-i}(B_x \otimes_R B_y) \xrightarrow{\sim} H^i(B_x \otimes_R B_y). \tag{4.19}$$

Example 4.13. Consider again BS(s, s) from Example Example 4.11. The (-1)-degree part is spanned by c_{00}, and the Lefschetz form with respect to ρ gives:

$$(c_{00}, c_{00})_L^{-1} = \langle c_{00}, \rho \cdot c_{00} \rangle = \langle c_{00}, \frac{\alpha_s}{2} c_{00} \rangle = \partial_s \left(\frac{\alpha_s}{2} \right) = 1 \tag{4.20}$$

This form is nondegenerate and positive definite, as expected from the choice of ρ as a dominant regular weight.

4.3. Construction of the asymptotic Hecke category

This section describes the construction of the asymptotic Hecke category as a categorification of the $\mathcal{J}$-ring. Following the approach of Elias and Williamson, we illustrate the construction steps in small examples and explain all needed structures.

Hidden in this subsection are non-trivial associators. While it might seem that a strict category such as the diagrammatic Hecke category cannot give a non-strict category we will get a non-strict one in all non-trivial cases. This will be the main focus of section 4.4.

The asymptotic category was also constructed in [51, Section 3.2]. However no associator data is computed there.

4.3.1. Motivation and more obstacles. We return to the motivating problem from the beginning of this chapter. The primary obstacle in categorifying the $\mathcal{J}$-ring construction lies in the asymmetry of morphisms: while projections onto $B_s(-1)$ are unique up to scalar, inclusions are not. Theorem 4.12 resolves this issue by providing a canonical isomorphism between the lowest and highest graded parts, once ρ is fixed. The new tensor product structure we will construct uses this isomorphism of perverse cohomology together with the (up to scalar) unique projections and inclusions. However, following [18, Theorem 5.1], we must first pass to certain subcategories and quotients, as we can no longer work inside the full diagrammatic Hecke category.

Example 4.14. We continue Example 4.11 in type $W = A_1$. Here, $\rho = \frac{\alpha_s}{2}$ is dominant regular since $\langle \rho, \alpha_s^\vee \rangle = 1$. For $B := B_s \otimes_R B_s$, the map $\eta^1 : H^{-1}(B) \to H^1(B)$ arises from the diagram

$$\begin{array}{ccc} \tau_{\leq -i}B/\tau_{\leq -i-1}B & \xrightarrow{\eta^i} & \tau_{\leq i}B/\tau_{\leq i-1}B \\ \text{canonical inclusion}\downarrow & & \uparrow\text{canonical projection} \\ B & \xrightarrow[\eta^i]{} & B \end{array} \tag{4.21}$$

modulo grading shifts. In terms of diagrams, this yields the identity on B_s:

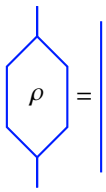

(4.22)

Indeed, for any $\rho = a\alpha_s + b$ with $a, b \in \mathbb{R}$ and $a \neq 0$, we obtain an isomorphism $B_s \to B_s$ (see [20, Example 17.25]). However, the term $b \in \mathbb{R}$ vanishes in perverse cohomology, and only for the normalized value $a = \frac{1}{2}$ do we get $\partial_s(\rho) = 1$, yielding exactly the identity without additional factors. Moreover, η satisfies the stronger Hodge-Riemann property precisely when $a > 0$, i.e., when ρ is dominant regular, motivating our restriction to this case.

The necessity of working with quotients becomes apparent even in small examples. Consider B_{ststs} in type $I_2(7)$. In the $\mathcal{J}$-ring, we have $j_{ststs} j_{ststs} = j_{sts} + j_s$ where all terms lie in a cell of **a**-value 1. However, in $\mathbb{S}$Bim we have:

$$B_{ststs} \otimes_R B_{ststs} \simeq B_{stststs}(v^{-3} + 2v^{-1} + 2v + v^3) \oplus B_{sts}(v^{-1} + v) \oplus B_s(v^{-1} + v). \tag{4.23}$$

Thus, the lowest degree summands belong to objects lying in higher cells, and η^i provides isomorphisms between objects in different cells. This suggests we should factor out objects and morphisms from higher cells.

This phenomenon is further illustrated in the following example showing non-unique projection morphisms:

Example 4.15 ([18, Example 2.2]). In type A_2, we have $\mathrm{BS}(ststst) \simeq B_{sts}(-1) \oplus B_{st} \oplus B_{sts}(+1)$. The degree 0 projection map onto B_{st} is not unique, having two generators. By Soergel's Hom formula, we obtain two possible maps corresponding to the light leaves expressions $(1, 1, 0, 0)$ and $(1, 0, 0, 1)$:

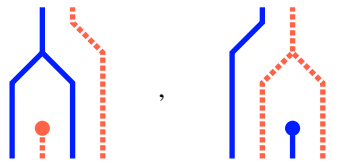

(4.24)

Similar to Section 4.1, this arises from factoring through higher cells: there exists a map in $\mathrm{Hom}^{-1}(\mathrm{BS}(ststst), B_{tst})$ and a map in $\mathrm{Hom}^{+1}(B_{tst}, B_{st})$ whose composition decomposes as the sum of both projections:

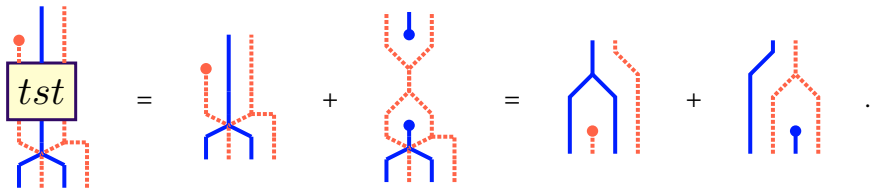

(4.25)

Here the second term vanishes by the needle relation.

4.3.2. Construction steps following Elias–Williamson. Before proceeding, we clarify notation between different sources.

- The category of Soergel bimodules is denoted by $\mathcal{B}$ in [18] and by $\tilde{C}$ in [50, 45]. We use $\mathbb{S}$Bim for consistency with earlier sections.

- The asymptotic category is denoted by $\mathcal{J}$ here and in [18], while in [45] it is denoted by $C^{\mathbf{c}}$ and in [50] by $C_{\mathbf{c}}$.
- The two-sided cell partial order is reversed: In [50, 45] and [18] the trivial element 1 lies in the highest cell, while in our notation it lies in the lowest cell.

We now describe how the asymptotic category $\mathcal{J}$ arises from the quotient construction and establish its key properties. Following Elias and Williamson's approach in [18], the construction proceeds in several steps that transform the category of Soergel bimodules $\mathbb{S}\mathrm{Bim}$ into a categorification of the $\mathcal{J}$-ring associated to a two-sided cell $\mathbf{c}$.

Let (W, S) be a Coxeter system and $\mathbf{c} \subseteq W$ a two-sided cell. Let a be the value of the $\mathbf{a}$-function on $\mathbf{c}$. Further assume ρ to be strictly dominant for the given type. We construct the category $\mathcal{J}_{\mathbf{c}}$ as follows:

(A) Let $\mathbb{S}\mathrm{Bim}_{>\mathbf{c}}$ be the full subcategory of $\mathbb{S}\mathrm{Bim}$ consisting of all direct sums of grading shifts of objects B_z with $z >_{\mathrm{J}} \mathbf{c}$. This category inherits a monoidal structure from $\mathbb{S}\mathrm{Bim}$.

(B) Let $I_{\mathbf{c}}$ denote the tensor ideal in $\mathbb{S}\mathrm{Bim}$ generated by morphisms factoring through objects of $\mathbb{S}\mathrm{Bim}_{>\mathbf{c}}$.

(C) Define $\mathbb{S}\mathrm{Bim}'_{\mathbf{c}} := \mathbb{S}\mathrm{Bim}\,/I_{\mathbf{c}}$ as the quotient category. Objects in $\mathbb{S}\mathrm{Bim}'_{\mathbf{c}}$ are the same as in $\mathbb{S}\mathrm{Bim}$, but morphisms are considered modulo those factoring through higher cells.

(D) Let $\mathbb{S}\mathrm{Bim}_{\mathbf{c}}$ be the full subcategory of $\mathbb{S}\mathrm{Bim}'_{\mathbf{c}}$ generated by $B^{\mathbf{c}}_x$ with $x \in \mathbf{c}$. This inherits the structure of a graded additive monoidal category.

(E) Finally, define $\mathcal{J}_{\mathbf{c}}$ as the full subcategory of $\mathbb{S}\mathrm{Bim}_{\mathbf{c}}$ consisting of direct sums (without shifts) of $J_x := B^{\mathbf{c}}_x$ for $x \in \mathbf{c}$. The monoidal structure is given by

$$B \star B' := H^{-a}(BB') \in \mathcal{J}_{\mathbf{c}} \tag{4.26}$$

Theorem 4.16 ([45, Section 18.15]). *By the construction above, $\mathcal{J}_{\mathbf{c}}$ is a semisimple abelian category and its Grothendieck ring is isomorphic to the asymptotic algebra $J_{\mathbf{c}}$.*

Sketch. Semisimplicity follows from the fact that $\mathcal{J}_{\mathbf{c}}$ consists only of $J_x = B^{\mathbf{c}}_x$ without grading shifts. By Soergel's hom formula (see Theorem 2.41), we have $\mathrm{Hom}(B_y, B_x) \simeq R$ if $x = y$ and $\mathrm{Hom}(B_y, B_x) = 0$ if $x \neq y$. Therefore the objects J_x are pairwise non-isomorphic simples, and any object in $\mathcal{J}_{\mathbf{c}}$ is a finite direct sum of simples, making the category semisimple.

For the Grothendieck ring isomorphism, the key observation is that the monoidal product $B \star B' := H^{-\mathbf{a}}(BB')$ on $\mathcal{J}_{\mathbf{c}}$ is precisely designed to match the structure constants of the asymptotic algebra $J_{\mathbf{c}}$. The definition of $J_{\mathbf{c}}$ is based on taking the lowest graded summand (namely degree $-\mathbf{a}$) of tensor products in $\mathbb{S}\mathrm{Bim}$, with objects from higher cells factored out. By construction, $\mathcal{J}_{\mathbf{c}}$ implements exactly this procedure: we quotient out by $I_{\mathbf{c}}$ (morphisms through higher cells) and take perverse cohomology at degree $-\mathbf{a}$. Thus the Grothendieck group, which records objects up to isomorphism and relations from short exact sequences, precisely recovers the algebraic structure of $J_{\mathbf{c}}$. □

For an H-cell $\mathbf{h} \subseteq \mathbf{c}$ we write $\mathcal{J}_{\langle}$ for the full subcategory of $\mathcal{J}_{\mathbf{c}}$ generated by all objects J_x for $x \in \langle$, or we leave out the index if it is clear.

The rigidity of $\mathcal{J}$ is proven in [18, Theorem 5.3].

We will explain the intricacies of this construction, starting with the quotient category.

Definition 4.17 ([26, §2.1]). Let $\Bbbk$ be a field and C a $\Bbbk$-bilinear monoidal category. A *tensor ideal* I in C is a collection of subspaces $I(X, Y) \subseteq \mathrm{Hom}_C(X, Y)$ for all $X, Y \in C$ such

that for all $X, Y, Z, T \in C$ and $\alpha \in I(X, Y), \beta \in \mathrm{Hom}(Y, Z), \gamma \in \mathrm{Hom}(Z, X), \delta \in \mathrm{Hom}(Z, T)$ we have:

(A) The concatenations $\alpha \circ \gamma$ and $\beta \circ \alpha$ lie in I, i.e. in $I(Z, X)$ and $I(Z, Y)$.
(B) The tensor products $\alpha \otimes \delta$ and $\delta \otimes \alpha$ lie in I, i.e. in $I(X \otimes Z, Y \otimes T)$ and $I(Z \otimes X, T \otimes Y)$.

Construction 4.18 (Quotient of categories). Let I be a tensor ideal in a k-bilinear monoidal category C. We define a new k-bilinear monoidal category C' called the *quotient of C by I* as follows: the objects in C' are the objects of C, but for $X, Y \in C'$ we set $\mathrm{Hom}_{C'}(X, Y) \coloneqq \mathrm{Hom}_C(X, Y)/I(X, Y)$. Composition and tensoring of morphisms is inherited from C and is well-defined by the tensor ideal properties.

One can show that most categorical properties of C, such as rigidity, or gradings, descend to C'. We now verify the key properties of the construction of $\mathbb{S}\mathrm{Bim}'_{\mathbf{c}}$ in a sequence of lemmas.

Lemma 4.19. *The collection $I_{\mathbf{c}}$ is a tensor ideal of* $\mathbb{S}\mathrm{Bim}$.

Proof. Let X, Y be objects of $\mathbb{S}\mathrm{Bim}$. First observe that $I_{\mathbf{c}}(X, Y)$ is a subspace of $\mathrm{Hom}(X, Y)$ as sums and compositions of morphisms factoring through objects in higher cells again factor through objects in higher cells.

For closure under composition, let $f \in I_{\mathbf{c}}(X, Y)$ factor through an object $R \in \mathbb{S}\mathrm{Bim}_{>\mathbf{c}}$. Then any composition with f again factors through R and thus lies in $I_{\mathbf{c}}$.

For the tensor product condition, note that by cell theory the monoidal product of two objects has only summands not lying below the two objects. Thus tensor products with morphisms in $I_{\mathbf{c}}$ remain in $I_{\mathbf{c}}$. □

Lemma 4.20. *In $\mathbb{S}\mathrm{Bim}'_{\mathbf{c}}$ any object isomorphic to $B^{\mathbf{c}}_x(m)$ for $\mathbf{c} <_{\mathrm{J}} x$ is not indecomposable.*

Proof. If $\mathbf{c} <_{\mathrm{J}} x$, then $B^{\mathbf{c}}_x \simeq B^{\mathbf{c}}_x \oplus B^{\mathbf{c}}_x$ since the space $\mathrm{Hom}_{\mathbb{S}\mathrm{Bim}'_{\mathbf{c}}}(B^{\mathbf{c}}_x, B^{\mathbf{c}}_x \oplus B^{\mathbf{c}}_x)$ contains only the zero morphism by construction. Hence, the objects $B^{\mathbf{c}}_x$ admit non-trivial decompositions into subobjects and are therefore not indecomposable. □

Since $I_{\mathbf{c}}$ is a tensor ideal (Lemma 4.19) and monoidal properties descend to quotient categories (see 4.18), $\mathbb{S}\mathrm{Bim}'_{\mathbf{c}}$ is a graded additive monoidal category.

Note that while perverse cohomology descends to $\mathcal{J}_{\mathbf{c}}$, we are no longer working in the diagrammatic Hecke category. Instead, morphism spaces in $\mathcal{J}_{\mathbf{c}}$ arise through quotients and other constructions. For practical computations, we will therefore typically perform calculations in $\mathcal{H}$ and then interpret the results in $\mathcal{J}_{\mathbf{c}}$. We will see explicit examples of such computations in the next subsection.

4.3.3. Small examples. We start with some basic examples to illustrate the construction.

Example 4.21. Let (W, S) be a finite Coxeter system with the geometric realization and let $\mathbf{c} \coloneqq \{1\}$ be the two-sided cell consisting only of the identity of W. We calculate $I_{\mathbf{c}}(B_1, B_1)$. In $\mathbb{S}\mathrm{Bim}$ the graded Hom space is $\mathrm{Hom}^\bullet(B_1, B_1) \simeq R$ generated by the identity map of B_1. For any $s \in S$ the concatenation of startdot $B_1 \to B_s$ and enddot $B_s \to B_1$

(4.27)

evaluates to $\alpha_s \, \mathrm{id}_{B_1}$, hence

$$I_{\mathbf{c}}(B_1, B_1) \supseteq \langle \alpha_s \mid s \in S \rangle_R. \tag{4.28}$$

Any other endomorphism of B_1 factoring through an object $B \in \mathbb{S}\mathrm{Bim}_{>\mathbf{c}}$ has positive degree, giving equality in (4.28). Therefore in $\mathbb{S}\mathrm{Bim}'_{\mathbf{c}}$ as well as in $\mathbb{S}\mathrm{Bim}_{\mathbf{c}}$ and $\mathcal{J}_{\mathbf{c}}$ we have

$$\mathrm{Hom}^\bullet(B_1^{\mathbf{c}}, B_1^{\mathbf{c}}) \simeq \mathbb{R}\,. \tag{4.29}$$

More generally in $\mathbb{S}\mathrm{Bim}'_{\mathbf{c}}$ and $\mathbb{S}\mathrm{Bim}_{\mathbf{c}}$ for any $m, n \in \mathbb{Z}$ we have

$$\mathrm{Hom}^\bullet(B_1^{\mathbf{c}}(m), B_1^{\mathbf{c}}(n)) \simeq \begin{cases} 0 & , \text{ if } m \neq n, \\ \mathbb{R} & , \text{ else.} \end{cases} \tag{4.30}$$

In $\mathcal{J}_{\mathbf{c}}$ this yields

$$\mathrm{Hom}(J_1^{\oplus m}, J_1^{\oplus n}) \simeq \mathbb{R}^{m \times n}, \tag{4.31}$$

hence as abelian (since now all morphisms have kernel and cokernels) $\mathbb{R}$-linear categories we have

$$\mathcal{J}_{\mathbf{c}} \simeq \mathbf{Vec}\,. \tag{4.32}$$

Since the $\mathbf{a}$-value on $\mathbf{c} = \{1\}$ is 0, the monoidal product is given by

$$J_1 \star J_1 = H^0(J_1 J_1) = J_1 J_1 \simeq J_1 \in \mathcal{J}.$$

Therefore $\mathcal{J}$ is even monoidally equivalent to **Vec**.

Example 4.22. Consider now the case W of type A_1 and the cell $\mathbf{c} = \{s\}$. Here $I_{\mathbf{c}}$ is zero as there are no $x \in W$ with $\mathbf{c} < x$. Hence $\mathbb{S}\mathrm{Bim}'_{\mathbf{c}} = \mathbb{S}\mathrm{Bim}$ and $\mathbb{S}\mathrm{Bim}_{\mathbf{c}}$ is generated by direct sums of grading shifts of B_s. While in any variant of $\mathbb{S}\mathrm{Bim}$ we have $\mathrm{Hom}(B_s, B_s) \simeq R$, there are no grading shifts in $\mathcal{J}$. Hence also here:

$$\mathrm{Hom}(J_s, J_s) \simeq \mathbb{R}, \tag{4.33}$$

and hence as abelian categories

$$\mathcal{J} \simeq \mathbf{Vec}\,. \tag{4.34}$$

For the monoidal structure, we get $J_s \star J_s \simeq J_s$ using the projections and inclusion maps from earlier. For the triple tensor product we find $B_s B_s B_s \simeq B_s(-2) \oplus B_s \oplus B_s \oplus B_s(+2)$ with perverse cohomology

$$H^{-2}(B) = \tau_{\leq -2} B / \tau_{\leq -3} B(-2) \simeq B_s(+2)(-2) \simeq B_s$$

and unique inclusion given by the Double Leave $\mathbb{LL}^s_{(1,0,0),(1)}$. Alternatively, considering $H^{-1}(H^{-1}(B_s B_s) B_s)$ or $H^{-1}(B_s H^{-1}(B_s B_s))$ gives equivalent projection maps that differ only by associativity and coassociativity in $\mathbb{S}\mathrm{Bim}$. So we are also monoidally equivalent.

4.4. Skeletal data of the asymptotic Hecke category

We develop an algorithm to compute the skeletal structure of the asymptotic Hecke category $\mathcal{J}_{\mathbf{c}}$. Building on Elias and Williamson's work, the method systematically extracts key categorical data from Soergel bimodules. By constructing idempotents, mapping cell interactions, and computing associator coefficients, we transform the original category into a more manageable representation. We keep to the notation from subsection 2.2.5.

Algorithm 4.23 (Skeletal Data Computation for Asymptotic Hecke Category). We fix (W, S) a Coxeter system with $\mathbf{c} \subseteq W$ a two-sided J-cell and $\mathbf{a}(\mathbf{c})$ its $\mathbf{a}$-value. Further let ρ be a strictly dominant weight. We write $\{j_x\}_{x\in\mathbf{c}}$ for all elements of $J_{\mathbf{c}}$. We again assume that we are multiplicity free, i.e. for all $j_x j_y = \sum_z n_z j_z$ we have $n_z \in \{0, 1\}$, see Remark 4.25 for the non-multiplicity free case.

We then compute the skeletal structure as follows:

(A) **Idempotent computation:** For each $x \in \mathbf{c}$ fix a reduced expression and construct the corresponding clasp idempotent e_x:  .

(B) **Projections and inclusions:** For all $(x, y) \in \mathbf{c} \times \mathbf{c}$:

(a) For each z with $n_z = 1$:

- Construct a canonical projection $p^z_{x,y} \in \mathrm{Hom}_{\mathbb{S}\mathrm{Bim}_{\mathbf{c}}}(B_x B_y, B_z(-\mathbf{a}(\mathbf{c})))$ with flip $\overline{p^z_{x,y}} \in \mathrm{Hom}_{\mathbb{S}\mathrm{Bim}'_{\mathbf{c}}}(B_z(+\mathbf{a}(\mathbf{c})), B_x B_y)$:

$$p^z_{x,y} = \quad \text{ 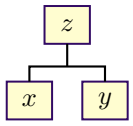 } \tag{4.35}$$

- Compute the coefficient $\kappa^z_{x,y} \in \mathbb{R}^*$ such that[1]

$$p^z_{x,y} \circ (\mathrm{id}_{B_x} \otimes \rho^{\mathbf{a}(\mathbf{c})} \otimes \mathrm{id}_{B_y}) \circ i^z_{x,y} = \kappa^z_{x,y} \cdot \mathrm{id}_{B_z}$$

$$\text{ 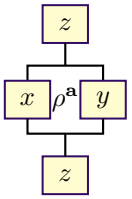 } \quad = \kappa^z_{x,y}\, \mathrm{id}_{B_z} \tag{4.36}$$

- Then we set $i^z_{x,y} := 1/\kappa^z_{x,y}(\mathrm{id}_{B_y} \otimes \rho^{\mathbf{a}(\mathbf{c})} \mathrm{id}_{B_z}) \circ \overline{p^z_{x,y}}$. These form a dual basis in sense of (2.42).

(C) **Associator Computation:** For all $(a, b, c) \in \mathbf{c}^3$:

(a) Compute $j_a j_b j_c = \sum_f n_f j_f$ in $J_{\mathbf{c}}$

(b) For each f with $n_f \neq 0$:

- Find all pairs (d, e) such that:

$$j_a j_b \supseteq j_d$$
$$j_b j_c \supseteq j_e$$

[1] The coefficient $\kappa^z_{x,y}$ is non-zero because $p^z_{x,y}$ is a non-zero morphism in $\mathbb{S}\mathrm{Bim}_{\mathbf{c}}$, where morphisms factoring through higher cells have been removed.

- Compute the associator coefficients $F^f_{a,b,c} \in \mathbb{R}$ via:

$$\frac{1}{\kappa^f_{a,e}\kappa^e_{b,c}}$$ 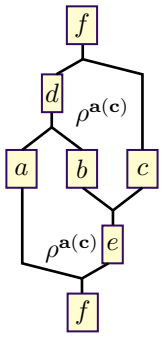

$$= \left[F^f_{a,b,c}\right]_{(d,e)} \mathrm{id}_{B_f} \tag{4.37}$$

Remark 4.24. This algorithm follows the notation from subsection 2.2.5. While $\mathcal{J}$ is not initially skeletal, this procedure provides a skeletal presentation. We fix one idempotent per element of the cell, along with canonical projection and inclusion maps. After completing these computations, we can regard $\mathcal{J}$ as a skeletal category. We will use the same letters to denote objects in both the original category and the skeletal category.

The existence of scalars κ and F follow from Lemma 3.6 as the composition is by construction a degree zero map.

Remark 4.25. If we encounter non-multiplicity-free cases, such as in type H_4, we proceed as in [20, Proposition 11.69]. Specifically, when $n_z > 1$ for some z, the space $\mathrm{Hom}^{-a}(B_xB_y, B_z)$ becomes n_z-dimensional. In such cases, we select a collection of projection and inclusion maps from this space. Compare to Remark 3.18.

All H-cells we consider are multiplicity free. As far as the author is aware for finite Coxeter groups only in type H_4 does one encounter multiplicities.

Remark 4.26. Two points require careful consideration in this algorithm:

- **Projection Map Selection:** The construction of projection maps is not straightforward. While light leaves span the morphism spaces for Bott–Samelson bimodules, many of those are orthogonal to the clasp idempotents, see Example 2.48. We must therefore always verify that they indeed do not give zero.
- **Coefficient Determination:** Calculating the coefficients $\kappa^z_{x,y}$ and F-symbols depends on the recursive structure of the idempotents, which can be very long. Already the number of summands in the expansion of the Jones–Wenzl projectors grow exponentially (the number of terms is given by the Catalan numbers).

We give the concrete maps in all examples we compute.

Remark 4.27. To establish rigidity, as in [18, Theorem 5.3], in the asymptotic Hecke category, we need to construct appropriate evaluation and coevaluation maps. The strategy is to utilize the canonical projection and inclusion maps we developed earlier, with careful attention to scaling factors.

For an object $x \in c$ we know by Proposition 1.44(P2) that $x^* = x^{-1}$, i.e., the dual is the inverse. In the J-ring, the product contains a Duflo involution with multiplicity 1: $j_x j_{x^*} \supseteq j_d$ (Then also $j_{x^*} j_x \supseteq j_{d'}$ for a possibly different Duflo involution).

The evaluation and coevaluation maps are then certain multiples of $p^d_{x^*,x}$ and $i^{d'}_{x^*,x}$. The right scalar multiple λ is determined by requiring that these maps satisfy the rigidity conditions Definition 2.9.

While we work with diagrammatic calculations for clarity, we must remain mindful that the category is not strict monoidal, and therefore we need to track associator coefficients carefully. The key calculation reduces to computing the following composition:

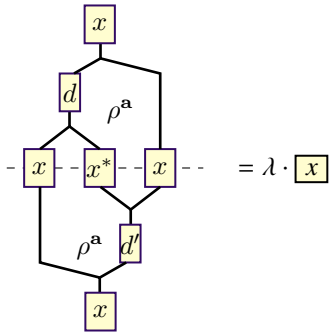

(4.38)

This is exactly the calculation done for computing the associator. Hence, the choice $\mathrm{ev}_{x^*} := p^d_{x^*,x}$ and $\mathrm{coev}_x := \frac{1}{\lambda} i^d_{x,x^*}$ for $\lambda = \frac{\left[F^x_{x,x^*,x}\right]_{d,d'}}{\kappa^x_{x,d}\kappa^{d'}_{x^*,x}}$ establishes the rigidity of J_x.

Lemma 4.28 (Dimensions in the Asymptotic Hecke Category). *For an object J_x in the asymptotic Hecke category $\mathcal{J}_{\mathbf{c}}$, its categorical dimension is determined by the composition of canonical pairing and associator coefficients:*

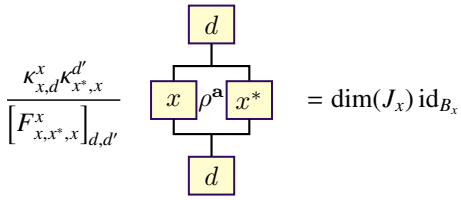

(4.39)

Hence, $\dim(J_x) = \frac{\kappa^x_{x,d}\kappa^{d'}_{x^*,x}}{\left[F^x_{x,x^*,x}\right]_{d,d'}\kappa^d_{x,x^*}}$.

Proof. The groundwork was laid in Remark 4.27. It remains to describe the pivotal structure. The dual is a vertical flip, so the double dual is a double flip. Therefore the identity provides the canonical pivotal structure: we have canonically $J_x \simeq J_{x^{**}}$ (see [18, Proposition 5.6(3)]). Now by definition of the dimension Definition 2.16 and κ^d_{x,x^*} we get our claim. □

4.5. Examples

In this section, we explicitly compute the skeletal structure and fusion data for several key examples of asymptotic Hecke categories. These computations illustrate the algorithm developed in the previous section and show us connections to categories described in subsection 2.1.2.

4.5.1. Type A_2. Consider the Coxeter system (W, S) of type $I_2(3) = A_2$ with generators s, t. We explore the construction of the quotient category and its skeletal structure. Here $\rho = \alpha_s + \alpha_t$.

Example 4.29. For the two-sided cell $\mathbf{c} = \{s, t, st, ts\}$ we only have $\mathbf{c} < sts$ for the longest word in A_2. Hence, in $\mathbb{S}\mathrm{Bim}_{\mathbf{c}}$ we get the relation:

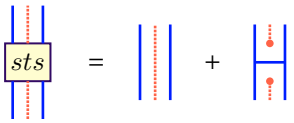

(4.40)

Specifically, composing with startdot and enddot on opposite sides yields:

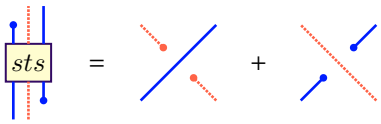

(4.41)

This relation dramatically simplifies the morphism spaces, as any blue crossing can be translated into a red crossing.

For this type, the projection maps are uniquely determined, as there is always only one map of degree -1 in $\mathbb{S}$Bim:

$p^{s}_{s,s} :=$ 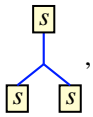

, $p^{st}_{s,st} :=$ 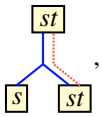

, $p^{ts}_{ts,s} :=$ 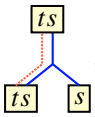

, $p^{t}_{ts,st} :=$ 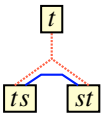

(4.42)

We then compute the coefficient $\kappa^{s}_{s,s}$:

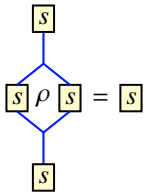

(4.43)

Hence, we get $\kappa^{s}_{s,s} = 1$. Similarly the calculations for $\kappa^{st}_{s,st}, \kappa^{ts}_{ts,s}, \kappa^{t}_{t,t}, \kappa^{ts}_{t,ts}, \kappa^{st}_{st,t}$ return the same. There is one exception:

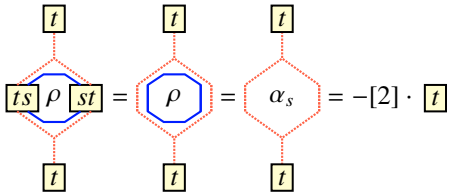

(4.44)

Hence, we get $\kappa^{t}_{ts,st} = -1$.

The associators reveal more interesting structural properties. First, note that $\alpha_{s,s,s}$ being trivial follows directly from associativity and coassociativity of the diagrammatic category:

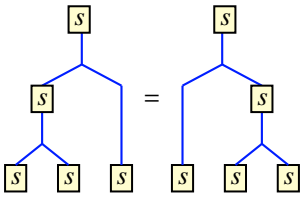

(4.45)

Alternatively we see this also in:

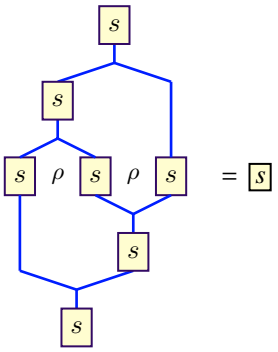

(4.46)

Hence, the associator here is 1, i.e. trivial. For most other triples they are also trivial. Here only for the triple (st, ts, st) and (ts, st, ts) we get using the quotient relation (4.41):

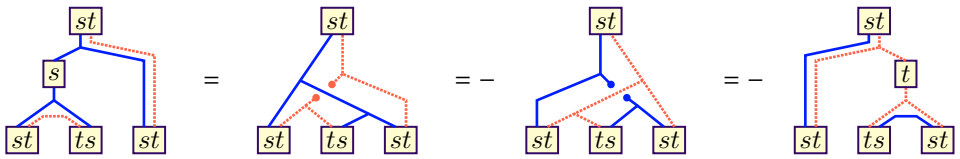

(4.47)

However, this computational strategy becomes impractical for more complex types. In type $I_2(4)$, for instance, the killed idempotent would have 5 summands, leading to 4 different summands where identifying zeros becomes challenging.

Following our algorithm we instead compute:

$$\frac{1}{\kappa^{st}_{st,t}\kappa^{t}_{ts,st}}\cdot$$

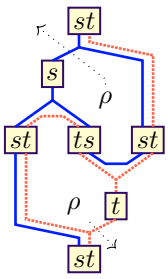

$$= \frac{1}{\kappa^{st}_{st,t}\kappa^{t}_{ts,st}}\partial_t(\rho)\partial_s(\rho)\cdot$$

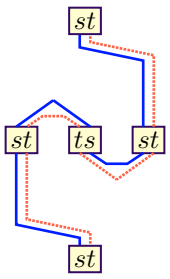

$$= -\boxed{st} \quad (4.48)$$

Here we can slide ρ trough as otherwise the trivalent sliding of the idempotents gives a needle relation. We can also read of the dimension here, as these are all coefficients needed in Lemma 4.28. All terms cancel out and we get $\dim(J_{st}) = (1, 0)$ as an element of $\mathrm{End}_{\mathcal{J}}(J_s \oplus J_t) \simeq \mathbb{R}^2$.

We give a summary over these computations:

Proposition 4.30 (Multifusion Structure for Type A_2). *For the Coxeter system of type A_2 with two-sided cell $\mathbf{c} = \{s, t, st, ts\}$, the asymptotic Hecke category $\mathcal{J}_{\mathbf{c}}$ is a multifusion category categorifying the asymptotic Hecke algebra $J_{\mathbf{c}}$. We have non-trivial associator $\alpha_{ts,st,ts} = -1$ and $\alpha_{st,ts,st} = -1$.*

4.5.2. Type $I_2(5)$. Consider the Coxeter system of type $I_2(5)$ with generators s, t. Since $2 - [2] \neq 1$, we choose $\rho = \frac{\alpha_s + \alpha_t}{2-[2]}$ as our dominant weight. Here we focus on the H-cell $\mathbf{h} = \{s, sts\}$.

For a product with a Duflo involution the projections look like in the smaller dihedral types. We then compute the additional projection maps required for this type. For the morphism spaces involving sts, we obtain:

$$p^{s}_{sts,sts} = \quad , \quad p^{sts}_{sts,sts} = \tag{4.49}$$

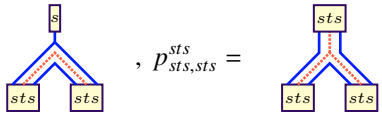

The coefficient $\kappa^{s}_{sts,sts}$ follows from:

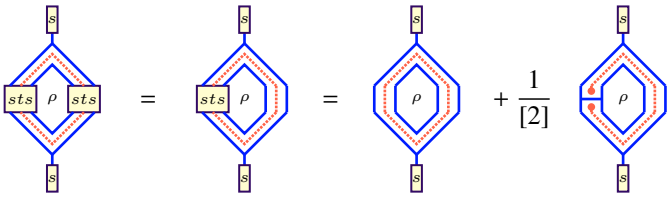

(4.50)

While $\kappa^{sts}_{sts,sts}$ is computed via:

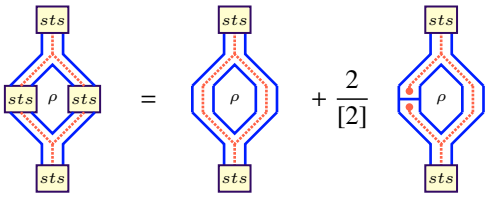

(4.51)

Here we use the identity $-[2] + \frac{2}{[2]} = \frac{-[2]^2+2}{[2]} = \frac{-[3]+[1]}{[2]} = -\frac{[4]}{[2]^2}$.

For the associators, we proceed systematically and compute $(\alpha_{sts,sts,sts})^{s}_{s}$:

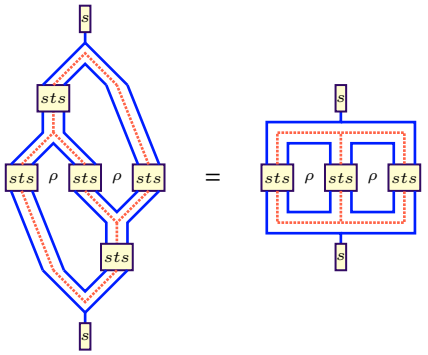

(4.52)

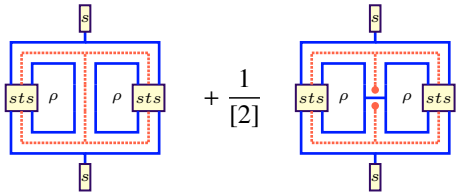

(4.53)

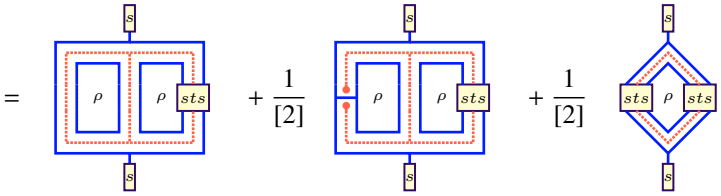

(4.54)

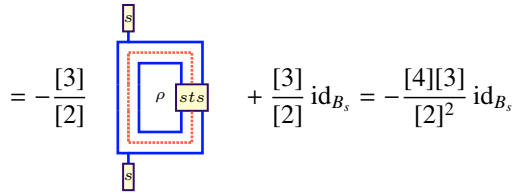

(4.55)

The calculation uses $-\frac{[3]}{[2]}[3] + \frac{[3]}{[2]} = \frac{[3]}{[2]}([1] - [3]) = -\frac{[3][4]}{[2]^2}$. With $\kappa^{sts}_{sts,sts} = -\frac{[2]^2}{[4]}$ and $\kappa^{s}_{sts,sts} = \frac{1}{[3]}$, this yields the F-symbol 1.

For $(\alpha_{sts,sts,sts})^{sts}_{sts}$ we have two different summands (denoted e, f in Algorithm 4.23), hence we will get a 2×2 matrix. For cases where s appears at top and bottom with one intermediate s this is a fast calculation:

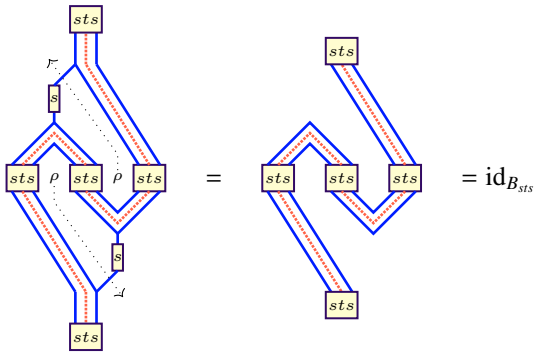

(4.56)

Normalization by $\kappa^{s}_{sts,sts}$ gives matrix entry $\frac{1}{[3]}$. Furthermore:

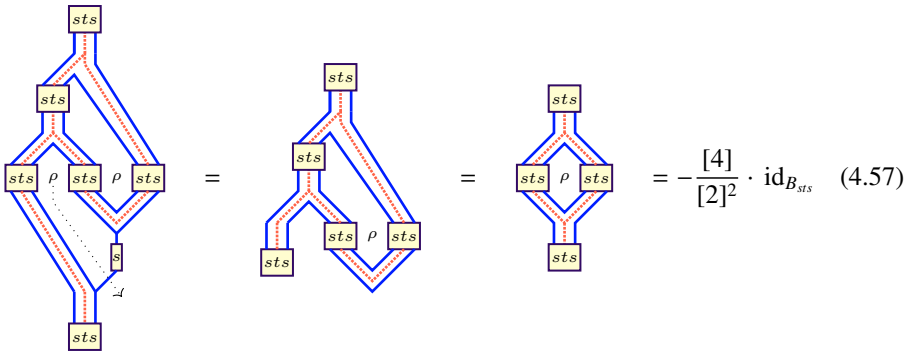

(4.57)

Normalization by $\kappa^{s}_{sts,sts}$ and $\kappa^{sts}_{sts,s}$ yields $-\frac{[3][4]}{[2]^2}$. For the flip, normalization by $\kappa^{sts}_{sts,sts}$ twice gives $-\frac{[2]^2}{[4]}$. The final computation requires more work. First note that we can write:

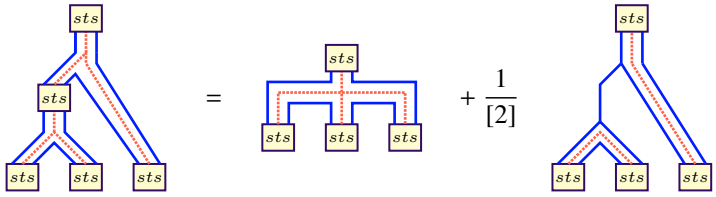

(4.58)

This calculation decomposes into three terms which we analyze systematically:

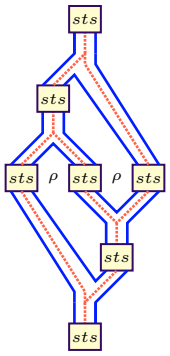

(4.59)

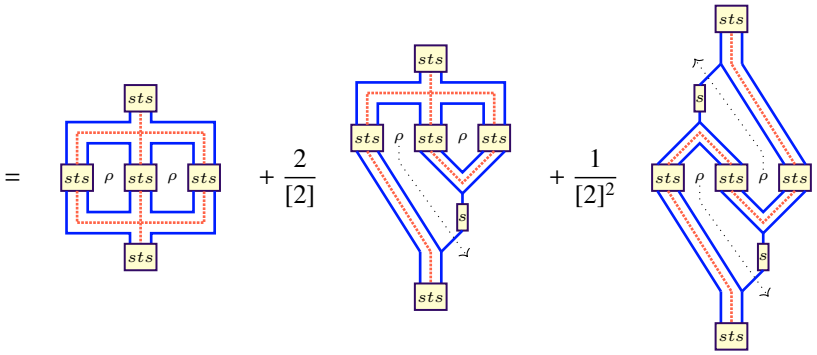

(4.60)

The rightmost term corresponds to the associator previously computed in Equation 4.56 , yielding $\frac{1}{[2]^2}$. The middle term evaluates to:

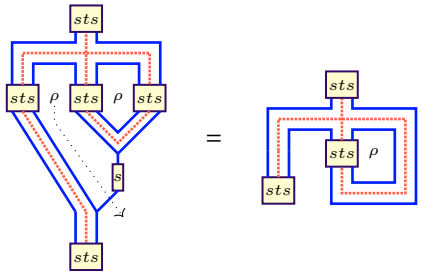

(4.61)

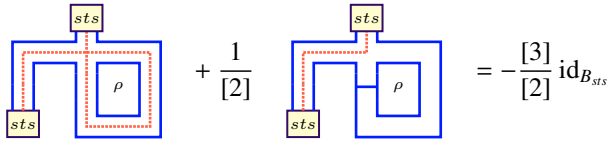

(4.62)

For the remaining term of (4.59), we compute:

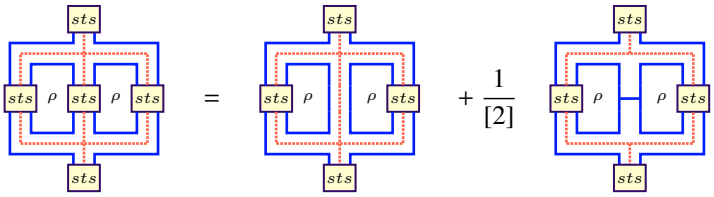

(4.63)

The second term in this equation evaluates to $-\frac{[4]}{[2]^3}$ as in the computation of $\kappa^{sts}_{sts,sts}$. For the first term, we have:

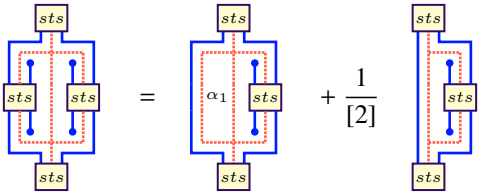

(4.64)

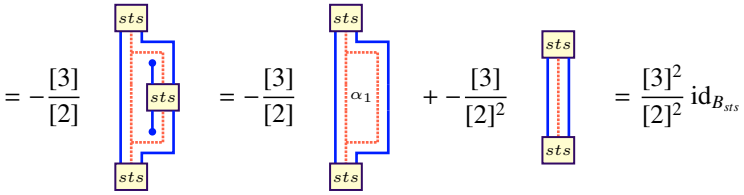

(4.65)

Combining all terms yields:

$$-\frac{[4]}{[2]^3}+\frac{[3]^2}{[2]^2}+\frac{2}{[2]}\left(-\frac{[3]}{[2]}\right)+\frac{1}{[2]^2}=\frac{[3]-[1]+[3]^2-2[3]+1}{[2]^2}=\frac{[5]-2[3]+3}{[2]^2} \tag{4.66}$$

$$=\frac{[6]-[4]+[2]}{[2]^3}=\frac{[7]+[1]}{[2]^4}=\frac{[9]+[7]+[5]+[3]}{[2]^4[3]}=\frac{[6][4]}{[3][2]^4} \tag{4.67}$$

After scaling by $\kappa^{sts}_{sts,sts}$ twice, we obtain $\frac{[6]}{[3][4]}$.

Proposition 4.31. *The fusion category $\mathcal{J}_{\mathbf{h}}$ for $\mathbf{h}=\{s, sts\}$ in type $I_2(5)$ is the Fibonacci category of Example 2.5.*

Proof. We computed the associators to be:

$$a_{sts,sts,sts}=\mathrm{id}_{B_s}\oplus\begin{pmatrix}\frac{[1]}{[3]} & -\frac{[2]^2}{[4]}\\ -\frac{[4]}{[2]^2[3]} & \frac{[6]}{[3][4]}\end{pmatrix}\mathrm{id}_{B_{sts}}. \tag{4.68}$$

By Table 2.1 this gives exactly the matrix of Example 2.5. □

Corollary 4.32. *Continuing with Proposition 4.31 we get:*

$$\dim(J_s)=[1],\ \dim(J_{sts})=[3] \tag{4.69}$$

Proof. Again we computed all κ and F-symbols needed. Note, that $\left[F^{x}_{x,x^*,x}\right]_{d,d'}$ is the top left entry of (4.66). We compute:

$$\dim(J_{sts}) = \frac{[3]}{[3]\frac{[1]}{[3]}} = [3]. \tag{4.70}$$

□

In the next chapter we will then extend these calculations to all dihedral groups, as well as the other H-cells chosen in section 1.4.

CHAPTER 5

Overview of Asymptotic Categories and their S-matrices

This chapter provides a comprehensive overview of asymptotic categories and the S-matrixes of their centers. As fusion data most of the asymptotic algebras J_h for the H-cells we consider here are well known in representation theory. Recall that the *Fibonacci ring* refers to the asymptotic algebra with relation $j_x^2 = j_1 + j_x$ (as seen in Example 2.5), and the $(\mathbb{Z}/2\mathbb{Z})$-*graded ring* refers to asymptotic algebras with relation $j_x^2 = j_1$ (as seen in Example 2.4 and earlier examples).

By Ostrik's classification of rank 2 fusion categories (see Remark 2.6), the Fibonacci ring and the $(\mathbb{Z}/2\mathbb{Z})$-graded ring admit only two different categorifications. One therefore has only two possibilities for the center and S-matrix in each case. Similarly in the dihedral group all categorifications of the asymptotic algebra are parametrized. Part of this chapter was already stated in [58]. However, in some cases it was not clear what the correct categorification should be. Now we are able to compute the associators and therefore can give a definitive statement. For many small Coxeter groups, such as type H_3 and H_4 an incomplete classification was also computed in [51, Section 8]. By computing the associators we can now give a complete classification for type H_3 and solve the smaller cells in type H_4.

We introduce type A_k fusion categories, describe their fusion structure, see how all asymptotic algebras we considered so far lie in Grothendieck rings of these categories. Then we can calculate all asymptotic Hecke categories and give statements about the S-matrixes.

5.1. Recoupling theory

The projection and inclusion maps in the small dihedral cases of the last chapter are coming directly from the Temperley–Lieb category. As no 2-valent vertices occur, one can find a preimage under the functor from the two-color Temperley–Lieb category.

Now we would like to extend the calculations of the asymptotic Hecke category to all dihedral groups. It turns out that such categories are already known in the literature. They are called categories with fusion rules A_k, as the monoidal product of the simple objects looks like the Dynkin diagram of type A_n. It is known how the associators and all braidings look like.

Since the fusion structure is already determined, we only need to compute a finite amount of data. For example the dimension of certain objects or a small number of F-symbols uniquely identify which version of $\mathcal{J}_{\mathbf{h}}$ our asymptotic Hecke category is equivalent to.

5.1.1. Type A_k fusion categories. We say that a fusion category C_k has fusion rules A_k if it has k simple objects, which we may label by $X_0, \dots, X_{k-1}$, such that

$$X_1 \otimes X_0 \simeq X_1 \simeq X_0 \otimes X_1,\ X_1 \otimes X_{k-1} \simeq X_{k-2} \simeq X_{k-1} \otimes X_1,\ X_1 \otimes X_i \simeq X_{i-1} \oplus X_{i+1} \quad (5.1)$$

for all $1 \leq i \leq k-2$. A summary of all possible categories with type A_k fusion rules can be found in [14]. The results were first obtained by [27]. We use the notation from [39]. These categories are also mentioned in [49, Section 2.2] under the name *Verlinde–Wess–Zumino–Witten*. A description can also be found in [24, Example 8.18.5].

Example 5.1. The category $\mathbf{Vec}_{\mathbb{Z}/2\mathbb{Z}}$ has fusion rules A_2. A category with fusion rules A_4 contains the Fibonacci category as a subcategory, as $X_2 \otimes X_2 \simeq X_0 \oplus X_2$. Also $\mathbf{Vec}_{\mathbb{Z}/2\mathbb{Z}}$ is the subfusion category generated by X_0, X_2 in a category with fusion rules A_3.

Note that the fusion rules resemble the multiplication of quantum numbers shifted by 1, i.e., we have $X_1 \otimes X_1 \simeq X_0 \oplus X_2$ and $[2][2] = [1] + [3]$. For fusion categories, we have different choices of associators. It was shown that the associators on type A_k fusion categories are classified by primitive roots of unity. We get that the two options described in Example 2.4, Example 2.5 are therefore all possibilities.

Remark 5.2. We can construct these type A_k fusion categories by starting with the Temperley–Lieb category and factoring out a Jones–Wenzl projector. For instance, in the Temperley–Lieb category we have the identity $JW_1 \otimes JW_1 = JW_2 \oplus JW_0$. Factoring out JW_2 eliminates this summand, leaving only $X_1 \otimes X_1 \simeq X_0$, which corresponds to the A_2 fusion category. For the following, we do not need the explicit construction; it suffices to understand the behavior of Jones–Wenzl projectors. For brevity, we denote a box labeled a as shorthand for JW_a.

Definition 5.3. We work in the Temperley–Lieb category $\mathcal{TL}(q)$ over $\mathbb{C}$ as defined in Definition 2.26. We do not yet specify what element of $\mathbb{C}$ we specialize the indeterminate q to; the concrete choice will determine the fusion category we obtain, and different specializations will be explored throughout this section.

We say that a triple of natural numbers (a, b, c) all smaller than k is *k-admissible* if

$$m \coloneqq \frac{a+b-c}{2},\ n \coloneqq \frac{a+c-b}{2},\ p \coloneqq \frac{b+c-a}{2} \tag{5.2}$$

are also natural numbers and $a + b + c \leq 2k - 2$. This is equivalent to saying that X_c occurs as a summand of $X_a \otimes X_b$ in C_k.

For a k-admissible triple, we define the (a, b, c)-projection as a morphism in $\mathcal{TL}(q)$:

$p^c_{a,b} \coloneqq$ 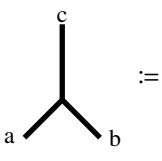

$\coloneqq$ 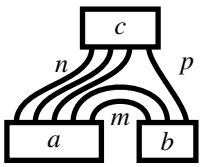

(5.3)

Dually we write $i^c_{a,b}$ for the flip.

Lemma 5.4. *Let (a, b, c) be a k-admissible triple.*

- *The trace of a (see Remark 2.36) is:*

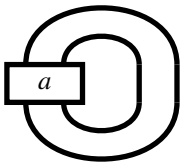

$= (-1)^a[a] =: \Delta_a$ (5.4)

- *The* theta net *is the coefficient* $\theta(a, b, c)$ *such that:*

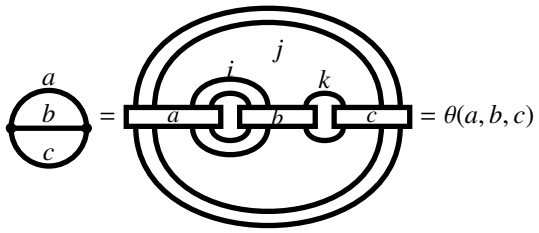

$$= \theta(a, b, c) \tag{5.5}$$

We have

$$\theta(a, b, c) := \frac{(-1)^{m+n+p}[m+n+p+1]![m]![n]![p]!}{[m+n]![m+p]![n+p]!}. \tag{5.6}$$

Sketch. While we can show the first claim using Lemma 2.31, the second claim requires a longer induction, see [39, Lemma 5.7]. We will replicate this in the asymptotic category in subsection 5.2.1. □

Example 5.5. We can verify these formulas with direct calculations for small examples.

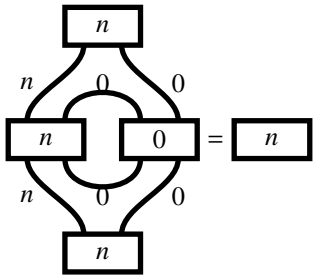

(5.7)

For another example :

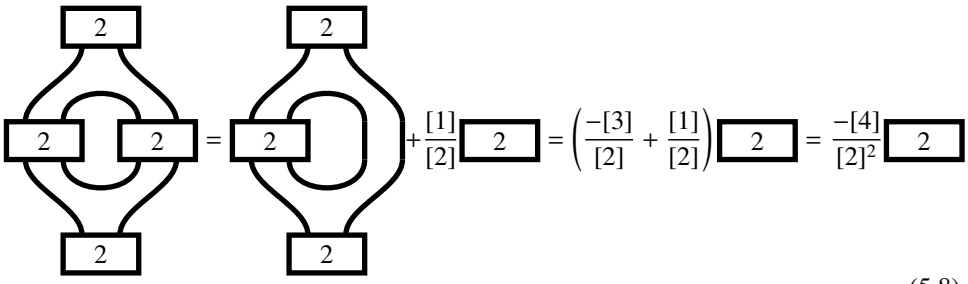

(5.8)

Here, we use the identity $\frac{[4]}{[2]} = [3] - [1]$.

Indeed, we see many similarities to the calculations in subsection 4.5.2. For the associator, we get a similar picture, see [39, Section 9.11].

Proposition 5.6. *For a collection of k-admissible triples* $(a,b,f),(b,c,e),(c,d,f)$ *and* (a,d,e) *we have:*

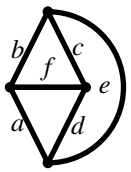

$$= \mathrm{Tet}\begin{bmatrix} a & b & e \\ c & d & f \end{bmatrix}, \tag{5.9}$$

where

$$\mathrm{Tet}\begin{bmatrix} a & b & e \\ c & d & f \end{bmatrix} = \frac{I!}{E!}\sum_{m\le s\le M}\frac{(-1)^s[s+1]!}{\prod_i[s-a_i]!\prod_j[b_j-s]!}, \tag{5.10}$$

here

$$a_1 \coloneqq \frac{a+d+e}{2},\ a_2 \coloneqq \frac{b+c+e}{2},\ a_3 \coloneqq \frac{a+b+f}{2},\ a_4 \coloneqq \frac{c+d+f}{2}, \tag{5.11}$$

$$b_1 \coloneqq \frac{b+d+e+f}{2},\ b_2 \coloneqq \frac{a+c+e+f}{2},\ b_3 \coloneqq \frac{a+b+c+d}{2}, \tag{5.12}$$

furthermore $m \coloneqq \max\{a_i\}, M \coloneqq \min\{b_j\}$*, and finally* $I! \coloneqq \prod_{i=1}^{4}\prod_{j=1}^{3}[b_j-a_i]!$ *and* $E! \coloneqq [a]![b]![c]![d]![e]![f]!$.

Furthermore:

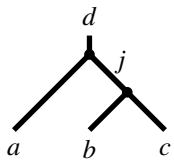

$$= \sum_i \begin{Bmatrix} a & d & i \\ c & b & j \end{Bmatrix}$$

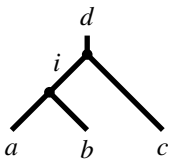

, (5.13)

where $\begin{Bmatrix} a & d & i \\ c & b & j \end{Bmatrix} = \mathrm{Tet}\begin{bmatrix} a & d & i \\ c & b & j \end{bmatrix}\frac{(-1)^i[i+1]}{\theta(a,b,i)\theta(d,c,i)}$.

Proof. This is the main part of [39, Chapter 8]. Furthermore, the numbers $\begin{Bmatrix} a & b & i \\ c & d & j \end{Bmatrix}$ satisfy orthogonality and the pentagon equations. □

Example 5.7. Take $a,b,c,d=2$. The only possible choices for i,j such that the triples with e,f are admissible are $\{0,2\}$. We compute these numbers explicitly as they give the associators for the Fibonacci category, and we saw them in subsection 4.5.2.

- First consider $i=j=0$. All a_i and b_1,b_2 are then 2, only $b_3=4$. Therefore $m=M=2$ and we have only one sum in the computation of Tet. We get:

$$\mathrm{Tet}\begin{bmatrix} a & b & i \\ c & d & j \end{bmatrix} = \frac{I!}{E!}\sum_{m\le s\le M}\frac{(-1)^s[s+1]!}{\prod_i[s-ai]!\prod_j[b_j-s]!} \tag{5.14}$$

$$= \frac{([4-2]!)^4}{([2]!)^4}\left(\frac{(-1)^2[3]!}{[4-2]!}\right) \tag{5.15}$$

$$= \frac{[3]!}{[2]!} = [3]. \tag{5.16}$$

Trivially $\Delta_0=[1]$ and for $(2,2,0)$ we get $(m,n,p)=(2,0,0)$, such that $\theta(2,2,0)=\frac{(-1)^2[3]![2]!}{[2]![2]!}=[3]$. Hence we get

$$\begin{Bmatrix} 2 & 2 & 0 \\ 2 & 2 & 0 \end{Bmatrix} = \frac{[3]}{[3][3]} = \frac{[1]}{[3]}. \tag{5.17}$$

- For $i = 0, j = 2$ the values change slightly, we have $(a_1, \dots, a_4) = (2, 2, 3, 3)$ and $(b_1, \dots, b_3) = (3, 3, 4)$, therefore $m = 3 = M$ and the tetraeder value is:

$$\mathrm{Tet}\begin{bmatrix} a & b & i \\ c & d & j \end{bmatrix} = \frac{I!}{E!} \sum_{m \le s \le M} \frac{(-1)^s [s+1]!}{\prod_i [s-a_i]! \prod_j [b_j - s]!} \tag{5.18}$$

$$= \frac{([2]!)^2}{([2]!)^5} \left(\frac{(-1)^3 [4]!}{[1]!} \right) \tag{5.19}$$

$$= -\frac{[4]!}{([2]!)^3} = -\frac{[3][4]}{[2]^2}. \tag{5.20}$$

  The other values do not change, hence

$$\begin{Bmatrix} 2 & 2 & 2 \\ 2 & 2 & 0 \end{Bmatrix} = -\frac{[3][4]}{[2]^2[3]^2} = -\frac{[4]}{[2]^2[3]}. \tag{5.21}$$

- For $i = 2, j = 0$ The calculation of the tetraeder returns the same. Now however for $\theta(2, 2, 2)$ we get $(m, n, p) = (1, 1, 1)$ and hence

$$\theta(2, 2, 2) = \frac{(-1)^3 [4]!}{([2]!)^3} = -\frac{[4][3]}{[2]^2}. \tag{5.22}$$

  Since $\Delta_2 = [3]$ we therefore get

$$\begin{Bmatrix} 2 & 2 & 0 \\ 2 & 2 & 2 \end{Bmatrix} = \frac{-\frac{[3][4]}{[2]^2}[3]}{\left(-\frac{[3][4]}{[2]^2}\right)^2} = -\frac{[2]^2}{[4]}. \tag{5.23}$$

- Next, for $i = j = 2$ we have for the first time two summands inside the tetreader calculation. All a_i's are 3 and all b_j's are 4, hence s can be 3 or 4. The sum gives:

$$\sum_{m \le s \le M} \frac{(-1)^s [s+1]!}{\prod_i [s-a_i]! \prod_j [b_j - s]!} = \left(\frac{(-1)^3 [4]!}{[1]} \right) + \left(\frac{(-1)^4 [5]!}{[1]} \right) = [4]! \frac{[2][6]}{[3]}. \tag{5.24}$$

  Here, we use, that $([5] - [1]) = [2]([4] - [2]) = [4]! \frac{[2][6]}{[3]}$. Altogether this gives:

$$\begin{Bmatrix} 2 & 2 & 2 \\ 2 & 2 & 2 \end{Bmatrix} = \frac{\frac{[6][4]}{[2]^4}}{\left(\frac{[3][4]}{[2]^2}\right)^2} = \frac{[6]}{[3][4]}. \tag{5.25}$$

- Finally for $\begin{Bmatrix} 2 & 0 & 2 \\ 2 & 2 & 2 \end{Bmatrix}$ we compute the following. Here $a_i = [2, 3, 3, 2]$, $b_j = [3, 4, 3]$, so $\mathrm{Tet}\begin{bmatrix} 2 & 0 & 2 \\ 2 & 2 & 2 \end{bmatrix} = \frac{[1]^4}{[2]^3}((-1)^3[4]!) = -\frac{[4][3]}{[2]^2}$. Additionally, $\Delta_i = [3]$ and $\theta(2, 2, 2) = -\frac{[3][4]}{[2]^2}$, $\theta(2, 2, 0) = [3]$. Therefore, $\begin{Bmatrix} 2 & 0 & 2 \\ 2 & 2 & 2 \end{Bmatrix} = \frac{-\frac{[4][3]}{[2]^2} \cdot (-1)^2 \cdot [3]}{-\frac{[3][4]}{[2]^2} \cdot [1]} = 1$.

All these matrix entries then give the associators for (X_2, X_2, X_2) to be:

$$\left(1\right) \oplus \begin{pmatrix} \frac{1}{[3]} & -\frac{[2]^2}{[4]} \\ -\frac{[4]}{[2]^2[3]} & \frac{[6]}{[3][4]} \end{pmatrix} \tag{5.26}$$

Theorem 5.8 (Classification of A_k Fusion Categories). *The fusion categories with fusion rules of type A_k are classified, up to monoidal equivalence, by integers $m \in \mathbb{Z}/(k+1)\mathbb{Z}$*

that are coprime to $k+1$. We denote these categories by C_k^m. The associators are then computed using the formula from the previous Proposition 5.6, with the $6j$-symbols:

$$\left[F^d_{a,b,c}\right]_{e,f} = \begin{Bmatrix} a & b & e \\ c & d & f \end{Bmatrix} \tag{5.27}$$

where all quantum numbers and functions depend on the chosen m, i.e. we have $[n] := [n]^m_{k+1}$. Different values of m that are coprime to $k+1$ yield non-equivalent monoidal categories.

Proof. The detailed proof can be found in [27]. □

Example 5.9. For the Fibonacci category we computed the associator in Example 5.7 above. When $m = 1$ we have $[2] = \phi$. For $m = 2$ we get $[2] = -\phi^{-1}$, exactly the two options of Example 2.5.

For $\mathbf{Vec}_{\mathbb{Z}/2\mathbb{Z}}$ we consider $\begin{Bmatrix} 1 & 1 & 0 \\ 1 & 1 & 0 \end{Bmatrix} = -[2]$. For $m = 1$ we have $[2] = 1$, this gives therefore the twisted version, for $l = 2$ we get $[2] = -1$ and get the non-twisted.

Remark 5.10. We can also read off the dimensions quickly and get $\dim(X_i) = [i]$. This also depends on the chosen root of unity. In the Fibonacci and $\mathbb{Z}/2\mathbb{Z}$-case the dimension of the non-trivial object describes the category. It is therefore often enough to only compute this one number.

5.1.2. The center of type A_k fusion categories. All braidings in type A_n are completely classified and well-understood in the literature. Since we are working with fusion categories, it suffices to specify mappings on the components. Braidings can therefore be described as tuples of invertible values. From a braided fusion category, one can construct its center directly if the S-matrix is invertible. Hence, in these small cases we will obtain Lusztig's Conjecture directly.

Definition 5.11. For a type A_k fusion category C_k^m, braidings are parametrized by l being coprime to $k+1$. We set $s := \exp\left(i\pi \frac{l}{4(k+1)}\right)$. Using this value we define a braiding on the summand X_c of $X_a \otimes X_b$ as follows. The collection of these braidings on all summands satisfies the hexagon axiom (see [39, Section 9.9]):

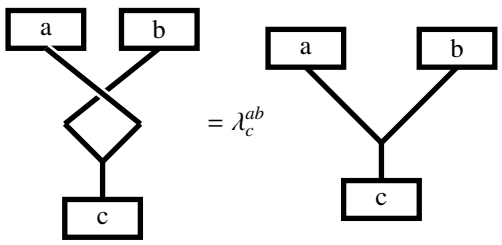

, (5.28)

where $\lambda_c^{ab} = (-1)^{\frac{a+b-c}{2}} s^{\frac{\mathbf{a}(a+2)+b(b+2)-c(c+2)}{2}}$.

Also following [39]:

Proposition 5.12. *For a type A_k fusion category with the braiding defined above, the corresponding S-matrix is given by:*

$$S_{i,j} = (-1)^{i \cdot j}[(i+1)(j+1)]. \tag{5.29}$$

Example 5.13. On C_3 for $m = 1$ we get two non-equivalent braiding structures. We compute:

$$\lambda_0^{00} = 1,\ \lambda_1^{01} = 1,\ \lambda_0^{02} = 1,\ \lambda_0^{11} = -s^3,\ \lambda_2^{11} = s^{-1},\ \lambda_1^{12} = -s^4,\ \lambda_0^{22} = s^8 \tag{5.30}$$

For example, for $l = 1$ and $l = 3$ the braidings on $X_1 \otimes X_1$ differ. We have

$$c_{X_1,X_1} : X_0 \oplus X_1 \simeq X_1 \otimes X_1 \to X_1 \otimes X_1 \simeq X_0 \oplus X_1,\ (-s^3, s^{-1}). \tag{5.31}$$

The corresponding S-matrix is:

$$S_3 := \begin{pmatrix} [1] & -[2] & [3] \\ -[2] & [4] & -[6] \\ [3] & -[6] & [9] \end{pmatrix} = \begin{pmatrix} 1 & -\sqrt{2} & 1 \\ -\sqrt{2} & 0 & \sqrt{2} \\ 1 & \sqrt{2} & 1 \end{pmatrix} \tag{5.32}$$

The S-matrix here is invertible over $\mathbb{C}$. This then gives directly an equivalence to its center:

Theorem 5.14. *Let C be a braided tensor category with invertible S-matrix. The center of C has the form:*

$$\mathcal{Z}(C) \simeq C \boxtimes C^{rev}, \tag{5.33}$$

where $(-)^{rev}$ denotes the category C with reverse braiding, i.e., $c'_{X,Y} = c^{-1}_{Y,X}$ for any braided object $(X, c_{X,-})$ in C and $\boxtimes$ the Deligne Tensor product.

Proof. This result is originally by Müger [54], see also [24, Propositions 8.6.1 and 8.20.12]. They show that the functors $C \to \mathcal{Z}(C),\ X \mapsto (X, c_{-,X})$ and $C^{rev} \to \mathcal{Z}(C),\ X \mapsto (X, c^{-1}_{X,-})$ combine into an equivalence of braided tensor functors:

$$C \boxtimes C^{rev} \to \mathcal{Z}(C). \tag{5.34}$$

□

Note that the center does not depend on the braiding chosen on C as long as the associated S-matrix is invertible. Hence, we can freely choose the braiding for computing the modular data of the center.

Example 5.15. Continuing with Example 5.13 and applying Theorem 5.14, we can compute the center $\mathcal{Z}(C_3)$ as $C_3 \boxtimes C_3^{rev}$. For example, $X_2 \boxtimes X_0 \simeq X_2$ with the same braidings as in C_3, while $X_0 \boxtimes X_2$ is an object of C_3 also isomorphic to X_2, but the braiding on X_1 has the component $-s^{12}$. Also, the S-matrix of $\mathcal{Z}(C_3)$ is then the Kronecker product $S_3 \boxtimes S_3$ (see (5.32)).

These are not directly the Fourier matrices from Lusztig. We will see the connection in section 5.3

5.1.3. Centers of the adjoint part. The adjoint part $\mathrm{Ad}(C_k)$ of a type A_k fusion category is a subfusion category consisting of the objects X_i where i is even. Understanding the Drinfeld center of this subcategory requires different approaches depending on the parity of k. We will see this again for the Fibonacci category and $\mathbf{Vec}_{\mathbb{Z}/2\mathbb{Z}}$. Describing their S-matrixes will be enough to show Lusztig's conjecture.

5.1.3.1. *The case of k even.* When k is even, the braiding of C_k, regardless of the choice, restricted to the adjoint part $\mathrm{Ad}(C_k)$ remains modular, meaning the corresponding S-matrix is still invertible. This allows us to apply Theorem 5.14 again:

Lemma 5.16 ([13, Lemma 3.1]). *For k even, we have*

$$\mathcal{Z}(\mathrm{Ad}(C_k)) \simeq \mathrm{Ad}(C_k) \boxtimes \mathrm{Ad}(C_k^{rev}). \tag{5.35}$$

Example 5.17. For $k = 4$, the adjoint part of $C_{k,m}$ for $m = 1$ is the Fibonacci category $\mathcal{F}$. The S-matrix is the restriction of the S-matrix of C_4 to the even rows and columns:

$$S_{\mathcal{F}} = \begin{pmatrix} [1] & [3] \\ [3] & [9] \end{pmatrix} = \begin{pmatrix} 1 & \varphi \\ \varphi & -1 \end{pmatrix}. \tag{5.36}$$

Note that $[9] = -[1] = -1$ and $[3] = \varphi$. This matrix is invertible, as expected.

The center $\mathcal{Z}(\mathrm{Ad}(C_4)) = \mathcal{Z}(\mathcal{F})$ can be visualized as a subcategory of $\mathcal{Z}(C)$ lying over the even graded objects:

$$\mathcal{Z}(\mathrm{Ad}(C_4)) = \begin{matrix} X_0 & \cdot & X_2 & \cdot \\ \cdot & X_0 \oplus X_2 & \cdot & X_2 \\ X_2 & \cdot & X_0 \oplus X_2 & \cdot \\ \cdot & X_2 & \cdot & X_0 \end{matrix} \tag{5.37}$$

where the black (non-gray) entries represent the objects in $\mathcal{Z}(\mathcal{F})$. Note that there are (gray) objects in the center that are even graded, but come from odd graded objects through the Deligne tensor product.

The S-matrix of $\mathcal{Z}(\mathcal{F})$ is then

$$S_{\mathcal{F}} \boxtimes S_{\mathcal{F}} = \varphi \begin{pmatrix} \varphi^{-1} & 1 & 1 & \varphi \\ 1 & -\varphi^{-1} & \varphi & -1 \\ 1 & \varphi & -\varphi^{-1} & -1 \\ \varphi & -1 & -1 & \varphi^{-1} \end{pmatrix}. \tag{5.38}$$

where the ordering of objects follows the pattern of the non-gray entries in the matrix above.

5.1.3.2. *The case of k odd.* When k is odd, the restriction of the S-matrix to the adjoint part is no longer invertible. For instance, in the case of C_3, restricting to the even rows and columns of (5.32) gives the degenerate matrix $\begin{pmatrix} 1 & 1 \\ 1 & 1 \end{pmatrix}$. Therefore, we need a different approach to determine the center.

Construction 5.18. Let C be a braided fusion category with braiding c. For any fusion subcategory $\mathcal{D} \subseteq C$, we write $\mathcal{D}'$ for the *centralizer*, i.e., the full fusion subcategory consisting of all objects $(X, c) \in C$ such that $c_{X,Y} \circ c_{Y,X} = \mathrm{id}_{X \otimes Y}$ for all $(Y, c) \in \mathcal{D}$.

Let G be a finite group. If we can decompose (as an abelian category) a fusion category C into components $C = \bigoplus_{g \in G} C_g$, such that all C_g are non-empty and for all objects $X \in C_g$, $Y \in C_h$ we have $X \otimes Y \in C_{gh}$, then we call C a *G-graded fusion category*. The trivial component $\mathcal{D} := C_0 \subseteq C$ is a fusion subcategory. By [30, Theorem 3.5], we have an isomorphism

$$\mathcal{Z}_{\mathcal{D}}(C)^G \simeq \mathcal{Z}(C). \tag{5.39}$$

The simple objects in $\mathcal{Z}(C)$ restricting to direct sums of the monoidal unit in C under the forgetful functor $\mathcal{Z}(C) \to C$ form a subcategory $\mathcal{E} \simeq \mathrm{Rep}(G) \subseteq \mathcal{Z}(C)$. We get an isomorphism

$$(\mathcal{E}')_G \simeq \mathcal{Z}(\mathcal{D}), \tag{5.40}$$

where $(-)_G$ stands for the *de-equivariantization*, which has the property $(\mathcal{C}^G)_G \simeq \mathcal{C}$. We refer to [30, Section 2.5] for details and see examples below.

Example 5.19. For $k = 3$, the category C_3 is $\mathbb{Z}/2\mathbb{Z}$-graded, and $\mathcal{D} \coloneqq \mathrm{Ad}(C_3)$ the adjoint part is equivalent to $\mathbf{Vec}_{\mathbb{Z}/2\mathbb{Z}}$.

The subcategory $\mathcal{E} \simeq \mathrm{Rep}(\mathbb{Z}/2\mathbb{Z})$ is generated by two copies of X_0. The first, the monoidal unit, has trivial braidings. It comes from $X_0 \boxtimes X_0$. The second copy's braidings, coming from $X_2 \boxtimes X_2$, are trivial on X_0 and X_2 but we have

$$c_{X_0,X_1} : X_1 \to X_1,\ (-1), \tag{5.41}$$

for the braiding on X_1. We write $(X_0, \tilde{c})$ for this second copy to distinguish it from the unit.

From this, we can compute the centralizer $\mathcal{E}'$. Since the braiding of $(X_0, \tilde{c})$ on X_1 is non-trivial, no copy of X_1 can lie in $\mathcal{E}'$ as their braidings on X_0 are trivial. All other objects, however, lie in the centralizer, i.e., the black (non-gray) objects in

$$\begin{matrix} X_0 & X_1 & X_2 \\ X_1 & X_0 \oplus X_2 & X_1. \\ X_2 & X_1 & X_0 \end{matrix} \tag{5.42}$$

Under the de-equivariantization, both copies of X_0 and X_2 in the corners will be isomorphic, while the object $X_0 \oplus X_2$ decomposes into two simple objects X_0 and X_2 not isomorphic to the others. In total, we get 4 simple objects in the center $\mathcal{Z}(\mathrm{Ad}(C_3))$.

The restriction of the S-matrix of $\mathcal{Z}(C_3)$ to the objects X_0, X_2, and $X_0 \oplus X_2$ has the form

$$\begin{pmatrix} 1 & 1 & 2 \\ 1 & 1 & -2 \\ 2 & -2 & 0 \end{pmatrix}, \tag{5.43}$$

while the S-matrix of $\mathcal{Z}(\mathrm{Ad}(C_3))$ has the form

$$\begin{pmatrix} 1 & 1 & 1 & 1 \\ 1 & 1 & -1 & -1 \\ 1 & -1 & 1 & -1 \\ 1 & -1 & -1 & 1 \end{pmatrix}. \tag{5.44}$$

We can observe that the sum of the third and fourth rows and columns corresponds to the entries for $X_0 \oplus X_2$ in the first matrix.

Theorem 5.20. *For $k = 2m + 1$ odd, the center $\mathcal{Z}(\mathrm{Ad}(C_k))$ has $m^2 + m + 2$ simple objects.*

Proof. By Theorem 5.14, $\mathcal{Z}(C_k) \simeq C_k \boxtimes C_k^{rev}$ has $k^2 = (2m + 1)^2$ simple objects $\{X_i \boxtimes X_j \mid 0 \le i, j \le 2m\}$.

The category C_k is $\mathbb{Z}/2\mathbb{Z}$-graded: the even-indexed objects $\{X_0, X_2, \ldots, X_{2m}\}$ form the trivial component $\mathrm{Ad}(C_k)$, and the odd-indexed objects $\{X_1, X_3, \ldots, X_{2m-1}\}$ form the non-trivial component. The subcategory $\mathcal{E} \simeq \mathrm{Rep}(\mathbb{Z}/2\mathbb{Z}) \subseteq \mathcal{Z}(C_k)$ acts on $\mathcal{Z}(C_k)$ by tensoring with $X_{k-1} \boxtimes X_{k-1}$, which maps $X_i \boxtimes X_j$ to $X_{k-1-i} \boxtimes X_{k-1-j}$. The centralizer $\mathcal{E}'$ consists of all $X_i \boxtimes X_j$ with $i + j$ even: there are $(m + 1)^2$ pairs with both indices even and m^2 pairs with both indices odd, giving $|\mathcal{E}'| = 2m^2 + 2m + 1$.

Under the $\mathbb{Z}/2\mathbb{Z}$-action, the object $X_i \boxtimes X_j$ is mapped to $X_{k-1-i} \boxtimes X_{k-1-j}$. Since tensoring with the non-trivial object in $\mathcal{E}$ is an autoequivalence, these two objects become isomorphic in the de-equivariantization $(\mathcal{E}')_{\mathbb{Z}/2\mathbb{Z}} \simeq \mathcal{Z}(\mathrm{Ad}(C_k))$.

The unique fixed point of this action in $\mathcal{E}'$ is $X_m \boxtimes X_m$ (since $k - 1 - m = m$ requires $k = 2m + 1$). By [30, Proposition 3.9], simple objects of $\mathcal{Z}(C_k)$ are parameterized by pairs

consisting of a conjugacy class K of $\mathbb{Z}/2\mathbb{Z}$ and a simple G_K-equivariant object. Since $\mathbb{Z}/2\mathbb{Z}$ has two irreducible representations, the fixed point $X_m \boxtimes X_m$ gives rise to two non-isomorphic simple objects in $\mathcal{Z}(\mathrm{Ad}(C_k))$.

The remaining $2m^2 + 2m$ objects in $\mathcal{E}'$ form $m^2 + m$ free orbits of size 2, each contributing one simple object. In total we get $m^2 + m + 2$ simple objects. □

The S-matrix entries for the objects arising from pairs $X_i \boxtimes X_j$ are inherited from those of $\mathcal{Z}(C_k)$. Those of the two simples arising from $X_m \boxtimes X_m$ can be determined from the restricted S-matrix and the de-equivariantization, as illustrated in the example of C_3 above.

After establishing that the asymptotic Hecke categories are always adjoint parts of some type A_k fusion categories, we will come back to their S-matrixes in the conclusion.

5.2. The asymptotic Hecke categories associated to two-sided cells

In this section, we finaly describe all asymptotic categories associated to the H-cells of section 1.4. We begin by investigating dihedral groups, where the recoupling theory describe the complete fusion data. In the other cases we argue by specific computations.

5.2.1. Recoupling for dihedral groups. We now investigate the recoupling theory for dihedral groups. Throughout this subsection, (W, S) denotes the dihedral group of type $I_2(k)$ with $S = \{s, t\}$. We use $\rho = \alpha_s + \alpha_t$ as our parameter (which will be properly scaled later).

Definition 5.21. For $x, y, z \in W$ in the subregular cell, let b, c, a be their respective lengths. We say that (x, y, z) is k-admissible if $(b-1, c-1, a-1)$ is k-admissible and x ends in the same reflection that z and y start in. We set m, n, p as:

$$m = \frac{b+c-a-1}{2},\ n = \frac{a+c-b-1}{2},\ p = \frac{a+b-c-1}{2} \tag{5.45}$$

We then define the unique projection:

$p^z_{x,y} :=$ 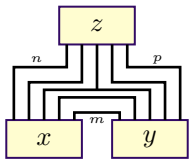

(5.46)

Lemma 5.22. *The projection $p^z_{x,y}$ is indeed the only map in* $\mathrm{Hom}(B_x B_y, B_z)$ *of degree* -1.

Proof. One can prove this either by computing with the Soergel Hom formula or by arguing via the light leaves construction. It is clear that this projection has degree -1. We want to show that any map $B_x B_y \to B(w_0) \to B_z$ has degree at least $+1$.

Consider the first map. A light leaf that maps to w_0 needs at least k many $U1$ decorations. The lowest possible degree occurs when all other decorations are $U0$. We calculate the minimal degree to be $b + c - k$. Now in a map $B(w_0) \to B_z$, we can have no $U0$ decorations as the first rex moves occur for the longest word. Hence we have $D0$ decorations giving us minimal degree $k-a$. In total, this gives minimal degree $(b+c-k)+(k-a) = b+c-a$.

Since $(a-1, b-1, c-1)$ is k-admissible we have that $0 \leq m = \frac{b+c-a-1}{2}$, hence the degree is at least $+1$. □

LEMMA 5.23. *For (x, y, z) k-admissible, the coefficient $\kappa^z_{x,y}$ is $\frac{(-1)^{a-1}[a]}{(2-[2])\theta(a-1,b-1,c-1)}$.*

PROOF. We have a computation similar to the one in the Temperley–Lieb category:

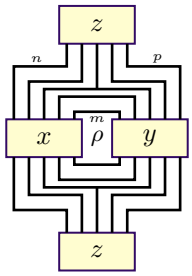

(5.47)

The main idea is to prove this using the functor $\mathcal{F}$ from the two-color Temperley–Lieb category to the dihedral Soergel category. However, the functor does not map directly to a diagram as in (5.47), as this contains a scalar factor ρ. Hence, we need to write this map without scalar factors. We also use different colors to better illustrate the calculations.

As a first step, we write the diagram as a sum of two diagrams with α_s and α_t in the middle. We assume that the innermost of the a-many strings is colored blue, just as s is.

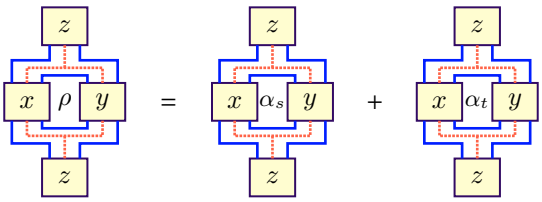

(5.48)

For the second diagram, we find a preimage in the Temperley–Lieb category immediately:

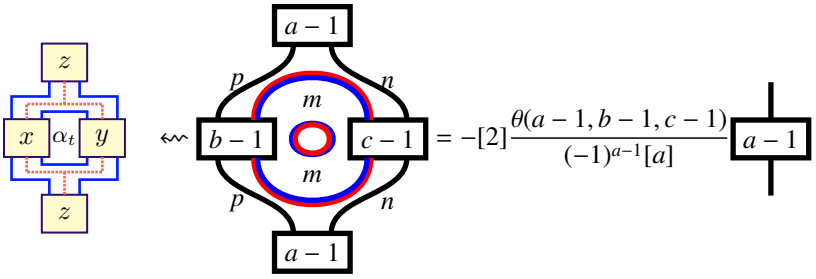

(5.49)

For the first diagram, we first apply one induction step from the Jones–Wenzl projectors to simplify the diagram. Note that most summands disappear due to the pitchfork rule. We write $\tilde{x}$ for $xs < x$.

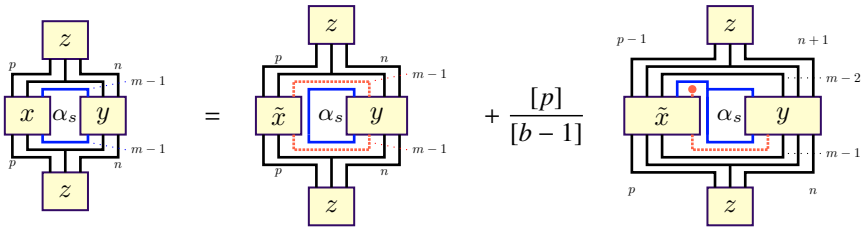

(5.50)

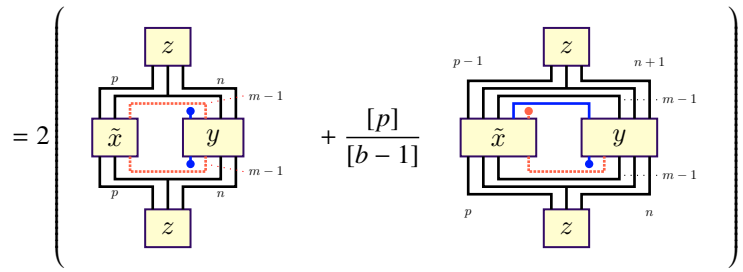

(5.51)

This has a preimage under the functor F:

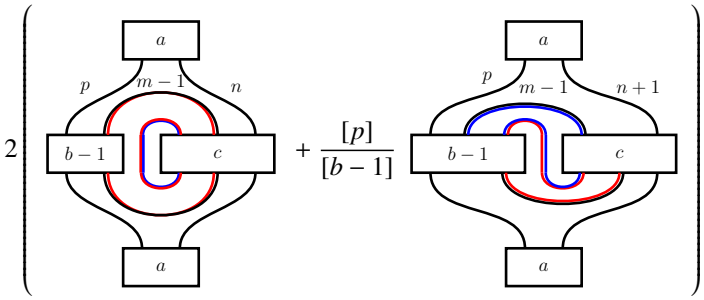

(5.52)

And finally, we use another Jones–Wenzl step to simplify further:

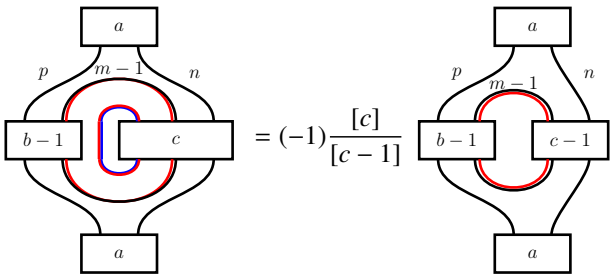

(5.53)

And using the recursive structure of the Jones–Wenzl projector we get:

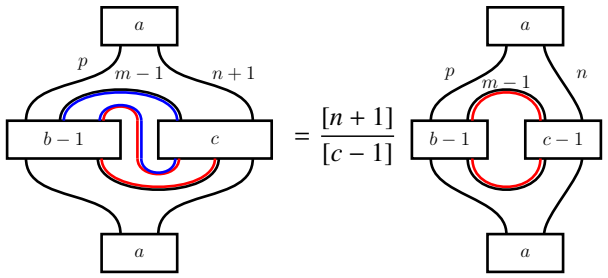

(5.54)

Now we bring all the diagrams into the same form, using the trace formula for Jones–Wenzl projectors from Lemma 2.31. This gives us:

$$
\begin{aligned}
&2\left(\frac{[p][n+1]}{[b-1][c-1]}-\frac{[c]}{[c-1]}\right)\frac{\theta(m-1,n,p)}{(-1)^{a-1}[a]}\\
&=2\left(\frac{[p][n+1]-[b-1][c]}{[b-1][c-1]}\right)(-1)^{m-1}\frac{[m+n+p]![n]![m-1]![p]!}{[n+p+1]![m+p-1]![m+n-1]!}\\
&=2\left(\frac{[p][n+1]-[m+p][m+n+1]}{[m+p][m+n]}\right)(-1)^{m-1}\frac{[m+n+p]![n]![m-1]![p]!}{[n+p+1]![m+p-1]![m+n-1]!}\\
&=2\left(\frac{-[m][m+n+p+1]}{[m+p][m+n]}\right)(-1)^{m-1}\frac{[m+n+p]![n]![m-1]![p]!}{[n+p+1]![m+p-1]![m+n-1]!}\\
&=2(-1)^m\frac{[m+n+p+1]![n]![m]![p]!}{[n+p+1]![m+p]![m+n]!}=2\frac{\theta(a-1,b-1,c-1)}{(-1)^{a-1}[a]}
\end{aligned}
\tag{5.55}
$$

Together we hence get:

$$
\kappa^z_{x,y}=\left((2-[2])\frac{\theta(a-1,b-1,c-1)}{\mathrm{tr}(JW_{a-1})}\right)^{-1}=\frac{(-1)^{a-1}[a]}{(2-[2])\theta(a-1,b-1,c-1)}. \tag{5.56}
$$

This concludes the computation of $\kappa^z_{x,y}$. □

Remark 5.24. We observe that the computation follows a similar approach to that used in the Temperley–Lieb category. The methods from [39] can be adapted to our new setting, demonstrating that we obtain the same values for the associator computations, but with appropriate shifts in the indices.

Theorem 5.25 (Classification of Asymptotic Hecke Categories for Dihedral Groups). *Let* $\mathbf{c}$ *be the subregular cell in type* $I_2(k)$ *and* $J_{\mathbf{c}}=\{j_x \mid x\in\mathbf{c}\}$ *the asymptotic Hecke algebra.*

For a triple $(x,y,z)\in\mathbf{c}\times\mathbf{c}\times\mathbf{c}$*, the associators are zero if* $j_xj_yj_z$ *is zero. Otherwise, the F-symbols for the associator are given by:*

$$
\begin{Bmatrix} x & w & e\\ z & y & f\end{Bmatrix}:=\begin{Bmatrix} \ell(y)-1 & \ell(w)-1 & \ell(e)-1\\ \ell(z)-1 & \ell(x)-1 & \ell(f)-1\end{Bmatrix} \tag{5.57}
$$

where w *ranges over all summands* j_w *of* $j_xj_yj_z$*, and* e *and* f *are chosen such that the tuples* (x,y,e)*,* (y,z,f)*,* (e,z,w)*, and* (x,f,w) *are* k*-admissible.*

Proof. This theorem formalizes the observation that the computation of the F-symbols is exactly the same as in the A_k fusion category. Now however, we have a category with mroe objects, specifically, for any given length, we have two elements in the dihedral group

(corresponding to whether the element begins with s or t). The computation of the associators then reduces to tracking which triples are k-admissible and applying the corresponding formulas with the appropriate shifts in indices. □

Remark 5.26. The main observation was that the computation of the associators for the asymptotic Hecke category, Lemma 5.23, works in the same way as the Recoupling theory, section 5.1.

We could also show this using [17, Proposition 1.1]: The (two-colored) Temperley–Lieb category embeds as the degree 0 morphisms into the category of Soergel bimodules of a dihedral group. By [19, Theorem 2.15] we even have a degree-zero equivalence.

We can also restrict to an H-cell in there.

Corollary 5.27. *Let $\mathbf{h}_s \subset \mathbf{c}$ be the* H*-cell consisting of elements that start and end with the simple reflection s. The fusion subcategory $\mathcal{J}_{\mathbf{h}_s} \subset \mathcal{J}_{\mathbf{c}}$ is equivalent to* $\mathrm{Ad}(C_{k-1})$*, the adjoint part of the fusion category C_{k-1}.*

Proof. This follows directly from Theorem 5.25 as now all triples are k-admissible. We get exactly the same structure constants. □

5.2.2. Asymptotic Hecke categories in $\mathbf{a}(1)$-finite groups. In the previous section, we provided a complete classification of the asymptotic Hecke category for the subregular cell in dihedral groups. This classification serves as a fundamental building block for understanding more general Coxeter groups.

For any Coxeter group (W, S) with a cell $\mathbf{c}$ of $\mathbf{a}(1)$, the structure of the asymptotic category can be related to the dihedral case. In particular, according to the classification of $\mathbf{a}(1)$-finite Coxeter groups, we have at most two simple reflections $s, t \in S$ with $m_{s,t} > 3$. The subgroup generated by $\{s, t\}$ is a dihedral group, and its subregular cell c' exhibits the structure we analyzed in detail in the previous section.

Corollary 5.28. *For the subregular cell $\mathbf{c}'$ generated by $\{s, t\}$ as described above, the asymptotic Hecke category $\mathcal{J}_{\mathbf{c}'}$ has the structure given in Theorem 5.25 for $k = m_{s,t}$.*

5.2.2.1. *Subregular cell in type H_3.* The cell $\mathbf{c}_1$ of $\mathbf{a}(1)$ in type H_3 contains 18 elements ordered in 3 left and right cells by the starting and ending reflection, see Figure 1.4.

$$\mathbf{c}_1 = \begin{array}{|c|c|c|} \hline 1{,}121 & 21{,}2121 & 32121{,}321 \\ \hline 12{,}1212 & 2{,}212 & 3212{,}32 \\ \hline 12123{,}123 & 23{,}213 & 3{,}32123 \\ \hline \end{array} \tag{5.58}$$

We know that the asymptotic category of $\mathbf{h} = \{3, 32123\}$ is equivalent to the dihedral case, however here the F-symbols differ by a gauge transformation. We track this one time to show that they are equivalent. This shows us that the asymptotic category of the whole subregular cell $\mathbf{c}$ has more F-symbol entries differing from the dihedral case.

The idempotent corresponding to 3 is clear. For 32123 consider the following pleth graph:

$$\Gamma(32123) = \quad 3 \longrightarrow 32 \rightleftarrows 321 \longrightarrow 3212 \dashrightarrow 32123 \ , \tag{5.59}$$

By Lemma 3.31 the idempotent 32123 has the recursive form:

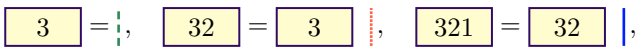

(5.60)

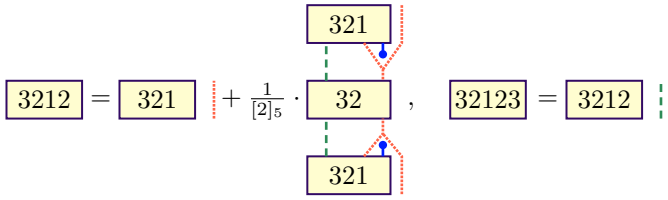

(5.61)

For computing the coefficients κ we state the following auxiliary lemma. By *partial traces*, we mean the traces that remain after removing one step in the full cup/cap computation (compare with the full trace in (2.64)).

Lemma 5.29. *We have the following computational rules for partial traces around* 32123.

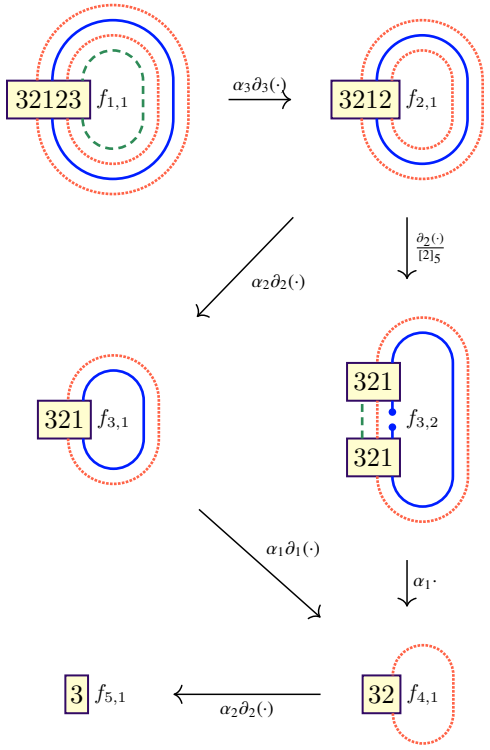

(5.62)

This is to be read as follows: We have for example $f_{2,1} = \partial_3(f_{1,1})\alpha_3$. *For* $f_{1,1} = \rho$ *we get in particular:*

$$f_{2,1} = \alpha_3,\ f_{3,1} = -\alpha_2,\ f_{3,2} = \frac{-1}{[2]_5},\ f_{4,1} = \frac{[3]_5}{[2]_5}\alpha_1,\ f_{5,1} = -[3]_5\alpha_2 \tag{5.63}$$

Proof. All equations follow directly from the recursive structure of the idempotents. Note that $[2]_3 = 1$ and that $[2]_5 - \frac{1}{[2]_5} = \frac{[2]_5^2-1}{[2]_5} = \frac{[3]_5}{[2]_5}$. □

Now we need to fix the inclusion and projection maps. In all cases there is only one light leaf that gives a map of degree -1. We have:

$p^3_{3,3} :=$  $, p^{32123}_{3,32123} :=$ 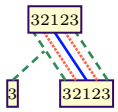 $, p^{32123}_{32123,3} :=$ 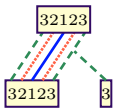 , (5.64)

$p^3_{32123,32123} :=$ 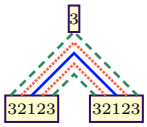 $, p^{32123}_{32123,32123} :=$ 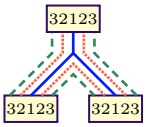 (5.65)

Using the previous Lemma 5.29 we can compute the coefficients κ:

Lemma 5.30.

- *We have* $\kappa^3_{3,3} = 1$*:*

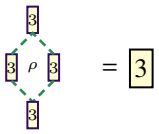 (5.66)

Similarly $\kappa^{32123}_{32123,3} = 1 = \kappa^{32123}_{3,32123}$.

- *We have* $\kappa^3_{32123,32123} = \frac{1}{[3]_5} = \varphi - 1$*:*

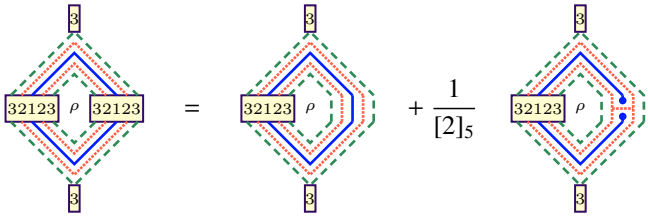 (5.67)

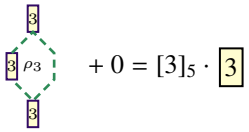 (5.68)

Here we use a pitchfork rule for the second term and then Lemma 5.29 to get that $\rho_3 = -[3]_5\alpha_2$

- *We have* $\kappa^{32123}_{32123,32123} = 2 - \varphi$*:*

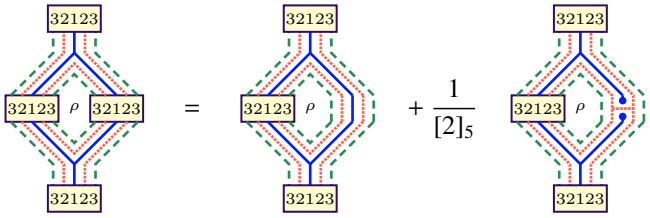

(5.69)

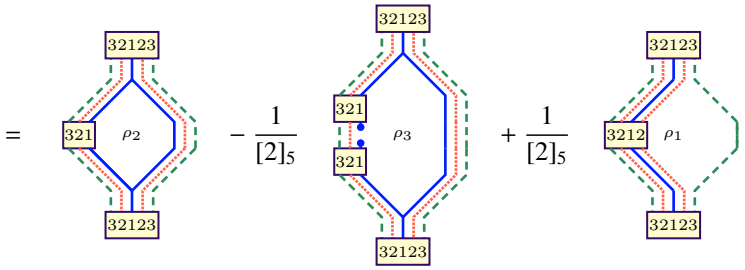

(5.70)

$$= \frac{[4]_5}{[2]_5^2} \boxed{32123} \tag{5.71}$$

Again, by Lemma 5.29 we have $\rho_2 = -\alpha_2$*,* $\rho_1 = -1$*,* $\rho_3 = \frac{1}{[2]_5}$*, so we have* $[2]_5 - \frac{2}{[2]_5} = \frac{[3]_5 - [1]_5}{[2]_5} = \frac{[4]_5}{[2]_5^2}$*. Therefore, since* $[4]_5 = 1$*, the coefficient is* $\frac{1}{\varphi^2} = 2 - \varphi$*.*

Next we will compute associators. We will see in Proposition 5.33 that the category is equivalent to the Fibonacci category, however with a gauge transformation.

Lemma 5.31. *We have the following identities:*

(A)

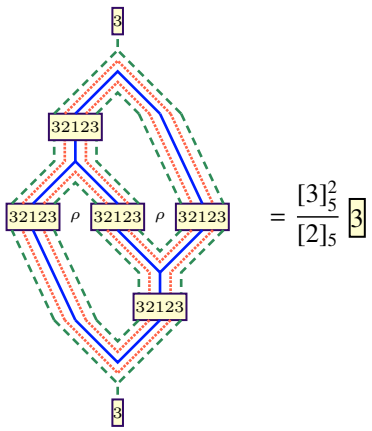

$$= \frac{[3]_5^2}{[2]_5} \boxed{3} \tag{5.72}$$

(B)

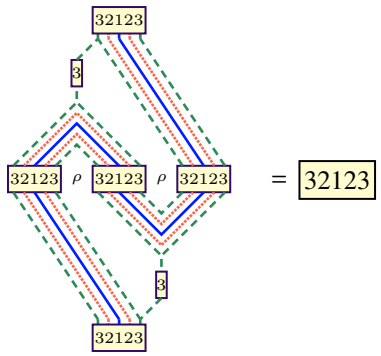

$$= \boxed{32123} \tag{5.73}$$

(C)

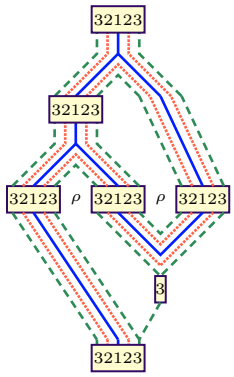

$$= \frac{[4]_5}{[2]_5^2} \boxed{32123} \tag{5.74}$$

(D)

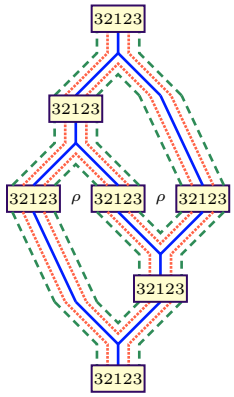

$$= \frac{[3]_5}{[2]_5^2} \boxed{32123} \tag{5.75}$$

Proof. In all cases we use trivalent sliding and properties of the idempotents.

(A) We simplify:

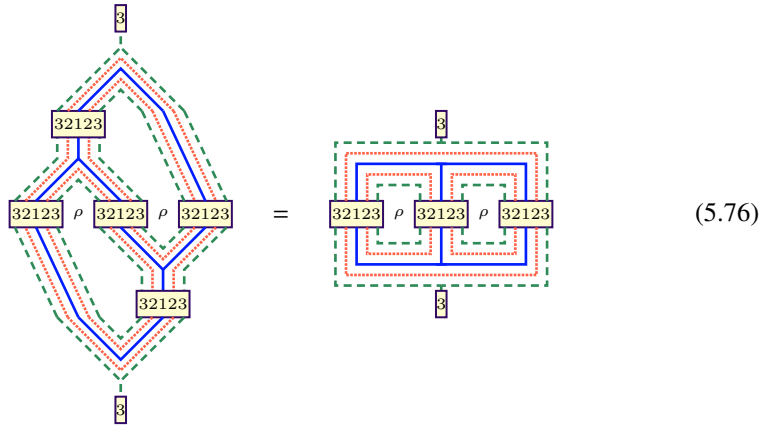

(5.76)

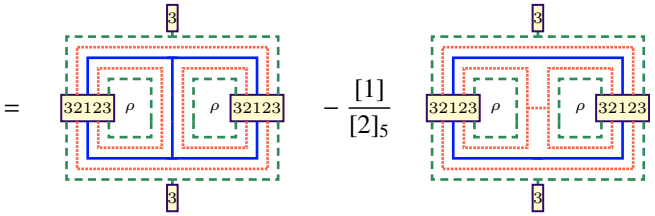

(5.77)

The first diagram can be simplified using the partial trace properties.

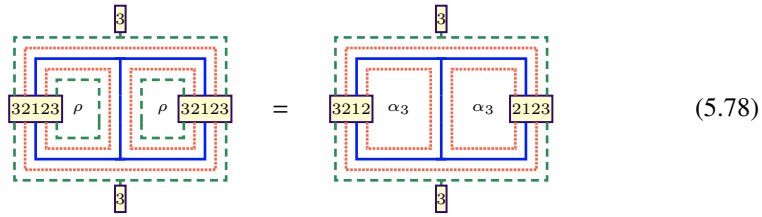

(5.78)

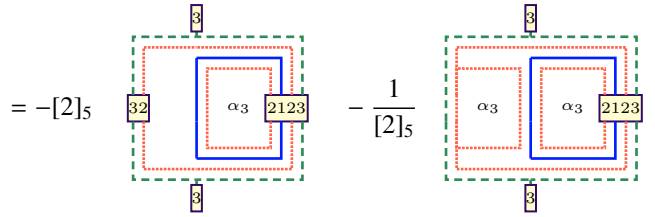

(5.79)

$$= \frac{-[3]_5}{[2]_5}$$ 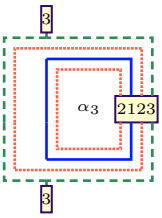

$$= \frac{-[3]_5^2}{[2]_5}\ \boxed{3} \tag{5.80}$$

The second term simplifies similarly:

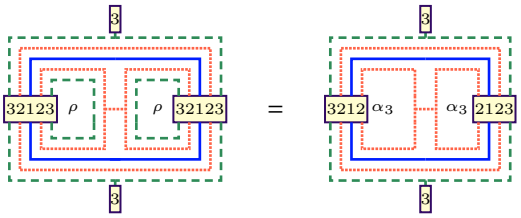

(5.81)

$= -$ 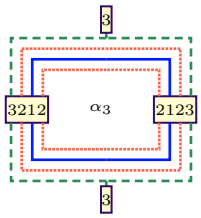

$= -[3]_5\ \boxed{3}$ (5.82)

This gives as coefficient $\frac{-[3]_5^2}{[2]_5} + [2]_5[3]_5 = \frac{[3]_5^2}{[2]_5}$.

(B) We directly have:

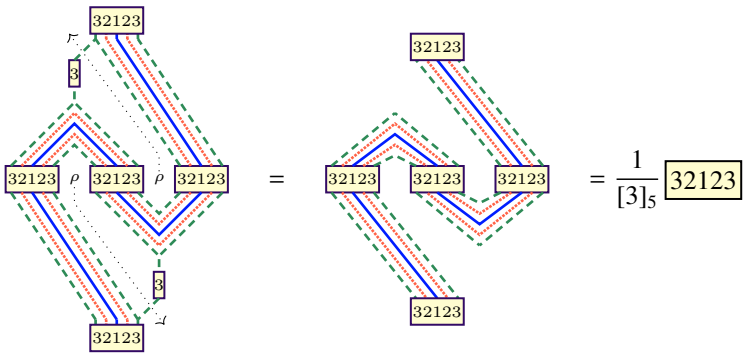

$= \frac{1}{[3]_5}\ \boxed{32123}$ (5.83)

(C) Next we consider:

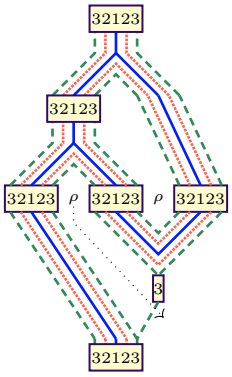

(5.84)

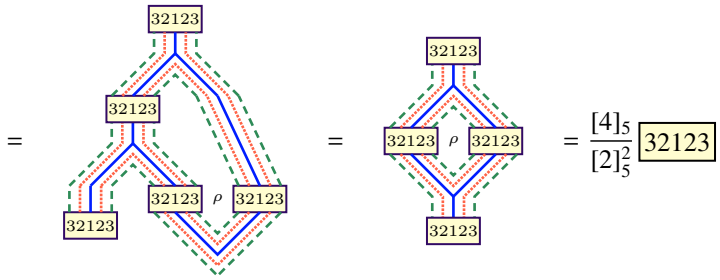

(5.85)

Here we use (5.71).

(D) The final term takes longer to compute. First we only look at the composition of the projections:

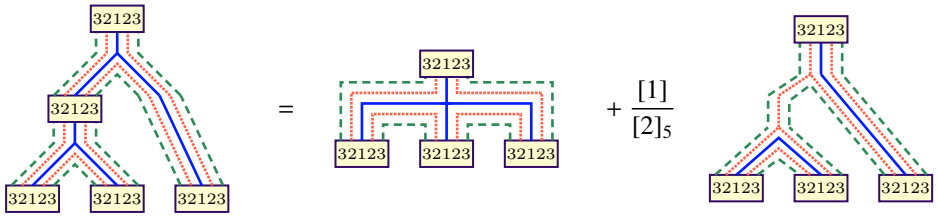

(5.86)

Note that the second summand factors on the left over the element 323, which is not inside the cell of $\mathbf{a}(1)$. Similar to (4.40) we use a quotient relation $\mathrm{id}_{323} = 0$ to get:

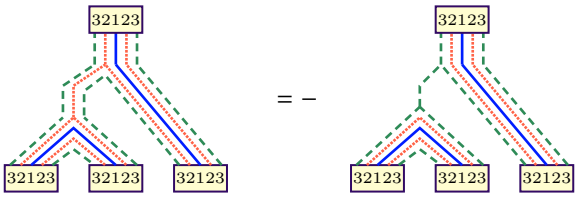

(5.87)

This means that the last term in the following computation was computed earlier:

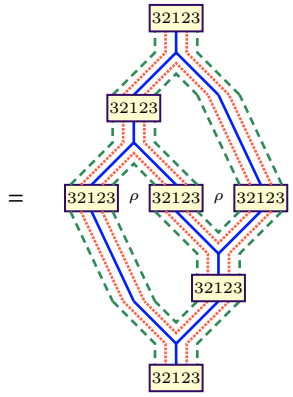

(5.88)

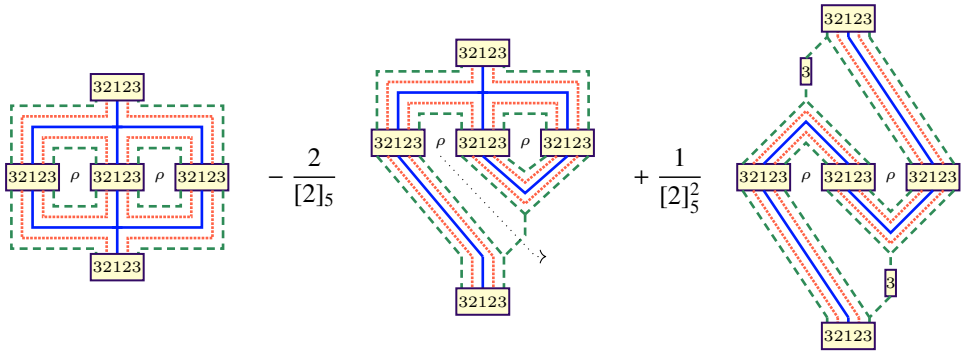

(5.89)

The first summand however inside the associator calculation gives

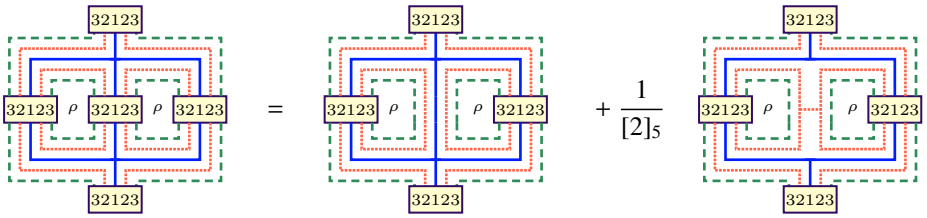

(5.90)

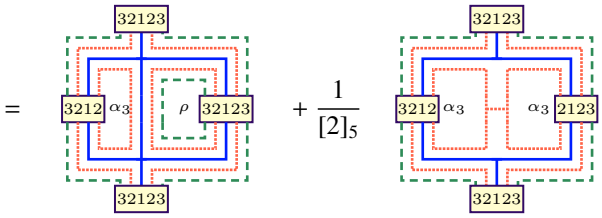

(5.91)

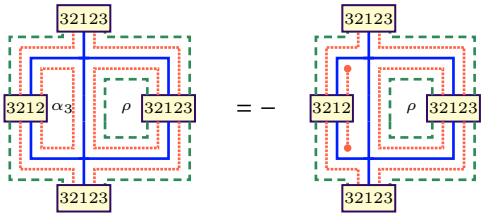

(5.92)

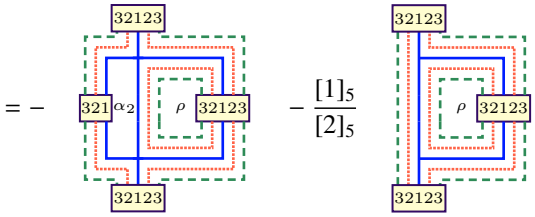

(5.93)

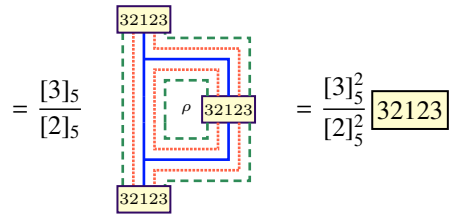

(5.94)

On the other hand:

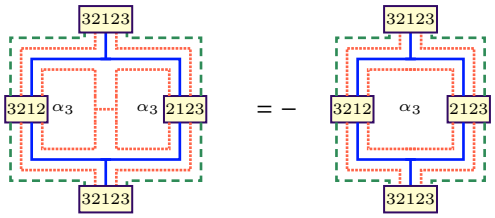

(5.95)

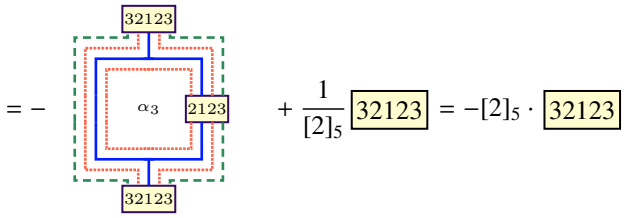

(5.96)

Where in the last line we use $\frac{[3]_5}{[2]_5} + \frac{[1]_5}{[2]_5} = \frac{[2]_5^2}{[2]_5} = [2]_5$. This coefficient is therefore $\frac{[3]_5^2}{[2]_5^2} - [1]_5$. It remains the middle term of (5.88):

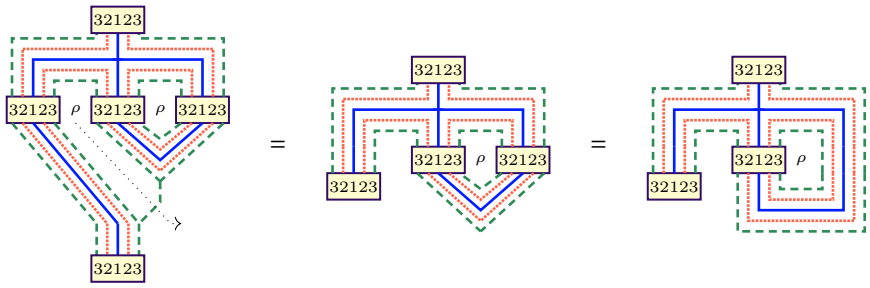

(5.97)

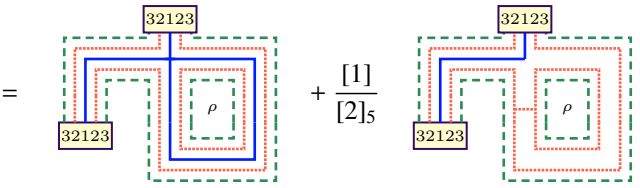

(5.98)

$$= \left([2]_5 - \frac{[1]}{[2]_5}\right) \boxed{32123} = \left(\frac{[3]_5}{[2]_5}\right) \boxed{32123} \tag{5.99}$$

In (5.88) we get $\frac{[5]+2[1]}{[2]^2} - 2\frac{[1]}{[2]}\frac{[3]}{[2]} + \frac{1}{[2]^2} = \frac{[5]-2[3]+3[1]}{[2]^2} = \frac{\left(\frac{[6]-[4]+[2]}{[2]}\right)}{[2]^2} = \frac{([4]-[2])([3]-[1])}{[2]^3} = \frac{\left(\frac{[6]}{[3]}\frac{[4]}{[2]}\right)}{[2]^3} = \frac{[6][4]}{[3][2]^4}$.

□

Corollary 5.32. *The associators in $\mathcal{J}_{\mathbf{h}}$ for $\mathbf{h} = \{3, 32123\}$ are trivial, except for:*

$$a_{32123,32123,32123} = \mathrm{id}_{B_3} \oplus \begin{pmatrix} \frac{[1]}{[3]} & \frac{[2]^2}{[4]} \\ \frac{[4]}{[2]^2[3]} & \frac{[6]}{[3][4]} \end{pmatrix} \mathrm{id}_{B_{32123}} . \tag{5.100}$$

Proof. We consider the computations of Lemma 5.31 and then scale by the coefficients κ of Lemma 5.30. □

Comparing with the Fibonacci category from Example 5.7, the F-symbol matrix in (5.100) differs in the off-diagonal entries: the matrix entries in positions $(1, 2)$ and $(2, 1)$ are negatives of those in the Fibonacci case. Both categories are equivalent, as we are witnessing a gauge transformation. We will see this in the next theorem in detail. In the general calculation for other cases we will only compute enough fusion data to find the right categorification.

Proposition 5.33. *The category $\mathcal{J}_{\mathbf{h}}$ for $\mathbf{h} = \{3, 32123\}$ in case H_3 is equivalent to the Fibonacci category.*

Proof. The freedom of choosing projection and inclusion maps gives different associators. We fixed 5 such maps in the beginning. We will now list how the associator changes when choosing different ones.

If we multiply $(p^3_{3,3}, p^{32123}_{3,32123}, p^{32123}_{32123,3}, p^3_{32123,32123}, p^{32123}_{32123,32123})$ by $(\alpha, \beta, \gamma, \delta, \epsilon)$, and then multiply the corresponding inclusions by $(\alpha^{-1}, \beta^{-1}, \gamma^{-1}, \delta^{-1}, \epsilon^{-1})$ we can then consider a general associator:

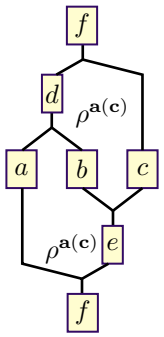

(5.101)

This describes all gauge transformations. We show the result in Table 5.1.

a	b	c	d	e	f	Gauge	Fibonacci	H3a1
1	**1**	**1**	**1**	**1**	**1**	1	1	1
1	**1**	**X**	**1**	**X**	**X**	α	1	1
1	**X**	**1**	**X**	**X**	**X**	1	1	1
X	**1**	**1**	**X**	**1**	**X**	$\gamma^{-1}\alpha^{-1}$	1	1
1	**X**	**X**	**X**	**1**	**1**	$\beta\alpha^{-1}$	1	1
1	**X**	**X**	**X**	**X**	**X**	1	1	1
X	**1**	**X**	**X**	**X**	**1**	$\gamma\beta^{-1}$	1	1
X	**1**	**X**	**X**	**X**	**X**	$\gamma\beta^{-1}$	1	1
X	**X**	**1**	**1**	**X**	**1**	γ^{-1}	1	1
X	**X**	**1**	**X**	**X**	**X**	1	1	1
X	**X**	**X**	**1**	**1**	**X**	$\beta\gamma^{-1}$	$\frac{1}{[3]_5}$	$\frac{1}{[3]_5}$
X	**X**	**X**	**X**	**X**	**X**	$\beta\delta\epsilon^{-2}$	$-\frac{[4]_5^2}{[2]_5^2[3]_5}$	$\frac{[4]_5^2}{[2]_5^2[3]_5}$
X	**X**	**X**	**X**	**1**	**X**	$\epsilon^2\delta^{-1}\gamma^{-1}$	$-\frac{[2]_5^2}{[4]_5}$	$\frac{[2]_5^2}{[4]_5}$
X	**X**	**X**	**X**	**X**	**X**	1	$\frac{[6]_5}{[3]_5[4]_5}$	$\frac{[6]_5}{[3]_5[4]_5}$
X	**X**	**X**	**X**	**X**	**1**	1	1	1

TABLE 5.1. Object notation from Example 2.5: **1** (unit object) and **X**

Solving this system of equations then gives $\alpha = \beta = \gamma = 1$ and leaves us with the choices: $\delta = -\epsilon^2$. One could choose $(\delta, \epsilon) = (-1, -1)$ or also $(1, i)$ would work. Nevertheless, both show that the categories are gauge equivalent.

□

In general, the F-symbols in the asymptotic category of the subregular cell can always be constructed out of the symbols in the dihedral case. This example shows us however that in the multifusion structure we get gauge freedoms everywhere. We will now only focus on H-cells as these are enough for the center computation (see Proposition 2.15).

5.2.3. The cases $\tilde{C}$, B_n and H_n.

THEOREM 5.34. *For the* H*-cell* $\mathbf{h} = \{24, 2124, 2z, 212z\}$ *(where* $z = 45\ldots(n-1)n(n-1)\ldots4$*) in type* $\tilde{C}_n$ *from Proposition 1.64, the asymptotic Hecke category* $\mathcal{J}_{\mathbf{h}}$ *is equivalent to* $\mathbf{Vec}_{(\mathbb{Z}/2\mathbb{Z})^2}$.

PROOF. We compute that the dimensions of all objects are 1. The maps shown in here are unique projections and inclusions. For this we need to compute with ρ^2 and the twisted Leibniz rule (see Remark 1.14). We have:

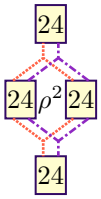

$$= 2\,\mathrm{id}_{B_{24}}, \tag{5.102}$$

since:

$$f_1 := \partial_2(\rho^2) = \partial_2(\rho)\rho + 2 \cdot \rho\partial_2(\rho) = \rho + 2 \cdot \rho \tag{5.103}$$

$$f_2 := \partial_4(f_1) = 2 \tag{5.104}$$

So $\kappa^{24}_{24,24} = \frac{1}{2}$. We use that $m_{2,4} = 2$. For the other calculation we will always start in the middle to use a Demazure operator. Then we calculate:

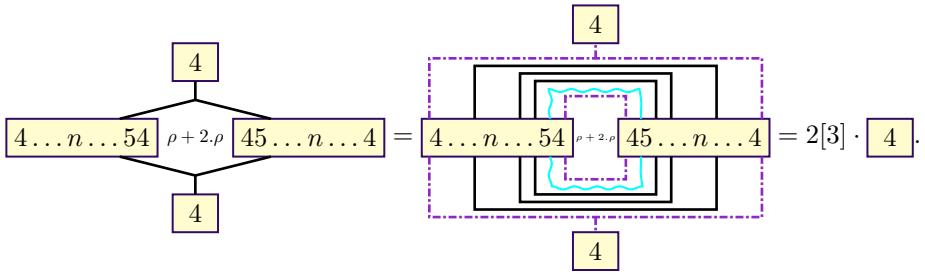

(5.105)

Similarly in the other cases, so we get:

$$\kappa^{24}_{2124,2124} = \frac{1}{2[3]}, \quad \kappa^{24}_{2z,2z} = \frac{1}{2[3]}, \quad \kappa^{24}_{212z,212z} = \frac{1}{4[3]^2}. \tag{5.106}$$

Also, note that $[3]_4 = 1$, hence this simplifies further. For the associators over 24 we then always get $\frac{1}{4}$ as in (B). Applying Lemma 4.28, since the numerator $\kappa^x_{x,24}\kappa^{24}_{x^*,x}$ and denominator $\frac{1}{4} \cdot \kappa^{24}_{x,x^*}$ consist of the same coefficients up to the associator factor, we get $\dim(J_x) = 1$ for all x. □

Remark 5.35. Associator computations can get quite difficult. However, when $x^* = x$ and the length of the Duflo involution equals the **a**-value of the cell, the first matrix entry of the F-symbol is easy to compute. In this case, breaking ρ^a through the d strands gives $\partial_d(\rho^a)$, while all other terms from polynomial forcing vanish. Thus:

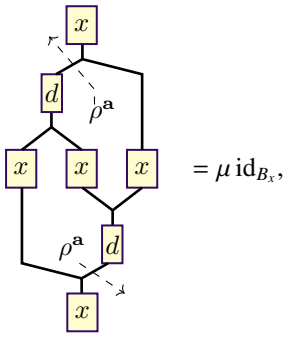

$$= \mu \, \mathrm{id}_{B_x}, \tag{5.107}$$

for $\mu = (\partial_d(\rho^a))^2$.

In types B_n and H_n this works in the same way.

Corollary 5.36. *For the cell* $\mathbf{h} = \{24, 2124\}$ *in type* B_n *we have* $\mathcal{J}_{\mathbf{h}} \simeq \mathbf{Vec}_{\mathbb{Z}/2\mathbb{Z}}$*, in type* H_n *we have* $\mathcal{J}_{\mathbf{h}} \simeq \mathcal{F}$.

5.2.4. Type F_n. We consider the H-cell $\mathbf{h} = \{24, 243524\}$ and the idempotents from Proposition 3.33. Note that $245324 = 425342$ using three rex moves. We therefore have:

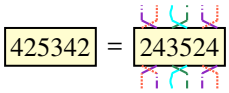

(5.108)

THEOREM 5.37. *For* $\mathbf{h} = \{24, 243524\}$ *in type* F_n *we have* $\mathcal{J}_{\mathbf{h}} \simeq \mathbf{Vec}_{\mathbb{Z}/2\mathbb{Z}}$.

PROOF. We compute, similar to Theorem 5.34, that $\kappa^{24}_{24,24} = \frac{1}{2}$. For $\kappa^{24}_{243524,243524}$ we use the rex moves from (5.108) to denote the unique degree -2 light leaf. Then in

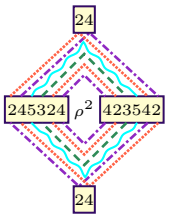

, (5.109)

the idempotent consists only of two terms, so expanding the middle gives 3 different diagrams, where we count one twice. The summands are:

$$a = \partial_{24}(\alpha_5\partial_5(\alpha_3\partial_3(\alpha_2\partial_2(\partial_4(\rho^2))))) = 4 \tag{5.110}$$

$$b = \partial_{24}(\alpha_5\partial_5(\alpha_3\partial_2(\alpha_4\partial_4(\rho^2)))) = -2[2] \tag{5.111}$$

$$c = \partial_{24}(\alpha_5\partial_5(\alpha_3\partial_2(\alpha_3)\partial_2(\alpha_4\partial_4(\rho^2)))) = 2[2]^2 \tag{5.112}$$

Now $a + \frac{2}{[2]} \cdot b + \frac{1}{[2]^2} \cdot c = 4 - 4 + 2 = 2$. Therefore $\kappa^{24}_{243524,243524} = \frac{1}{2}$. Similarly, the associator is $\frac{1}{4}$, hence by Lemma 4.28 the dimension of all objects is 1. □

5.2.5. Asymptotic Hecke Categories in Remaining Cases in Type H. This section completes our analysis of asymptotic Hecke categories for the remaining cells in types H_3 and H_4. We establish the categorical equivalences for each case through computation of dimensions. In all cases we solve, we have a categorification via the Fibonacci category $\mathcal{F}$ or the $\mathbb{Z}/2\mathbb{Z}$-graded vector spaces. It is therefore enough to compute the dimension of the non-unit, as this will give us which associator we have on the category.

5.2.5.1. *Cell* $\mathbf{h}_2$ *in Type* H_4.

THEOREM 5.38. *For the* H*-cell* $\mathbf{h} = \mathbf{h}_2 = \{d := 31, x := 312143\}$ *in type* H_4*, we have* $\mathcal{J}_{\mathbf{h}} \simeq \mathcal{F}$.

PROOF. It is enough to compute the dimensions of the objects in our cell. First, we observe that $312143 = 341213$ using simple rex moves

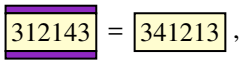

, (5.113)

where we build the idempotent on the right differently from x. We use this to make the projection contain fewer rex moves. For the projections, we have:

$$p^{31}_{31,31} \coloneqq$$ 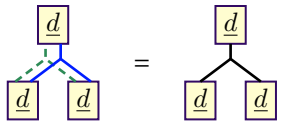 (5.114)

$$p^{31}_{312143,312143} \coloneqq$$ 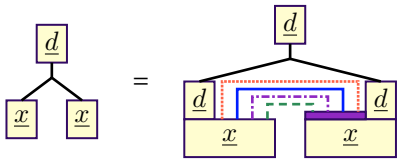 (5.115)

This leads to the following calculations. For $\kappa^{31}_{31,31}$:

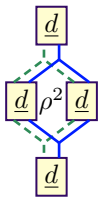 $= \partial_3(\partial_1)(\rho^2)\,\mathrm{id}_{B_{31}} = 2\,\mathrm{id}_{B_{31}},$ (5.116)

by the twisted Leibniz rule as 1 and 3 commute. On the other hand, in the calculation of $\kappa^{31}_{312143,312143}$ when we expand the right side, we get a pitchfork rule:

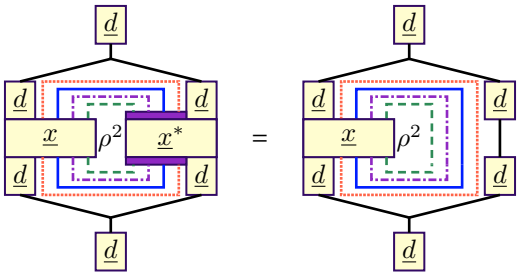 (5.117)

We simplify the middle part of that:

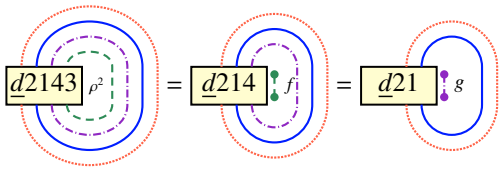

(5.118)

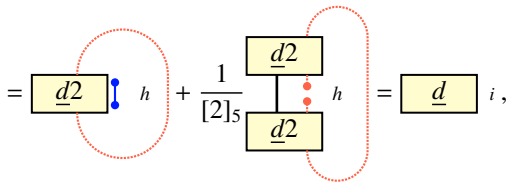

(5.119)

where $f = \partial_3(\rho^2)$, $g = \partial_4(\alpha_3 f)$, $h = \partial_1(\alpha_4 g)$, and $i = \alpha_2(\partial_2(\alpha_1 h)) + \frac{\alpha_2 h}{[2]_5}$. One then computes $\partial_3(\partial_1(i)) = 2[3]$. The first F-entry of the associator $(\alpha_{312143,312143,312143})^{312143}_{312143}$ is by Remark 5.35 $\frac{1}{4}$, hence by Lemma 4.28 we have $\dim(J_{312143}) = [3]$. Since the dimensions match those of the Fibonacci category, we conclude $\mathcal{J}_{\mathbf{h}} \simeq \mathcal{F}$ by Remark 5.10.

□

5.2.5.2. *Cell* $\mathbf{h}_3$ *in Type* H_4. We again take the cell $\mathbf{h} = \mathbf{h}_3 = \{d = 232, x = 232123\}$ and idempotents from Proposition 3.24.

Theorem 5.39. *The asymptotic Hecke category* $\mathcal{J}_{\mathbf{h}}$ *is equivalent to* $\mathbf{Vec}_{\mathbb{Z}/2\mathbb{Z}}$.

Proof. Here the partial trace computations from before are a little more involved. For $\kappa^d_{d,d}$ we consider:

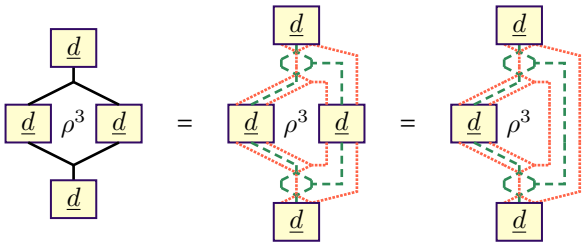

$= \partial_{232}(\rho^3)\,\mathrm{id}_{B_d}$ (5.120)

Here one uses the pitchfork rule for d, and then polynomial forcing and the needle relation. Then one computes $\partial_{232}(\rho^3) = 6$, so $\kappa^d_{d,d} = \frac{1}{6}$. For $\kappa^d_{x,x}$ we note that $232123 = 323123 = 321323$ by simple rex moves, hence one can describe the unique projection in:

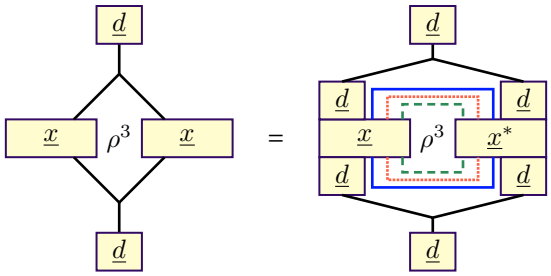

(5.121)

Here, however, the computation is a little more complicated. On the right side not all summands disappear. To help calculate we first consider:

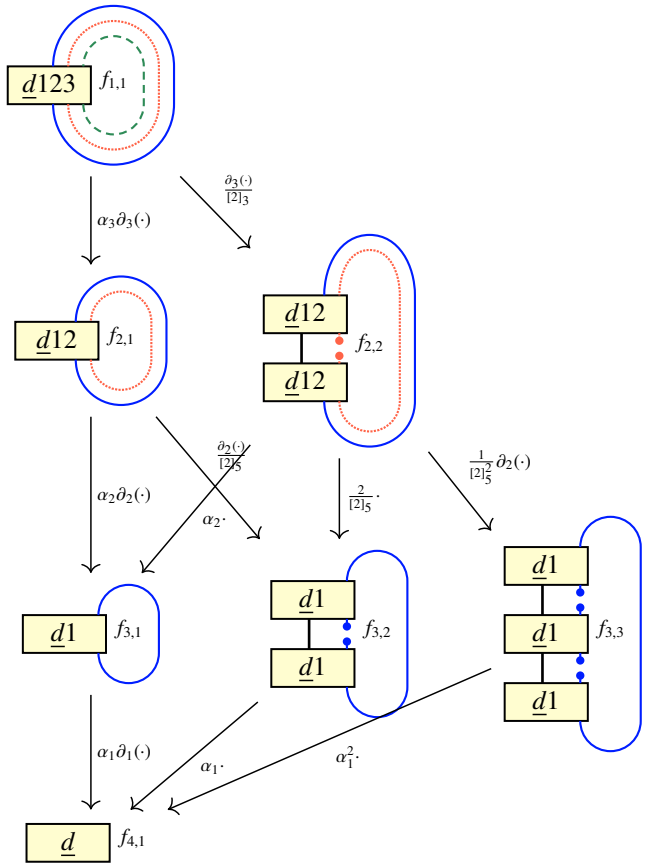

(5.122)

Plugging in $f_{1,1} := \rho^3$ and then taking $\partial_{232}(f_{4,1})$ gives one summand of the coefficient in equation (5.121). More terms to consider are:

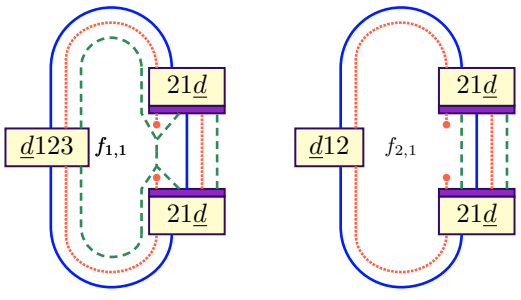

, (5.123)

One can draw similar diagrams showing how the idempotents decompose. In the end one will get:

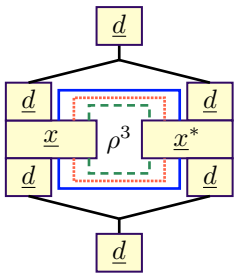

$$= 6\,\mathrm{id}_{B_d} \tag{5.124}$$

Also the F-symbol will be $\frac{1}{36}$, similar to the computation in Remark 5.35, so the dimensions are $\dim(J_x) = 1$. □

5.2.5.3. *Cell* $\mathbf{h}_6$ *in Type* H_3. For Theorem 5.40 we have explicit computer calculations in [21]. For $\mathbf{h} = h_6 = \{x, d\}$ where $d := 12121321213212$ and $x := 1212132121$, we provide some comments on the calculations.

The coefficient $\kappa^d_{x,x}$ is calculated via: In th

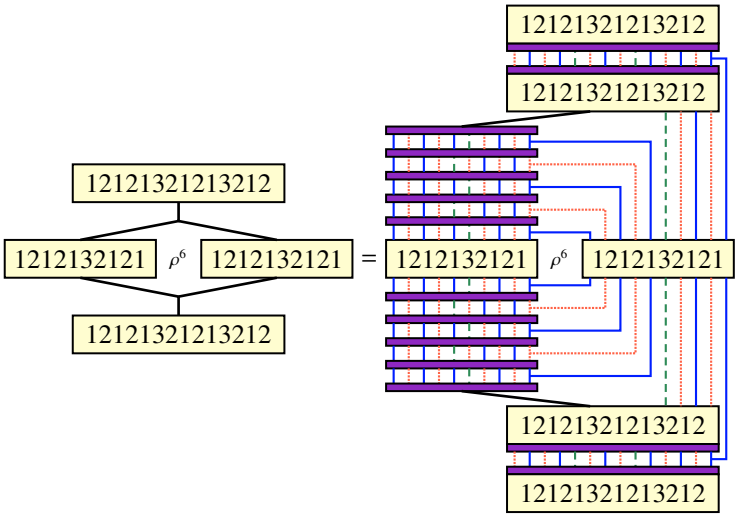

(5.125)

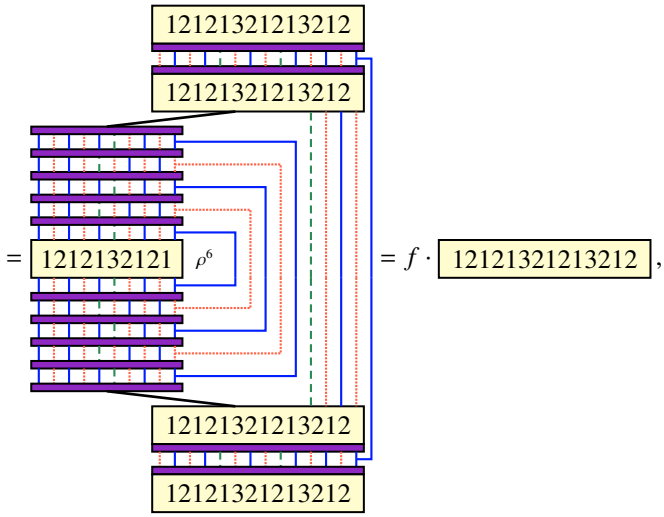

(5.126)

where $f = \partial_1(2.(1.(2.(3.(\partial_1(\partial_2(\partial_1(\partial_2(\partial_1(\rho^6)))))))))) = 1080\phi + 660$. We observe that the given map has degree -6. As the calculations will show, f is not zero; hence, this leaf does not lie in the cell above. The second equality of (5.126) can be derived through the following observation: when we use the recursive structure of $\underline{10}$, the terms generated without any summands containing $\kappa_{a,b}$ precisely yield the third term in the equation. All other summands contain needles or pitchforks and therefore have no impact on the result. Specifically, expanding $\underline{10}$ on the right side, until we have only summands constructed from $\underline{5}$, produces needles that locally resemble:

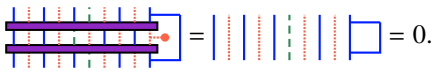

(5.127)

Expanding all terms of $\underline{5}$ then yields pitchforks, except for the identity summand. To obtain f, we break ρ^6 and all subsequent terms through the first 5 strands, then apply the respective action, and finally apply one last Demazure operator to arrive at the claimed equation.

For $\kappa^d_{d,d}$ the picture looks similar:

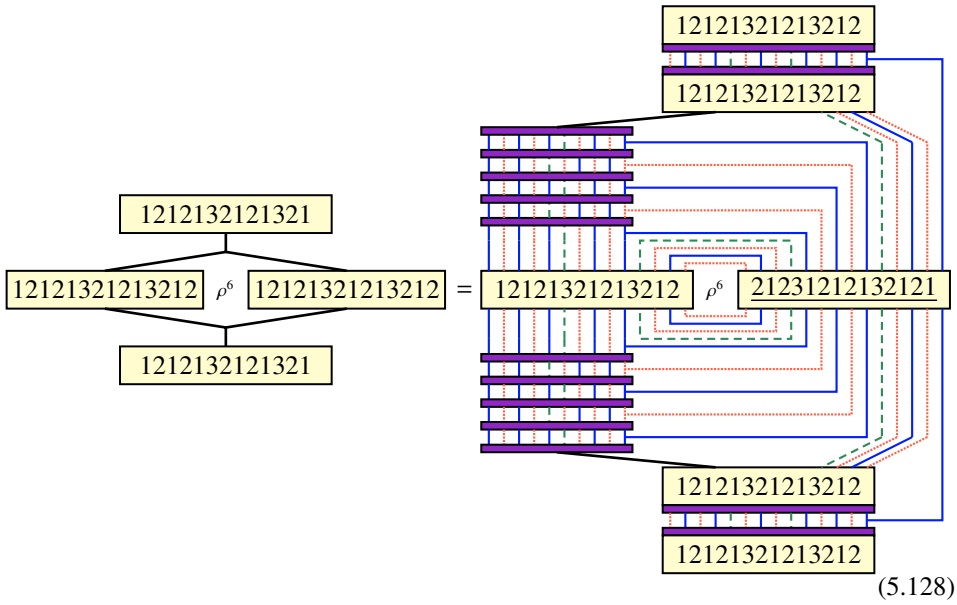

(5.128)

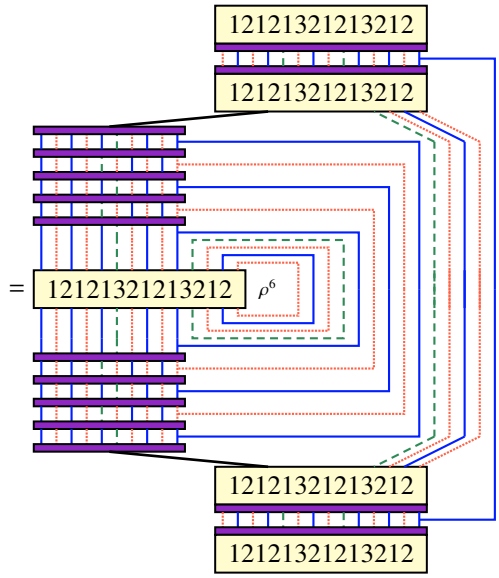

$= g \cdot$ 12121321213212 , (5.129)

where $g = 660\phi + 420$. A similar argument applies to the second equation (5.128). The computation of g, however, is more time-consuming when performed manually. A manual calculation would produce a graphic similar to that in (5.122). The following is an excerpt

of this process:

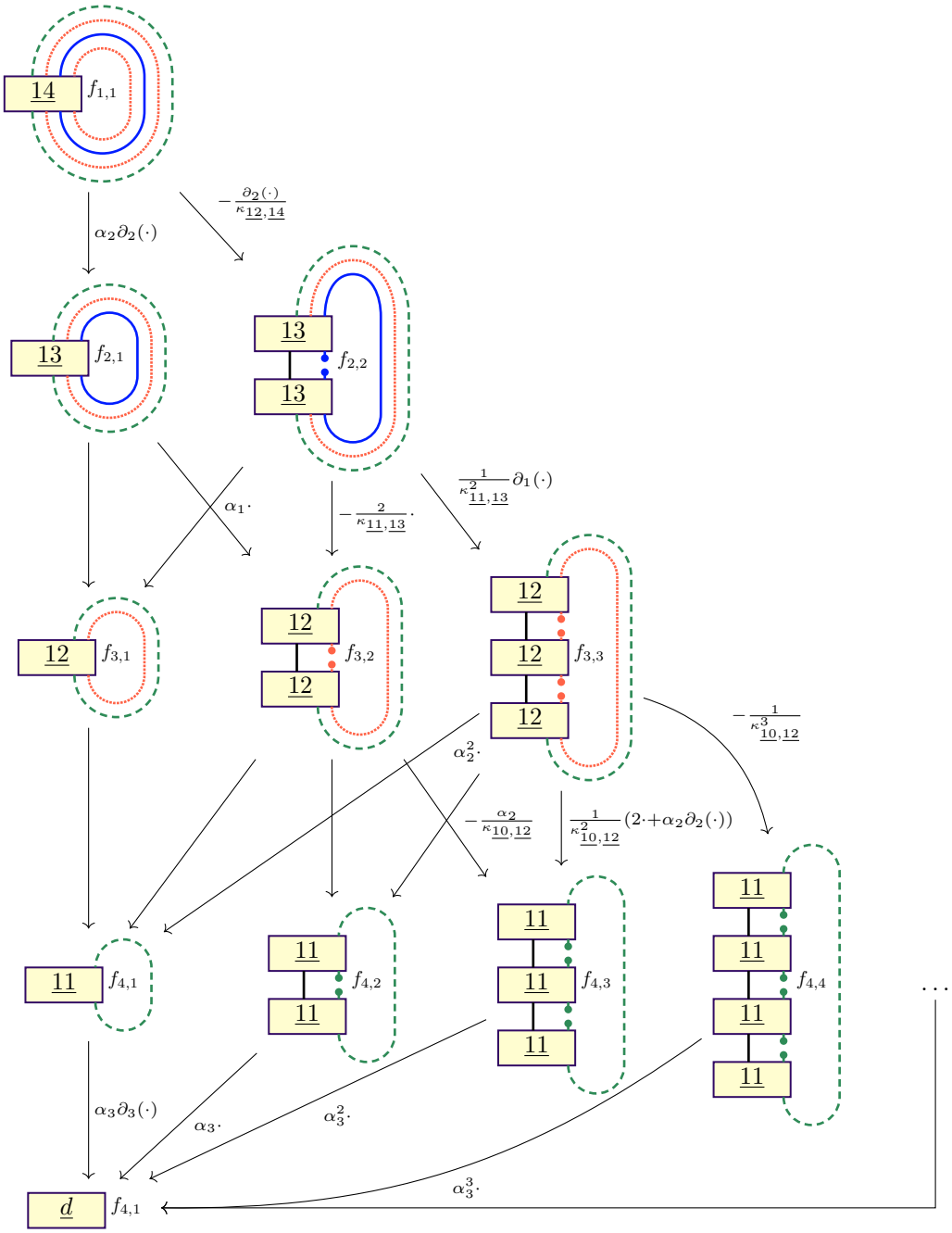

(5.130)

o where in place of ... we get a lot more terms involving $\kappa_{x,\underline{12}}$ all of which occur using the recursion on the terms in the line above. In the end the dimension of $\mathcal{J}_x$ can then be computed to $\frac{f}{g} = \phi$.

THEOREM 5.40. *For the* H*-cell* $\mathbf{h}_6$ *(of* $\mathbf{a}$*-value* 6*) in type* H_3 *(see subsection 1.4.3), the asymptotic Hecke category* $\mathcal{J}_{\mathbf{h}_6}$ *is equivalent to the Fibonacci category* $\mathcal{F}$*.*

REMARK 5.41. We summarize the asymptotic Hecke categories computed in this chapter:

- **Type** H_3**:** All non-trivial H-cells have been analyzed. The interesting cases are the subregular cell $\mathbf{h} = \{3, 32123\}$ (equivalent to $\mathcal{F}$, see Proposition 5.33), the cell $\mathbf{h}_3$ in $\mathbf{a}$-value 3 (Proposition 3.24), and $\mathbf{h}_6$ in $\mathbf{a}$-value 6 (equivalent to $\mathcal{F}$, see Theorem 5.40). For cells with $|h| = 1$, the category is simply $\mathbf{Vec}_{\mathbb{C}}$.
- **Type** H_4**:** We computed the two smallest non-trivial H-cells, $\mathbf{h}_2$ in $\mathbf{a}$-value 2 and $\mathbf{h}_3$ in $\mathbf{a}$-value 3 (see subsubsection 5.2.5.1 and subsubsection 5.2.5.2). The middle and higher cells in H_4 have elements of length up to 59, making the computations currently infeseable.

Now we have computed all (feasible) asymptotic Hecke categories. Therefore, we can proceed to analyze their S-matrixes in the next section.

5.3. Lusztig's Conjecture

We present the Fourier data from Lusztig. He uses a different convention for the S-matrix than we do. After a slight reordering and normalization, we obtain the same matrices. Then, combining knowledge from previous sections, we see how his data coincides with our computations.

So far we only considered $\mathcal{H}$ and therefore $\mathcal{J}$ to be defined over $\mathbb{R}$. To have the braidings as in subsection 5.1.2 we now work over $\mathbb{C}$. Since the Kazhdan–Lusztig combinatorics and the asymptotic algebra are defined over $\mathbb{Z}$, this base change does not affect the structure of the asymptotic category.

EXAMPLE 5.42. The dihedral fusion datum by Lusztig, [49, Section 3.10], is of the following form: For $p \geq 3$, we consider the pairs (i, j) with $0 < i < j < i + j < p$ or $0 = i < j < \frac{p}{2}$. If p is even, we also include two special tuples $(0, \frac{p}{2}), (0, \frac{p'}{2})$. For a pair (i, j) with $i > 0$, we denote by $(i, p - j)$ its involution, otherwise elements are self-dual.

We define a pairing via

$$\langle (i, j), (k, l) \rangle := \frac{\xi^{il+jk} + \xi^{-il-jk} - \xi^{ik+jl} - \xi^{-ik-jl}}{p} \tag{5.131}$$

on non-special tuples. Here ξ is a p-th root of unity. This expression resembles an expression in quantum numbers; the connection has been described in [42, Section 3.4].

The tuples (i, j) correspond to the object $X_{j-i-1} \boxtimes X_{j+i-1}$ in $C_p \boxtimes C_p^{rev}$. Both special elements correspond to two different subobjects of $X_{\frac{p-1}{2}} \boxtimes X_{\frac{p-1}{2}}$, see subsubsection 5.1.3.2.

For any tuple of pairs $((i, j), (k, l))$, the S-matrix value of the corresponding entry $(X_{j-i-1} \boxtimes X_{j+i-1}, X_{l-k-1} \boxtimes X_{l+k-1})$ is then

$$(-1)^{j+l-i-k-2}[(j - i)(l - k)][(j + i)(l + k)]. \tag{5.132}$$

The quantum part of this expression gives

$$\frac{q^{(j-i)(l-k)} - q^{-(j-i)(l-k)}}{q-q^{-1}} \frac{q^{(j+i)(l+k)} - q^{-(j+i)(l+k)}}{q-q^{-1}} \tag{5.133}$$

$$= \frac{(q^{lj-il-kj+ik} - q^{il-lj+kj-ik})(q^{jl+jk+il+ik} - q^{-jl-jk-il-ik})}{(q-q^{-1})^2} \tag{5.134}$$

$$= \frac{q^{2lj+2ik} - q^{-2il-2jk} - q^{2il+2kj} + q^{-2ik-2lj}}{(q-q^{-1})^2}, \tag{5.135}$$

where q is a $2p$-th root of unity, i.e., $q^2 = \xi$. Indeed, this gives the result of the pairing by Lusztig modulo a term of the form $\frac{(q-q^{-1})^2}{p}$.

This normalization is also seen in [24, Section 8.12]. Often, we normalize the entries in the S-matrix by $\dim(C)$, which is defined as the sum of the dimensions of the objects.

Remark 5.43 (Normalization). For $n = 2m$ even, we have m^2 objects in $\mathcal{Z}(\mathrm{Ad}(C_n))$. The values of the normalized S-matrix coincide with the calculations done in [42].

As one example, we can examine the entry corresponding to the unit object. In the S-matrix it is 1, while in the normalized S-matrix it is $\frac{1}{\dim(C_n)}$. The value of Lusztig's pairing $\langle (0,1),(0,1)\rangle$ is $-\frac{(q-q^{-1})^2}{p}$, which is expected.

Example 5.44. In type $I_2(5)$, we get the tuples $(0,1),(0,2),(1,2),(1,3)$ corresponding to $X_0 \boxtimes X_0 \simeq X_0$, $X_1 \boxtimes X_1 \simeq X_0 \oplus X_2$, $X_0 \boxtimes X_2 \simeq X_2$, and $X_1 \boxtimes X_3 \simeq X_2$. Under the involution, we pair the first and second, and third and fourth entries. If we denote the S-matrix under this permutation, we get:

$$\varphi \begin{pmatrix} \varphi^{-1} & \varphi & 1 & 1 \\ \varphi & \varphi^{-1} & -1 & -1 \\ 1 & -1 & -\varphi^{-1} & \varphi \\ 1 & -1 & \varphi & -\varphi^{-1} \end{pmatrix} \tag{5.136}$$

We are therefore only off by a factor of $\frac{\varphi}{\sqrt{5}} = \frac{2+\varphi}{5}$.

Theorem 5.45. *Let* $\mathbf{c}$ *be an* H*-cell in a Coxeter group of type* $I_2(p)$*,* H_3*, or one of the smaller cells in* H_4*. Let* n *be such that* $J_{\mathbf{c}}$ *is the Grothendieck ring of* $\mathrm{Ad}(C_n)$*. The* S*-matrix of the center of the asymptotic Hecke category* $\mathcal{Z}(\mathcal{J}_{\mathbf{c}})$ *is, after a reordering following the procedure in Example 5.42 and a normalization as described in Remark 5.43, the same as Lusztig's datum in [49, Section 3.10] and [8, Section 7.3].*

Proof. This follows from the observations presented here. For cells where the asymptotic algebra is the Fibonacci ring, we have consistently seen that in the categorification we have $\mathcal{F}$. If we are $(\mathbb{Z}/2\mathbb{Z})$-graded, then $\mathbf{Vec}_{\mathbb{Z}/2\mathbb{Z}}$ also occurs. For the trivial algebras, the S-matrix will also be trivial. For general dihedral cases, we have seen in the earlier examples that Lusztig's pairing and our notation on the S-matrix coincide. □

Remark 5.46. We conclude this theorem with a comment on the missing cases in H_4. The higher cells of H_4 have the same asymptotic algebras as the lower cells, i.e., we also only get two choices of categorification. Computing idempotents in this case, however, is beyond our current capabilities. The elements reach lengths up to 59, causing any branching graph to explode. Even the computational implementations used in [21] are insufficient. There computations are performed in the localized Hecke category, which provides a nice way to represent diagrams but is highly inefficient. For a map between $\mathrm{BS}(\underline{w}) \to \mathrm{BS}(\underline{v})$,

we need a $2^{\ell(w)} \times 2^{\ell(v)}$ matrix to represent it. Thus, the idempotent of the element of length 14 in case H_3 is represented as a 16392×16392 matrix where the entries are elements of the fraction field of R. Despite using some optimizations, these calculations are nearly at the limit of what is computationally feasible. Calculating traces and associators is similarly limited. The algorithmic approaches and current computational limitations are discussed in detail in [22].

In the middle cell of H_4, we obtain a completely new fusion category. Here, one has different options depending on the chosen $\mathcal{H}$-cell. We have 14, 18, or 24 objects, as described in subsection 1.4.4, however computing the entire categorification is currently not possible.

To advance further in this area, one needs to develop a Software package capable of calculating with the idempotents directly and utilizing their recursive structure.

Computing the center may then be possible using recent work from [53], where Mäurer and Thiel describe an algorithm that can compute the center and the S-matrix from a given fusion category.

References

[1] D. Alvis. "Subrings of the asymptotic Hecke algebra of type H_4". In: *Experimental Mathematics* 17.3 (2008), pp. 375–383. DOI: 10.1080/10586458.2008.10129042.

[2] D. Barter, J. C. Bridgeman, and R. Wolf. "Computing associators of endomorphism fusion categories". In: *SciPost Phys.* 13 (2022), p. 029. DOI: 10.21468/SciPostPhys.13.2.029.

[3] A. A. Beilinson, J. Bernstein, and P. Deligne. "Faisceaux pervers". In: *Analysis and topology on singular spaces, I (Luminy, 1981)*. Vol. 100. Astérisque. Soc. Math. France, Paris, 1982, pp. 5–171.

[4] M. Belolipetsky. "Cells and representations of right-angled Coxeter groups". In: *Selecta Mathematica (New Series)* 10 (3 2004), pp. 325–339. DOI: 10.1007/s00029-004-0355-9.

[5] M. V. Belolipetsky and P. E. Gunnells. "Cells in Coxeter groups, I". In: *Journal of Algebra* 385 (2013), pp. 134–144. DOI: https://doi.org/10.1016/j.jalgebra.2013.03.016.

[6] M. V. Belolipetsky, P. E. Gunnells, and R. A. Scott. "Kazhdan-Lusztig cells in planar hyperbolic Coxeter groups and automata". In: *Internat. J. Algebra Comput.* 24.5 (2014), pp. 757–772. DOI: 10.1142/S0218196714500325.

[7] M. Broué, G. Malle, and J. Michel. "Towards spetses. I". In: *Transform. Groups* 4.2-3 (1999), pp. 157–218. DOI: 10.1007/BF01237357.

[8] M. Broué and G. Malle. "Zyklotomische Heckealgebren". de. In: *Représentations unipotentes génériques et blocs des groupes réductifs finis - Avec un appendice de George Lusztig*. Astérisque 212. Société mathématique de France, 1993. URL: http://www.numdam.org/item/AST_1993__212__119_0/.

[9] X. Chen and H. Hu. *The boundedness of Lusztig's a-function for Coxeter groups of finite rank*. 2025. URL: https://arxiv.org/abs/2503.06432.

[10] A. H. Clifford. "Matrix Representations of Completely Simple Semigroups". In: *American Journal of Mathematics* 64.1 (1942), pp. 327–342. DOI: 10.2307/2371687.

[11] H. S. M. Coxeter. "The Complete Enumeration of Finite Groups of the Form $R_i^2 = (R_iR_j)^{k_{ij}} = 1$". In: *Journal of the London Mathematical Society* s1-10.1 (1935), pp. 21–25. DOI: https://doi.org/10.1112/jlms/s1-10.37.21.

[12] F. du Cloux. "Positivity results for the Hecke algebras of noncrystallographic finite Coxeter groups". In: *Journal of Algebra* 303.2 (2006). Computational Algebra, pp. 731–741. DOI: https://doi.org/10.1016/j.jalgebra.2005.10.004.

[13] C. Edie-Michell. "The Brauer-Picard Groups of fusion categories coming from the ADE subfactors". In: *International Journal of Mathematics* 29 (2017), p. 1850036.

[14] C. Edie-Michell and S. Morrison. *A field guide to categories with A_n fusion rules*. 2017. DOI: 10.48550/ARXIV.1710.07362.

[15] B. Elias. "The two-color Soergel calculus". In: *Compos. Math.* 152.2 (2016), pp. 327–398. DOI: 10.1112/S0010437X15007587.

[16] B. Elias, L. Rogel, and D. Tubbenhauer. "Code and more related to the paper "On the asymptotic category"". In: (2024). https://github.com/dtubbenhauer/acat.

[17] B. Elias and G. Williamson. "Soergel calculus". In: *Represent. Theory* 20 (2016), pp. 295–374. DOI: 10.1090/ert/481.

[18] B. Elias and G. Williamson. "Relative hard Lefschetz for Soergel bimodules". In: *J. Eur. Math. Soc. (JEMS)* 23.8 (2021), pp. 2549–2581. DOI: 10.4171/jems/1061.

[19] B. Elias. "Quantum Satake in type *A*. Part I". In: *Journal of Combinatorial Algebra* 1.1 (2017), pp. 63–125. DOI: 10.4171/jca/1-1-4.

[20] B. Elias, S. Makisumi, U. Thiel, and G. Williamson. *Introduction to Soergel Bimodules*. RSME Springer Series. Springer International Publishing, 2020. DOI: 10.1007/978-3-030-48826-0.

[21] B. Elias, L. Rogel, and D. Tubbenhauer. *Idempotents, traces, and dimensions in Hecke categories*. 2025. URL: https://arxiv.org/abs/2507.10061.

[22] B. Elias, L. Rogel, and D. Tubbenhauer. *Computing in the asymptotic category*. To appear. 2026.

[23] B. Elias and G. Williamson. "The Hodge theory of Soergel bimodules". In: *Ann. of Math. (2)* 180.3 (2014), pp. 1089–1136. DOI: 10.4007/annals.2014.180.3.6.

[24] P. Etingof, S. Gelaki, D. Nikshych, and V. Ostrik. *Tensor categories*. Vol. 205. Mathematical Surveys and Monographs. American Mathematical Society, Providence, RI, 2015, pp. xvi+343. DOI: 10.1090/surv/205.

[25] P. Etingof, D. Nikshych, and V. Ostrik. "On fusion categories". In: *Annals of Mathematics* 162.2 (2005), pp. 581–642. DOI: 10.4007/annals.2005.162.581.

[26] P. Etingof and V. Ostrik. "On Semisimplification of Tensor Categories". In: *Representation Theory and Algebraic Geometry: A Conference Celebrating the Birthdays of Sasha Beilinson and Victor Ginzburg*. Ed. by V. Baranovsky, N. Guay, and T. Schedler. Cham: Springer International Publishing, 2022, pp. 3–35. DOI: 10.1007/978-3-030-82007-7_1.

[27] J. Fröhlich and T. Kerler. *Quantum groups, quantum categories and quantum field theory*. Vol. 1542. Lecture Notes in Mathematics. Springer-Verlag, Berlin, 1993, pp. viii+431. DOI: 10.1007/BFb0084244.

[28] M. Geck. "PyCox: computing with (finite) Coxeter groups and Iwahori–Hecke algebras". In: *LMS J. Comput. Math.* 15 (2012), pp. 231–256. DOI: 10.1112/S1461157012001064.

[29] M. Geck and N. Jacon. *Representations of Hecke Algebras at Roots of Unity*. 1st ed. Algebra and Applications. Springer London, 2011, pp. XII, 404. DOI: 10.1007/978-0-85729-716-7.

[30] S. Gelaki, D. Naidu, and D. Nikshych. "Centers of graded fusion categories". In: *Algebra Number Theory* 3.8 (2009), pp. 959–990. DOI: 10.2140/ant.2009.3.959.

[31] J. Gibson, L. T. Jensen, and G. Williamson. "Calculating the p-Canonical Basis of Hecke Algebras". In: *Transformation Groups* 28.3 (2023), pp. 1121–1148. DOI: 10.1007/s00031-023-09799-z.

[32] J. Gibson, G. Williamson, and L. T. Jensen. *Magma package ASLoc*. https://github.com/joelgibson/asloc. 2022.

[33] J. A. Green. "On the Structure of Semigroups". In: *Annals of Mathematics* 54 (1951), p. 163.

[34] R. M. Green and T. Xu. "Classification of Coxeter groups with finitely many elements of **a**-value 2". In: *Algebr. Comb.* 3.2 (2020), pp. 331–364. DOI: 10.5802/alco.95.

[35] R. M. Green and T. Xu. *Kazhdan–Lusztig cells of* **a***-value 2 in* **a**(2)*-finite Coxeter systems*. 2021. arXiv: 2109.09803 [math.CO].

[36] A. Gruen and S. Morrison. "Computing Modular Data for Pointed Fusion Categories". In: *Indiana University Mathematics Journal* 70.2 (2021), pp. 561–593. DOI: 10.1512/iumj.2021.70.8560.

[37] S. Hart. "How many elements of a Coxeter group have a unique reduced expression?" In: *Journal of Group Theory* 20.5 (2017), pp. 903–910. DOI: doi:10.1515/jgth-2017-0009.

[38] N. Iwahori and H. Matsumoto. "On some Bruhat decomposition and the structure of the Hecke rings of p-adic Chevalley groups". In: *Inst. Hautes Études Sci. Publ. Math.* 25 (1965), pp. 5–48.

[39] L. H. Kauffman and S. L. Lins. *Temperley-Lieb Recoupling Theory and Invariants of 3-Manifolds (AM-134)*. Princeton University Press, 1994. DOI: 10.1515/9781400882533.

[40] D. Kazhdan and G. Lusztig. "Representations of Coxeter groups and Hecke algebras". In: *Invent. Math.* 53.2 (1979), pp. 165–184. DOI: 10.1007/BF01390031.

[41] L. Kong and H. Zheng. "The center functor is fully faithful". In: *Advances in Mathematics* 339 (2018), pp. 749–779. DOI: https://doi.org/10.1016/j.aim.2018.09.031.

[42] A. Lacabanne. "Crossed S-matrices and Fourier matrices for Coxeter groups with automorphism". In: *Journal of Algebra* 558 (Sept. 2020), pp. 550–581. DOI: 10.1016/j.jalgebra.2019.10.013.

[43] N. Libedinsky. "Sur la catégorie des bimodules de Soergel". In: *J. Algebra* 320.7 (2008), pp. 2675–2694. DOI: 10.1016/j.jalgebra.2008.05.027.

[44] G. Lusztig. "Some examples of square integrable representations of semisimple *p*-adic groups". In: *Trans. Amer. Math. Soc.* 277.2 (1983), pp. 623–653. DOI: 10.2307/1999228.

[45] G. Lusztig. *Hecke algebras with unequal parameters*. Vol. 18. CRM Monograph Series. American Mathematical Society, Providence, RI, 2003, pp. vi+136. URL: https://arxiv.org/abs/math/0208154.

[46] G. Lusztig. *Characters of Reductive Groups over a Finite Field.* Princeton University Press, 1984. URL: http://www.jstor.org/stable/j.ctt1b9x10c.

[47] G. Lusztig. "Cells in Affine Weyl Groups". In: *Advanced Studies in Pure Mathematics* 6 (1985), pp. 255–287. DOI: https://doi.org/10.2969/aspm/00610255.

[48] G. Lusztig. "Cells in affine Weyl groups, II". In: *Journal of Algebra* 109.2 (1987), pp. 536–548. DOI: https://doi.org/10.1016/0021-8693(87)90154-2.

[49] G. Lusztig. "Exotic Fourier transform". In: *Duke Mathematical Journal* 73.1 (1994), pp. 227–241. DOI: 10.1215/S0012-7094-94-07309-2.

[50] G. Lusztig. “Truncated convolution of character sheaves”. In: *Bull. Inst. Math. Acad. Sin. (N.S.)* 10.1 (2015), pp. 1–72. URL: https://web.math.sinica.edu.tw/bulletin/archives_articlecontent16.jsp?bid=MjAxNTEwMQ==.

[51] M. Mackaay, V. Mazorchuk, V. Miemietz, D. Tubbenhauer, and X. Zhang. “Simple transitive 2-representations of Soergel bimodules for finite Coxeter types”. In: *Proceedings of the London Mathematical Society* (2023). DOI: 10.1017/S1474748018000555.

[52] G. Malle. “Appendix: An exotic Fourier transform for H_4”. In: *Duke Math. J.* 76.1 (1994), pp. 243–248. URL: http://dml.mathdoc.fr/item/1077288615.

[53] F. Mäurer and U. Thiel. *Computing the center of a fusion category*. 2024. URL: https://arxiv.org/abs/2406.13438.

[54] M. Müger. “On the Structure of Modular Categories”. In: *Proceedings of the London Mathematical Society* 87.2 (2003), pp. 291–308. DOI: https://doi.org/10.1112/S0024611503014187.

[55] W. Munn. “Matrix representations of semigroups”. In: *Proc. Cambridge Philos. Soc.* 53 (1957), pp. 5–12. DOI: 10.1017/s0305004100031935.

[56] V. Ostrik. “Multi-fusion categories of Harish-Chandra bimodules”. In: *Proceedings of the International Congress of Mathematicians—Seoul 2014. Vol. III*. Kyung Moon Sa, Seoul, 2014, pp. 121–142. URL: https://api.semanticscholar.org/CorpusID:117941895.

[57] V. Ostrik. “Fusion categories of rank 2”. In: *Mathematical Research Letters* 10.2 (Apr. 2003), pp. 177–183. DOI: 10.4310/MRL.2003.v10.n2.a5.

[58] L. Rogel and U. Thiel. “The center of the asymptotic Hecke category and unipotent character sheaves”. In: (2023). URL: https://arxiv.org/abs/2307.07276v2.

[59] P. Selinger. “A Survey of Graphical Languages for Monoidal Categories”. In: *New Structures for Physics*. Ed. by B. Coecke. Berlin, Heidelberg: Springer Berlin Heidelberg, 2011, pp. 289–355. DOI: 10.1007/978-3-642-12821-9_4.

[60] W. Soergel. “Kategorie $\mathcal{O}$, perverse Garben und Moduln über den Koinvarianten zur Weylgruppe”. In: *J. Amer. Math. Soc.* 3.2 (1990), pp. 421–445. DOI: 10.2307/1990960.

[61] W. Soergel. “The combinatorics of Harish-Chandra bimodules”. In: *J. Reine Angew. Math.* 429 (1992), pp. 49–74. DOI: 10.1515/crll.1992.429.49.

[62] W. Soergel. “Kazhdan–Lusztig-Polynome und unzerlegbare Bimoduln über Polynomringen”. In: *J. Inst. Math. Jussieu* 6.3 (2007), pp. 501–525. DOI: 10.1017/S1474748007000023.

[63] B. Steinberg. *Representation theory of finite monoids*. Universitext. Springer, Cham, 2016, pp. xxiv+317. DOI: 10.1007/978-3-319-43932-7.

[64] Y. Zhang. “From the Temperley-Lieb Categories to Toric Code”. PhD thesis. Jan. 2016. DOI: 10.25911/5d9efb1734330.

Scientific Career

Education

04/2021 – 11/2025	PhD student in Mathematics University of Kaiserslautern–Landau Supervisor: Ulrich Thiel
08/2018 – 03/2021	Master of Science (M.Sc.) Technical University Kaiserslautern
10/2015 – 07/2018	Bachelor of Science (B.Sc.) Technical University Kaiserslautern
08/2007 – 03/2015	Abitur Heinrich Heine Gymnasium Kaiserslautern

Employment

10/2016 – 03/2021	Teaching Assistant in Mathematics Technical University Kaiserslautern
04/2021 – 11/2025	PhD student in Mathematics University of Kaiserslautern–Landau

Wissenschaftlicher Werdegang

Ausbildung

04/2021 – 11/2025	Promotionsstudium in Mathematik Rheinland-Pfälzische Technische Universität Kaiserslautern–Landau Betreuer: Ulrich Thiel
08/2018 – 03/2021	Master of Science (M.Sc.) Technische Universität Kaiserslautern
10/2015 – 07/2018	Bachelor of Science (B.Sc.) Technische Universität Kaiserslautern
08/2007 – 03/2015	Abitur Heinrich Heine Gymnasium Kaiserslautern

Beschäftigung

10/2016 – 03/2021	Wissenschaftliche Hilfskraft in Mathematik Technische Universität Kaiserslautern
04/2021 – 11/2025	Wissenschaftlicher Mitarbeiter in Mathematik Rheinland-Pfälzische Technische Universität Kaiserslautern–Landau